ABSTRACT

Title of Thesis: DATA REQUIREMENTS TO ENABLE PHM FOR LIQUID HYDROGEN STORAGE SYSTEMS FROM A RISK ASSESSMENT PERSPECTIVE

Camila Asunción Correa Jullian,
Master of Science, 2021

Dissertation directed by: Dr. Katrina Groth,
Department of Mechanical Engineering

Quantitative Risk Assessment (QRA) aids the development of risk-informed safety codes and standards which are employed to reduce risk in a variety of complex technologies, such as hydrogen systems. Currently, the lack of reliability data limits the use of QRAs for fueling stations equipped with bulk liquid hydrogen storage systems. In turn, this hinders the ability to develop the necessary rigorous safety codes and standards to allow worldwide deployment of these stations. Prognostics and Health Management (PHM) and the analysis of condition-monitoring data emerge as an alternative to support risk assessment methods. Through the QRA-based analysis of a liquid hydrogen storage system, the core elements for the design of a data-driven PHM framework are addressed from a risk perspective. This work focuses on identifying the data collection requirements to strengthen current risk analyses and enable data-driven

approaches to improve the safety and risk assessment of a liquid hydrogen fueling infrastructure.

DATA REQUIREMENTS TO ENABLE PHM FOR LIQUID HYDROGEN STORAGE SYSTEMS FROM A RISK ASSESSMENT PERSPECTIVE

by

Camila Asunción Correa Jullian

Dissertation submitted to the Faculty of the Graduate School of the
University of Maryland, College Park, in partial fulfillment
of the requirements for the degree of
Master of Science
2021

Advisory Committee:
Professor Katrina M. Groth, Chair
Professor Mohammad Modarres
Professor Reinhard Radermacher
Dr. William Buttner, Special Member

Dedication

To

Mercedes Poblete
&
your guardian angel

Acknowledgments

First, I would like to sincerely thank my advisor, Dr. Katrina Groth, for both her technical insight and her encouragement and support, for helping me to become a better researcher and not lose track of what is important. You told me once that we should give our 100% everyday, but that there are also some days that just getting out of bed is the 100% and that this is ok, too.

I would also like to thank the other members of my committee, Dr. Mohammad Modarres, Dr. Reinhard Radermacher, both with whom I had the pleasure of taking courses. Like this thesis, the variety of backgrounds and insights have proven to be a challenge to harmonize. As a special member in my committee, I would like to thank Dr. William Buttner and his team at NREL which have given invaluable insight and the opportunity to present my work to a greater audience.

I would like to thank the U.S. Department of Energy Office of Energy Efficiency and Renewable Energy Hydrogen and Fuel Cell Technologies Office for funding this work[1].

I would also like to thank my research colleagues at the SyRRA Lab, especially Madison West, Vincent Paglioni and Austin Lewis who read through this and helped me wrestle the stubborn English language.

Three-quarters of this thesis was writing during a pandemic. As an international student, missing my friends and family back in Chile has been challenging. A silver-lining of all of this is that I can appreciate all your love and support throughout the years from a different perspective. I'd like to give special thanks to my parents, Margarita Jullian and Leopoldo Correa, for being there in your own unique ways. I'd also like to mention Sebastian Romo and Christopher Howard, who have made this past year stuck at my-far-away-home brighter.

Finally, I would like to thank Sergio Manuel Ignacio Cofré Martel with all my heart. Ignacio, thank you for your never-ending patience, witty humor, and unwavering confidence in me. Thank you for all our long-winded conversations and for always making me strive to improve. Sunnier days are ahead of us!

[1] This work was supported by the NREL, operated by Alliance for Sustainable Energy, LLC, for the U.S. DOE under Contract No. DE-AC36-08GO28308. Funding provided by U.S. DOE-EERE Hydrogen and Fuel Cell Technologies Office. The views expressed in this document do not necessarily represent the views of the DOE or the U.S. Government.

Table of Contents

Dedication ii
Acknowledgments iii
Table of Contents iv
List of Tables vii
List of Figures ix
List of Abbreviations xi
Chapter 1. Introduction 1
1.1. Context and Motivation 2
1.2. Objectives & Approach 6
1.2.1. Task 1: LH_2 Storage System Risk Scenario Identification 7
1.2.2. Task 2: Failure Data Collection and Quantification in LH_2 Systems 8
1.2.3. Task 3: LH_2 Storage PHM Framework Concept Design 8
1.3. Thesis Outline 9
Chapter 2. Background and Literature Review 10
2.1. Hydrogen Fueling Stations 10
2.1.1. Hydrogen Safety Codes and Standards 12
2.2. Quantitative Risk Assessment 19
2.2.1. Risk Technical Background 20
2.2.2. General QRA Framework 23
2.3. Risk Assessments of Hydrogen Systems 25
2.3.1. QRA-based Hydrogen Risk Assessment Model Software 26
2.3.2. QRA Applications in Gaseous Hydrogen Stations 29
2.3.3. QRA Applications in Liquid Hydrogen Stations 35
2.4. Prognostics and Health Management 37
2.4.1. Introduction to Elemental PHM Concepts 38
2.4.2. PHM Frameworks and Applications 43
2.4.3. Challenges in Data-Driven PHM Applications 46
Chapter 3. LH_2 Storage System Risk Scenario Identification 48
3.1. Methodology 48
3.1.1. LH_2 Storage System Design Selection 48
3.1.2. Analysis of Hydrogen Failure Scenarios 49
3.1.3. Failure Mode and Effect Analysis 49

3.2. Hydrogen Fueling Station Generic Design 51
3.2.1. Bulk LH_2 Storage System 55
3.2.2. Compression and Cooling Subsystem 56
3.2.3. Gas Cascade Storage 57
3.2.4. Dispenser Subsystem 57
3.3. Survey of Available Scenario Data Sources 58
3.3.1. Hydrogen Risk Scenario Data Sources 58
3.3.2. Liquid Hydrogen Risk Scenarios 59
3.4. Results of FMEA for LH_2 Storage System 63
3.4.1. FMEA System Decomposition 63
3.4.2. Results: FMEA Risk Scenario Identification 66
3.4.3. Discussion of Identified Risk Scenarios 70
Chapter 4. Quantitative Risk Analysis of LH_2 Storage System 72
4.1. Methodology 72
4.1.1. Review of Hydrogen-related Reliability Data 72
4.1.2. Event Sequence Diagrams and Fault Trees 73
4.1.3. Fault Tree Analysis 73
4.2. Survey of Available Frequency and Reliability Data Sources 74
4.2.1. Hydrogen Frequency Data Sources 74
4.2.2. Data Sources from Other Industries 80
4.3. Results of QRA for LH_2 Risk Scenarios 82
4.3.1. Event Sequence Diagrams for High-Risk Scenarios 83
4.3.2. Fault Trees for LH_2 Release Initiating Event 88
4.4. Discussion and Identified QRA Data Requirements 100
Chapter 5. Conceptual Development of PHM Framework for LH_2 Storage Systems 105
5.1. Methodology 105
5.2. Data Collection in PHM Applications 106
5.2.1. Data Types for Diagnostics and Prognostics 106
5.2.2. PHM-Related Standards 109
5.2.3. Benchmark Datasets 111
5.3. PHM Applications in Engineering Systems 113
5.3.1. Variable Renewable Energy Systems 113
5.3.2. Lithium-ion Batteries and Fuel Cells 116
5.4. Potential Condition-Monitoring Data Sources in LH_2 Storage Systems 120

5.4.1. LH_2 Storage Tank and Pipelines 121
5.4.2. Centrifugal Pump for LH_2 Cryogenic Applications 124
5.4.3. Proposed Condition-Monitoring Data Sources in LH_2 Storage System 125
5.5. PHM Framework Design Stages for LH_2 Storage System 127
5.5.1. System Failure Characterization 127
5.5.2. System Behavior Characterization 128
5.5.3. Anomaly Detection 129
5.5.4. Diagnosis of Faulty Behavior 130
5.5.5. Prognosis of Future Health States 131
5.5.6. Framework Integration to System Operation 132
5.6. Proposed PHM and QRA Integration Framework 136
Chapter 6. Discussion and Conclusions 142
6.1. Summary and Technical Contributions 143
6.2. Discussion and Limitations 145
6.3. Recommendations and Future Work 148
Appendices 153
Appendix A. Hydrogen Fuel Properties 153
Appendix B. Additional Risk Scenarios and Mitigations in HAZOP study 155
Appendix C. Hydrogen Fueling Station P&IDs 157
C.1. Liquid Storage Subsystem 158
C.2. Compression and Cooling Subsystem 159
C.3. Cascade Storage Unit 160
C.4. Cascade Storage System 161
C.5. Fuel Dispenser Subsystem 162
C.6. Subsystem components by P&ID Nomenclature 163
Appendix D. Frequency Data Sources 165
D.1. HyRAM Frequency Data 165
D.2. OREDA 167
D.3. Purple Book Loss of Containment Frequency Data 186
Appendix E. Extended QRA Results 192
E.1. FMEA Full Results 192
E.2. Full Fault Tree 204
References 206

List of Tables

Table 2-1: NFPA 2 Performance-Based Option Required Design Scenarios..... 14
Table 2-2: NFPA 2 Performance-Based Option Criteria Requirements..... 15
Table 2-3: NFPA 2 Critical HAZOP Scenarios during normal system operation..... 17
Table 2-4: Developed Risk Scenarios in HyRAM 3.0..... 28
Table 2-5: Comparison of approaches used in PHM Frameworks..... 40
Table 3-1: Simplified Risk Matrix..... 51
Table 3-2: H2@SCALE hydrogen fueling station subsystem description..... 54
Table 3-3: H2@SCALE hydrogen fueling station components description..... 55
Table 3-4: P-28 Alternative-release scenarios..... 60
Table 3-5: Range of effects on employees, the public, and the environment..... 61
Table 3-6: P-28 HAZOP Consequences in Node #2..... 61
Table 3-7: P-28 HAZOP Consequences in Node #5..... 62
Table 3-8: P-28 Safeguards for large range consequence scenarios in Nodes #2-#5. 62
Table 3-9: LH_2 storage functional description..... 63
Table 3-10: LH_2 Storage Decomposition Functional Description..... 65
Table 3-11: Storage subsystem identified liquid hydrogen-related failure modes..... 68
Table 3-12: Control subsystem identified liquid hydrogen-related failure modes..... 69
Table 3-13: Process subsystem identified liquid hydrogen-related failure modes..... 69
Table 4-1: ESD General Release Event Description. To be continued..... 84
Table 4-2: ESD General Release Event Description. Continued..... 85
Table 4-3: Identified liquid hydrogen-related high-risk failure modes..... 85
Table 4-4: Relevant Failure Modes from OREDA database..... 89
Table 4-5: Selected Failure Rate values for Top Event: LH_2 Leakage..... 91
Table 4-6: Selected LOC Frequencies for Top Event: LH_2 Leakage..... 91
Table 4-7: Event Tree Nomenclature. To be Continued..... 96
Table 4-8: Event Tree Nomenclature. Continued..... 97
Table 4-9: Probability of Failure Events, Trilith Nomenclature..... 98
Table 4-10: Ranking of Minimal Cut-sets by Estimated Unreliability..... 99
Table 5-1: Measurement techniques for various diagnostics models. NIST (2014). 110
Table 5-2: Opportunities for PHM applications in LH_2 Storage Systems..... 125
Table 5-3: Design of implementation stages for PHM frameworks..... 133

A-Table 1: P-28 HAZOP Consequences in other system nodes..... 155
A-Table 2: P-28 Other safeguards for large range consequence scenarios..... 156
A-Table 3: HyRAM Probability Data..... 165
A-Table 4: Random leak frequency parameters per components. To be continued. 166
A-Table 5: Random leak frequency parameters per components. Continued..... 167
A-Table 6: Relevant Failure Modes from OREDA database..... 169
A-Table 7:OREDA Topside Data Table Format..... 170
A-Table 8: Top failure mode and mechanisms - Centrifugal pumps..... 172
A-Table 9: Failure rates for Centrifugal Pump in Cooling Systems..... 172
A-Table 10: Top failure mode and mechanisms - Electric motors..... 173
A-Table 11:Failure rates for Electric Motors in Centrifugal Pump-Cooling Systems. 174

A-Table 12: Top failure mode and mechanisms - Relief valves..... 175
A-Table 13: Failure rates for Conventional PSV Relief Valves..... 175
A-Table 14: Top failure mode and mechanisms - Shut-off valves..... 176
A-Table 15: Failure rates for Shut-off valves. To be continued..... 176
A-Table 16: Failure rates for Shut-off valves. Continued 177
A-Table 17: Top failure mode and mechanisms - Input devices..... 177
A-Table 18: Top failure mode and mechanisms - Pressure input devices..... 178
A-Table 19: Failure rates for various input devices..... 179
A-Table 20: Top failure mode and mechanisms - Fire & gas detectors..... 180
A-Table 21: Failure rates for Fire & gas detectors. To be continued..... 180
A-Table 22: Failure rates for Fire & gas detectors. Continued..... 181
A-Table 23: Top failure mode and mechanisms – CLUs..... 181
A-Table 24: Failure rates for CLUs..... 182
A-Table 25: Top failure mode and mechanisms - Heat exchangers..... 183
A-Table 26: Failure rates for Heat Exchangers. To be continued..... 183
A-Table 27: Failure rates for Heat Exchangers. Continued..... 184
A-Table 28: Top failure mode and mechanisms – Vessels..... 185
A-Table 29: Failure rates for Vessels. To be continued..... 185
A-Table 30: Failure rates for Vessels. Continued..... 186
A-Table 31: Consequence modeling for storage and piping LOC events..... 187
A-Table 32: LOC data for pressure and atmospheric tanks..... 189
A-Table 33: LOC data for pipelines..... 189
A-Table 34: LOC data for centrifugal pumps..... 190
A-Table 35: LOC data for heat exchangers..... 191
A-Table 36: LOC data for PRDs..... 191
A-Table 37: FMEA Results for System 1.1 Storage Tank. To be continued..... 193
A-Table 38: FMEA Results for System 1.1 Storage Tank. Continued..... 194
A-Table 39: FMEA Results for System 1.2-1.4 PSV. To be Continued..... 195
A-Table 40: FMEA Results for System 1.2-1.4 PSV. Continued..... 196
A-Table 41: FMEA Results for System 1.5 Block-and-bleed valve..... 197
A-Table 42: FMEA Results for System 2.1 Air-operated valve (FV)..... 198
A-Table 43: FMEA Results for System 2.2-2.6 FV Control System..... 199
A-Table 44: FMEA Results for System 3.1 Cryogenic Pump..... 200
A-Table 45: FMEA Results for System 3.2 Isolation Hand Valve..... 201
A-Table 46: FMEA Results for System 3.3 Ambient air Evaporator..... 202
A-Table 47: FMEA Results for System 4.1 Piping Lines..... 203

List of Figures

Figure 1-1: Types of data needed to perform QRA for a hydrogen system. Moradi and Groth (2019)..... 4
Figure 1-2: Number of journal publications on PHM in Web of Science. Meng and Li (2019)..... 6
Figure 1-3: Overview of thesis methodology. 9
Figure 2-1: Block diagram of a hydrogen fueling station. 11
Figure 2-2: General QRA Framework Outline. 23
Figure 2-3: Summary of QRA methodology implemented in HyRAM. Groth and Hecht (2017)..... 27
Figure 2-4: Event Sequence Diagram for GH_2 releases in HyRAM 3.0. 28
Figure 2-5: Exceeded Pressure Set Point Sub-Fault Tree. Casamirra et al. (2009). ... 30
Figure 2-6: Risk Matrix used in Kikukawa et al. (2008). 31
Figure 2-7: Event Tree for Accumulator Connection Piping Hydrogen Leakage. Tsunemi et al. (2019) 33
Figure 2-8: Proposed BN for fire and explosions risks. Huang and Ma (2018). 34
Figure 2-9: Publications related RUL prediction. Lei et al. (2018). 41
Figure 2-10: A holistic PHM Framework. Moradi and Groth (2020). 43
Figure 2-11: Example of applied PHM framework. Nguyen and Medjaher (2019)... 46
Figure 3-1: Code Compliant Base Case Liquid Full Station Layout. Ehrhart et al. (2020)..... 53
Figure 3-2: Schematic of LH_2-based fueling station design. 54
Figure 3-3: LH_2 storage functional block diagram. 56
Figure 3-4: LH_2 Storage Decomposition Functional Block Diagram. 64
Figure 4-1: Maintenance by Known Equipment in Retail Stations. NREL (2019). ... 76
Figure 4-2: Maintenance by Known Equipment in all Stations. NREL (2018)..... 76
Figure 4-3: Safety Reports in Retail Stations. Adapted from NREL CDPs (2019).... 77
Figure 4-4: Safety Reports in all Stations. Adapted from NREL CDPs (2018). 78
Figure 4-5: Example of maintenance causes and effects analysis. NREL (2020). 79
Figure 4-6: Historical Failure Rate Estimation by Number of Fills in hydrogen fueling stations. NREL (2020). 80
Figure 4-7: Proposed Event Sequence Diagram for LH_2 releases. 84
Figure 4-8: High risk scenario 1 - Malfunction of the pressure relief valve system... 86
Figure 4-9: High risk scenario 2 - Operation failure of the air-operated valve. 87
Figure 4-10: High risk scenario 3 - Rupture of the evaporator. 88
Figure 4-11: Fault Tree Developed for LH_2 Leakage Top Events. 92
Figure 4-12: Fault Tree Developed Event 2: Pump Leakage Events. 93
Figure 4-13: Fault Tree Developed Event 3: Evaporator Leakage Events. 94
Figure 4-14: Fault Tree Developed Event 4: Piping Leakage Events. 94
Figure 4-15: Fault Tree Developed Events 4-5 Undetected Random Leaks. 95
Figure 4-16: Types of data needed to perform QRA for a liquid hydrogen system. Adapted from Moradi and Groth (2019). 102
Figure 5-1: Examples of PHM applications: Health-state diagnosis in bearings. Lei et al. (2018). 108

Figure 5-2: Examples of PHM applications: Health-state prognosis. Jouin et al. (2016). 108
Figure 5-3: The predicted and observed voltage curves in four seasons. Hong, Z. Wang, and Y. Yao (2019)..... 118
Figure 5-4: Estimated RUL probability distribution. Cheng, Zerhouni, and Lu (2018). 120
Figure 5-5: Defect localization on the cylinder: effect of excited frequencies. Yang et al. (2019)..... 122
Figure 5-6: Monitoring System Layout for LH_2 Storage Systems..... 126
Figure 5-7: Examples of dimensionality reduction for system diagnosis..... 129
Figure 5-8: Examples of anomaly and fault characterization for diagnosis. 130
Figure 5-9: Examples of RUL prognosis in a CNC milling machine. Wang et al. (2020). 132
Figure 5-10: Gradual Implementation of PHM Framework based on Available Data. 135
Figure 5-11: Information Flow in PHM Framework for maintenance decisions. 137
Figure 5-12: Information Flow in QRA for risk-informed code development. 138
Figure 5-13: Combined QRA-PHM Framework. 140

A-Figure 1: Reference Station P&ID - Liquid Storage..... 158
A-Figure 2: Reference Station P&ID - Compression and Cooling..... 159
A-Figure 3: Reference Station P&ID – Cascade Gas Storage Unit..... 160
A-Figure 4: Reference Station P&ID - Cascade Storage System. 161
A-Figure 5: Reference Station P&ID – Dispenser..... 162
A-Figure 6: Example of HyRAM Fault Tree for Random Leaks. 166
A-Figure 7: Maintainable items relative contribution to the total failure rate, %..... 171
A-Figure 8: Top failure modes and mechanisms in centrifugal pumps, %..... 171
A-Figure 9: Top failure modes and mechanisms in electric motors, %..... 173
A-Figure 10: Top failure modes and mechanisms in relief valves, %..... 175
A-Figure 11: Top failure modes and mechanisms in shut-off valves, %..... 176
A-Figure 12: Top failure modes and mechanisms in input devices, %. 178
A-Figure 13: Top failure modes and mechanisms in pressure input devices, %..... 178
A-Figure 14: Top failure modes and mechanisms in fire & gas detectors, %. 180
A-Figure 15: Top failure modes and mechanisms in CLU, %..... 182
A-Figure 16: Top failure modes and mechanisms in heat exchangers, %..... 183
A-Figure 17: Top failure modes and mechanisms in vessels, %. 185
A-Figure 18: Complete Fault Tree for LH2 Release Top Event..... 205

List of Abbreviations

AE	Auto-encoder
CBM	Condition-Based Maintenance
CEC	California Energy Commission
CGA	Compressed Gas Association
CNN	Convolutional Neural Networks
DBN	Deep Belief Networks
DL	Deep Learning
FCEV	Fuel Cell Electric Vehicle
FMEA	Failure Mode and Effects Analysis
FTA	Fault Tree Analysis
GH_2	Gaseous Hydrogen
HFTO	Hydrogen and Fuel Cell Technologies Office
HI	Health Indicator
HIAD	Hydrogen Incidents and Accidents Database
HyRAM	Hydrogen Risk Assessment Model
ISO	International Organization for Standardization
k-NN	k-Nearest Neighbors
KPI	Key Performance Indicator
LH_2	Liquid Hydrogen
LSTM	Long-Short Term Memory
ML	Machine Learning
NN	Neural Networks
NREL	National Renewable Energy Laboratory
OREDA	The Offshore Reliability Data Handbook
PHM	Prognostics and Health Management
QRA	Quantitative Risk Analysis
RNN	Recurrent Neural Networks
RUL	Remaining Useful Life
SVM	Support Vector Machine

Chapter 1. Introduction

Limited availability of hydrogen fueling stations represents an important barrier for the increase in Fuel Cell Electric Vehicles' (FCEVs) deployment [1], [2]. Access to hydrogen-based fuel is restricted in urban areas due to the requirements established in pertinent Safety Codes and Standards (SCS) that ensure that new technologies maintain acceptable risk levels. As hydrogen technologies are developed and deployed, continuous efforts have been invested into increasing the safety of hydrogen infrastructure, as well as incorporating scientific, risk-informed requirements into the development of corresponding SCS [3].

Quantitative Risk Assessment (QRA) frameworks provide a systematic and science-based foundation for the design and implementation of SCS. These frameworks have been used in key hydrogen SCS including multiple aspects of both the U.S. National Fire Protection Association *NFPA 2* code for gaseous hydrogen (GH_2) stations [4] and the international standard *ISO 19880-1* [5]. However, to date, most QRA efforts have focused on GH_2 systems and storage, while liquid hydrogen (LH_2) risks have been less explored [6].

The limited availability of reliability and safety data for LH_2 systems represents a barrier to fully employ risk-informed tools, such as QRA [7]. As stated by the U.S. Department of Energy's Fuel Cell Technologies Office (FCTO), new approaches for data generation, collection, and analysis are critical to close safety and reliability knowledge gaps regarding hydrogen infrastructure [2]. This work seeks to explore the suitability of

new methods for data collection and analysis, with a specific focus on LH_2 storage systems for on-site equipment at fueling stations.

Recent trends in Prognosis and Health Management (PHM) research have focused on proactive asset management, as well as operation and maintenance scheduling optimization in complex systems based on the use of sensor and condition-monitoring data [8], [9]. Given the wide variety of PHM applications in complex engineering systems, these frameworks could provide valuable tools for expanding available risk and reliability analysis for hydrogen systems. In particular, while risk analysis generally consists of the identification and management of system-level risks, PHM could enable the study of the operational conditions which lead to the development of the identified risk scenarios.

The purpose of this thesis is to provide a context for the development of a PHM framework in hydrogen systems. This study is carried out through the analysis of a general design for a liquid hydrogen-based fueling station. Traditional QRA approaches are utilized to determine the system's operation and failure logic, as well as identifying critical failure modes and risk scenarios. Current data collection requirements are discussed from a QRA and PHM perspective. A conceptual design of a PHM framework is developed to illustrate the potential of incorporating new risk-informed mitigations based on QRA and PHM into existing SCS. Ultimately, this could lead to both safer hydrogen systems and less restrictive codes and standards requirements.

1.1. Context and Motivation

The International Energy Agency (IEA) has identified that the cost reduction of the installation, operation, and maintenance of hydrogen fueling station as critical to the deployment of FCEV. Particularly, safety requirements have been identified as some of the

costliest elements in hydrogen stations [10]. In the U.S., the main organization devoted to the development of SCS addressing the risks and effects of fire-related hazards is the National Fire Protection Association (NFPA) [11]. The *NFPA 2 Hydrogen Technologies Code* is the principal code that guides the design and implementation of hydrogen-related infrastructure [4]. During each revision cycle, this code is updated based on new developing technologies, methodologies, data sets, and good practices identified within the industry. A key aspect of the code has been the use of QRA to risk-inform various requirements, e.g., the separation distances [12], indoor refueling provisions [13] and performance-based compliance options [14] for GH_2 stations. Similarly, QRA has been used for the corresponding international standard *ISO 19980-1* referring to GH_2 stations [15].

In contrast, there is limited research available to support risk-informed mitigation measures in LH_2 storage systems. The use of LH_2 presents advantages over GH_2 in terms of storage volume, as it is significantly more energetically dense than its gaseous counterpart. LH_2 storage systems must also consider unique risks related to damages and injuries caused by unsafe releases of liquid hydrogen at cryogenic temperatures (-243°C) [7]. However, the behavior of LH_2 releases and dispersion is not well known and limits the widespread use of the fuel.

QRAs are used to identify and prioritize which risks need to be reduced to reach the accepted levels and to develop specific provisions of *NFPA 2* and *ISO 19880-1* [4]. The use of QRA also allows a comprehensive assessment of alternative risk mitigation measures tailored to specific station designs. In [7], Moradi & Groth highlight challenges and research gaps present in risk and reliability analysis of hydrogen systems. Lack of

cohesive databases of hydrogen-specific degradation, failure, and accident data is recognized as one of the biggest hindrances to credible QRAs. A systematic collection of various data types such as the ones described in Figure 1-1 [7] is needed to overcome this limitation. The use of contextual information enriches the risk assessment of relevant hazards, adding to a systematic analysis of the system's configuration, event frequency, and accident scenario consequence. This allows a more realistic portrayal of the risks present in the system, both structural and contextual-wise.

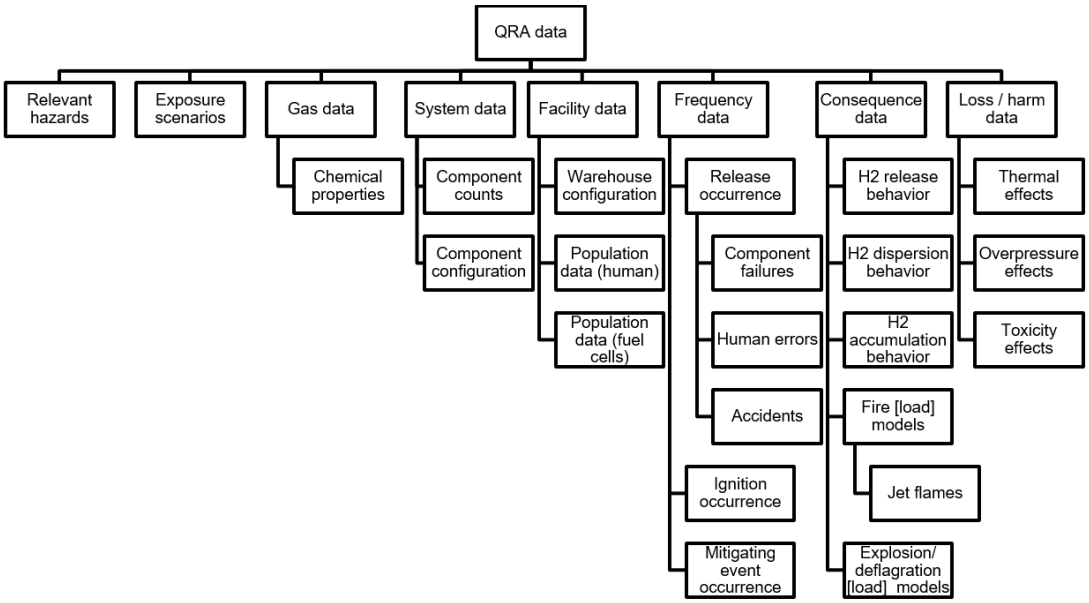

Figure 1-1: Types of data needed to perform QRA for a hydrogen system. Moradi and Groth (2019).

Standards for hydrogen fueling stations have been developed mostly based on modern integrated risk assessment techniques which consider three core elements 1) different contexts and infrastructure involved, 2) the probability of system failures, leaks, and ignition, and 3) the physical behavior of hydrogen releases, accumulation, and combustion. The Hydrogen Risk Assessment Model (HyRAM) is a compendium QRA tool containing both probabilistic information and deterministic models to simulate GH_2 releases, thermal and pressure effects of resulting deflagrations, detonations, and jet fires

[16]. HyRAM calculates risk metrics based on the structural description of the system and other contextual information, such as the presence of people on the premises, aiding and accelerating the process of risk analysis. Initial versions of HyRAM were gas-specific [17]–[19]. Recently, the HyRAM tool was expanded to include deterministic physical models of LH_2 behavior [20]. However, HyRAM 3.0 still needs new probabilistic data and models for hazards and failure scenarios specific to LH_2 systems. Given the current limitations of public hydrogen failure data, the continued use of GH_2-based data in risk assessments for future stations with LH_2 storage might lead to unrepresentative risk values, inadequate prevention and mitigation measures, and undesirable new accident scenarios. Consequently, there is a clear need for new probabilistic data to represent the new conditions present in LH_2 systems. In addition, there is an opportunity to explore how new data types and techniques used in other areas of reliability engineering can be further used within hydrogen codes and standards development.

Recent advances in Condition-Based Maintenance (CBM) and Prognosis and Health Management (PHM) may have benefits for hydrogen QRA. PHM is an important component in modern engineering systems, in which algorithms are designed and used to detect anomalies, diagnose faults, and predict future states of the system. These methods diverge from traditional probability theory-based reliability analysis to model the life cycle of the studied system, enabling real-time health assessment under its actual operating conditions [21]. PHM is an extension of CBM decision-making frameworks, combining various research disciplines, computational methods, and data sources to enable a system's health-state prognosis. In the past decades, there has been a proliferation of different approaches for this purpose, in part driven by the development of Machine Learning (ML)

and Deep Learning (DL) applications for data analysis. These data-driven approaches have made data collection and analytics within diagnostic technologies essential components and high-priority research topics [22]. Figure 1-2 shows the number of journal publications referring to PHM applications in the last decade [23].

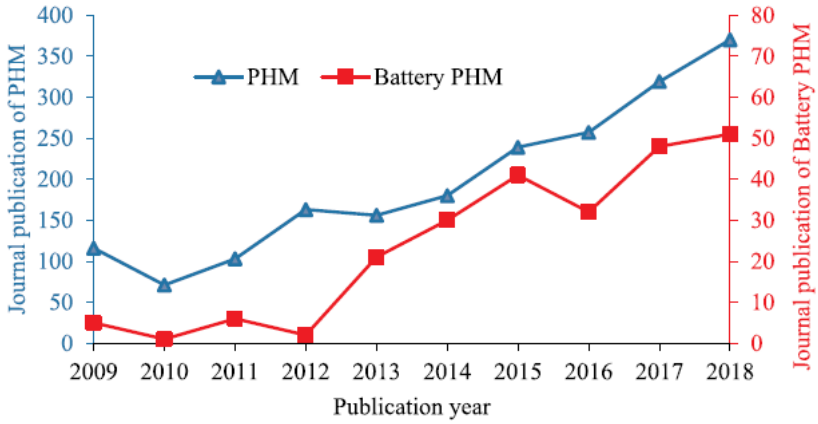

Figure 1-2: Number of journal publications on PHM in Web of Science. Meng and Li (2019).

Applications in engineering systems frequently focus on estimating the Remaining Useful Life (RUL) of a component or a system. This, to opportunely schedule maintenance activities with minimum impact on the system's availability and reduce operational costs. Common applications explore mechanical and electrical failure phenomena, such as lithium-ion battery degradation [23] and crack propagation [24]. Up to date, PHM research related to hydrogen has focused solely on fuel cells [25].

1.2. Objectives & Approach

The purpose of this research is to explore the suitability of new methods from reliability engineering to enhance risk assessment and safety codes and standards for LH_2 storage systems. This includes identifying existing data sources, conducting QRA on a

generic station, and creating a risk-informed conceptual PHM framework for an LH_2 on-site storage system.

To achieve this, the research involves three main objectives:

1. Identify hazards and risk scenarios for a generic design and site layout for a hydrogen fueling station equipped with bulk LH_2 storage for use in QRA and reliability modeling.
2. Apply QRA methods to the selected design to determine and model risk scenarios and associated data requirements for credible risk assessments of LH_2 storage systems.
3. Identify condition-monitoring data sources and design the concept of a PHM-based framework for safety and risk assessment of a LH_2 storage system.

The development of this thesis has been organized under three tasks contributing to the conceptual development of a PHM algorithm for a LH_2-based fueling station system. These are graphically represented in Figure 1-3 and described as follows.

1.2.1. Task 1: LH_2 Storage System Risk Scenario Identification

Task 1 refers to the hydrogen station design selection, familiarization, analysis, and risk scenario identification for unsafe hydrogen releases. To select the system's layout, meetings were conducted with external experts in hydrogen station designs. Several teleconferences were held with external partners from private industry and U.S. Department of Energy (DOE) national labs to identify important elements of designs for use in this research. Relevant documentation of hydrogen fueling station designs were reviewed and considered for the generic layout design. After the selection of the bulk LH_2

storage system as the subsystem of interest, a qualitative risk screening was conducted through a Failure Mode and Effects Analysis (FMEA). The LH_2 storage system was decomposed into functional sections and through a probability and severity classification, the failure modes and resulting scenarios which represent the highest risk in the system were identified.

1.2.2. Task 2: Failure Data Collection and Quantification in LH_2 Systems

Task 2 refers to the reliability quantification of the selected LH_2 station design. This task aims to characterize data availability and requirements for risk and reliability assessments of LH_2 systems. First, the work is focused on identifying the available data sources related to frequency analysis in QRAs for LH_2 systems. Through a literature survey of relevant QRAs developed in the hydrogen context, common logic-modeling tools and databases are identified. Following this, the design's reliability quantification is addressed. The modeling of the system's failure logic is carried out through Event Sequence Diagrams (ESD) developed for the high-risk scenarios identified through the FMEA process, and Fault Tree Analysis (FTA) are utilized to determine the frequency of LH_2 releases. Considering the current data limitations, future data collection tasks are proposed.

1.2.3. Task 3: LH_2 Storage PHM Framework Concept Design

Task 3 refers to an early development of the PHM framework oriented towards risk assessment applications in LH_2 systems. For this, based on relevant literature and applications in similar engineering systems, condition-monitoring data sources for PHM frameworks in LH_2 systems are identified and documented. An outline of the design stages of a data-driven framework is described in terms of data requirements, possible techniques, and integration schemes. Methods are proposed to integrate PHM tools to risk analysis

processes for these systems, i.e., what engineering decisions can be informed through these tools.

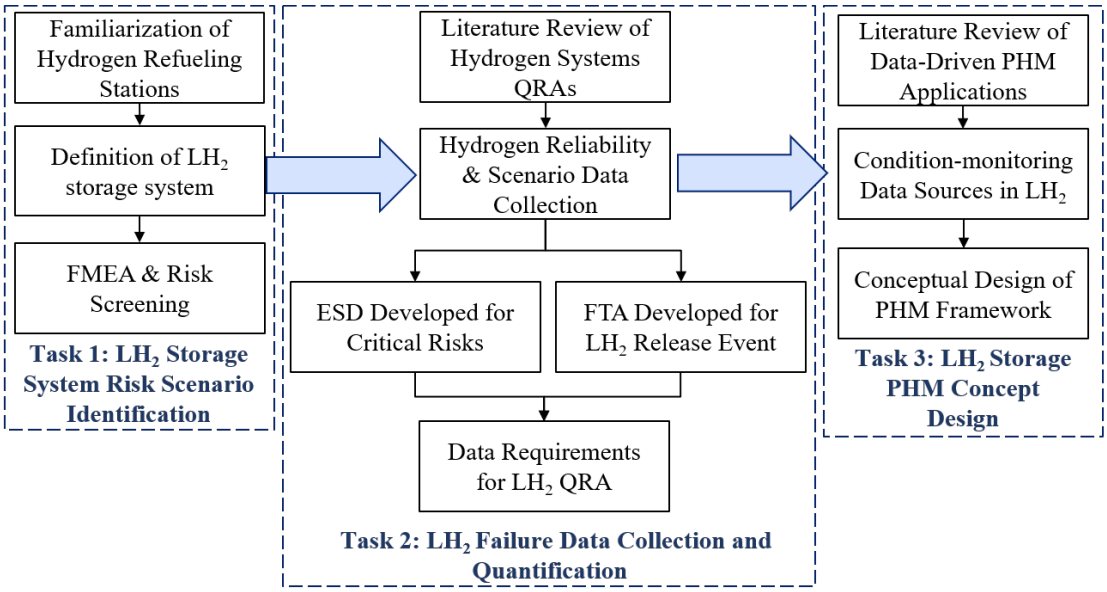

Figure 1-3: Overview of thesis methodology.

1.3. Thesis Outline

The remainder of this thesis is organized as follows. Chapter 2 provides the background of this work, including a review of related published literature encompassing risk assessments in hydrogen systems and an overview of PHM frameworks. Chapter 3 presents the development of Task 1, based on the analysis of failure modes identified in a LH_2 storage system. Chapter 4 presents the main results of Task 2, focusing on the discussion on the data requirements to improve QRA. Chapter 5 presents the conceptual development of the PHM framework described in Task 3 based on related published literature and case studies. Chapter 6 concludes this thesis with a summary and discussion of the completed work, the limitations of the presented analysis, and suggestions regarding future work.

Chapter 2. Background and Literature Review

In this chapter a review of three relevant topics for the development of the thesis are presented. The first is a technical background on hydrogen fueling stations, including important regulating aspects of SCS. The second topic consists of a technical background overview of QRA frameworks and a literature review of QRAs applied to hydrogen systems. Finally, the third topic covered in this chapter is an overview of PHM frameworks, including approaches and current challenges.

2.1. Hydrogen Fueling Stations

Hydrogen fueling stations are a critical distribution infrastructure for the deployment and market participation of hydrogen-powered vehicles, both FCEV and hydrogen internal combustion engine vehicles (HICE) [1]. Hydrogen station designs vary depending mainly on storage type and capacity, as well as the source of hydrogen. In terms of infrastructure, major differences are found whether hydrogen is obtained on-site or delivered to the site [26]. The main components that can be found in a hydrogen fueling station are shown in Figure 2-1. A generic hydrogen station can be characterized through the following elements:

- The source of hydrogen fuel can vary whether it is produced on-site or off-site and then delivered to the fueling site through pipelines, road or rail tanker, or ships. This can occur for both gaseous and liquid hydrogen.
- Hydrogen storage units, such as bulk liquid hydrogen reservoir tanks (if delivered as liquid), bulk low-pressure hydrogen storage tanks (if delivered as a compressed

gas or after conversion of liquid to gas), and high-pressure cascade GH_2 hydrogen storage tanks (at dispensing pressures).

- A compressor stage or air booster for high-pressure storage of compressed hydrogen, typically to above 35 or 70 MPa (350-700 bar).
- Heat exchangers operating for both the controlled evaporation of liquid hydrogen prior to the compressor stage and the cooling of hydrogen gas during fueling.
- Dispensers for filling on-board high-pressure hydrogen tanks on FCEV, usually with 35 or 70 MPa (350-700 bar) nozzles. This allows drivers of FCEV to refuel their tanks in about the same time as for gasoline vehicles, that is, in three to five minutes.
- A control system that allows the controlled flow of hydrogen through the liquid and gaseous phases of the system. This includes emergency shut-off systems and hydrogen gas detection systems.

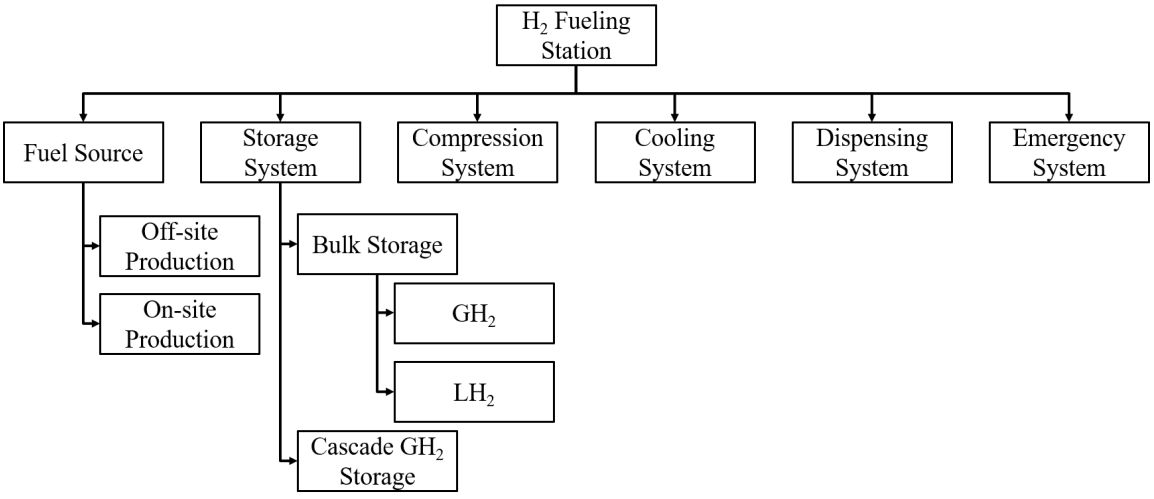

Figure 2-1: Block diagram of a hydrogen fueling station.

By 2013 there were 224 operating hydrogen fueling stations distributed in twenty-eight countries: 43% located in North and South America, 34% in Europe, and 23% in Asia. The countries which led in number of hydrogen stations were the USA, Japan, Germany, and South Korea. Around 49% of the stations produced hydrogen on-site, while 26% had the fuel delivered from off-site production sites [1]. According to the U.S DOE's Alternative Fuels Data Center (AFDC), there are currently fifty-one operational retail stations in the country [27].

2.1.1. Hydrogen Safety Codes and Standards

SCS are developed and used to ensure and promote safety, functionality, efficiency, reproducibility, and comparability in both design and operation for a wide variety of engineered systems. For systems whose operation exposes users and neighboring facilities to certain hazards, permitting processes require the demonstration that the proposed designs meet safety requirements, frequently relying on SCS as evidence of compliance and safety [28]. In the U.S., The National Fire Protection Association (NFPA), American Society of Mechanical Engineers (ASME), Compressed Gas Association (CGA), International Organization for Standardization (ISO), among others, are commonly used to guide and permit hydrogen infrastructure designs.

Risk acceptance criteria vary between SCS and the methods each code uses to estimate and obtain risk values. These also vary depending on contextual information particular to each station or based on determined performance criteria (such as the *NFPA 2*). Currently, SCS for hydrogen facilities specify that these designs should include certain safety features, comply with material requirements, and maintain specific maintenance, operational, and site characteristics. One important requirement is for minimum separation

distances. These safety distances are defined as the minimum setback distances from neighboring infrastructure from hydrogen systems and usually depend on the amount of hydrogen stored or used in the location and its likelihood of resulting in a hazardous condition. However, these requirements are based on generic designs and may not apply to other stations, as risks and mitigation measures inherently depend on hazards specific to a station's location, design, and operation. A significant step towards modernizing and developing comprehensive SCS is the inclusion of risk-related concepts [6]. For instance, the *ISO 19880-1 Hydrogen Fueling Station and Vehicle Interface Technical Specification (2016)* establishes the individual risk limit of $10^{-6}yr^{-1}$ for vulnerable external populations to the hydrogen fueling stations, while this value reduces to $10^{-4}yr^{-1}$ for hydrogen fueling station workers [5]. For this reason, it is important to develop and harmonize the technical bases for risk mitigation measures. These could then be applied without relying on expert opinion for their application in specific designs which differ from those described in the SCS [6], [12].

2.1.1.1. NFPA 2 Hydrogen Technologies Code

In 2006, the NFPA created the Technical Committee on Hydrogen Technology to develop a comprehensive document establishing the requirements for hydrogen technologies. The *NFPA 2* [4] code addressed aspects of hydrogen storage, use, and handling, and it is built upon existing NFPA codes (e.g. *NFPA 52*, *NFPA 55* and *NFPA 853*). With each revision of the standards, efforts have led to the incorporation of hydrogen-specific requirements for both GH_2 and LH_2 systems.

The *NFPA 2* code contains definitions and descriptions of general fire safety and hydrogen requirements, as well as specific standards for fueling facilities, generation

systems, fuel cell power applications, combustion applications, laboratory operations, and parking and repair garages, among others. Compliance with the code can be obtained under two different options: prescriptive-based or performance-based. For the latter, the code allows the calculation of safety measures, such as separation distances, based on performance criteria. This safety-oriented design is based on the hydrogen station's performance in the case of a select number of risk scenarios. The minimum design scenarios that must be considered for permitting process are presented in Table 2-1. As stated in the *NFPA 2* code [4]: "*Each design scenario used in the performance-based design proposal shall be translated into input data specifications, as appropriate for the calculation method or model".* A description of required performance criteria from the *NFPA 2* code is presented in Table 2-2. It should be noted that none of the scenarios nor criteria explicitly refer to risks present in LH_2-based fueling station.

Table 2-1: NFPA 2 Performance-Based Option Required Design Scenarios.

Design Scenario	**Description [NFPA 2: 5.4 Section]**
Fire Scenario	Performance-based building design for life safety affecting the egress system shall be in accordance with this code and the requirements of the adopted building code.
Explosion Scenario 1	Hydrogen pressure vessel burst scenario shall be the prevention or mitigation of a ruptured hydrogen pressure vessel.
Explosion Scenario 2	Hydrogen deflagration shall be the deflagration of a hydrogen-air or hydrogen-oxidant mixture within an enclosure such as a room or within large process equipment containing hydrogen.
Explosion Scenario 3	Hydrogen detonation shall be the detonation of a hydrogen-air or hydrogen-oxidant mixture within an enclosure such as a room or process vessel or within piping containing hydrogen
Hazardous Material Scenario 1	Unauthorized release of hazardous materials from a single control area.
Hazardous Material Scenario 2	Exposure fire on a location where hazardous materials are stored, used, handled, or dispensed.
Hazardous Material Scenario 3	Application of an external factor to the hazardous material that is likely to result in a fire, explosion, toxic release, or other unsafe condition.
Hazardous Material Scenario 4	Unauthorized discharge with each protection system independently rendered ineffective.

Table 2-2: NFPA 2 Performance-Based Option Criteria Requirements.

Criteria Type	Description [NFPA 2: 5.2 Section]
Fire Conditions	No occupant who is not intimate with ignition shall be exposed to instantaneous or cumulative untenable conditions.
Explosion Conditions	The facility design shall provide an acceptable level of safety for occupants and for individuals immediately adjacent to the property from the effects of unintentional detonation or deflagration.
Hazardous Materials Exposure	The facility design shall provide an acceptable level of safety for occupants and for individuals immediately adjacent to the property from the effects of an unauthorized release of hazardous materials or the unintentional reaction of hazardous materials to cryogenic hydrogen or precooled hydrogen at the dispenser is established for this analysis.
Property Protection	The facility design shall limit the effects of all required design scenarios from causing an unacceptable level of property damage.
Occupant Protection from Untenable Conditions	Means shall be provided to evacuate, relocate, or defend in place occupants not intimate with ignition for sufficient time so that they are not exposed to instantaneous or cumulative untenable conditions from smoke, heat, or flames.
Emergency Responder Protection	Buildings shall be designed and constructed to reasonably prevent structural failure under fire conditions for sufficient time to enable fire fighters and emergency responders to conduct search and rescue operations.
Occupant Protection from Structural Failure	Buildings shall be designed and constructed to reasonably prevent structural failure under fire conditions for sufficient time to protect the occupants.

An important concept for compliance under the performance-based option is equivalency, under which risk mitigation measures not considered explicitly in the *NFPA 2* are incorporated into permitting hydrogen fueling station designs. Equivalency is defined in *NFPA 2* Section 1.5 as: *"Nothing in the* NFPA 2 *code is intended to prevent the use of systems, methods, or devices of equivalent or superior quality, strength, fire resistance, effectiveness, durability, and safety over those prescribed by this code. Technical documentation shall be submitted to the AHJ*[2] *to demonstrate equivalency. The system, method, or device shall be approved for the intended purpose by the AHJ"*[4].

[2] AHJ is defined as an organization, office, or individual responsible for enforcing the requirements of a code or standard, or for approving equipment, materials, an installation, or a procedure [4].

In 2014 the *NFPA 2* and *NFPA 55* Technical Committees established a task group to develop separation distances for bulk LH_2 storage based on a risk-informed methodology parallel to the process used in the previous update of the gaseous requirements. A QRA procedure was used to evaluate the risk from unintended releases of hydrogen to identify and quantify scenarios, risk contributors, and potential accident prevention and mitigation strategies for risk reduction under acceptable levels [6]. *NFPA 2* code utilizes risk insights obtained from QRA combined with deterministic analysis of accident scenarios, frequency of leakage events, and use of safety factors to account for uncertainties in data, methods, and scope of the risk evaluation.

The most recent edition of the *NFPA 2* Hydrogen Technologies Code (2020 Edition) incorporates the results of a Hazard and Operability (HAZOP) study developed for a generic hydrogen station with an LH_2 storage system. This design is based on previous work of the CGA *P-28 Risk Management Plan Guidance Document for Bulk Liquid Hydrogen Systems* [29]. This document contained a representative HAZOP which identified various situations where deviations from normal operating parameters could potentially have hazardous consequences. Event likelihood and hazard severity classes were utilized to determine the risk associated with the identified scenarios. Nine possible high-risk failure scenarios were identified to present the highest risk levels, and three of these occur during normal operating conditions of the hydrogen fueling station. These are presented in Table 2-3. It was stated that for further quantification of the presented risks, characterizing pooling and evaporation effects are fundamental steps to effectively model the required safety distances. The complete QRA procedure used for LH_2 systems is currently pending the development of physical models to analyze the consequences

referring to jet and plume behavior (COLDPLUME), as well as multiphase network flow (NETFLOW) under Sandia National Labs.

Table 2-3: NFPA 2 Critical HAZOP Scenarios during normal system operation.

HAZOP Number	HAZOP Description	Modeling Notes (NETFLOW, COLDPLUME)	Separation Distance Driver
2.1	High pressure because of leak in inner vessel allowing hydrogen into the vacuum area.	Characterize flow out of casing vent.	Modeling results of hydrogen concentration plume and heat flux from subsequent fire will be used for all other separation distance exposure because this is the highest risk priority during normal operations.
4.15	Loss of containment from pipe leading from tank to vaporizer or vaporizer itself caused by thermal cycles or ice falling from vaporizers.	Characterize temperature and concentrations from the releases to the air. Model is needed to characterize pooling and evaporation effects.	
6.15	Misdirected flow caused by operator error resulting in large low-level release of cold gaseous hydrogen through bottom drain valve of vent stack during normal tank venting process.	Quantify gas flow through drain vent and vent stack. Characterize temperature and concentrations from the releases to the air. Model is needed to characterize pooling and evaporation effects.	

Additional to the material and procedural requirements for hydrogen fueling station designs, there also are requirements for hydrogen monitoring systems. In *NFPA 2* these refer to gas detectors set to detect gas at a limit lower than the 4 vol % lower hydrogen flammable limit. The location and number of sensors required depend on the design and must ensure effective hydrogen detection. No other sensors are explicitly mentioned in the code regarding their use as risk mitigation or failure detection measures. This represents a major gap to transition towards comprehensive risk-informed standards and proactive health management in hydrogen systems.

2.1.1.2. CGA Standards for Hydrogen Systems

The CGA is a member and an accredited standard developer of the American National Standards Institute (ANSI) [30]. Codes related to hydrogen technology focus on

guidelines and standards for shipping, storage, and filling systems used in hydrogen fuel technologies. Some of the relevant codes are briefly described in this section concerning possible condition-monitoring data and risk scenario identification.

The *H-5 Standard for Bulk Hydrogen Supply Systems* contains minimum requirements for location and equipment selection, installation, startup, maintenance, and the removal of bulk hydrogen supply systems. This document covers both GH_2 and LH_2 bulk systems, as well as discussing health hazards and safety considerations [31]. Regarding monitoring and maintenance activities, the CGA *H-5* standard recommends the temperature monitoring in the intermediate section and discharge line of the cryogenic pump. Cavitation can be identified through motor current amperage sensors or temperature sensing devices on the pump discharge line. Additionally, maintenance and inspection activities should be performed annually. This includes inspection for physical damage, leak tightness, ground system integrity, vent system operation, equipment identification, warning signs, operator information and training records, scheduled maintenance and retest records, alarm operation and other safety-related features. Finally, scheduled maintenance and retest activities shall be formally documented, and records shall be maintained for a minimum of three years.

The *H-3 Standard for Cryogenic Hydrogen Storage* contains the suggested minimum design and performance requirements for shop-fabricated, vacuum-insulated cryogenic tanks intended for above ground storage of LH_2. These standards apply to LH_2 storage tanks with maximum allowable working pressures (MAWP) up to 1210 kPa (175 psi). Tanks less than 3785 L (1,000 gal) gross volume or greater than 94,600 L (25,000 gal) gross volume and all transportable containers are excluded. Tanks outside these pressure

and volume constraints may also meet the requirements of this standard when agreed upon by the purchaser/manufacturer and the AHJ [32]. Regarding monitoring and testing procedures, the CGA *H-3* standard recommends that in vacuum-insulated vessels, absolute pressure measurements in annular space should be continuously monitored. Identification criteria of loss of vacuum also includes monitoring temperature difference between the outer jacket and ambient temperature, inner vessel pressure, condensation of ice on the outer vessel, and unusual venting indicated by frost or condensate on the vent stack. Further, external piping should be installed together with instrumentation rated for warm and cold operation, and special considerations should be taken to account for hidden failures of these. Finally, vacuum integrity testing should include warm and cold vacuum retention test. Temperature and vacuum pressure should be recorded at least twice daily for seventy-two hours and compared to the fluctuations accepted by the specific design.

These standards recommend specific monitoring, testing and maintenance policies highly relevant for the operation of LH_2 systems. This includes the use of pressure, temperature, and current amperage to detect anomalous behavior in the main components of these systems. Hence, stations designed considering these guidelines are expected to have access to this kind of monitoring data and thus, could explore the use of data-driven models for safety and reliability management. When combined with the maintenance records, these data sources can potentially be used to reduce the number of unscheduled maintenance events.

2.2. Quantitative Risk Assessment

A Quantitative Risk Assessment (QRA) is a valuable tool for determining the risk of the use, handling, transport, and storage of dangerous substances. QRAs are used to

demonstrate the risk caused by an activity and to provide the competent authorities with relevant information to enable decisions on the acceptability of risk related to developments on-site, or around the establishment or transport route [33].

QRA frameworks consists of several stages including hazard scenario identification and development, frequency data quantification and consequence modeling, leading to risk characterization. For the results of a QRA to be integrated into a decision-making process, these need to be verifiable, reproducible, and comparable. In the context of dangerous substances, the information recollection needed to develop a complete QRA varies from technical information such as scenario and event probabilities, release, dispersion and harm models for hazard exposure to policy and decision-making procedures. A brief technical description of risk concepts and modeling procedures are provided in this section.

2.2.1. Risk Technical Background

Traditional risk assessment techniques have been used to assess hydrogen infrastructure safety. To adequately frame the context of this project a brief definition of risk and reliability-related terms is presented [34].

Risk analysis formally involves three stages: assessment, management, and communication. The risk assessment stage is a process used to identify and characterize risk in a system, involving the quantification of the likelihood of an event occurring and the severity of its consequences. Risk management involves the evaluation and control of each of the risk contributors identified. Finally, risk communication addresses how both risk assessment and management aspects are shared and discussed with the system's stakeholders and the public. The assessment stage is conceptually addressed in this thesis.

Risk is formally characterized by a set of hazard exposure scenarios (i), consequences associated with each scenario (c_i), and the probability of occurrence of these consequences (p_i). A common expression used to calculate risk therefore is:

$$R = \sum_{i=1}^{n} p_i \times c_i \tag{1}$$

which represents the total risk contributed by each of the n hazard exposure scenarios identified in the system under study. A hazard or accident scenario may be a single or a combination of hazardous events, defined as an unplanned event or sequence of events which start with an initiating event that result in undesirable consequences [35].

To identify and describe hazardous scenarios, techniques such as Failure Mode and Effects Analysis (FMEA) and Hazard and Operability Analysis (HAZOP) are used. On the one hand, FMEA is an inductive technique for reliability analysis which can be used in both the design and implementation stages of a system or a project. It aims to describe the inherent causes that lead to a system failure, determine the consequences of said failures and the methods to detect and minimize the occurrences of hazardous events. On the other hand, HAZOP studies analyze the significance of hazardous situations associated with a process or activity. This methodology uses qualitative techniques to pinpoint weakness in the design and operation of facilities that could lead to accidents [35].

The probability of occurrence of an event can be expressed as a frequency over a duration of time. Initiating events, in the context of engineered systems, generally refer to the failure of a component, given an internal malfunction, external accident, or a combination of both. Reliability refers to the probability that a component or system can perform its intended function at a given prescribed time. Through the mathematical

background of probability and statistics theories, data-based prognostic tasks and maintenance-scheduling procedures are performed. Frequentist approaches can be applied when there is sufficient historical data related to failure or maintenance events to determine the time-to-failure of a system or component. Statistical data analysis procedures allow the use of parametric or non-parametric models to determine the occurrence of future events. Bayesian approaches allow the analysis of systems and situations which have few recorded data to support prognostics tasks. The techniques derived from Bayesian probability theory allow the combination of different data sources in parametric models, as well as updating these models based on new information.

To determine the frequency of occurrence of an event, the operational logic of the system and the physical or operational barriers which protect against hazard exposures must be considered. Logic-modeling tools such as Event Tree Analysis (ETA) and Fault Tree Analysis (FTA) are used for this purpose. ETAs are an inductive process that provides a systematic method of recording the accident sequences between the initiating events and subsequent events that can result in hazards exposure. Events can be ordered by chronological or causal order, and the sequence is characterized by the probability of occurrence of each event [35]. Event Sequence Diagrams (ESDs) are graphical, logically equivalent tools which aid the formal development of Event Trees (ETs). These diagrams are used to represent a sequence of pivotal events stemming from a common initiating event and leading to different end-states. The quantification of ETs and ESDs allow the estimation of each outcome's frequency based on the initiating event's frequency.

Given the complexity of an initiating or pivotal event, FTAs can be used to obtain their probability of occurrence. This is a deductive process that provides a method to

identify the cause or combination of causes that can lead to the top event and quantify the probability of this event's occurrence. The smallest set of event combinations that lead to the top failure event is called minimal cut-set. Based on component reliability data, the failure probability of a system can be determined and used to characterize an initiating or intermediate event in ETAs and ESDs.

2.2.2. General QRA Framework

The general main steps of a QRA framework are presented in Figure 2-2 [33]. This process begins with defining the scope of the analysis, in this case, oriented towards verifying the code-compliance of a design. Then, the system under study must be described in depth, clearly defining components, system boundaries, and functional logic under normal operational conditions.

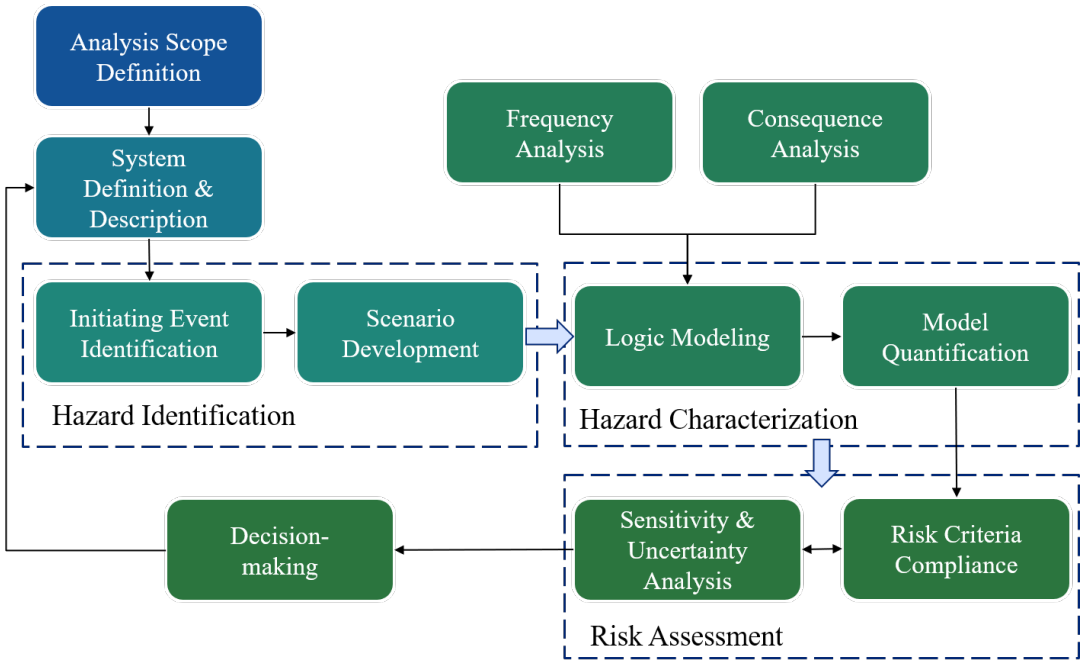

Figure 2-2: General QRA Framework Outline.

Based on the technical knowledge of this type of system, the potential hazards must be identified and characterized. Exposure to hazards is caused by a sequence of incidents

which begin with an initiating event and then develop into particular accident scenarios. These accident scenarios are represented through logic-modeling tools regarding the likelihood of occurrence (frequencies and probabilities) and the consequence of hazard exposure (simulation, experimental or empirical models). To fully characterize these hazards and each risk-contributing factor, various types of data are needed to quantify the logic models as discussed in Figure 1-1. The end-value of risk associated with the defined system must then be compared to thresholds given by formal SCS or societal guidelines. Sensibility and uncertainty analysis are employed to construct robust risk assessments. If the resulting risk is deemed not tolerable, the system's design, prevention and mitigation barriers must be modified to reduce the effect of the most prominent risk contributor, and then re-evaluated.

Risk assessment and mitigation procedures often require the participation of groups of experts and access to detailed technical information. However, the QRA framework is adaptable to the level of complexity required. For an initial screening, qualitative techniques such as FMEA and HAZOP are used to help identify potential safety hazards and determine necessary prevention and mitigation features. Following the high-risk event identification and scenario development, either quantitative or qualitative severity and probability classifications are employed to characterize risk. Frequently, tools such as ETA and FTA are used to model the failure logic of the system and correlation harm models are employed to determine the expected damage from hazard exposure. This categorization of risk can be communicated through risk matrices, a useful method to prioritize which hazardous scenarios need to be addressed to comply with the acceptance criteria. The

scenarios which represent the highest risk levels can be further quantified in depth to further develop full QRAs to aid design and permitting-related decision-making.

2.3. Risk Assessments of Hydrogen Systems

From a safety and risk assessment perspective, hydrogen systems are of particular interest given the intrinsic hazard related to the stored substance and resulting release conditions under failure scenarios. Location options for hydrogen fueling stations are limited in urban areas due to the minimum separation distances required between hydrogen storage systems and various components that represent risk hazards. These safety distances are required to maintain an acceptable level of risk associated with the use, storage, and handling of this alternative fuel. Hydrogen hazards caused by undesired GH_2 releases include leakage, fire, deflagration, and explosion [36]. The main hazard associated with GH_2 infrastructure is the uncontrolled accumulation in confined spaces that allow delayed ignition events [37]. In contrast, stations with LH_2 systems have the most serious potential failures due to factors such as collisions, overfilling tanks, and pressure relief valve venting [38]. Storage tanks, pipelines, pumps and dispensers are faced with pressure and thermal cyclical stresses which can lead to hydrogen releases in either liquid or gaseous states [39]. The use of LH_2 must also consider hazards related to unsafe releases of cryogenic liquid hydrogen, leading to either GH_2-related risks or to cryogenic temperature-induced damages [40].

In the past few years, a growing number of works regarding hydrogen system safety have been published, pushed by the development of new technologies and the growing pressure to fin viable alternatives to decarbonize energy and transport sectors. FMEA and HAZOP studies are frequent tools used to complement and enrich QRA procedures in

hydrogen station designs [14], [41]–[44]. Generally, major hazards are described, as well as modifications in the design implemented to reduce the overall risk. However, most of these works are based on risk assessments developed over a decade ago, as are the first approaches to risk-inform hydrogen SCS. Therefore, a literature review covering relevant QRA applications developed for hydrogen systems is presented in this section. Finally, the effort to build user-friendly software tools and facilitate the use of risk assessment methodologies have led to the development of tools such as Sandia National Laboratory's HyRAM discussed in Section 2.3.1.

2.3.1. QRA-based Hydrogen Risk Assessment Model Software

The HyRAM tool was developed in Sandia National Laboratories with the purpose of aiding decision-makers in the hydrogen community as well as enabling access to current models and frameworks necessary for fast and efficient QRA in hydrogen systems [16]. The graphical representation of this QRA framework developed for HyRAM is presented in Figure 2-3.

This flexible platform allows the estimation of the number and type of hydrogen release events per year depending on the specific design of a hydrogen fueling station while also enabling fast physics-based analysis of hydrogen releases [16]. In the latest version released in September 2020, the HyRAM tool has incorporated LH_2 properties, release and dispersion models, as well as updated the available leak frequency values [20]. HyRAM was initially developed based on gaseous-specific hydrogen data [16]. Based on hydrogen behavior and harm models, as well as leak event probability distributions for different components found in generic hydrogen fueling station designs, this framework can be used

to characterize the main risk scenarios expected following an unintended GH_2 release shown in Figure 2-4.

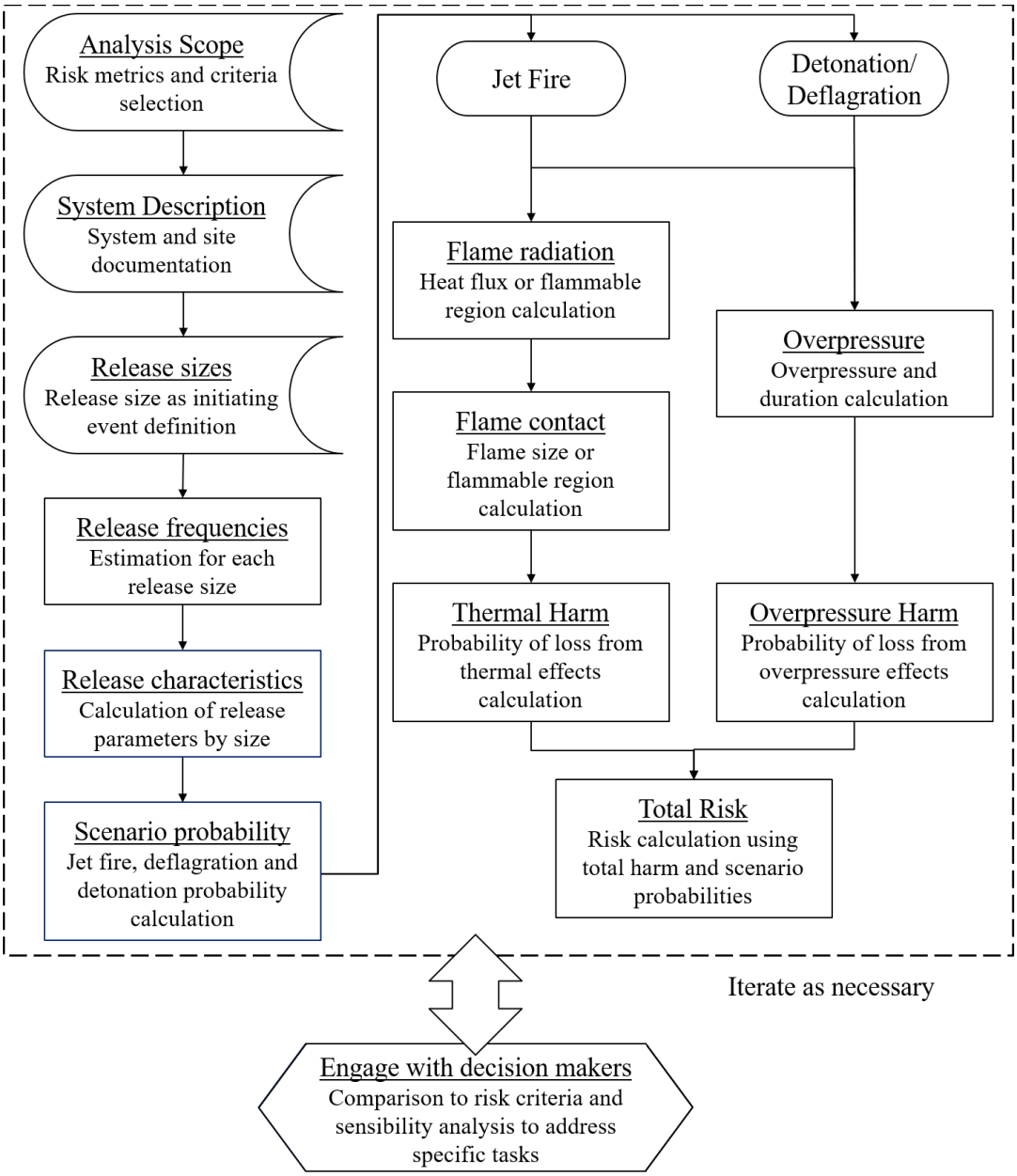

Figure 2-3: Summary of QRA methodology implemented in HyRAM. Groth and Hecht (2017).

The transitions between events following a GH_2 release are characterized by probabilities of detection and isolation, immediate or delayed ignition, and whether thermal or pressure effects dominate the specific scenario. A description and the values used to

quantify these frequency and probability-related events are presented in Annex D.1. The three main scenarios which represent the highest consequences are described in Table 2-4 [45]. Each of these scenarios have been modeled with experimentally-validated thermal and pressure effects expressions to obtain valuable risk metrics in terms of personnel injuries, fatalities, and infrastructure damage consequences.

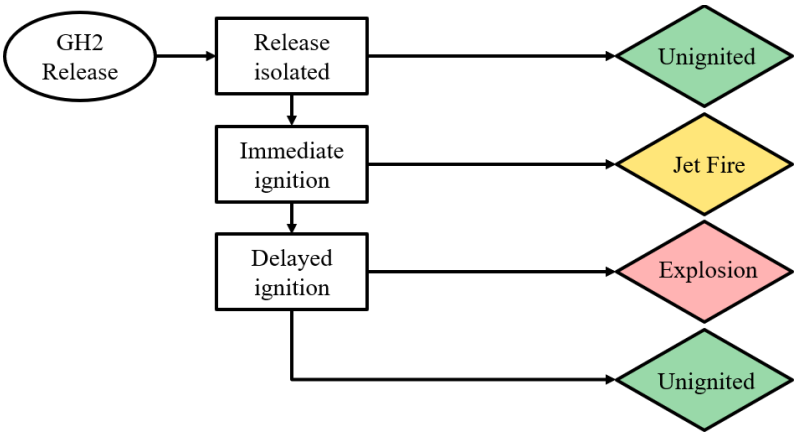

Figure 2-4: Event Sequence Diagram for GH_2 releases in HyRAM 3.0.

Table 2-4: Developed Risk Scenarios in HyRAM 3.0.

Physical Consequences	**Pivotal Events**	**Combustion Description**	**Hazard**
Jet fire	Continuous release (i.e., until H2 supply is exhausted); immediate ignition	A non-premixed turbulent flame, momentum driven. The speed of the combustion is roughly equal to the gas release rate.	Thermal effects
Explosion (Detonation or Deflagration)	Deflagration or detonation of accumulated gas, delayed ignition	Rapid flame propagation in a confined area (detonations also result in a shock wave)	Thermal and Overpressure effects

Several publications in recent years related to risk assessment in hydrogen systems have utilized either the leakage frequency database or the physics module provided by HyRAM. Together with the original publication describing this framework [16], LaFleur, Muna & Groth demonstrated its capacity to aid performance-based permitting of hydrogen fueling stations [14]. In this work, a methodology for assessing a hydrogen fueling station

design which does not comply with specific prescriptive separation distances is presented. As mentioned in Section 2.1.1.1, compliance through a performance-based design implies demonstrating equivalent risk values to those of designs required explicitly by the *NFPA 2* code. Baseline results for a code-compliant generic outdoor GH_2-based fueling station show that HyRAM obtains acceptable risk values for all three scenarios, as expected. Thus, HyRAM software presents an opportunity to simplify QRA of hydrogen fueling stations for performance-based code compliance, delivering a flexible tool for designers and an additional verification tool for decision-makers.

2.3.2. QRA Applications in Gaseous Hydrogen Stations

An early work by Casamirra et al. [46] developed a safety analysis of the design of a high-pressure storage equipment in a GH_2-based fueling station through the integrated use of FMEA, HAZOP and FTA techniques in 2009. Utilizing the risk and reliability tools mentioned, authors obtained a coherent risk analysis of the design based on industrial failure data. As the focus of this work was frequency analysis, consequences are addressed in a qualitative manner. An FMEA was conducted to screen for the most relevant failure modes, assigning a risk priority number (RPN) based on probability and severity classes. Following this analysis, a HAZOP for two top events was developed: hydrogen loss in the environment and overpressure of the storage vessel during the hydrogen filling phase. Finally, an FTA was carried out for the top event referring to the storage vessel overpressure. The fault tree for pressure excess is presented in Figure 2-5 as an example [46]. Further, minimal cut-sets identified in the system are analyzed and it was found that the events that caused the highest unavailability coincide with the elements previously identified with a high RPN.

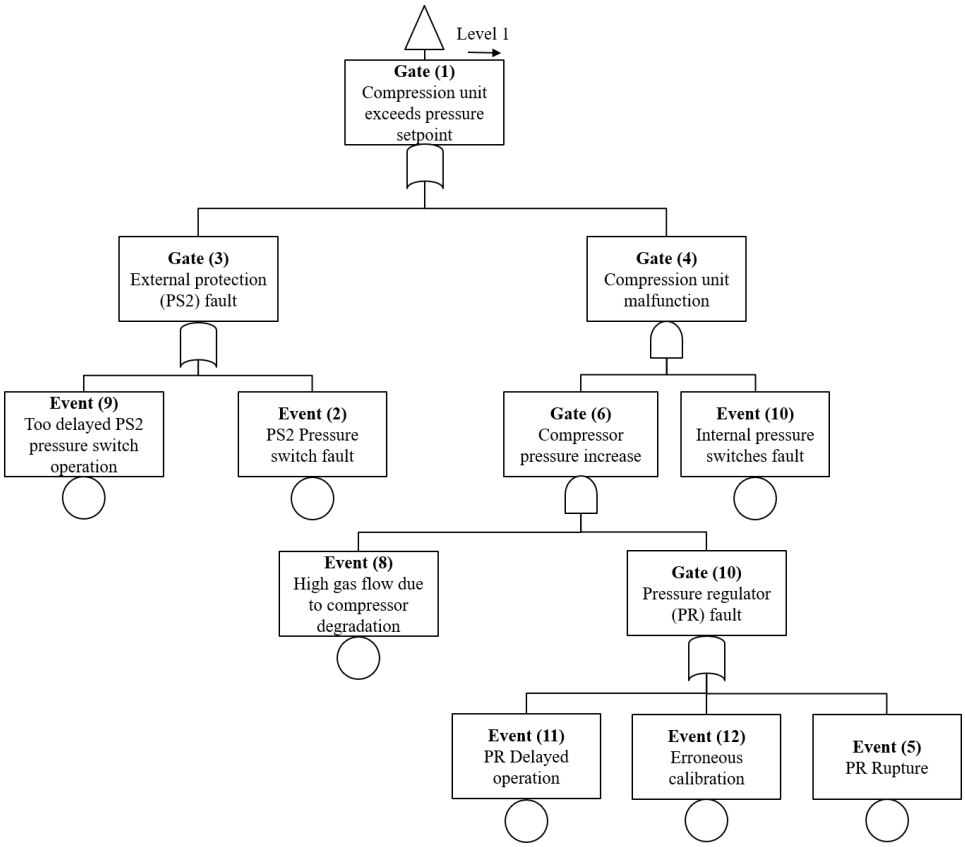

Figure 2-5: Exceeded Pressure Set Point Sub-Fault Tree. Casamirra et al. (2009).

Another relevant work is Kikukawa et al. in 2008 [47], who employed a combination of HAZOP, FMEA and physics-based consequence models for explosions and jet fires following a hydrogen leak. While most of the consequences were successfully estimated through available experimental data, probability data was addressed qualitatively. Hence, the risk assessment was carried out based on the matrix shown in Figure 2-6. This leads to the risk classification of 'High', 'Medium' and 'Low'. As a result, safety measures were suggested to mitigate the identified hazards, including features not available in the market at the time, such as dispenser break-away devices and excess flow valves.

		Probability Level			
Consequence Severity Level		A Improbable	B Remote	C Occasional	D Probable
1	Extremely Severe Damage	H	H	H	H
2	Severe Damage	M	H	H	H
3	Damage	M	M	H	H
4	Limited Damage	L	L	M	H
5	Minor Damage	L	L	L	M

Figure 2-6: Risk Matrix used in Kikukawa et al. (2008).

LaChance et al. (2009) proposed to formally risk-inform the hydrogen fueling station permitting process based on the development of SCS which incorporate risk-informed analysis to establish adequate safety measures [6]. In this context, QRA techniques are presented as robust methodologies to aid this process in identifying and quantifying risk scenarios and contributors, as well as potential prevention and mitigation strategies to reduce risk to acceptable levels. The authors argue this approach can aid AHJ in permitting non-standard facility designs facing important space limitations, such as in urban locations. As part of the U.S. DOE Fuel Cells & Infrastructure Technologies Program, LaChance proposed a QRA-based methodology to identify code requirements, specifically regarding minimum separation distances in a GH_2 -based fueling station [28].

These works are examples of a combination of risk assessment tools based on the identification of possible failure modes present in the design, the development of the hazardous scenarios caused by these, the quantification of the frequency of these occurrences and finally, the ranking of their relative importance. Similar methodologies are presented in several works published in the following years, focused on developing more robust risk assessment procedures, aiding the development of adequate safety regulations, and applying these techniques to specific case studies.

Recently, Gye et al. (2019) [42] conducted a QRA for an GH_2-based fueling station in a highly populated and congested urban area in Seoul. This station is located next to a highway and shares the lot space with a liquefied petroleum gas (LPG) fueling station that operates with delivery from tube-trailers. From a HAZOP study, the risk scenarios chosen to be developed refer to a catastrophic rupture of the tube-trailer and dispenser leakage. Given the station's setting, authors argue that the most relevant consequence is an explosion scenario. Consequences from heat flux and overpressure effects were estimated through *The Purple Book* [33], while frequency analysis was performed using the HyRAM software (See Section 2.3.1) as well as local wind behavior. Their analysis concluded that additional mitigation measures, including physical safety barriers and hydrogen leakage detection systems, are required to be implemented on the compressor and dispenser systems to reduce individual and societal risk levels.

Another example is the research published by Tsunemi et al. (2019), in which three accident scenarios are analyzed in depth: hydrogen leakage events from dispenser external piping, and from the connection piping in the accumulator and compressor [43]. The leakage frequency and consequence effects are estimated from methods and sources similar to the previous works to obtain a spatial distribution of risk in the vicinity of these hazard sources. The novelty of this work is the inclusion of safety barrier failure estimation through the development of specific ETs, as shown in Figure 2-7 [43]. Authors argue that the risk reduction effect of these components may have been overestimated in previous works as their failure probabilities have not been incorporated explicitly.

Similarly, Suzuki et al. (2020) [48] present a QRA for modern Japanese hydrogen fueling station, arguing local regulations were established over a decade ago and recent

technology advances could warrant future modifications. Specific leakage nodes are defined in a general design of GH_2-based fueling station, including the delivery tube-trailer, compressor, piping, storage cylinders, and dispensers. HAZOP and FMEA are employed to determine credible hazards for each node. A piping and instrumentation diagram (P&ID) of the design is presented, enabling a deeper analysis than most of the other published works described above. Frequency analysis is based on ETA, using HyRAM's leak frequency and ignition probability data (See Section 2.3.1). However, the obtained risk contours reveal that unacceptable risk levels are present for personnel and customers inside the station. Further, jet fires were identified as the most significant risk contributor resulting from compressor and dispenser leakage events. Authors argue that unacceptable risk levels are obtained due to conservative assumptions, such as not including safety barriers (e.g., fire walls) in the analysis, as suggested by Tsunemi et al. [43].

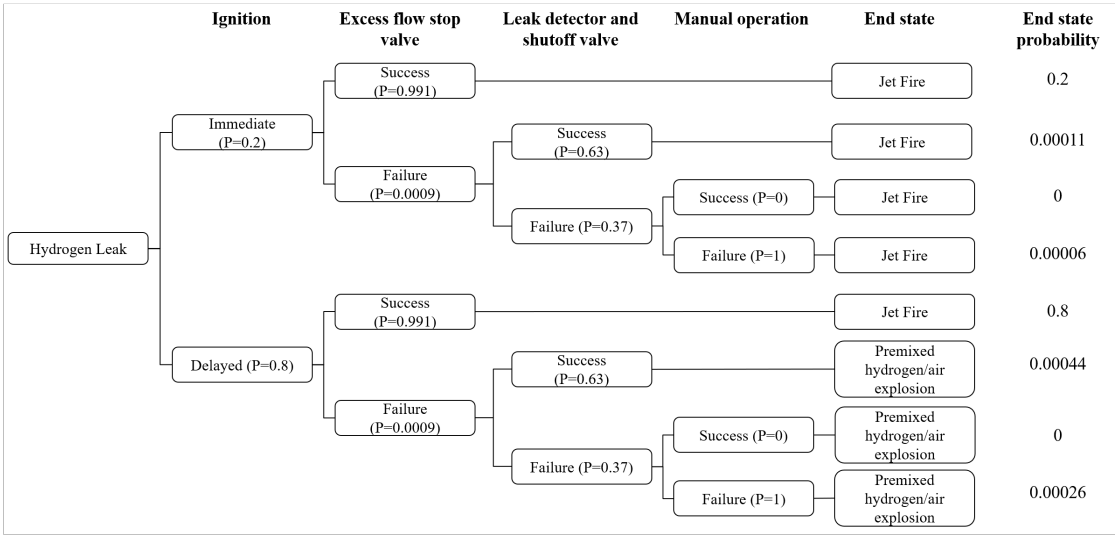

Figure 2-7: Event Tree for Accumulator Connection Piping Hydrogen Leakage. Tsunemi et al. (2019)

Uncertainty analysis in QRAs, such as for values used for frequency of occurrence of the risk scenarios, is still a complex issue in hydrogen systems. For instance, in [49] the frequency analysis phase of the risk assessment is based on a hierarchical Bayesian model.

An existing database including leak frequencies in diverse industries and hydrogen fueling stations was used to determine prior distributions for leakage events. Accident data collected from compressed natural gas stations in the U.S. and gasoline stations in Japan were used as evidence to update the specified priors. Thus, authors estimated the median of posterior leak frequency distribution to represent the accidents' occurrence probability.

Similarly, Kodoth et al. (2020) [50] compared Bayesian and frequentist methods to obtain leak frequency values in hydrogen systems. In [51], a Bayesian Network (BN) model was employed to developed a grid-based risk-screening method for accident scenarios in hydrogen fueling stations with the purpose of explicitly assessing the interaction between different risk factors. In contrast to many cited QRA procedures based on ETAs and FTAs which focus on mayor risk scenarios independently, BNs allow the analysis of fire and explosion scenarios occurring simultaneously as shown in Figure 2-8 [51].

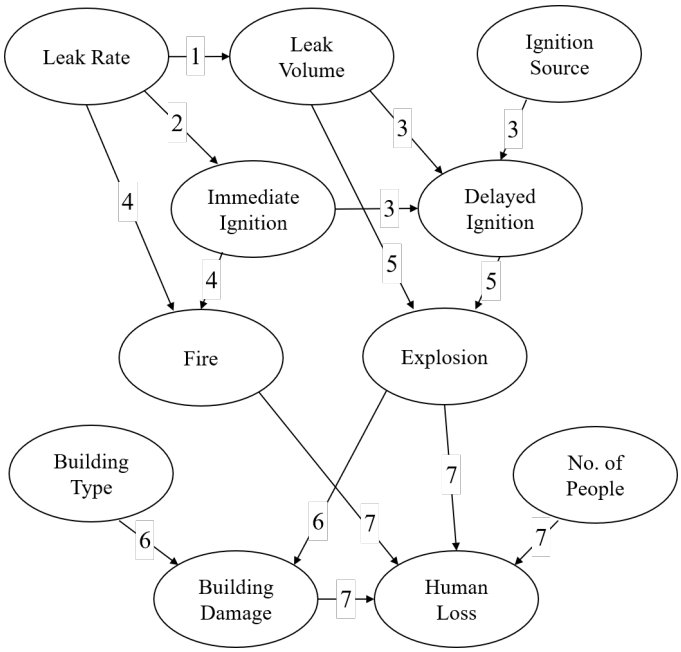

Figure 2-8: Proposed BN for fire and explosions risks. Huang and Ma (2018).

Based on generic leakage frequencies and physics-based consequence models, spatial distributions of human loss and building damage risks were obtained for the entire area surrounding the station. Authors argue that the proposed method is a simple approach to obtain a transparent, explainable, and efficient risk-screening procedure compared to regular QRA.

2.3.3. QRA Applications in Liquid Hydrogen Stations

In the case of hydrogen fueling stations equipped with LH_2 storage systems, risk-related research has focused more on discovering, simulating, and quantifying the dispersion, accumulation, and ignition behavior of liquid releases rather than on reviewing the values used for leakage frequency analysis. Hydrogen as a liquid is stored at cryogenic temperatures (-273°C), which induces different thermal stresses on storage, piping, instrumentation, and process equipment than GH_2-storage, which is stored at high pressure but at temperatures close to ambient conditions. In a regular GH_2-based fueling station the only section regularly under significant thermal and pressure stresses is the dispensing system, given that precooling is needed to maintain low temperatures during vehicle fueling (-40°C). For LH_2-based fueling stations, these potentially hazardous situations are found in the delivery, bulk storage, and processing stages prior to the vaporization stage at even more extreme conditions. Examples of LH_2 release consequences these are frostbite, hypothermia, ice formation on vents and valves, air condensation and oxygen enrichment, moisture within storage due to inadequate purging, and damage to boil-off valves and release valves [40].

Although QRAs developed specifically for fueling stations with LH_2 storage are fewer then the GH_2 counterpart, the followed methodologies are similar in nature. For

example, Al-shanini, Ahmad and Khan (2014) [52] develop in-depth accident scenario analysis through barrier failure modeling. Various FTA and ETA are developed for a delivery LH_2-based fueling station with intermediate high-pressure GH_2 storage prior to the refueling facility. Failures related to technical, operational, human, management, and natural disasters aspects are considered based on frequency data retrieved from failures in other related industries (natural gas, chemical process, etc.). Lack of specific failure and consequence data have been a significant challenge for research related to LH_2 systems, even when these studies are coupled to BN techniques [53].

In [54], Lowesmith, Hankinson and Chynoweth (2014) explored risks related to the liquefaction, storage, and transport of LH_2 through an incident analysis and Hazard Identification (HAZID) procedures. Relevant findings from the incident analysis include that storage vessels (including fittings, valves, and reliefs) accounted for 36% of incidents detected in liquefaction and storage stages, followed by the vent system and pipework (28%); pumps, compressors, and vaporizers (15%); valves, connecting components, and fittings (15%); transfer lines and pipelines (13%); and finally, the liquefier and purifier (5%). These incidents were classified into categories, in which the leading cause was due to incorrect operational, procedural deficiency or poor maintenance (46%). Other major causes cited were design or construction failure and inadequate hazard assessment (31%) and equipment failure (21%). Consequence analysis produced the following breakdown, including overlapping events: no release (13%), accumulation or dispersion (36%), fire (23%), explosion (13%) and boiling liquid expanding vapor explosion (BLEVE) (3%), leading to injury in 8% of the incidents, and non-trivial damage in 59% of the cases. When compared to the developed HAZID based on the incidents, although identified scenarios

and cases were similar, the most notable discrepancy surged from the fact that equipment failures were overestimated, and operational failures underestimated. Authors highlight the value of conducting a HAZID procedure to identify relevant risk scenarios but insist on the need to improve the tools available for full QRAs in LH_2 systems, such as release models and quantitative large-scale experimental, failure frequency and ignition probability data.

It is unusual to find completely developed QRAs and other risk analyses in published literature, as depending on the complexity of the system, hundreds or even thousands of hazards and risk scenarios may be developed. Despite the mentioned limitations, QRA-based frameworks are considered to be robust risk assessment methodologies and significant efforts have been invested into improving the quality of these tools, harmonizing international risk assessment procedures in hydrogen fueling stations, and developing SCS incorporating sound science and risk concepts [55].

2.4. Prognostics and Health Management

Prognostics and Health Management (PHM) frameworks are a modern engineering approach designed to enable a system's real-time health assessment based on its actual operating conditions [21]. This is a non-intrusive alternative for condition-based decision-making in engineering systems. PHM combines various disciplines and data sources: sensor technology, physics of failure and degradation analysis, modern statistics, traditional reliability engineering, as well as novel applications of data-driven techniques. In the last two decades, data-driven health-monitoring techniques have gained significant popularity due to the widespread deployment of low-cost sensors, high connectivity, and improvements in computational processing power [56]. These are fundamental elements of what is known as the Internet of Things (IoT). As a consequence, it is expected that data-

driven applications become even more widespread in the transition to the Industry 4.0 era [57]. The overview presented in this section serves as an introduction to the purpose and characteristics of PHM research for the hydrogen community.

The premise of PHM frameworks to aid CBM decisions is the life-cycle cost reduction, as well as the improved reliability and safety of a system. During the last decade there has been significant advances in both the complexity and variability of applications. In this section, a literature review presents a brief description of some applications of PHM frameworks in other engineering systems. Given the wide variety of applications developed in different industries and research areas, a summary of related standards is also reviewed, as well as aspects of data collection fundamental to the design and implementation of these frameworks. Finally, examples of data-driven applications in other complex engineering systems are summarized and some challenges of these methods are highlighted.

2.4.1. Introduction to Elemental PHM Concepts

It is known that most engineering systems enter a deterioration stage at some point over their lifetime, subject to stresses from prolonged operation or environmental conditions. Failures may occur for multiple causes, and as the complexity of a system increases, characterizing failures and anomalies in the system based on traditional reliability approaches can become unfeasible. Early fault detection is an important step in improving the availability of any equipment or mechanism. This allows to take appropriate maintenance measures in order to prevent further degradation and unexpected component failure. In this context, research interests have shifted from time-to-failure probability-based models towards the extraction of useful information to monitor the system's operational conditions.

The use of condition-monitoring data to build reliability models is known as CBM. The analysis of various sensor measurements, particularly signal analysis, have been used to perform anomaly and damage detection through the development of diagnostic models. These health assessment tools are then used to inform maintenance-related decisions for scheduling and aiding preventive maintenance, seeking to reduce overall costs and increase the perceived reliability of the system. Fault diagnostics can be achieved through various techniques, from simulation and model-based approaches to data-driven methods [22]. However, CBM frameworks are not designed to perform prediction tasks to determine the future behavior of a system's state of health. The latter is known as prognostics and is a fundamental tool to increase the impact of maintenance-scheduling activities, transitioning from corrective actions (i.e., when there is already significant damage detected in the system) to proactive and preventive maintenance policies based on the system's current operational state (i.e., performing maintenance actions before damage is detected).

Prognostics is understood as a process entailing the ability to predict future damage, degradation paths and the RUL of a system. Formally, it is defined in the *ISO 13381-1:2015 Condition monitoring and diagnostics of machines — Prognostics — Part 1: General guidelines* standard as: "an estimation of time-to-failure and risk for one or more existing and future failure modes" [58]. PHM frameworks rely either on physics-based, data-driven, or hybrid techniques to derive health indicators (HI) from the system's performance. A summary of their main characteristics is presented in Table 2-5 [23]. The main differences lay in the availability of a physical model of the system which integrates information from operational conditions and, in contrast, the use of monitoring data to identify underlying characteristics and relationships extracted of the damaged state of a system.

Table 2-5: Comparison of approaches used in PHM Frameworks.

Approaches	Advantages	Disadvantages
Physics-based	Accurate description of degradation and failure behavior; do not require plenty of data.	Hard to observe degradation directly; limited simulation of real environment conditions.
Data-driven	Not required to model degradation and failure behavior precisely; requires little domain knowledge.	Reliance on system-specific relevant and quality data; low adaptation to new conditions.
Hybrid	Combine advantages of both approaches.	Complexity of model selection and parameter tuning.

Physics-based approaches are usually identified as being the more system-specific of the two, tackling well-described local phenomena such as crack propagation. However, as the complexity of the analyzed systems increase, the challenges to obtain precise physical models that describe the degradation under real industrial conditions have also increased [59]. On the other hand, data-driven approaches can be subdivided into traditional statistical model-based tools and AI-based tools. Figure 2-9 shows an overview of publications reviewed in 2018 that cover some of these techniques [24]. Here, statistical model-based methods refer to models such as auto-regression (AR), Wiener and Gamma processes, as well as Markov and Proportional Hazard (PH) models. AI-based approaches include well-known Machine Learning (ML) techniques, such as Support Vector Machine (SVM), Gaussian Process Regression (GPR), k-Nearest Neighbors (k-NN), and Artificial Neural Networks (ANN).

These algorithms bridge over to more complex and hierarchical structures known as Deep Learning (DL) models based on Deep Neural Networks (DNN). Many variants of DNN architectures have been derived and used for specific tasks, such as Auto-encoders (AE), Deep Belief Networks (DBN), Convolutional Neural Networks (CNN), Recurrent Neural Networks (RNN) and Long-Short Term-Memory cells (LSTM). Finally, hybrid approaches attempt to combine the knowledge of the system used in physics-based models

and the generalization capabilities of data-driven approaches. Frequently employed combinations of the mentioned statistical techniques include GPR, SVM and DNN, as well as Particle Filters (PF) and Kalman Filters (KF).

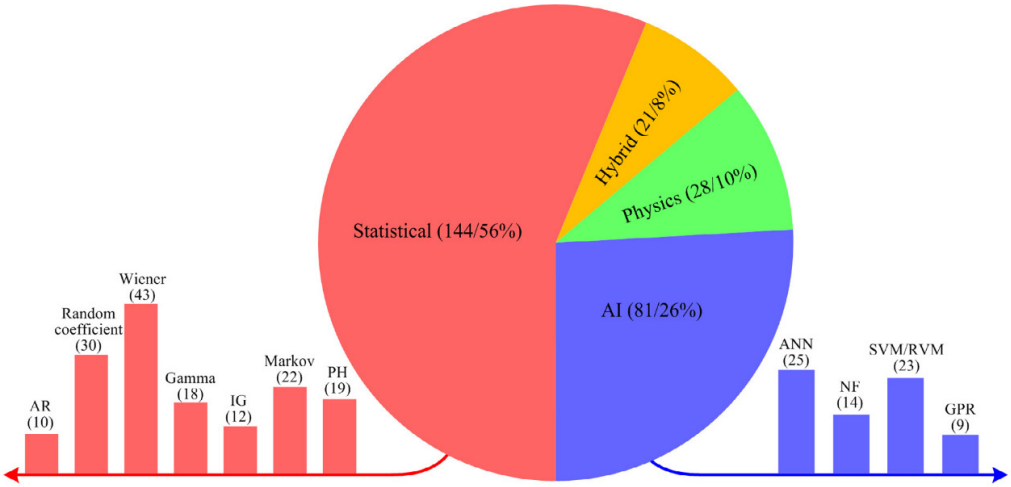

Figure 2-9: Publications related RUL prediction. Lei et al. (2018).

At present, a variety of ML techniques exist, designed for specific purposes and datasets. Generally, these models are described as black boxes in which the outputs are calculated based on certain input data. The learning phase of a model is understood as the optimization of its parameters according to the data provided for the training process. These parameters must be adjusted to obtain the most accurate representation of the training data for the model to perform adequately when presented with new unseen data (i.e., obtain parameters to adequately represent outputs based on new input data). Depending on the selected ML/DL algorithm and its corresponding task, a model's ability to provide reliable predictions will be affected by the architecture or hyperparameters selected beforehand, as well as the quality of the training data (e.g., number of samples, model architecture, optimization function and algorithm, among others).

When applied to PHM, the selected data-driven applications differ based on the knowledge of the system's true health state. On the one hand, if information is available relating the input data to the system's health state, supervised models can be trained. On the other hand, if no previous knowledge of the system's health state is available, unsupervised models can be trained to extract information hidden within the data's structure [60]. Given these characteristics, unsupervised models have been widely applied for anomaly detection tasks. Detection of faulty behavior can be performed by comparing the data to thresholds which can be known beforehand (faults) or established through statistical analysis (anomalies). Another alternative is the construction of HI or key performance indexes (KPI) to represent the state of the system.

In contrast, supervised methods require samples of known correlations between sensor measurements and system's health states to train the models. For instance, these labeled samples can either represent HIs used to identify a specific failure mode through classification models or the evolution of the RUL at each time step of measurements through regression models [60]. Hence, the training of the models consists of an optimization process aimed at replicating known relationships between the model's input and output data. Prognostic tasks are generally supervised tasks, where current conditions are used to predict future states of the system. As with diagnosis tasks, the system's performance and health-state predictions can be developed based on specific HI and KPI. Several methods have been designed to label data either for diagnosis or prognosis tasks yet, these are frequently system-specific and based on expert knowledge. Some of these include data-driven unsupervised clustering methods, such as k-NN and AE models.

2.4.2. PHM Frameworks and Applications

In many of the articles published in the last decade, authors discuss the necessary steps to design phases of data-driven PHM frameworks. While these vary between areas, systematic approaches to design applications have been discussed from an engineering perspective, including the logical, functional, and physical design of the system [61]. Most PHM frameworks define similar stages from data acquisition to decision-making. For instance, Figure 2-10 presents four distinct phases with subtasks corresponding to data acquisition, diagnostics and prognostics assessments, which are then followed by a health management decision-making support stage [62].

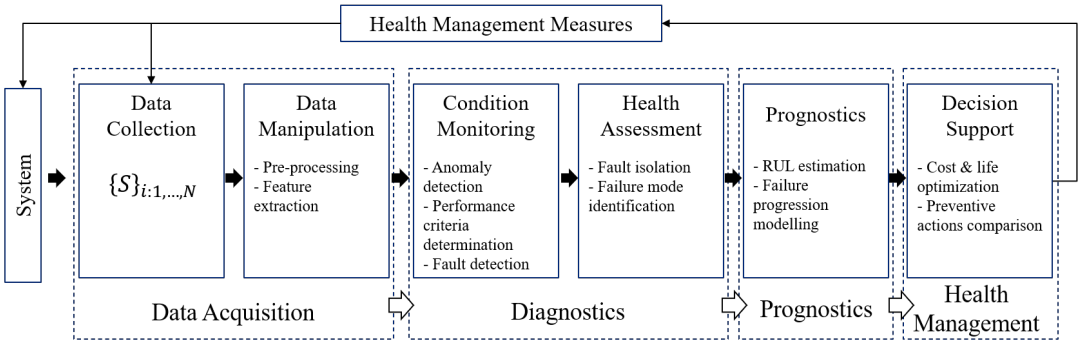

Figure 2-10: A holistic PHM Framework. Moradi and Groth (2020).

Data acquisition is an initial and essential step of PHM frameworks, encompassing both sensor and event data [63]. A complex engineering system yields operational information acquired through different sensor measurements, denoted as $\{S\}_{i:1,\dots,N}$. On the one hand, condition-monitoring data are measurements collected via a variety of installed sensors in components whose performance is linked to the overall system's health state. On the other hand, event data include the information on maintenance actions (component replacement, repairs, etc.) taken during such events (failure, breakdown, installation, etc.) that have occurred in the system.

Data acquisition is followed by a stage of data preprocessing of the raw sensor measurements and event data. These data cleaning and preprocessing stages should consider the system's inherent characteristics, as common practices like outlier detection and removal can lead to unrepresentative datasets if no expert knowledge of the system is available [64]. This also applies to feature selection and extraction from sensor data, where statistical and signal processing techniques have been extensively used in predictive maintenance procedures, including those based on conventional ML models [65]. In this context, combined with the increased computational processing power developed, it was argued that DL algorithms possessing automatic feature extraction capabilities could be applied to analyze raw and minimally treated data [56].

Early and real-time anomaly detection are tasks that have benefited from the surge of data-driven CBM applications, aiming for more comprehensive and flexible tools. Traditional model-based anomaly and fault detection tools rely on given thresholds or the simulation of the system's performance under real operational conditions. Yet, this limits the ability to capture unknown safety issues that are not explicitly defined by rule-based thresholds. Data-driven applications for anomaly detection aim to replace physics-based models for the simulation of the systems' behavior by implicitly extracting it from sensor data under nominal and historic operating conditions. Therefore, anomalous behavior is identified when the observed behavior strays from the simulated expected behavior. For instance, in [66] a SVM regression (SVR) framework is implemented as a real-time safety monitoring tool in the context of commercial aircraft. Here, Lee et al. (2020) argue that, as in many industries, current aircraft monitoring methods depend on predefined and fixed thresholds to identify anomalous behavior. In this work, as system health metrics are not

directly available, performance anomalies are detected based on statistical deviations from predicted flight behavior based on in-flight data. Hence, a SVR decision boundary was formed under the assumption that anomalous behavior is caused by abnormal operational conditions or the degraded state of the system's subcomponents.

Despite the wide range of techniques and models developed for anomaly and fault detection, there are challenges in system diagnostics which have not been overcome yet. Insensitivity to different operational conditions, false alarms and high uncertainty present in real-time processing have been identified as some of the more pressing issues [22]. Both physics-based and data-driven techniques have limited applicability in complex systems, as there are too many assumptions, complex processes, and relationships between components to be simulated or replicated accurately. System-specific knowledge and data characterizing healthy, degraded, and failed states are required to enable and validate an adequate health assessment and prognostics of the system. Linking maintenance events to previous operating conditions and anomalous behavior recorded is the basis for both health-state diagnostics and prognostics tasks. These tasks are implemented to inform engineering decision-making to increase system safety and operation reliability [67]. A variety of models are available for fault diagnosis, including popular ML and DL algorithms such as SVM, RF, AE, DBN, and CNN. On the other hand, RNN and LSTM models have been consistently used for prognostics tasks [56].

Finally, the decision-making stage for planning and executing maintenance measures is included. Few published research papers address the implementation of the decision-making phase. As stated in [65], predictive maintenance studies can be divided into prognostics and maintenance optimizations. The latter is frequently performed over

"known" degradation behavior and prognostics results; hence maintenance decisions are dealt separately and often are system-specific. In this work, Nguyen and Medjaher (2019) [65] present a two-stage framework to schedule maintenance operations in a simulated system shown in Figure 2-11. Based on the C-MAPSS dataset (discussed in Section 5.2.2), an LSTM model was used to predict the RUL of turbofan engines from simulated sensor run-to-failure data. Given the estimated RUL, the framework classified whether the system would fail before or after a certain time-window defined by the operation planner, hence enabling maintenance and repair logistic decisions based on prognostic information. Although this work considers limited assumptions such as simulated data and perfect repairs, it demonstrates the framework's ability to obtain lower costs than regular periodic maintenance schemes [65].

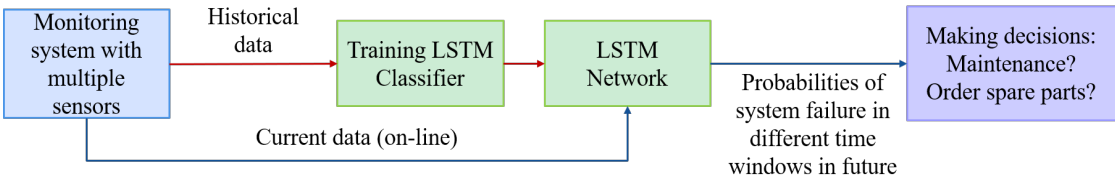

Figure 2-11: Example of applied PHM framework. Nguyen and Medjaher (2019).

2.4.3. Challenges in Data-Driven PHM Applications

Many PHM applications at the component level struggle with issues such as optimum sensor selection and localization, feature extraction, framework integration and uncertainty quantification. These issues are only amplified when considering system-level applications. A review of data-driven techniques applied to PHM frameworks conducted in [68] highlighted some of the following challenges:

- Data scarcity in the industrial context: Significant historical data is needed to construct robust models. The main drawback of data-driven models is that their

performance strongly relies on the amount and quality of data in the training process [25].

- Black-box model selection: The role of feature extraction stages was significantly reduced with the growing popularity of DL models. Yet, the reduced transparency and explicability of the model's decisions coupled to the lack of public datasets for model validation is a hindrance to their applicability in real complex systems [69].
- Real-time integration to maintenance decision-making: Few studies have assessed the operation of PHM frameworks. A critical aspect of data-driven models is to be representative of the system its applied to, i.e., periodic retraining of the model can avoid erroneous health assessments even when the operational conditions of the system have changed.

The challenges summarized above should be considered when designing and implementing PHM frameworks for system-level data-driven diagnostics and prognostics tasks.

Chapter 3. LH_2 Storage System Risk Scenario Identification

The layout of a hydrogen station can vary significantly depending on the available space and components present in the system. Hence, the most prominent risks and required safeguards will vary according to the code-compliant design's particular design. For research purposes it was necessary to have a baseline, generic design to carry out the risk scenario screening process. This chapter presents the description of the selected LH_2 storage system design and is followed by the identification of its most relevant failure modes through an FMEA process.

3.1. Methodology

This section refers to the methodology followed to determine the generic LH_2 storage system to be analyzed and the initial risk screening through an FMEA process. It should be noted that this corresponds to a high-level analysis, as the studied system corresponds to a preliminary design for hydrogen stations equipped for liquid delivery and with both bulk LH_2 and GH_2 storage systems [70].

3.1.1. LH_2 Storage System Design Selection

For the development of this work, the selection of the specific system to be analyzed was conducted through the discussions held with hydrogen experts. The meetings held with external hydrogen partners involved several teleconferences with representatives from the private hydrogen station sector, as well as from the H2@SCALE project occurring at U.S. DOE National Laboratories Sandia and NREL. These meetings with external partners focused on the design of the hydrogen fueling station and LH_2 storage system. As described in Section 2.1, the basic design of a hydrogen station generally consists of delivery, storage, compression, and dispensing sections. Based on a theoretical station design equipped for

LH_2 delivery and storage discussed in the context of the H2@SCALE project, details such as fueling capacity, component characteristics, and basic layout are documented to enable an initial risk screening. This documentation focused on the functioning logic of the LH_2 storage system, including relevant connecting elements located between the main components of this subsystem.

3.1.2. Analysis of Hydrogen Failure Scenarios

To analyze the selected LH_2 bulk storage system design, a review of typical risk scenarios in these systems was conducted. This includes a revision of user-reported database portals such as H2 Lessons Learned and Hydrogen Incidents and Accidents Database (HIAD). Given the predominant participation of GH_2 stations in the hydrogen fueling market, scarce information is available of operating systems with LH_2 bulk storage. Nevertheless, as mentioned in Section 2.1.1.1, the latest version of the *NFPA 2* code included a HAZOP study on LH_2 bulk storage stations. The main results in this stage are summarized to provide necessary context for the risk screening of the selected design.

3.1.3. Failure Mode and Effect Analysis

FMEA is an inductive technique for reliability analysis which can be used in both the design and implementation stages of a system or a project. It aims to describe the inherent causes that lead to a system failure, determine the consequences of said failures and the methods to detect and minimize the occurrences of hazardous events. A criticality rating can be assigned to each identified failure mode, based on their probability and consequence severity classification. Naturally, the procedure and specific classifications vary with the studied system and the author's field, for which it is usual that FMEAs are developed by a team of experts with different backgrounds.

The objectives of FMEA applied to a system's or product's design process are summarized as a) identifying and ranking failure modes accordingly to their effect on the system's performance and thus establish a priorities for design improvements; b) identifying design actions to eliminate potential failure modes or reduce the occurrence of the respective failures; and c) document the rationale behind product design changes and provide future reference for analyzing field concerns, evaluating new design changes, and developing advanced designs [71].

The main outline describing an FMEA should consist of the following steps:

1. Define the system decomposition level to be analyzed. Identify internal and interface system functions, restraints, and develop failure definitions.
2. Construct a block diagram of the system, depending on the desired level of decomposition.
3. Identify all potential item failure modes and define their effects on the immediate function or item, on the system, and on the mission to be performed.
4. Evaluate each failure mode in terms of the worst potential consequence and assign a severity classification category.
5. Identify failure detection methods and compensating provisions for each failure mode.
6. Identify corrective designs or other actions required to eliminate the failure or control the risk.
7. Document the analysis and identification of the problems that could not be corrected by design.

Generally, FMEAs are carried out between a group of experts. This design FMEA has been mostly developed based on previous literature and the analysis of the generic station design. A review of the *NFPA 2* and CGA codes, *The Purple Book*, OREDA and HyRAM documentation have enriched this FMEA process, addressed in Section 4.2. For the purpose of this project, only steps 1-5 are addressed.

The identified failure modes are then characterized by the estimated severity of resulting consequences and the relative likelihood of their occurrence to obtain a representative risk level. A simplified risk matrix, as the one presented in Table 3-1 is used to rank the most relevant failure modes and risk scenarios identified in the selected LH_2 storage system design. This matrix consists of three levels of severity classes (minor, moderate, and critical) and three probability classes (low, medium, and high). This leads to a three-level risk ranking: high (H), moderate (M), and low (L).

Table 3-1: Simplified Risk Matrix.

Severity Class	Probability Class		
	Low	Medium	High
Minor	L	L	M
Moderate	L	M	H
Critical	M	H	H

3.2. Hydrogen Fueling Station Generic Design

The Hydrogen Fueling Infrastructure Research and Station Technology (H2@SCALE) is a project initiated by the U.S. DOE and executed by Sandia National Laboratories (SNL) and the National Renewable Energy Laboratory (NREL). This project addresses the research and development (R&D) barriers towards the deployment of hydrogen fueling infrastructure in urban areas. This ongoing project is based on generic

designs for which the P&IDs are available for analysis [70]. The generic design selected is based primarily on these documents, which served as an initial step in characterizing the LH_2 storage system's components for further analysis. As the documentation available is focused on estimating the layout of different station designs compliant with the *NFPA 2* (2020 Ed.), technical details of specific supporting and connecting elements (i.e., valves, piping, emergency systems, etc.) are not included.

The station design has the following general characteristics, regarding its location and main components. It is a stand-alone hydrogen fueling station located in an urban area, in a lot that also contains a convenience store. The corresponding code-compliant layout is shown in Figure 3-1 [70]. This station's design equipped for LH_2 delivery and storage considers a lot size of 52x38 m (170x125 ft.), with a total area of 1,974 m^2 (21,250 ft^2). It should be noted that non-hydrogen related components contribute significantly to the station's footprint, particularly parking and traffic flow (Figure 3-1b). LH_2 is delivered through trailer trucks to the liquid storage tank, the latter acting as a hydrogen reservoir for the rest of the system.

A centrifugal cryogenic pump is used to transport LH_2 from the liquid storage towards the evaporator previous to the compression stage. After the compression stage, gaseous hydrogen is stored in a pressure cascade configuration. From the cascade system, hydrogen is cooled through a chiller system and dispensed under active demands. Minor components include temperature and pressure sensors located at relevant points in the system, valves such as motor-operated valves, gate valves, and check valves. The configuration of the hydrogen storage, compression, and cooling components is shown

schematically in Figure 3-1c. These are kept in the open to minimize the potential risk of hydrogen accumulation should the system leak.

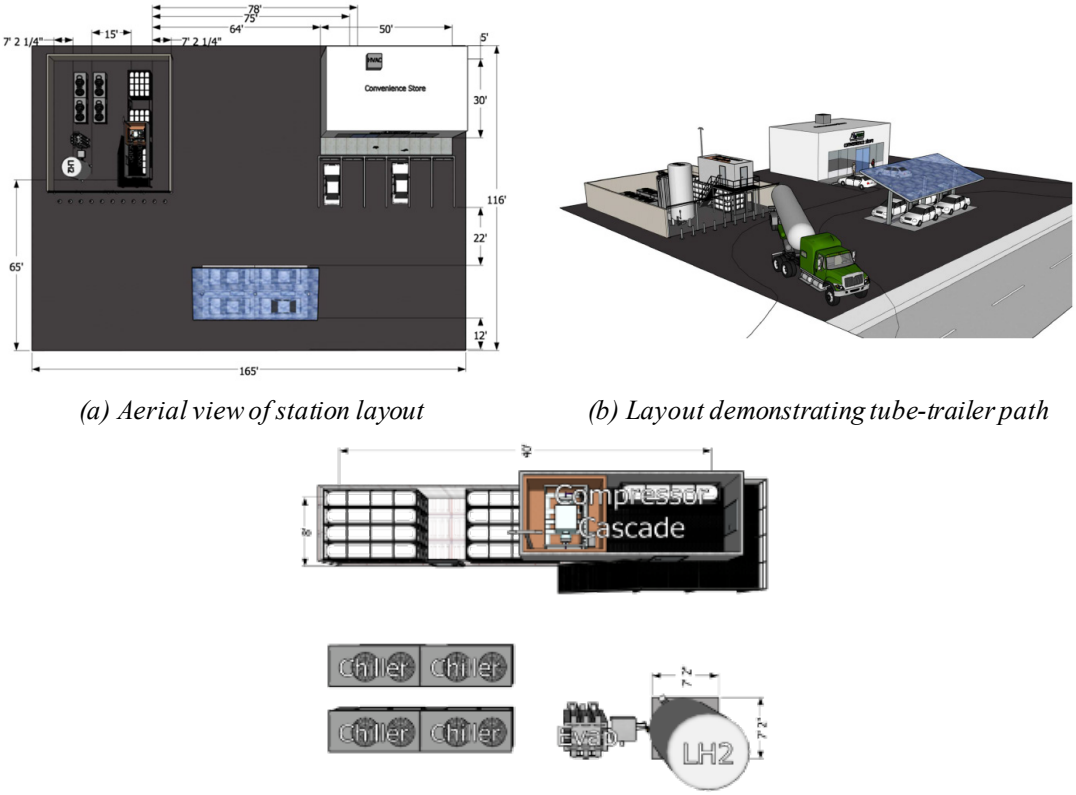

(a) Aerial view of station layout *(b) Layout demonstrating tube-trailer path*

(c) Schematic layout hydrogen storage, compression, and cooling components.

Figure 3-1: Code Compliant Base Case Liquid Full Station Layout. Ehrhart et al. (2020).

This station's documentation is divided into five subsystems, not including the delivery stage: liquid storage, compression stage, gaseous cascade storage, cooling system, and dispensers. A schematic adaptation of the full station's layout is presented in Figure 3-2, in which the liquid storage subsystem is highlighted. It must be noted that the cascade GH_2 units are connected to a vent system to address pressure-adjusting and unexpected releases in a safe manner. A list of the station's subsystems is presented in Table 3-2, while technical details of the components are detailed in Table 3-3. A description of the main components of each subsystem is presented in the following sections.

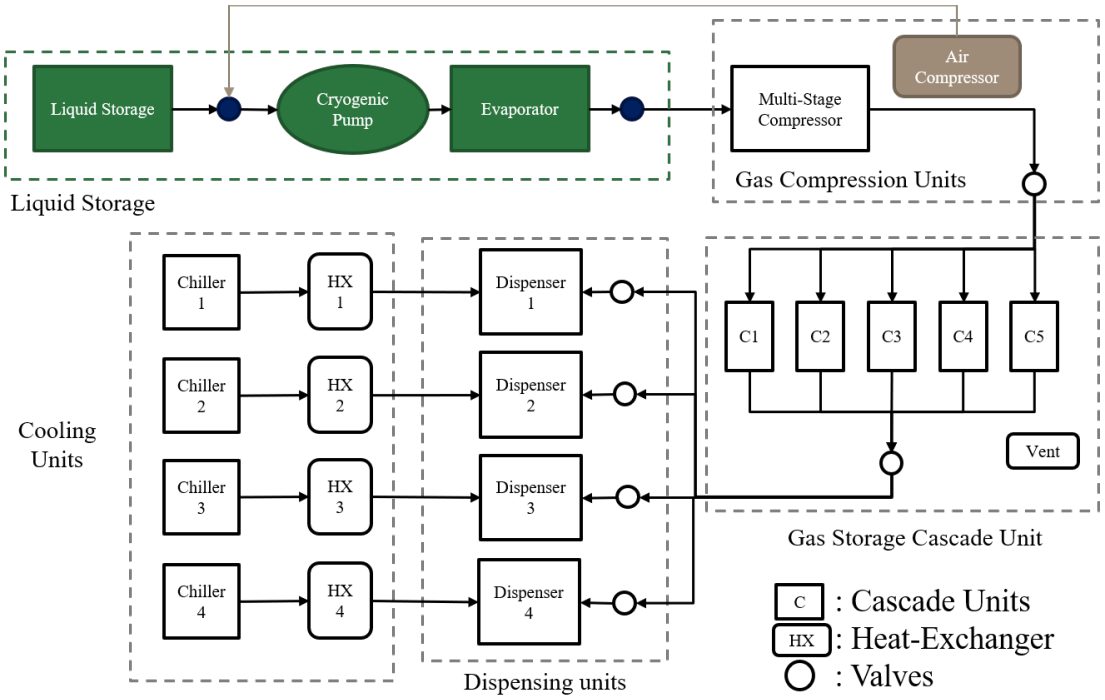

Figure 3-2: Schematic of LH_2-based fueling station design.

Table 3-2: H2@SCALE hydrogen fueling station subsystem description.

Subsystem	Function	Main Components	Valves	Sensors	Connects To
Liquid Storage	Liquid hydrogen storage	Liquid Storage Tank	Motorized valve, gate valve	Temperature, pressure	Gas storage
Gas Storage	Gaseous hydrogen storage	Gas Storage Tank	-	-	Compression
Compression	Compression of hydrogen gas and control air	Multi-stage hydrogen gas compressor, process air compressor	Motorized valve, gate valve, check valve	Pressure	Cascade Storage
Cascade Storage	Storage of hydrogen gas	Gas cylinder storage	Motorized valve, gate valve	Pressure	Dispenser
Dispenser	Vehicle refueling	Dispenser nozzle, users	Motorized valve		Cooling
Cooling	Dispenser cooling	Chillers, heat exchangers	Gate valve		

Table 3-3: H2@SCALE hydrogen fueling station components description.

Components	Capacity	Coupled To	Number	System
Storage Tank	800 kg	Temperature, pressure sensors	1	Liquid Storage
Cryogenic Pump	16 kW	-	1	Liquid Storage
Ambient Air Evaporator	25 kg/hr.	-	1	Liquid Storage
Multiple Stage Compressor	25 kg/hr.	480V-60kW motor, air blown coolers, centrifugal pump	1	Compression
Air Compressor	-	Air dryer	1	Compression
Chillers	25.2 kW, 94.4 MPa	Aluminum cooling block (1330 kg)	4	Cooling
Gas Cylinders	MAWP 95 MPa (13780 psig), 60 kg/hr. outlet flowrate.	10 cascade units, each with 5 pressure vessels (1:1:3)	50	Cascade Storage
Dispensers	70 MPa, -40°C	Internal controls 120V, 15A	4	

3.2.1. Bulk LH_2 Storage System

A simplified representation of the main components of the system is shown in Figure 3-3. The bulk liquid storage system of the station is composed of a double-walled storage tank with an estimated capacity of 800 kg of LH_2 assuming a density of 70.8 g/L at 0.6 MPa (88.2 psi). This gives an LH_2 volume of 11,299 L (2,985 gal.) stored within a bulk cryogenic storage tank with a net capacity of 11,470 L (3,030 gal.), a diameter of 2.18 m (7.2 ft), and a height of 5.8 m (19 ft). This tank is equipped with temperature and pressure sensors as well as a pressure relief valve (PSV) and a maintenance valve (HV-1). The piping on the outlet of the bulk storage tank is assumed to have an outer diameter (OD) of 25.40 mm (1 in.) and inner diameter (ID) of 14.27 mm (0.562 in.). The generic pressure rating selected is of 137.9 MPa (43,000 psi).

The liquid bulk storage tank is connected through double-walled piping to a 16-kW centrifugal cryogenic pump (CNL) that feeds the LH_2 to an ambient air evaporator (EV)

with a 25kg/hr. rated mass flow rate. This is regulated by an air-operated motorized valve located prior to the cryogenic pump, which is controlled by the process air system (ZZO-Air). In the evaporator, liquid hydrogen is heated at ambient air temperature and transformed into gas. From the evaporator, the GH_2 flows towards the compressor subsystem and can be closed by a gate valve for safety and maintenance purposes (HV-2). The storage subsystem counts with a dedicated IR thermal flame detector and alarm system.

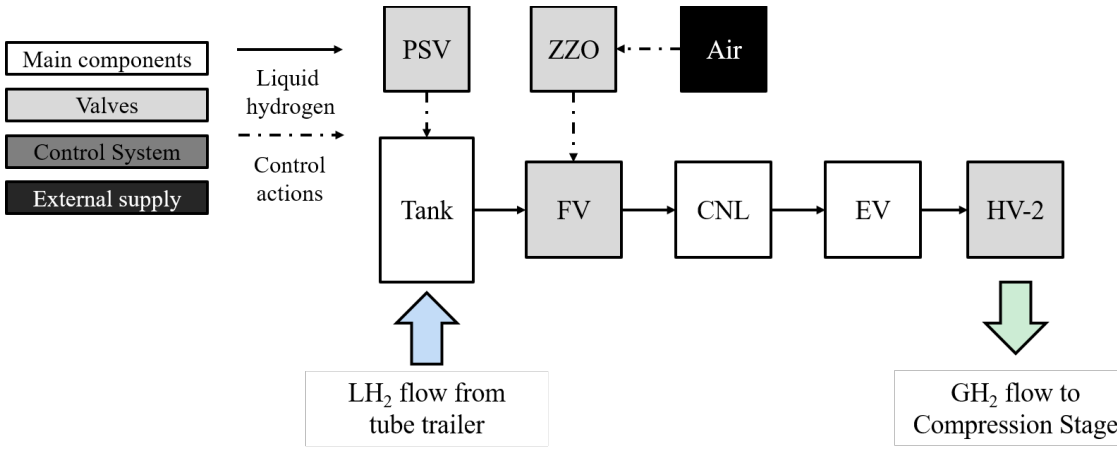

Figure 3-3: LH_2 storage functional block diagram.

3.2.2. Compression and Cooling Subsystem

From an intermediate gas storage system after the evaporation process, the hydrogen gas must be compressed from 0.6 MPa to 94.4 MPa to be delivered to the cascade storage and dispensing system. This subsystem is primarily composed of the multi-stage compressor (102 kW, 25 kg/hr. capacity, 480 V-60 kW motor-driven) and the numerous air-actuated valves acting as pressure regulators. The air compressor and the cooling system (four units of 25.2 kW, 94.4 MPa capacity) are also included in this section.

3.2.3. Gas Cascade Storage

The storage of GH_2 for dispensing purposes is stored in a cascade pressure system. Thus, when gas is dispensed, the flow is taken from the lower-pressure vessels and sequentially increasing until the FCEV's tank is filled. There are ten cascade units, each with five pressure vessels (C) with a pressure ratio of 1:1:3 from high to low pressures. The default pressures are set to 33.0 MPa, 61.3 MPa, and 80.2 MPa, respectively. The gas cylinders have a MAWP of 95.0 MPa (13,780 psig). A recirculation system towards the compressor allows the pressure regulation in the distribution network in the station. Each unit of them is equipped with air-actuated valves, pressure indicators and transmitters, as well as hand valves and two-way pressure relief valves. A total of 630 kg of GH_2 is stored in the cascade storage, with an estimated output flow of 60 kg/hr. towards the dispensing system.

3.2.4. Dispenser Subsystem

The dispensing subsystem counts with four fueling positions for delivering gaseous hydrogen at 70 MPa at -40°C through high-pressure, break-away nozzles. These units have an internal control system and user interface which regulates the fueling phase (WUN-902 FV/Controls Internal 120V, 15A). These are connected to heat exchangers each consisting of 1,330 kg aluminum cooling blocks (heat exchangers, HX) for temperature control.

For details on all stages and additional details of the storage system, refer to Appendix C original P&IDs for the main subsystems including LH_2 bulk storage, compression, GH_2 cascade storage, and dispensing elements are attached.

3.3. Survey of Available Scenario Data Sources

To develop a credible FMEA of the LH_2 storage system, a survey of identified risk scenarios in hydrogen fueling stations was conducted. It must be noted that public datasets recording hydrogen-related incidents are available for scenario development analysis. However, given the higher number of stations equipped with bulk GH_2 storage rather than LH_2, scarce information has been collected referring to the latter. Instead, a HAZOP study developed for a generic station with bulk LH_2 is presented as a base for the FMEA conducted. These are described in the following sections.

3.3.1. Hydrogen Risk Scenario Data Sources

HIAD is an international systematic data collecting initiative on hydrogen-related undesired events [72], [73]. The main purpose of this database is to assist stakeholders in a better understanding of hydrogen events to facilitate the safe introduction of hydrogen technologies and applications for a more sustainable development in Europe. HIAD was developed within the EC-funded Network of Excellency HySafe project under the coordination of Det Norske Veritas and the European Commission Joint Research Centre (JRC) EU Science Hub.

On the other hand, H2 Lessons Learned is a database-driven website intended to facilitate the sharing of lessons learned from hydrogen-related incidents [74]. This is part of the Hydrogen Tools Portal developed by the Pacific Northwest National Laboratory through support from the U.S. DOE EERE. The goal of this Portal is to support implementation of the practices and procedures that will ensure safety in the handling and use of hydrogen in a variety of fuel cell applications. Both these public, online databases are a significant input for analysis of failure modes, causes, and risk mitigations measures.

Yet, these depend on the quality of the incident's reports, mostly referring to general descriptions and lacking in-depth quantitative analysis of these failures.

The California Energy Commission (CEC) has identified 153 relevant failure modes at hydrogen delivery stations, including those using LH_2 and compressed GH_2, and at on-site hydrogen production stations [75]. Out of these designs, stations with LH_2 delivery are identified as having the most serious consequences due to factors such as external accidents and collisions, overfilling tanks, and relief valve venting [1], [38].

3.3.2. Liquid Hydrogen Risk Scenarios

The U.S. Occupational Safety and Health Administration (OSHA) Process Safety Management (PSM) and the U.S. Environmental Protection Agency (EPA) Risk Management Program (RMP) establish safety requirements for certain types of U.S. industrial gas facilities. The *P-28 OSHA Process Safety Management and EPA Risk Management Plan Guidance Document for Bulk Liquid Hydrogen Systems* is intended to provide information that is required to meet safety and risk mitigation requirements [29]. A typical system HAZOP in a generic bulk LH_2 system, as well as the hazard assessment for release scenarios typical of the standard hydrogen station tanks used in the gas industry are provided to guide the design and implementation of code-conforming systems.

A typical hydrogen system is described, including a storage tank, flow controls, vaporizers, low temperature protection, and other safety systems. For the development of the HAZOP deviation matrix, hazards of the process, previous incidents, engineering and administrative controls, consequences of failure of controls, general human factors and facility-sitting items were considered for the analysis organized with the following classification: Node #1: Delivery trailer, hose, and fill line to storage vessel; Node #2:

Storage tank; Node #3: Pressure build-up circuit and economizer; Node #4: Hydrogen line – liquid through vaporizer to the customer; Node #5: Hydrogen pump; Node #6: Vent stacks; and Node #7: General items. For the RMP development purposes, off-site consequences must be addressed, including a worst-case release scenario as well as alternative-release scenarios. The worst-case scenario for a LH_2 tank is modeled as a catastrophic release in which the entirety of the tank content is instantaneously released to the atmosphere, forming an explosive cloud that detonates. Alternative-release scenarios refer to other less catastrophic events which are more likely to occur, such as the ones stated in Table 3-4 [29].

Table 3-4: P-28 Alternative-release scenarios.

Alternative-release scenario		Conclusions
1	Transfer hose release due to splits or sudden hose uncoupling.	The likelihood of sudden hose uncoupling due to inadvertent movement of the liquid hydrogen trailer during the off-loading process is minimized by the trailer tow-away protection. Hose splits would result in a liquid release at grade. The flow rate for such a release generally would be less than that for a process piping failure since the flow is limited by the trailer pressure and trailer pump (if used).
2	Process piping releases from failures at flanges, joints, welds, valves, and valve seals, and drains or bleeds.	A release from a gaseous piping failure would be less severe than from a liquid line of the same size. Failure of a liquid line would result in a liquid hydrogen spill at grade.
3	Process vessel or pump releases due to cracks, seal failure, or drain/bleed/plug failure.	Likely to be small flow releases with no offsite impact.
4	Vessel overfilling and spill, or over-pressurization and venting	Releases through a well-designed vent stack. Not expected to have any offsite impact.
5	Shipping container mishandling and breakage or puncturing leading to a spill.	A trailer (shipping container) failure would be no worse than the worst case for a single stationary container of the same size. Other failures associated with the trailer would fall into one of the previous four types.

Of these, the most likely scenario to have off-site consequences is the process piping failure resulting in LH_2 release at grade. This kind of incident may be caused by a mechanical failure, corrosion, failure of a piping component (such as a joint or valve), or

impacted by a vehicle, among other events. Table 3-5 [29] presents the consequence classification criteria used for the HAZOP analysis. These consequences classification assume all safety and protection measures have failed, thus, reference the worst-case scenarios. Some of the most relevant anomalous system variations are summarized in Table 3-6 regarding the liquid storage tank and Table 3-7 for the cryogenic pump.

Table 3-5: Range of effects on employees, the public, and the environment.

Release Size	Description of effect on persons and the environment
Small	A release that could potentially cause injury, adverse health effects, or death to personnel in the immediate vicinity of the release with little or no likelihood of environmental damage.
Medium	A release that could potentially cause injury, adverse health effects, or death to personnel throughout the unit/process that is under review; or localized acute environmental impact within the facility that could require special operations.
Large	A release that could potentially cause injury, adverse health effects, or death to people (both employees, and the public) either throughout the facility or outside the facility, or widespread acute environmental impact either within or outside the facility that could require special operations.

Table 3-6: P-28 HAZOP Consequences in Node #2.

#	Deviation	Caused by	Consequences
2.1	High pressure	Loss of vacuum	PRDs opening or possible rupture of inner or outer vessel resulting in hydrogen release with possible fire/explosion, equipment damage, and personal injury.
		Pressure build regulator fails open	
		PRDs fail closed or vent-line restricted.	
2.4	High temperature	External fire or hydrogen leak and fire	Possible loss of vacuum with functioning of the relief system, hydrogen release, and possible fire/explosion, equipment damage, and personal injury.
		Loss of vacuum	Functioning of the relief system, hydrogen release, and possible fire/explosion, equipment damage, and personal injury.
2.5	Low temperature (outer vessel or external lines)	Hydrogen leak from the inner vessel into the vacuum space	Escalating leak can result in inner vessel failure with hydrogen release, possible fire/explosion, equipment damage, and personal injury. Casing failure.
2.16	Loss of containment	External impacts	Hydrogen release, and possible fire/explosion, equipment damage, and personal injury.
		Natural disasters	PRD functions. Hydrogen release, and possible fire/explosion, equipment damage, and personal injury.
		External fire	

Table 3-7: P-28 HAZOP Consequences in Node #5.

#	Deviation	Caused by	Consequences
5.1	High pressure	Pump dead-headed	Pump or line rupture with hydrogen release, possible fire/explosion, equipment damage, and personal injury. PRD functions.
		Operator error- improper valve sequences (closes valve downstream of pump)	
5.16	Loss of containment	External fire	Hydrogen release, and possible fire/explosion, equipment damage, and personal injury.
		External impacts	

Other failures regarding the delivery system, pressure build-up circuit, vaporizer, and other general failures can be found in A-Table 1. No large consequence scenarios were identified in the vent stacks. Following this analysis, several safety measures were introduced and suggested to counter the identified hazards. Safeguards related to the storage unit and the cryogenic pump are presented in Table 3-8, including ones referring to storage tank material selection, design considerations, and vacuum-insulated layer pressure monitoring. Other relevant safeguards developed for the other system's nodes are presented in A-Table 2.

Table 3-8: P-28 Safeguards for large range consequence scenarios in Nodes #2-#5.

#	Deviation	Safeguards	
2.1	High pressure	Mechanical integrity program. PRD vent system has a dedicated tank connection.	Rupture disks provide redundant protection again relief valve failure.
2.4	High temperature	Inner vessel relief valves are sized for this condition. Proper material of construction of outer vessel. Fusible links. Fire-rated isolation valves. Proper tank sitting in accordance with NFPA 55.	Equipment designs to recognize codes. Insulation of tank legs over 18 in high. Mechanical integrity program. Properly designed PRD vent system.
2.5	Low temperature	Vacuum space pressure gauge.	Mechanical integrity program.
2.16	Loss of containment	Proper tank sitting in accordance with NFPA 55.	Foundation design.
5.1	High pressure	Operating procedures. Properly labeled lines and valves.	Properly designed PRD vent system.
5.16	Loss of containment	Proper tank sitting in accordance with NFPA 55.	Area fencing and traffic posts.

3.4. Results of FMEA for LH_2 Storage System

The FMEA presented is used as an exploratory assessment of failure modes present in the LH_2 storage system related to the effect of cryogenic temperatures, thermal and pressure cycling. As discussed in Section 2.3, several FMEA have been previously developed for hydrogen fueling stations, although most of these are focused on risks related to GH_2 release. This section contains the documentation of the FMEA and resulting insights regarding the design of the LH_2 storage system in the context of risk analysis.

3.4.1. FMEA System Decomposition

A functional description of the main components of this system are available in Table 3-9. The main component in the liquid storage system is the double-walled 800 kg liquid storage tank. Therefore, special attention must be brought to the risk mitigation components of this item, such as the pressure relief valve (PSV) system, including pressure and temperature sensors. Following the storage tank, both the cryogenic pump (CNL) and the ambient-pressure evaporator (EV) play a fundamental role in the transport and phase transformation of the hydrogen fuel. Hence, connecting elements such as the double-walled piping, and valves are also considered. The supply of process air and electricity are considered external to the system.

Table 3-9: LH_2 storage functional description.

System Code	System Name	Functional Description	Components Involved
1	Storage	Storage of liquid hydrogen under safe pressure levels.	PI, PT, PSV, HV-1, Tank
2	Control	Controlled transport of liquid hydrogen from storage to process components.	FV, ZI, ZSO, ZSC, ZZO
3	Process	Pressure, temperature, and phase control of hydrogen fuel towards the station.	CNL, HV-2, EV
4	Piping	Physical transport of liquid hydrogen from storage to process components.	Piping

The fully decomposed layout of the LH_2 storage system and identified subsystems is presented in Figure 3-4 and Table 3-10. System boundaries are defined concerning the storage tank onwards to the distribution network towards the evaporator. This does not include the fuel delivery process, emergency fire cabinet operation or the supply of external elements such as process air or electricity.

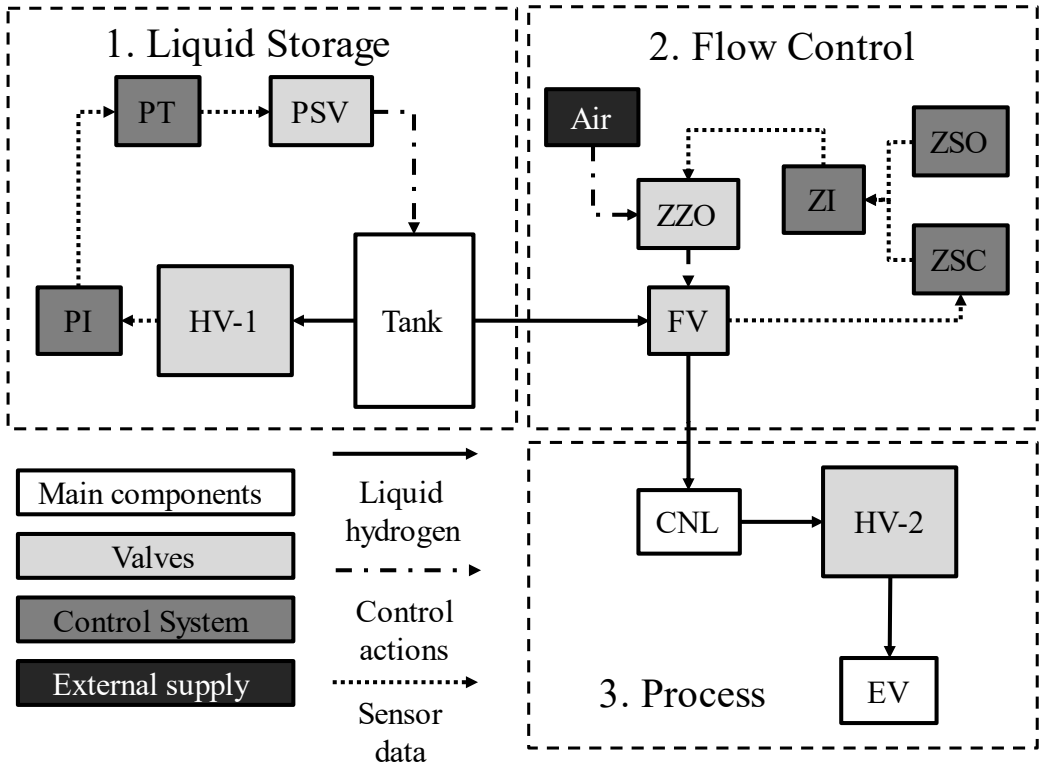

Figure 3-4: LH_2 Storage Decomposition Functional Block Diagram.

For the LH_2 subsystem any major failure can potentially result in the unintended release of hydrogen. However, a distinction should be made between liquid and gaseous releases of hydrogen as these can lead to different failure scenarios with varying severity classifications. Unintended LH_2 release will be primarily caused by leakage or rupture of components such as: storage tank, piping, valves, pump, and evaporator. Large ruptures will result in LH_2 releases at cryogenic temperatures. The effect of these releases over

infrastructure, instrumentation, and humans is yet to be completely quantified, as well as possible pooling and subsequent evaporation and ignition risks [76].

Table 3-10: LH_2 Storage Decomposition Functional Description.

Component Code	Nomenclature	Component Name	Function
1.1	Tank	Liquid storage tank	Storage of liquid hydrogen.
1.2	PI	Pressure Indicator	Indicates pressure inside tank.
1.3	PT	Pressure Transmitter	Transmission of pressure sensor reading to control system.
1.4	PSV	Pressure Release Valve	Controlled releases of gaseous hydrogen from tank in case of high pressure (>1MPa).
1.5	HV-1	Block and bleed ball valve	Block flow and bleed off remaining gaseous hydrogen.
2.1	FV	Air operated valve	Flow control of hydrogen
2.2	ZZO	Position actuator	Controls operation of FV
2.3	ZI	Position Indicator	Indicates position of FV
2.4	ZSO	Switch position open	Indicates open position of FV
2.5	ZSC	Switch position closed	Indicates closed position of FV
2.6	Air	Air	Process air supply
3.1	CNL	Cryogenic Pump	Transport of liquid hydrogen
3.2	HV-2	Isolation Hand Valve	Isolates flow to system downstream
3.3	EV	Ambient air evaporator	Liquid to gas phase transformation
4.1	Piping	Piping	Liquid and gaseous hydrogen transport

Small ruptures will likely lead to limited LH_2 release and subsequent evaporation. If the release rate is low, the GH_2 will most likely disperse. It is unclear how the conditions under which the LH_2 is released, and at which rate, affects the evaporation rate. In this case, the probability of the event 'liquid hydrogen evaporating into gaseous state' will be required to assess known ignition and explosion risks related to GH_2 releases. No explicit information on failure detection methods is available other than the Fire & Gas cabinets shown in Appendix C. It is assumed that detection leads to a system shutdown based on shut-off valve operation (HV).

3.4.2. Results: FMEA Risk Scenario Identification

As specific data on stations with LH_2 storage systems is limited, a qualitative estimation of even probabilities was used to assess the risk of the identified failure modes. Considering the LH_2 storage system studied, the most relevant release scenarios refer to releases from either a rupture of the storage tank or to releases from process piping connecting elements, process vessel or pump releases, and vessel overfilling and spill, or over-pressurization and venting (See Table 3-4). Of these, the scenario most likely leading to severe consequences is process piping failure, particularly in LH_2 lines. In [29] it is also assumed that releases from process vessels or pumps will likely lead to small flow releases with no off-site impact. Yet, these still represent causes which affect the overall availability of hydrogen fueling stations as discussed in Section 4.2.1.

Hydrogen releases from the storage tank and piping lines represent possible high-risk scenarios due to the number of locations at which these can occur, especially at connecting elements (valves, fittings, and seals). However, safety measures should also focus on process equipment, such as the cryogenic pump and the evaporator heat exchanger, as these components are exposed to thermal cycling and could be a major source of leaked hydrogen. The main failure modes for critical subsystems identified in the system are as follows:

- Storage tank and piping: Main failure mode includes loss of containment in either the inner or outer jacket due to overpressure and fatigue wear. Also, connecting elements are under thermal degradation failure modes. Specific safety measures exist to counter these failures, mainly material and maintenance requirements, although specific LH_2 leakage frequency data is unavailable.

- Pressure relief devices and air-actuated valves: Considered failure modes refer to failures to operate or to close under demand. It must be noted that the operation of these elements depends on instrumentation and control systems which may fail by exposure to cryogenic temperatures, although these effects remain unquantified.
- Cryogenic pump and evaporator: These elements are potential sources of hydrogen leakage. The effect of failures in connecting elements, fittings, and seals are similar to those expected from the storage and piping components. However, failures due to thermal or pressure cycles stresses could also lead to abnormal pressure conditions in the piping lines in the vicinity of the pump or releases of a liquid/gaseous mixture from the evaporator. It must be noted that specific LH_2 leakage frequency data is unavailable.

The identified failure modes particularly affected by LH_2 are summarized in Table 3-11 regarding the storage tank, Table 3-12 regarding the valve and control system and Table 3-13 regarding the process equipment. These tables present the identified failure mode and cause and the failure mode model. Based on the risk matrix presented in Table 3-1, the corresponding risk level (R) is obtained: Low (L), Medium (M) and High (H). In these components, the following high-risk failure modes were identified:

1. Malfunction of the pressure relief valve system due to cryogenic temperatures.
2. Operation failure at prescribed time of the air-operated valve.
3. Rupture due to collision or external accident of the evaporator.

Based on the estimated probability class, the medium-risk level failure modes identified include:

1. Storage tank rupture due to an external accident or collision.
2. Failure of the outer wall of the storage tank due to external fire.
3. Premature operation of the air-operated valve.
4. Leakage from cryogenic pump due to seal failure or installation error.
5. Premature operation of the cryogenic pump due to controller failure.
6. Leakage from fittings and connecting piping in the evaporator.

Table 3-11: Storage subsystem identified liquid hydrogen-related failure modes.

Item	Failure Cause	Failure Mode	Severity	Probability	Risk	Notes
Storage Tank	Fittings fail due to manufacturing defect or installation error	Failure to meet functional specifications	Minor	Medium	L	Evaporation rate is required to assess liquid/gaseous release scenario.
	Tank rupture due to accident or collision	Failure conditions caused by the operational environment	Critical	Low	M	
	Failure of outer tank wall due to external fire	Failure conditions caused by the operational environment	Critical	Low	M	Loss of insulation would cause evaporation before effective leakage; hence risk is related to GH_2.
Pressure Sensor	Circuit malfunction due to cryogenic temperatures	Failure conditions caused by the operational environment	Moderate	Low	L	Early detection of malfunction should reduce potential risk.
Pressure Relief Valve	Malfunction due to cryogenic temperatures	Failure conditions caused by the operational environment	Critical	High	H	Loss of insulation would cause evaporation before effective leakage; hence risk is related to GH_2.

The complete list of failure modes identified in the storage design are presented from A-Table 37 to A-Table 47. Here, failure modes which are particularly affected by LH_2 are highlighted in blue.

Table 3-12: Control subsystem identified liquid hydrogen-related failure modes.

Item	Failure Cause	Failure Mode	Severity	Probability	Risk	Notes
Air operated valve	Mechanical failure, unable to close	Failure to meet functional specifications	Minor	Medium	L	Evaporation rate is required to assess liquid/gaseous release scenario
	Operation failure	Premature operation	Critical	Low	M	Evaporation rate is required to assess liquid/gaseous release scenario
	Operation failure	Failure to operate at prescribed time	Critical	High	H	Evaporation rate is required to assess liquid/gaseous release scenario

Table 3-13: Process subsystem identified liquid hydrogen-related failure modes.

Item	Failure Cause	Failure Mode	Severity	Probability	Risk	Notes
Cryogenic Pump	Leakage from pump due to seal failure or installation error	Failure to meet functional specifications	Moderate	Medium	M	Evaporation rate is required to assess liquid/gaseous release scenario
	Pump operates prematurely due to controller failure	Premature operation	Critical	Low	M	
Evaporator	Leakage from fittings and connecting piping	Failure to meet functional specifications	Moderate	Medium	M	
	Rupture due to collision or accident	Failure conditions caused by the operational environment	Critical	Medium	H	

3.4.3. Discussion of Identified Risk Scenarios

This following analysis is based on the reviewed literature regarding storage components and the effect of hydrogen on surrounding infrastructure. It should be noted that the three high-risk failure modes identified can lead to unintended release of hydrogen in both liquid and gaseous forms, depending on conditions of the release. However, the evaporation rate is required to assess the transition between liquid/gaseous release scenarios. Further, risks related to leakage and rupture of the storage tank and cryogenic pump are considered less probable than in components which have not been specifically designed for cryogenic temperatures (evaporator, instrumentation, etc.).

Regarding the storage tank, these double-walled cryogenic vessels are constructed with a vacuum jacket which serves as an additional safety barrier for leaks and ruptures. Also, hydrogen has a low adiabatic expansion energy at cryogenic temperatures [77]. This would imply that in the case of leakage or tank rupture, immediate ignition of the release hydrogen at cryogenic temperatures is unlikely. However, the low temperatures can damage adjacent valves or pressure relief devices which have not been designed for operating under cryogenic conditions [7]. Additionally, leakage and ruptures have varying consequences whether there is a loss of insulation prior to the leakage. In this scenario, loss of insulation would result in the vaporization of the hydrogen and the development on the GH_2 release events [41]. On the contrary, if the leakage or rupture compromises both barriers instantly, LH_2 will be released.

Double-walled vacuum-insulated pipes are also used in the sections in contact with LH_2 at low temperatures. As the volume of hydrogen transported is minor in comparison to the storage tank, only risks related to leakage through the outer wall are considered. At

low temperatures, effects other than hydrogen embrittlement must be considered. Examples of these are the change of mechanical characteristics, thermal expansion and contractions phenomena and brittleness [78]. The likelihood of leakage events due to stress cycling and exposure to low temperatures during operation have not been quantified. Thus, additional safety measures regarding instrumentation, valves, pump, and evaporator should be considered in the future. For this reason, special attention should focus on the evaporator given the amount of hydrogen fuel stored within (hence a high severity class). The initial design on the station does not include the dimensions of this component, nor it is specified which special safety measures it counts with to counter the effect of both the GH_2 (embrittlement) or the thermal cycling due to the LH_2 entering at cryogenic temperatures.

These failure modes identified serve as a basis for the use of failure logic-modeling tools in the QRA context, as well as the resulting data collection priorities presented in Chapter 4.

Chapter 4. Quantitative Risk Analysis of LH_2 Storage System

Hydrogen infrastructure is susceptible to hazards caused by undesired hydrogen releases, both in liquid and gaseous states. The cause, frequency, and consequences of hydrogen releases have been studied in the context of risk assessment and mitigation, leading to safer designs. In this chapter, the high-risk scenarios identified in the LH_2 storage system are developed and the structural reliability of the system is assessed. Based on the analysis of hydrogen-related risk and reliability databases, it is determined that there is insufficient data to support the quantification of a full risk assessment in LH_2 systems. Thus, the analysis is carried out semi-quantitatively based on generic industry data and supported by the review of previous work which address hydrogen LH_2 infrastructure. The work developed includes ESDs and FTAs built for the most severe risk scenarios identified and initiating leak events. Finally, recommendations regarding frequency data requirements to enable the full development of these tools are discussed.

4.1. Methodology

The following section refers to the methodology followed to analyze the generic LH_2 storage system defined in Section 3.2. Insights derived from the developed FMEA and risk scenario identification shed light on the current frequency data requirements, as well as considerations for future risk assessments and advanced reliability tool incorporation to the analysis of LH_2 storage systems.

4.1.1. Review of Hydrogen-related Reliability Data

A comprehensive and representative frequency database is needed to support the development of credible QRAs. As reviewed in Section 2.3, hydrogen risks are characterized by component leak frequencies. A review of publicly available hydrogen

accident and leak frequency databases is required to identify useful sources and information gaps regarding LH_2 risks. This review includes safety and maintenance reports from currently operating hydrogen fueling stations in the U.S. and from generic industry failure databases.

4.1.2. Event Sequence Diagrams and Fault Trees

Logic-modeling techniques such as ESDs are employed to develop the high-risk scenarios identified. These tools are graphical representations of specific series of events which may lead to an accident. In this work, ESDs are developed for the high-risk scenarios identified through the FMEA and risk-ranking process. These are based on the ESDs developed for GH_2 releases defined in the HyRAM software (addressed in Section 2.3.1 and Appendix D.1.) and adapted to include LH_2 releases, which ultimately can also lead to the GH_2 accident scenarios. The construction of the ESDs is aimed at identifying current data gaps to quantify LH_2 release scenarios.

4.1.3. Fault Tree Analysis

An FTA is carried out on the LH_2 storage system designed. This incorporates hydrogen-specific and generic industrial failure data from dedicated sources discussed in Section 4.2. Once the fault tree's minimal cut-sets are known, the reliability or the unavailability can be calculated through the quantification of these minimal cut-sets. By incorporating failure rates and frequencies, the storage subsystem's overall unreliability is estimated through the use of Trilith software [79]. Finally, the relative importance of each cut-set of component failures is analyzed and ranked. A relevant result to this analysis is the identification of which component failures should be further studied or monitored, with

the purpose of preventing unexpected failures in the system and reducing unexpected downtime of the stations.

4.2. Survey of Available Frequency and Reliability Data Sources

Data collection and analysis are fundamental components of risk and reliability assessments. The need for comprehensive databases regarding multiple aspects of hydrogen systems is still a remaining challenge, in particular for LH_2 technologies [7]. In this section, available hydrogen failure data for traditional reliability frameworks is discussed to frame the development and quantification of the risk scenarios identified.

4.2.1. Hydrogen Frequency Data Sources

Reliability, safety, and performance data collection from operational hydrogen fueling stations is a valuable initiative to characterize in-situ behavior of component failures. The quantification and analysis of the availability of station components and fueling capability is fundamental to understand the current state of technology deployed. Through the "Hydrogen Station Component Validation" Project developed by NREL [80], [81] in cooperation with the CEC, industrial data collaborators deliver periodic performance safety and incidents reports. Internal processing and analysis lead to the preparation of Composite data Products (CDPs) [82], in which data is aggregated across multiple systems, sites, and teams. This, with the objective of publishing useful information without revealing proprietary data of said data providers and collaborators. These include stations funders, station providers, and other organizations who participate in the hydrogen station communities. CDPs have been published since 2012 and are currently updated each six months.

The main data types reported in NREL's CDPs cover energy, reliability, safety, performance, cost, deployment, and utilization aspects of the stations. The data collection tool consists of a template for reporting data from hydrogen infrastructure and is divided into reports covering all stations and only retail stations. Given the nature of both types of stations, there are some inconsistencies regarding the level of detail collected from the maintenance and safety reports. Fuel log records, safety and leaks checks, and maintenance events are recorded, enabling the estimation of time between fueling events and overall unavailability of the retail stations.

Maintenance events are dominated by failures at dispenser subsystems. Safety reports by equipment indicate that dispensers (including hose and nozzle) present the highest number of leakage events, as shown in Figure 4-1 for retail stations in 2019 and in Figure 4-2 for all stations in 2018 [80]. Further, failures at the compressor and chiller components are also significant. Pipes, fittings, and valves, as well as sensors and storage are also mentioned in the reports. GH_2 releases with no accumulation and equipment malfunction are the events most often described. Additionally, NREL has determined key measurement locations for leak rates in dispenser cabinets and compressor systems. In dispenser cabinets, leaks are typically small and slow, occurring through valves. They may occur over a relatively long period of time and can go unnoticed for a significant time. In compressor systems leaks frequently develop from seal failures and can result in larger and shorter leaks compared to the dispenser systems [83].

This type of information is crucial to develop station- and component-level reliability models, enabling the prediction of type and duration of maintenance events. However, as information is recollected through manual reporting tasks, the quality of the

data can vary significantly from station to station. In particular, safety and maintenance events are estimated to be the most under-reported section, limiting the utility for scenario development or consequence data. Figure 4-3 presents a breakdown of these maintenance and safety incident reports by primary factors, equipment involved, and event descriptions. Based on these reports, the most frequent cause of station or dispenser unavailability is inadequate or non-working equipment, the most common being the fueling hoses, and most likely leading to minor GH_2 leakage events. It must be noted that there is a significant number of events with an undefined cause (Figure 4-3a). Similar information is presented in Figure 4-4 presenting all the safety records from stations during 2018.

(a) Maintenance hours: Total 22,807 hours and 77% unscheduled.

(b) Maintenance events: Total 10,074 events and 65% unscheduled.

Figure 4-1: Maintenance by Known Equipment in Retail Stations. NREL (2019).

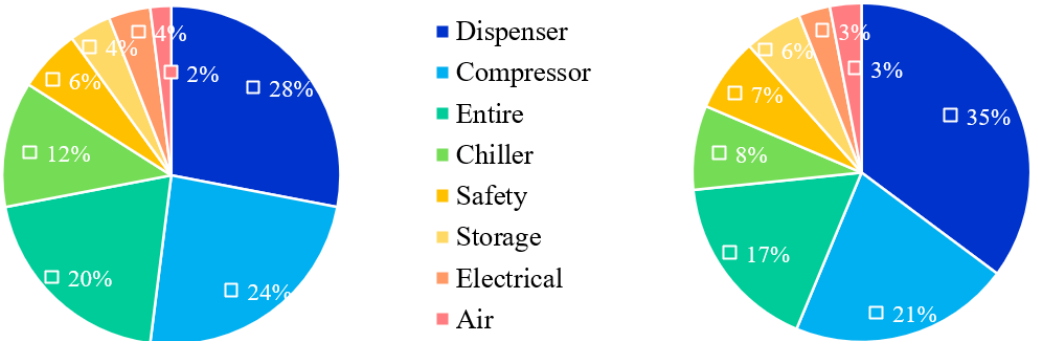

(c) Maintenance hours: Total 23,907 hours and 58% unscheduled.

(d) Maintenance events: Total 7,913 events and 57% unscheduled.

Figure 4-2: Maintenance by Known Equipment in all Stations. NREL (2018).

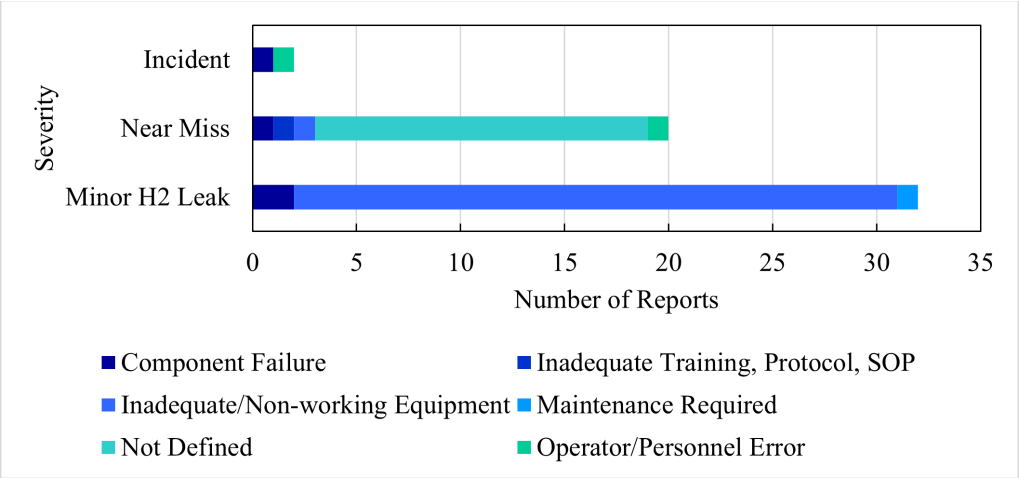

(a) By Primary Factor

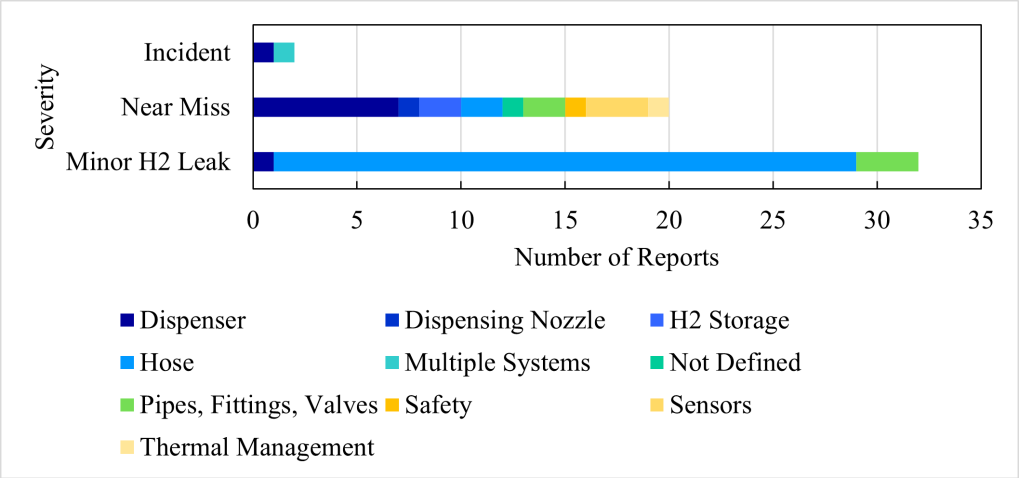

(b) By Equipment Involved

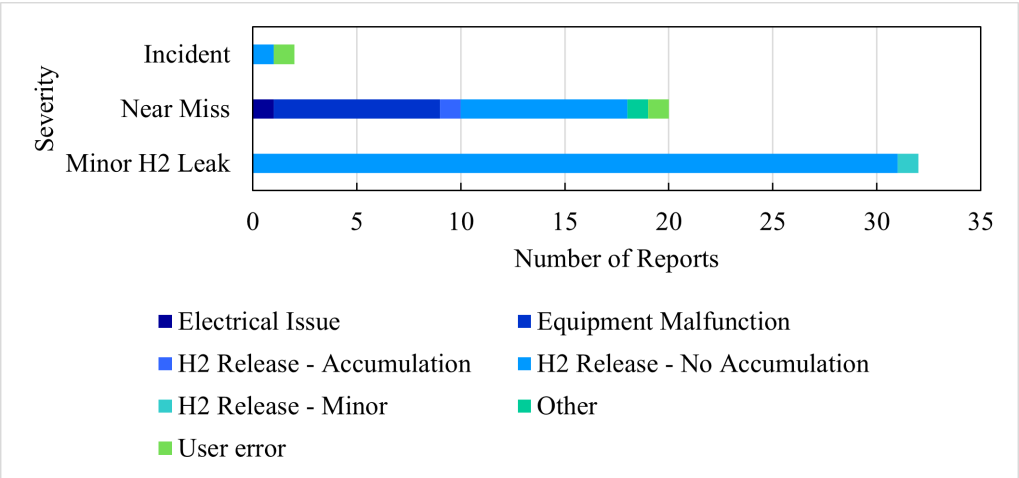

(c) By Event Description

Figure 4-3: Safety Reports in Retail Stations. Adapted from NREL CDPs (2019).

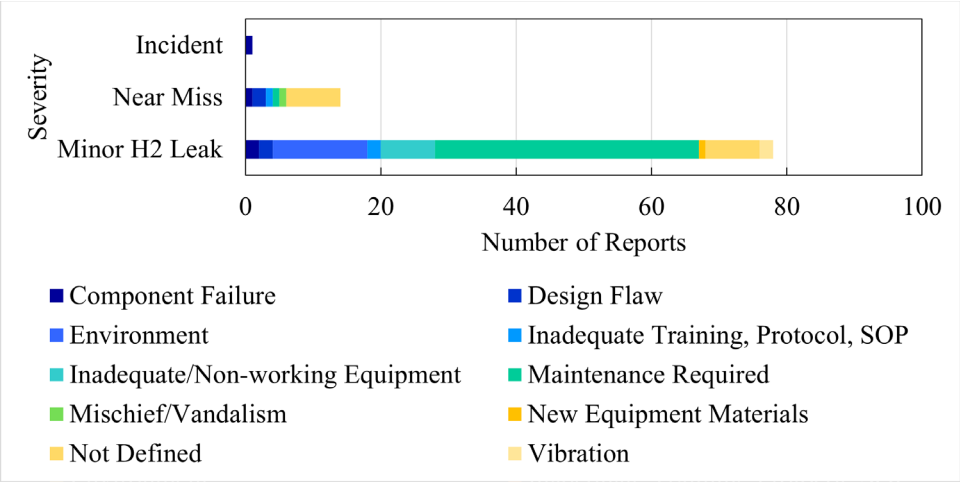

(a) By Primary Factor

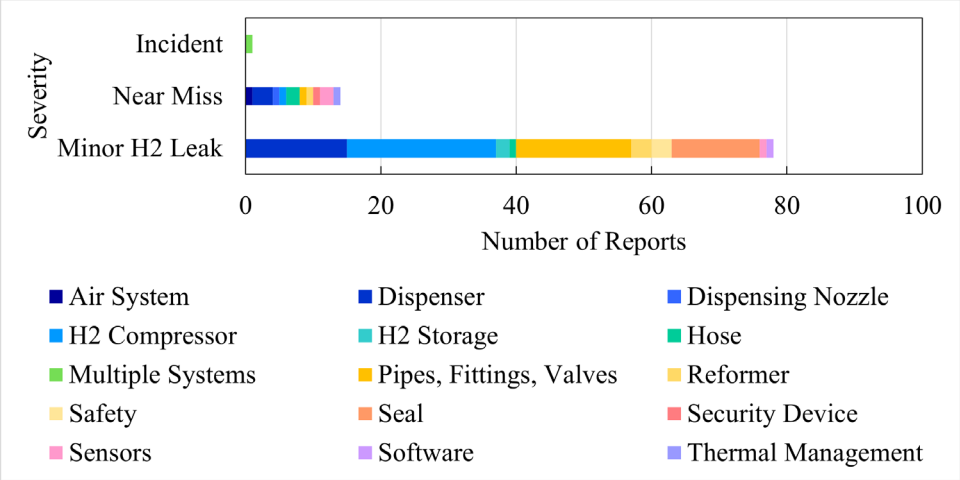

(b) By Equipment Involved

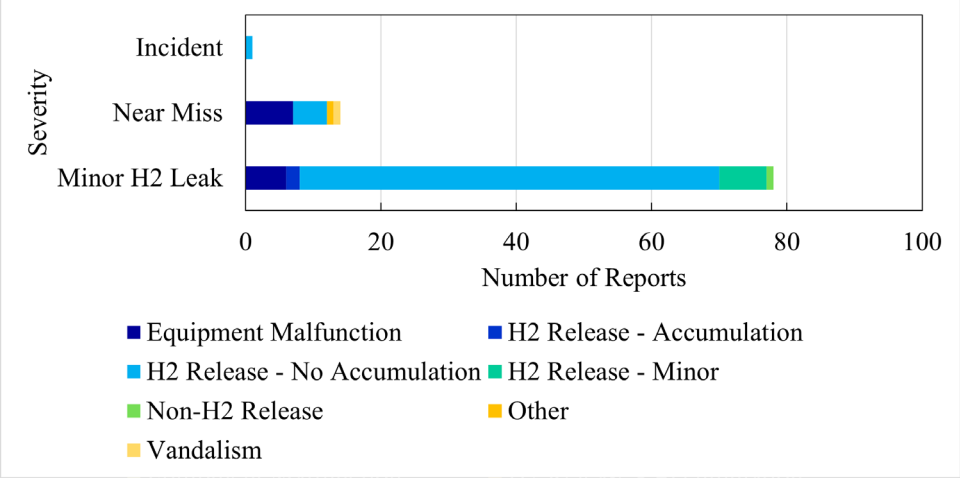

(c) By Event Description

Figure 4-4: Safety Reports in all Stations. Adapted from NREL CDPs (2018).

Further, information collected from maintenance records allows the breakdown of failed parts per component for some of the most relevant elements of the system. An example is shown in Figure 4-5 for the compressor from information gathered in retail stations.

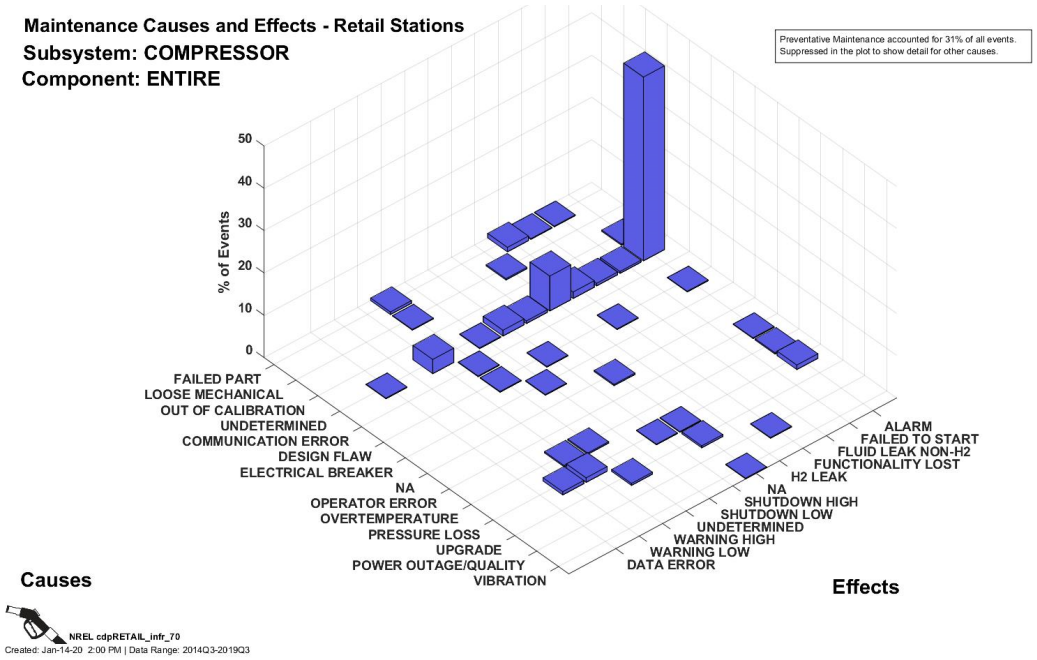

Figure 4-5: Example of maintenance causes and effects analysis. NREL (2020).

However, it should be noted that the majority of the reported maintenance events fall under the category 'undefined'. For this reason, the initial reliability models developed for hydrogen fueling stations refer to general failures and as a function of either number of fills or amount of hydrogen dispensed. Figure 4-6 presents the determined failure rate by number of fills based on the historic collected data.

Overall, documented failure frequency and probability data specific to hydrogen systems is limited, given the low number of stations deployed worldwide and the sensitive nature of failure or maintenance-related information [48]. More so, is failure and

degradation data related to the effect of cryogenic temperatures on the system's components for risk assessment purposes, as the number of operational LH_2-based stations is significantly lower than their gaseous counterpart [80]. Given the limited availability of reliable failure frequency data specific to hydrogen infrastructure, many works have utilized generic industrial data, reduced records from accidents in hydrogen systems, and incorporated Bayesian analysis to address the uncertainties these estimations carry.

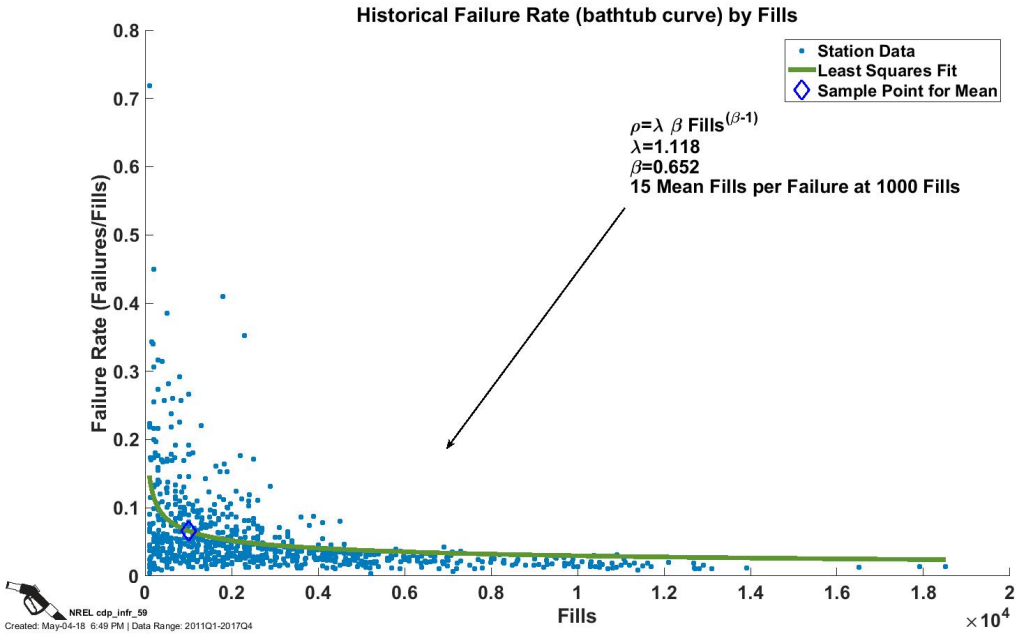

Figure 4-6: Historical Failure Rate Estimation by Number of Fills in hydrogen fueling stations. NREL (2020).

4.2.2. Data Sources from Other Industries

Documented frequency failure data is scarce, limiting the development of credible QRAs for hydrogen fueling station permitting processes. Thus, analysis must rely on up-to-date industrial failure data and adapted to on-site conditions through Bayesian approaches as discussed in Section 2.3.2. During the development of the HyApproval project under the European Integrated Hydrogen Project (EIHP2), a survey of reliability

data sources relevant to hydrogen systems was conducted [84]. Aimed at the publication of a standardized Handbook for Approval of Hydrogen Refueling Stations [85], the project determined that documented failure data in hydrogen systems were limited. Thus, they concluded that QRA and reliability analysis were to be conducted relying on up-to-date failure data from similar industries. The Identification and Review of Databases for Reliability Data [86] reported several data sources pertinent to hydrogen systems. Some of the most current versions of the reliability data sources are described below:

- The Offshore Reliability Data Handbook, OREDA Handbook (2015), 6th edition – Volume I. The intention of the handbook is to provide both quantitative and qualitative information as a basis for Reliability, Availability, Maintainability, and Safety (RAMS) analyses [87].
- The 'Purple Book': Guideline for Quantitative Risk Assessment in the Netherlands (2001) [33]. This handbook contains failure frequency data for general industrial components, denominated as 'Loss of Containment' (LOC).
- SINTEF PDS Data Handbook: Reliability Data for Safety Instrumented Systems (2013). Data dossiers for field devices (detectors, transmitters, valves, etc.) and control logic (electronics) are presented [88].
- RMQSI – Nonelectric Parts Reliability Data (2016) Quanterion. This publication provides historical reliability data on a wide variety of part types [89].
- SwedPower: T-Book, Reliability Data of Components in Nordic Nuclear Power Plants (2005). Data collection of Swedish nuclear power plants the Finnish company TVO [90].

- Concawe: Western European Cross-country oil pipelines, 30-year performance statistics, report no. 2/02 (2002) [91].

Based on the assessment presented in [86], OREDA has been considered the most relevant database as it is based on data from the oil and gas industry. Regarding safety-related equipment, the SINTEF PDS is considered as an important database, also based on data from the oil and gas industry. The T-book has been mostly used for reliability analysis of electrical equipment, as this is not covered in depth by the previous sources. Concawe is also recommended for pipeline reliability.

In both OREDA and *The Purple Book*, hydrogen-specific and cryogenic-related failure probabilities remain unquantified. Yet, these failure probabilities and frequencies can still be incorporated for risk quantification using a Bayesian approach. Both sources contain information from similar fluids and represent the most robust starting point for further analyses.

4.3. Results of QRA for LH_2 Risk Scenarios

This section consists of the documentation regarding the main results derived from applying risk and failure logic-modeling tools used in QRAs to the selected LH_2 storage system. Firstly, the high-risk scenarios identified through the FMEA process are developed and described through separate ESDs, considering they could have significantly different frequencies of occurrence. Secondly, based on an analysis of generic industrial data from the OREDA database and *The Purple Book*, an estimate of the storage system unreliability is obtained, as well as a ranking of the cut-sets leading to unexpected LH_2 releases.

4.3.1. Event Sequence Diagrams for High-Risk Scenarios

The identified high-risk failure modes described in Section 4.2.2 can potentially lead to unintended release of hydrogen in both liquid and gaseous forms. Hence, there is a need to identify and describe risk scenarios related to LH_2 releases. These risk scenarios are developed below. However, the complexity of the new scenarios depends on physics and probability data not yet fully developed. This section is divided in a discussion regarding the ESD events probabilities of occurrence and the construction of separate ESDs for each high-risk scenario identified.

4.3.1.1. ESD Transition Probabilities

The proposed ESDs models are based on HyRAM's ESD for GH_2 releases, however an updated ESD should incorporate a prior event of LH_2 release. A general draft of this ESD concept is presented in Figure 4-7. A summary of the GH_2 and LH_2 events represented in this diagram are found in Table 4-1 and Table 4-2.

The release of LH_2 may lead to either GH_2 or LH_2 specific risks, such as the ones described in Appendix D.1. as well as scenarios unique to cryogenic liquid releases such as pooling and the formation of a cryogenic plume. Both these events should be described in depth and supported with experimental data as a method to quantify potential damages caused by these prior or in combination with GH_2-related scenarios. Further, there is a need for more scientific information on how system operational conditions (e.g., pressure and temperature) affect the release behavior of *liquid* hydrogen. These could potentially affect the likelihood and consequences of immediate and delayed ignition and thus the overall system risk, leading to a different risk profile than that of GH_2 releases.

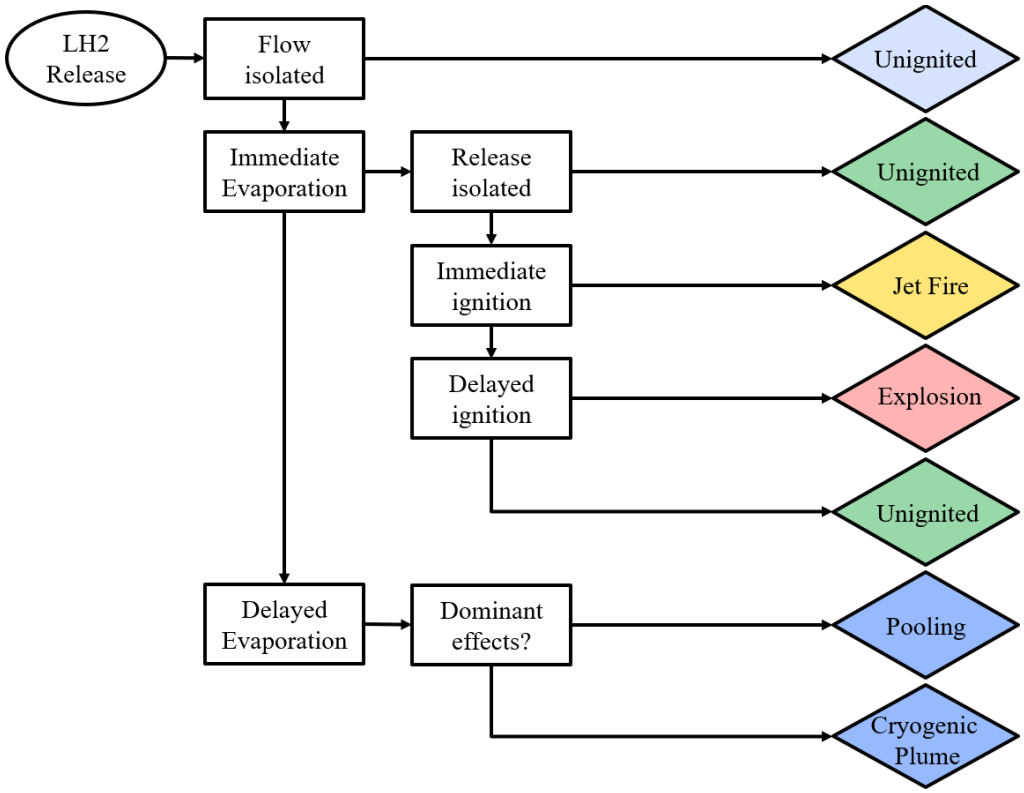

Figure 4-7: Proposed Event Sequence Diagram for LH_2 releases.

Table 4-1: ESD General Release Event Description. To be continued.

ESD Event	Data Type	Source	Notes
Component leak frequencies for GH_2	Release frequencies obtained for components per leak size.	HyRAM	See D.1.
GH_2 Release Detection	Constant Probability Value	HyRAM	See D.1.
GH_2 Immediate Ignition	Constant Probability Value	HyRAM	See D.1.
GH_2 Delayed Ignition leading to Explosion	Constant Probability Value	HyRAM	See D.1.
GH_2 Unignited Release	Constant Probability Value	HyRAM	See D.1.

Table 4-2: ESD General Release Event Description. Continued.

ESD Event	Data Type	Source	Notes
Component leak frequencies for LH_2	Release frequencies obtained for components per leak size.	N/A	Component reliability data describing failure modes that lead to LH_2 releases could also be used.
LH_2 Release Detection	Constant Probability Value	N/A	A priori the same value for GH_2 detection and isolation could be used. Depends on detection method.
LH_2 Immediate Evaporation	Constant Probability Value	N/A	Possible dependency on physics-based model.
LH_2 Delayed Evaporation leading to Pooling	Constant Probability Value	N/A	Possible dependency on physics-based model.
LH_2 Delayed Evaporation leading to Cryogenic Plume	Constant Probability Value	N/A	Possible dependency on physics-based model.

4.3.1.2. ESD Construction

In this context, conceptual ETAs are proposed for the three high-level risks identified through the FMEA shown in Table 4-3. These are qualitative in nature and further argument the need for specific LH_2 leak frequency data to adequately characterize different form of LH_2 releases and relevant consequences.

Table 4-3: Identified liquid hydrogen-related high-risk failure modes.

Item	Failure Modes and Causes	Failure Mode Model	Notes
Pressure Relief Valve	Malfunction due to cryogenic temperatures	Failure conditions caused by the operational environment	Loss of insulation would cause evaporation before effective leakage; hence risk is related to GH_2
Air operated valve	Operation failure	Failure to operate at prescribed time	Evaporation rate is required to assess liquid/gaseous release scenario
Evaporator	Rupture due to collision or accident	Failure conditions caused by the operational environment	Evaporation rate is required to assess liquid/gaseous release scenario

In the case of "High-risk scenario 1 - Malfunction due to cryogenic temperatures of the pressure relief valve system" presented in Figure 4-8, it appears evident that if the increase of pressure within the storage tanks leads to leakage or burst of the inner tank, the loss of thermal insulation and subsequent evaporation would directly lead into the already determined ESDs regarding GH_2 releases. This scenario is considered more likely than a burst of the outer tank due to the expansion of the evaporating hydrogen (which would lead to a mixed release) or a complete burst of the storage tank (inner and outer walls) due to overpressure based on the cited literature [7], [41], [77].

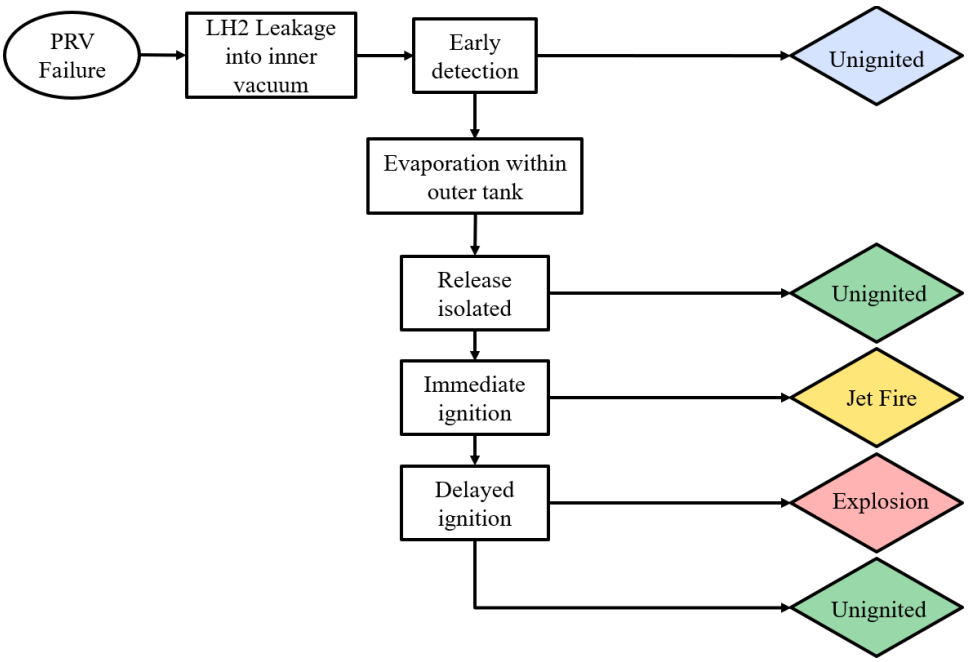

Figure 4-8: High risk scenario 1 - Malfunction of the pressure relief valve system.

Figure 4-9 presents the developed sequence for "High-risk scenario 2 - Operation failure at prescribed time of the air-operated valve". Here, the scenario caused by the repeated malfunction of the air-operated valve could lead to a reduced flow towards the cryogenic pump. This, as the valve's normal position is closed, pressurized air opens the valve in "active" state, and it has a return spring mechanism for return to normal state.

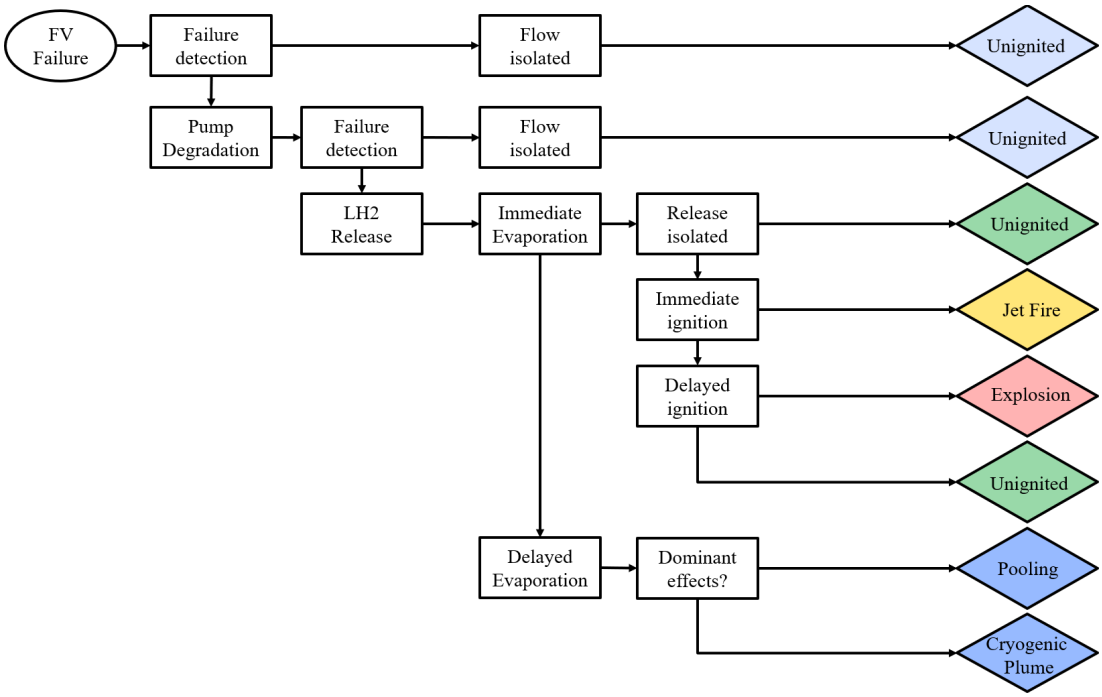

Figure 4-9: High risk scenario 2 - Operation failure of the air-operated valve.

Failure to close of the FV valve may cause pressure issues upstream, however other control mechanism may interact to reduce associated risks. Failure to open, on the other hand, may result in pressure issues upstream (regulated with the pressure relief valve, refer to high-risk scenario 1) and potential damage to the cryogenic pump's operation. This scenario refers to the latter risk, where if early failure detection procedures are implemented, pump seal degradation or more serious pump degradation scenarios (i.e., cavitation) could be avoided. If the disruption of normal operation of the pump continuous unnoticed it may be damaged and LH_2 leakage may occur. The consequence of this depends on the magnitude of the leakage, as small leakages, could lead to the already described GH_2 release scenarios. For greater leakages (plume) or other conditions which lead to delayed evaporation (pooling), ignition probabilities have not been quantified, yet could lead to jet fires, flash fires, or explosions, additional to the potential damage of other infrastructure due to cryogenic temperatures.

In the case of "High-risk scenario 3 - Rupture due to collision or external accident of the evaporator", the development is similar to the high-risk scenario 2. However, as shown in Figure 4-10, in this case that leakages lead to evaporated GH_2 ignition, if LH_2 still remains in the evaporator, the resulting ignition of mixed hydrogen may result in consequences not contemplated by the implemented harm models.

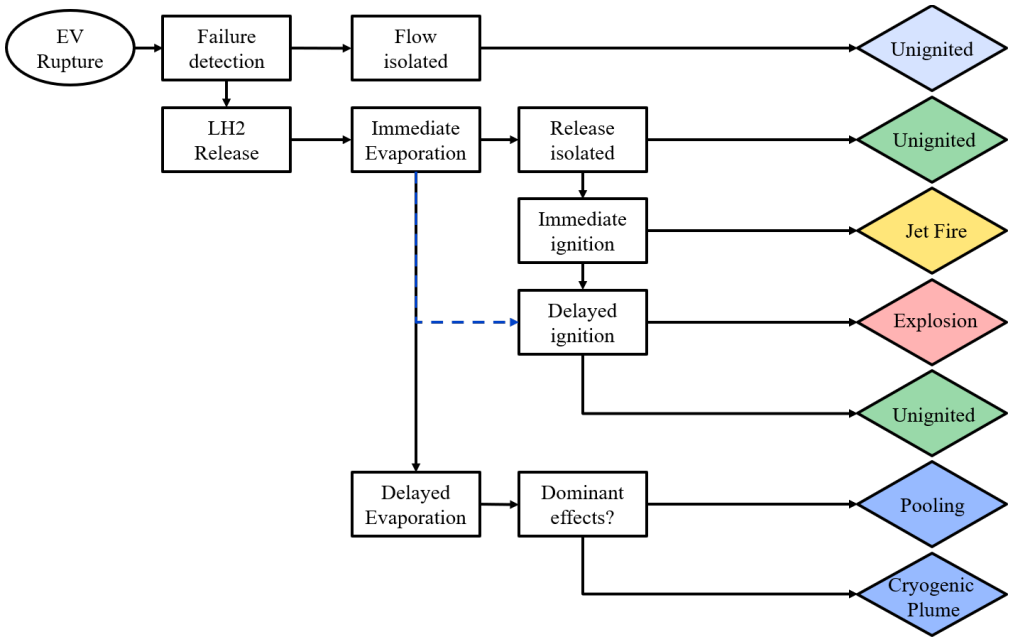

Figure 4-10: High risk scenario 3 - Rupture of the evaporator.

4.3.2. Fault Trees for LH_2 Release Initiating Event

An FTA is carried out with the purpose of determining a general initiating event frequency for LH_2 release in the system described in Figure 4-7. This section is divided into a discussion of failure data (i.e., probabilities and rates) to support the FTA, the construction of the fault tree based on the most prominent failure modes identified in the literature, followed by the evaluation and analysis of the model.

4.3.2.1. FTA Failure Probabilities

Failure mode taxonomies and leak frequency data are based on OREDA and *The Purple Book* failure and leak frequency data, yielding an initial estimation of the LH_2 storage system's reliability. Both these inputs are valuable for FMEA and FTA analysis, primarily, as a method to prioritize failure modes to monitor in the system. OREDA holds a collection of failure data, failure modes, and failure mechanisms recorded for specific components in engineering systems. This includes data regarding pumps, electric motor, valves, instrumentation input devices, heat exchangers, and process vessels, among others. Each equipment type is described as a function of their subcomponents and corresponding *maintainable items*. Each failure mode is associated to the most probable combination of a maintainable item and failure mechanism. A list of relative contributions of each maintainable item and failure mechanisms to the total failure rate is presented decomposed for each failure mode. A detailed analysis of the OREDA data and the relative importance of failure modes of the main LH_2 storage systems was carried out in Appendix D.2. , cross-referencing with the identified risk scenarios previously developed. Table 4-4 presents the failure modes selected as relevant for the analysis of the LH_2 storage system.

Table 4-4: Relevant Failure Modes from OREDA database.

FM	Description	FM	Description
AOL	Abnormal output - low	FTF	Fail to function on demand
ELP	External leakage - process medium	NOO	No output
ELU	External leakage - utility medium	STD	Structural deficiency
ERO	Erratic output	VIB	Vibration

The Purple Book reports 'Loss of Containment' (LOC) event frequencies for various components and installation configurations. These LOC frequencies refer to random events under normal operational conditions for various pressure and atmospheric tanks, pipelines, pumps, heat exchangers, and pressure relief devices models. Leakage

events are further classified by their type and severity, e.g., instantaneous release of complete inventory or continuous release from specific hole diameters. It also allows to characterize external accidents leading to LOC events by modifying reported frequencies by a factor of $5 \times 10^{-6}\ yr^{-1}$. Failure frequencies reported in *The Purple Book* are more general in nature, except for LOC events in storage tanks (See Appendix D.3.). For this reason, OREDA data is used to represent specific failures from failure modes identified through the FMEA procedure, while LOC data is used to represent "random failures", i.e.: caused by external events.

4.3.2.2. FTA Construction

An FTA was carried out for the top event "Major Liquid Hydrogen Leakage" in the storage system and supported by the recollected failure data. Each event in the FTA corresponds to a component failure based on the reported data from OREDA and *The Purple Book*. The worst-case scenario is considered for both event development and failure rate data selected. Failure modes and mechanisms were ranked in order of relative importance according to each component to identify relevant information. Corresponding values are summarized in Table 4-5 for OREDA and in Table 4-6 for *The Purple Book*. It is important to note that the available data is generic and does not account for cryogenic temperatures or thermal cycling effects. In the case of OREDA data, calendar time is utilized to characterize most failure rates, with the exception of the pump, as passive leak events are only caused by abnormal operation (i.e., vibration-induced degradation). The following paragraphs describe the modeled failure logic of the system and each identified subevent shown in Figure 4-11.

Table 4-5: Selected Failure Rate values for Top Event: LH_2 Leakage.

System Component	OREDA Component	Severity Class	Failure Mode	Mean	SD	n/t	Time
CNL	Centrifugal Pump in Cooling Systems	Critical	VIB	2.84	2.01	2.84	†
		Degraded	ELP	7.68	3.44	7.68	†
FV	Valves, Shut-off, Ball	Critical	ELU	24.74	24.74	24.74	*
HV-2	Valves, Shut-off, Gate	All modes	All	4.03	5.7	-	*
ZI-ZZO	Input Devices, General	Critical	FTF	1.73	2.11	0.29	*
		Degraded	AOL	0.65	1.02	0.07	*
EV	Heat Exchanger	Critical	ELP	1.3	0.94	1.33	*
		Critical	STD	2.2	2.15	2.67	*
Piping	Vessels	Critical	ELP	2.86	3.73	2.98	*
		Degraded	STD	5.96	2.07	6.39	*
Control System (General)	Control Logic Devices (CLU)	Incipient	FTF	5.21	5.76	5.7	*
Emergency Alarm System	Fire & Gas detectors (F&G)	Critical	FTF	1.02	1.83	1.22	*
		Critical	NOO	0.63	1.11	0.69	*

Note: All failure rates are given in (10^{-6} hrs.). Time: Operational (†), Calendar (*).

Table 4-6: Selected LOC Frequencies for Top Event: LH_2 Leakage.

System Component	Purple Book Component	Failure Mode	LOC (yr^{-1})	Final LOC (yr^{-1})	Failure Rate (hrs.)
Tank	Atmospheric tank with protective outer shell	G1-b	5×10^{-7}	5.5×10^{-6}	1.2×10^{-9}
EV	Dangerous substance outside pipes.	G1	5×10^{-5}	5.5×10^{-5}	6.28×10^{-9}

Note: An external accident factor of 5×10^{-6} (yr^{-1}) is added to the reported LOC values.

External accidents leading to release of hydrogen: This section of the event tree refers to leakage events caused by external accidents such as collisions in storage tank and evaporator (LOC). Both these can result in large amounts of released hydrogen, depending on the size of the rupture.

Large leakage events due to multiple component failures: This section of the event tree corresponds to releases caused by degraded component operation. First, in regard to

the cryogenic pump, the event of vibration-induced structural degradation (VIB) combined with air-valve and the isolation shut-off valve instrumentation (AOL) and control unit failure (CLU-FTF) is considered. Abnormal pressure conditions can be created downstream or upstream due to the air-controlled valve (FV) and the isolation valve (HV-2) failing closed, respectively. Coupled to vibration-induced degradation, repeated occurrences of these failures can lead to leakage events in the pump's connecting elements (fittings and seals), assuming structural integrity of the pump's casing. The detailed model of this section of the fault tree is shown in Figure 4-12.

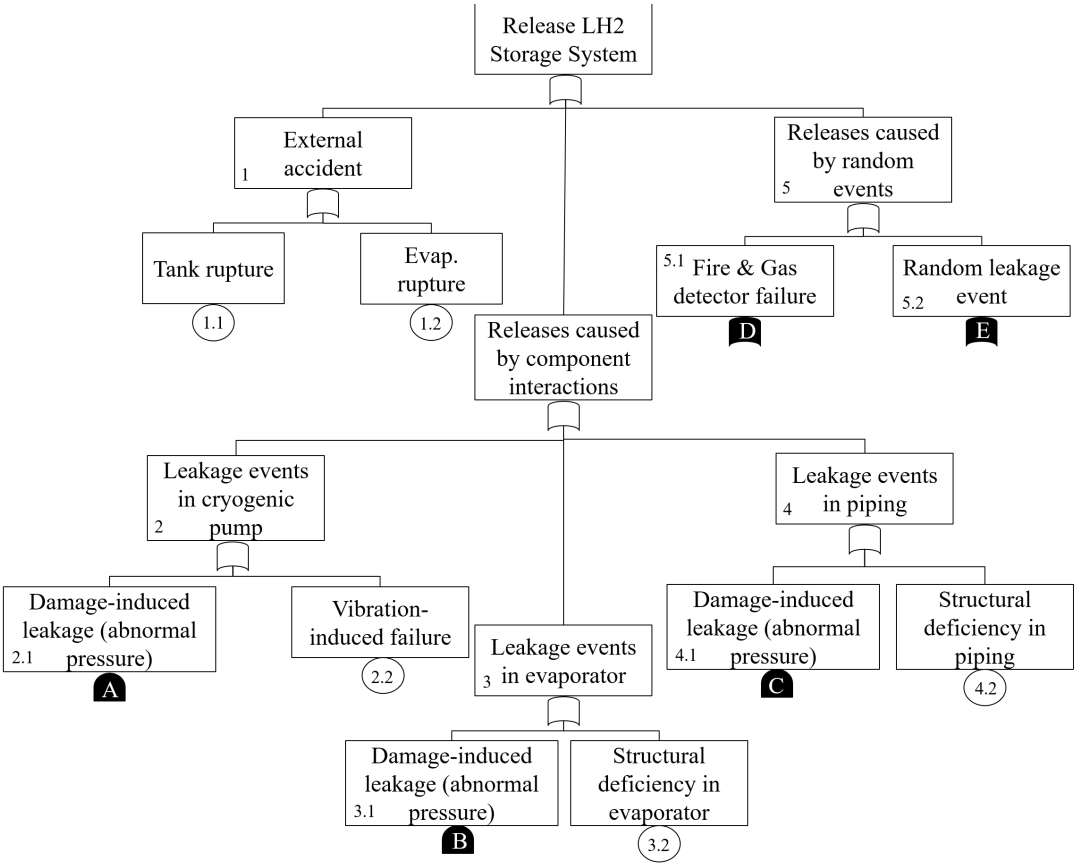

Figure 4-11: Fault Tree Developed for LH_2 Leakage Top Events.

In the case of the evaporator, structural deficiency (STD) combined with pump, air-valve, and isolation shut-off valve instrumentation (AOL) and control unit (FTF) failures

are considered. Similar to the situation described for the pump, abnormal pressure conditions can be created downstream due to the isolation valve (HV-2) failing closed or upstream to the cryogenic pump failing to stop operation (CLU-FTF) while the air-operated valve (FV) has failed open (CLU-FTF). Repeated occurrences of these failures can lead to leakage events in the evaporator's connecting elements (fittings and seals) or casing. The latter could lead to a release of liquid/gaseous hydrogen mixture, as discussed in the previous section. The detailed model of this section of the fault tree is shown in Figure 4-13.

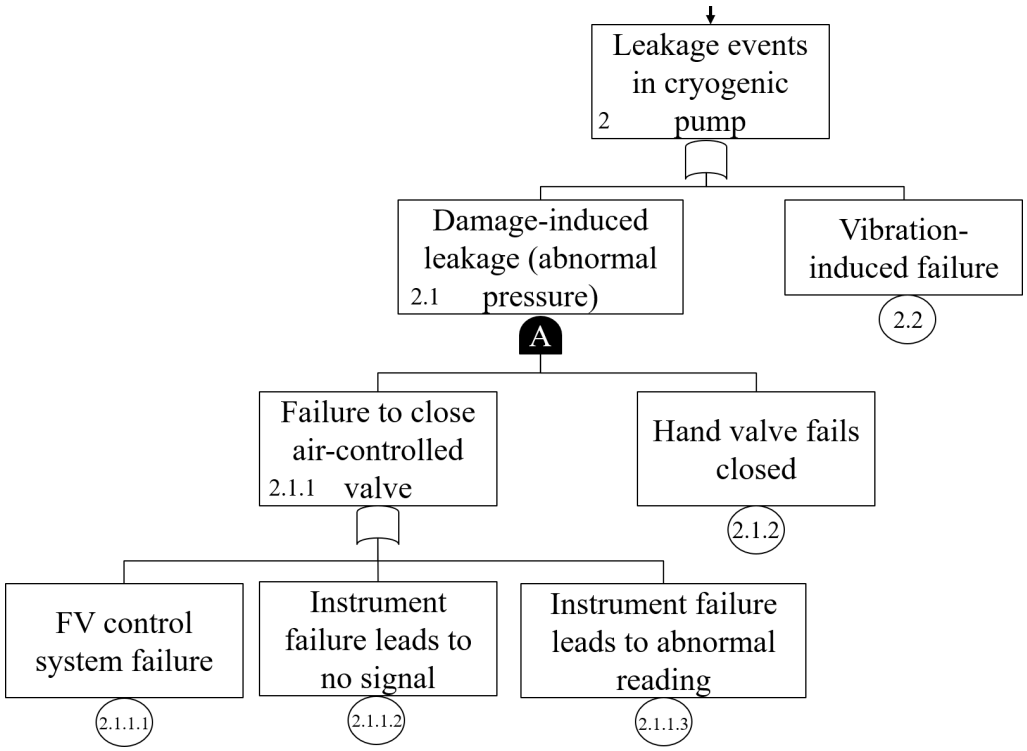

Figure 4-12: Fault Tree Developed Event 2: Pump Leakage Events.

In relation to the piping sections, a combination of failure modes leading to structural deficiency (STD) combined with pump, air-valve, and shut-off valve control unit failure (CLU-FTF) is considered. Similar to previously described leakage events, abnormal pressure conditions can lead to leakage events in the piping's connecting elements (fittings

and seals) or significant structural damage leading to leakage events. The detailed model of this section of the fault tree is shown in Figure 4-14.

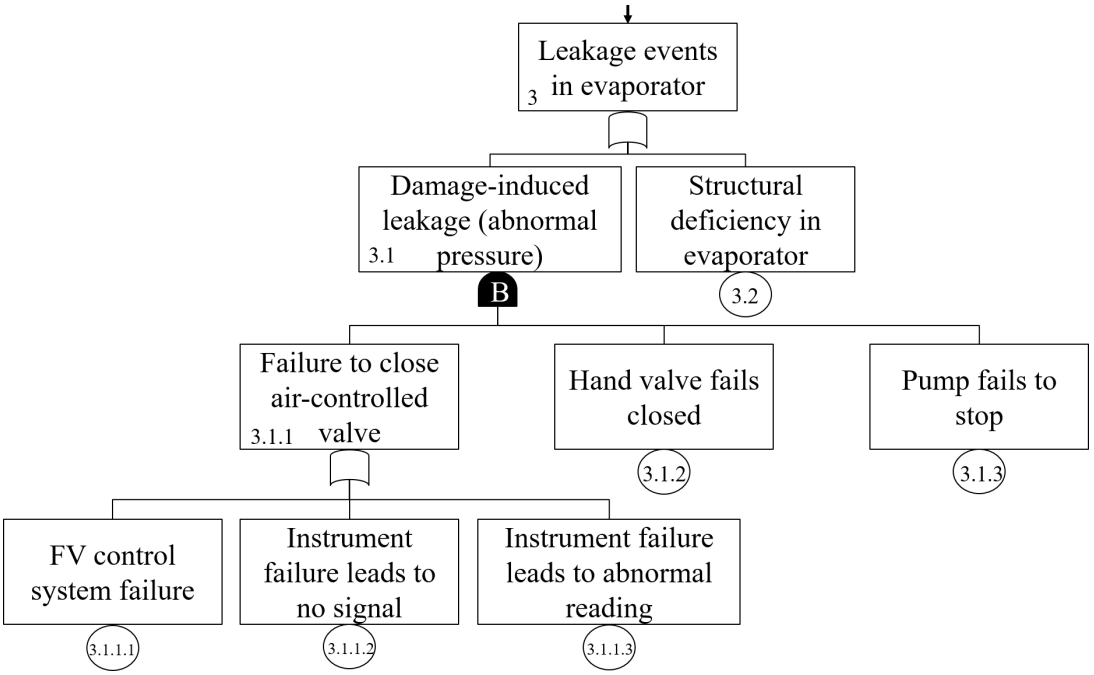

Figure 4-13: Fault Tree Developed Event 3: Evaporator Leakage Events.

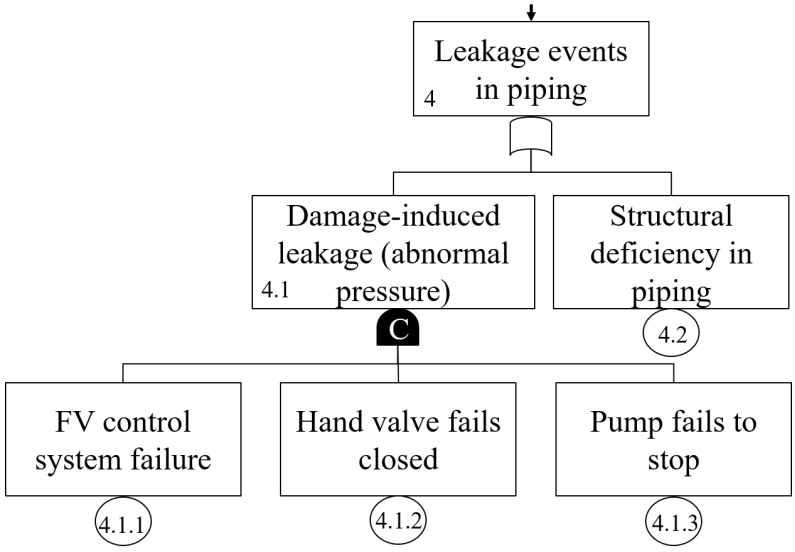

Figure 4-14: Fault Tree Developed Event 4: Piping Leakage Events.

Undetected leakages in various components: This section of the event tree corresponds to random releases of hydrogen in the system, hence, component reliability

related to leakage failure modes (ELU, ELP) is considered. Here, a difference must be made between the elements which contain the LH_2 during operation (such as the piping sections, cryogenic pump, and the evaporator) and those who interact with it under demand (mainly, the air-controlled valve). These leakage failures only lead to the risk of hazardous exposure if these are not detected by the Fire & Gas detectors in the emergency systems (FTF) or fail to shut down the system due to reading failures (NOO). Hydrogen sensors are frequently relied on to determine if a leak has occurred in the system, and further discussion is needed regarding unrevealed leaks and inspection policies [92]. The detailed model of this section of the fault tree is shown in Figure 4-15.

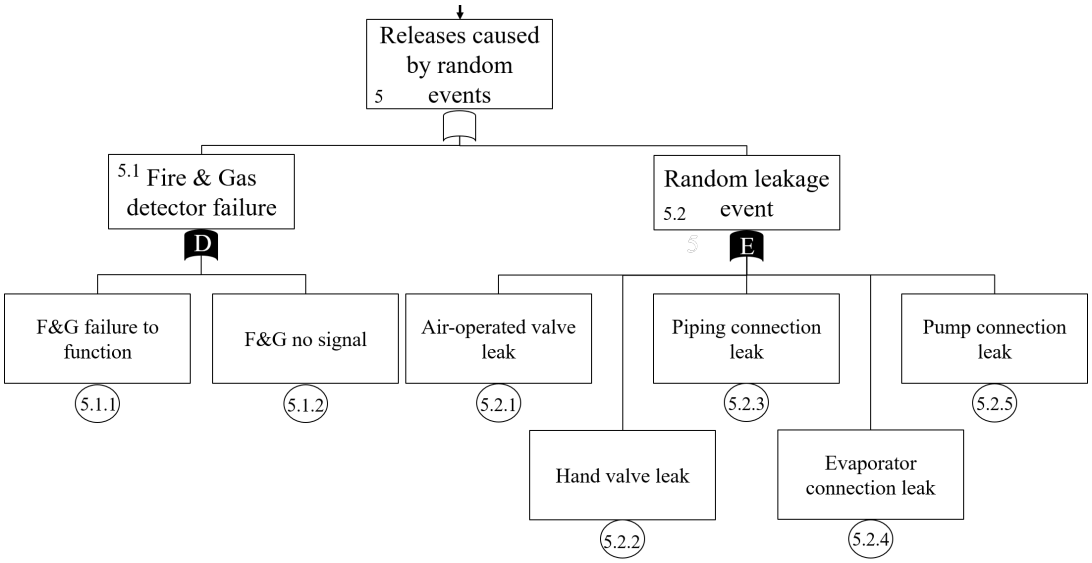

Figure 4-15: Fault Tree Developed Events 4-5 Undetected Random Leaks.

As the worst-case scenario is considered, these events are considered both to contribute separately to the overall failure of the system. The full tree shown in A-Figure 18. The nomenclature used to identify each of the events in the fault tree are described in Table 4-7 and Table 4-8, together with the related failure mode identified.

From this FTA's structure, it can be observed that the most repeated failure events are related to failures of the air-operated valve (FV), leading to abnormal pressure conditions in the piping lines, stressing connecting elements in components. However, it should be noted that under real operational conditions, this is expected to lead to hazardous situations after repeated occurrences or in combination with other degradation factors (such as vibration-induced material fatigue).

Table 4-7: Event Tree Nomenclature. To be Continued.

Event Number	Event Name	Related Failure Modes	Nomenclature
1	External accident		
1.1	Tank rupture	LOC	TK-EXT
1.2	Evap. rupture	LOC	EV-EXT
2	Leakage events in cryogenic pump		
2.1.1.1	FV control system failure	FTF	CLU-FTF
2.1.1.2	Instrument failure leads to no signal	FTF	IN-FTF
2.1.1.3	Instrument failure leads to abnormal reading	AOL	IN-AOL
2.1.2	Hand valve fails closed	FTF	HV-FTF
2.2	Vibration-induced failure	VIB	CNL-VIB
3	Leakage events in evaporator		
3.1.1.1	FV control system failure	FTF	CLU-FTF
3.1.1.2	Instrument failure leads to no signal	FTF	IN-FTF
3.1.1.3	Instrument failure leads to abnormal reading	AOL	IN-AOL
3.1.2	Hand valve fails closed	FTF	HV-FTF
3.1.3	Pumps fails to stop	FTF	CNL-FTF
3.2	Structural deficiency in evaporator	STD	EV-STD

Table 4-8: Event Tree Nomenclature. Continued.

Event Number	Event Name	Related Failure Modes	Nomenclature
4	Leakage events in piping		
4.1.1	FV control system failure	FTF	CLU-FTF
4.1.2	Hand valve fails closed	FTF	HV-FTF
4.1.3	Pumps fails to stop	FTF	CNL-FTF
4.2	Structural deficiency in piping	STD	PIP-STD
5	Releases caused by random events		PIP-STD
5.1.1	F&G failure to function	FTF	FG-FTF
5.1.2	F&G no signal	NOO	FG-NOO
5.2.1	Air-operated valve leak	ELU	FV-LEAK
5.2.2	Hand valve leak	ELU	HV-LEAK
5.2.3	Piping connection leak	ELP	PIP-LEAK
5.2.4	Evaporator connection leak	ELP	EV-LEAK
5.2.5	Pump connection leak	ELP	CNL-LEAK

4.3.2.3. FTA Evaluation

To quantify the developed fault tree based on OREDA and *The Purple Book* databases, it must be noted that both sources consider constant failure rates. Although this is a strong assumption, it can be expected that a component's failure rate to remain constant over its useful life. Further, given that the failure rates λ reported are assumed to be constant over the components' lifetime, the probability that a component fails within T units of time can be expressed as:

$$P(t \leq T) = F(t;\lambda) = 1 - e^{-\lambda t} \qquad (2)$$

The Trilith software was used to quantify the developed FTA and obtain an initial estimation of unreliability of the system. Trilith allows a simple and straightforward construction and quantification of fault trees, in which the probability of the events presented in Table 4-9 were used as input based on the mean values reported for failure

rates. It should be noted that these are the instantaneous values for the probability of failure of each component, which in this case are represented by exponential distributions (i.e., constant failure rate). The calculated unreliability of the overall system and the relative contribution of each minimal cut-set is presented in Table 4-10. This estimation yields an instantaneous unreliability $Q(t) = 1.12 \times 10^{-5}\ yr^{-1}$ which over the course of a year ($t = 8760\ hrs.$) amounts to a 0.1042 probability of failure of the overall system. This is equivalent to a failure occurring roughly each 5.6 weeks. The loss of structural integrity along the piping lines (PIP-STD) is identified as the most significant cut-set, accounting for 53.04% of the estimated unreliability.

Table 4-9: Probability of Failure Events, Trilith Nomenclature.

Component	Failure Mode	Probability (t, hours)	Trilith Nomenclature
CNL	FTF	5.21E-06	CNL-FTF
	ELP	7.68E-06	CNL-LEAK
	VIB	3.07E-06	CNL-VIB
EV	LOC	6.28E-09	EV-EXT
	ELP	1.30E-06	EV-LEAK
	STD	2.20E-06	EV-STD
F&G	FTF	1.02E-06	FG-FTF
	NOO	6.30E-07	FG-NOO
FV	FTF	5.21E-06	CLU-FTF
	ELU	2.47E-05	FV-LEAK
HV-2	FTF	5.21E-06	HV-FTF
	ELU	4.03E-06	HV-LEAK
ZI-ZZO	AOL	6.50E-07	IN-AOL
	FTF	1.73E-06	IN-FTF
Piping	ELP	2.86E-06	PIP-LEAK
	STD	5.96E-06	PIP-STD
Tank	LOC	1.20E-09	TK-EXT

Note: A-Figure 18 replicates the FTA developed, incorporating the Trilith nomenclature for clarification purposes.

This is followed by leakage in the pump (CNL-VIB) and in the evaporator (EV-STD) caused by vibration-induced vibration and loss of structural integrity, respectively.

It should be noted that these events represent 99.93% of probable failures within a year and the downtime of these events could potentially be reduced significantly by introducing adequate monitoring systems and maintenance policies. This effect can be seen by analyzing the 'Random releases' branch in Figure 4-11 where it was considered that leakage events could be detected by the Fire & Gas detectors. Thus, a failure could only occur if the leakages were undetected due to detector failures, such as failure function (FTF) or no signal outputted (NOO). The corresponding probability of failures related to the cut-sets in this branch are lower by several orders of magnitude ($10^{-3} - 10^{-5}\ yr^{-1}$) when compared to unmonitored components (see cut-sets #7-8, #10-12, #14-18 in Table 4-10).

Table 4-10: Ranking of Minimal Cut-sets by Estimated Unreliability.

Ranking	Minimal Cut	Unreliability (t, hrs.)	Unreliability (1 yr.)	Relative %
1	PIP-STD	5.96E-06	5.09E-02	53.04%
2	CNL-VIB	3.07E-06	2.65E-02	27.32%
3	EV-STD	2.20E-06	1.91E-02	19.58%
4	EV-EXT	6.34E-09	5.50E-05	0.06%
5	TK-EXT	1.02E-09	1.05E-05	0.01%
6	HV-FTF, CLU-FTF	2.71E-11	1.99E-03	0.00%
7	FG-FTF, FV-LEAK	2.52E-11	1.73E-03	0.00%
8	FG-NOO, FV-LEAK	1.56E-11	1.07E-03	0.00%
9	HV-FTF, IN-FTF	9.01E-12	6.71E-04	0.00%
10	FG-FTF, CNL-LEAK	7.83E-12	5.79E-04	0.00%
11	FG-NOO, CNL-LEAK	4.88E-12	3.58E-04	0.00%
12	FG-FTF, HV-LEAK	4.11E-12	3.09E-04	0.00%
13	HV-FTF, IN-AOL	3.39E-12	2.53E-04	0.00%
14	FG-FTF, PIP-LEAK	2.92E-12	2.20E-04	0.00%
15	FG-NOO, HV-LEAK	2.54E-12	1.91E-04	0.00%
16	FG-NOO, PIP-LEAK	1.08E-12	1.36E-04	0.00%
17	FG-FTF, EV-LEAK	1.33E-12	1.01E-04	0.00%
18	FG-NOO, EV-LEAK	8.19E-13	6.23E-05	0.00%
	TOP Event	**1.12E-05**	**0.1042**	

However, there are important limitations in this analysis. For instance, events referring to external accidents and resulting LOC events in the storage tank (TK-EXT) and the evaporator (EV-EXT) assume that the frequency of external accidents involving these components is 1 per year. Given specific station data, the relative importance of these failures could increase and warrant either the development of physics-based release models from ruptured components or increased required safety barriers surrounding these components.

Additionally, the selected databases did not provide sufficient information for failure events related to the control and instrumentation systems which repeatedly appeared in the FTA construction. Overall failure rates might be underestimated, as the exposure to cryogenic temperatures is not accounted for and could reasonably lead to shorter equipment lifespans, particularly in connecting elements present in various components. This aspect is further discussed in the following section.

4.4. Discussion and Identified QRA Data Requirements

A first step toward characterizing LH_2 system-related risk scenarios is the identification of relevant failure modes. One means for doing this is through a FMEA, a useful qualitative technique that can be used as a fundamental step in the development of QRAs for hydrogen fueling stations. The QRA analysis primarily refers to risks presented by the liquid hydrogen aspect of LH_2 systems. In the previous chapter, an FMEA process was applied to a generic LH_2 storage design to 1) identify liquid hydrogen-related failure modes and 2) qualitatively assess probability and severity classes. Based on this analysis, the failure scenarios which represent the highest risk of LH_2 releases are:

a) Malfunction due to cryogenic temperatures of the pressure relief valve system in the liquid storage tank.

b) Failure of the air-operated valve between the storage tank and the cryogenic pump.

c) Rupture of the evaporator due to collision or external accident.

These three high-risk failure modes can lead to unintended release of GH_2 and LH_2, depending on the pressure and temperature conditions of the release. To further extend the work, ESDs and FTAs of a the LH_2 storage system were developed and frequency data requirements which will enable QRA on these systems were identified. For instance, leakage and failure rates in different components are fundamental to properly assess risk. While the ESD facilitates the discussion of the sequence of events which lead to specific hazardous scenarios, it also highlights the need to update the transition probabilities between liquid-gaseous events. On the other hand, the FTA enables an initial estimation of the system's unreliability, as well as a structural analysis of its operation and failure. Although several limitations are present in the failure probability quantification process, it has allowed the identification of potential improvements in the design with the inclusion of monitoring systems dedicated to detecting vibration- and abnormal pressure- induced structural damage in the pump, evaporator, and piping lines.

As stated previously, HyRAM is currently incorporating LH_2 consequence models into the risk assessment framework based on ESDs. For this, both the frequency of leakage events and the consequence of the LH_2 release must be considered. In Section 1.1, the data requirements to carry out QRAs for hydrogen systems were discussed. These include valuable contextual information regarding the system, which combined with adequate consequence models and representative accident frequency data, can aid the accurate

estimation of risks present in the system. An updated conceptual diagram of the needed data in LH_2 systems is presented in Figure 4-16.

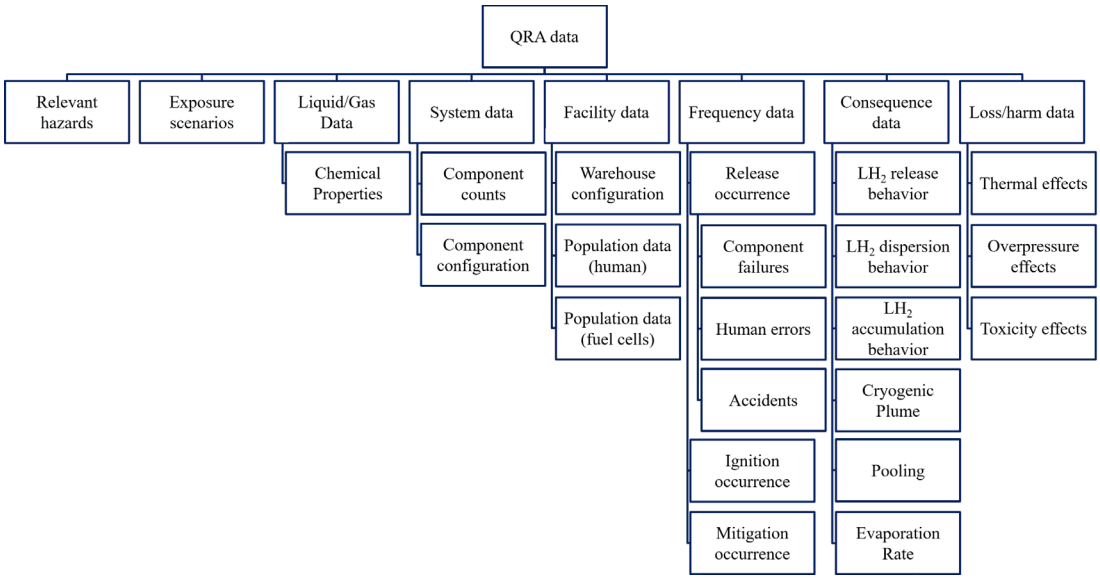

Figure 4-16: Types of data needed to perform QRA for a liquid hydrogen system. Adapted from Moradi and Groth (2019).

Based on the high-risk scenarios identified in the previous section, the following aspects must be considered:

- Physics models describing the effect of evaporation rates on ignition probabilities. Similar to the quantified probability transitioning between jet flame and explosion scenarios caused by GH_2 releases, the probability of a leak to display either evaporation, pooling, or cryogenic plume release behavior in LH_2 releases is relevant to these scenarios. Additionally, their respective ignition probabilities are fundamental for risk assessment procedures, and whether consequence analysis should distinguish different severity classes depending on the gaseous/liquid proportion of releases hydrogen.

- Component leak frequencies under cryogenic temperatures (particularly in components which have not been described previously in the GH_2 context such as cryogenic pumps and evaporators). Component reliability analysis is still an underdeveloped task regarding hydrogen infrastructure despite the potential application towards failure event frequency quantification and maintenance scheduling. Traditional reliability data includes time-logs of failure events, ideally classified regarding the failure modes present in the system. Expansions of this framework include the statistical estimation of reliability models developed in data-intensive industry for reliability-centered maintenance scheme designs. An alternative approach to transitioning from generic reliability data is based on Bayesian updating procedures as previously mentioned.

As it has been discussed, advances in physics-based hydrogen release, dispersion, ignition and overpressure consequence and harm models have allowed improving QRA procedures to justify performance-based hydrogen fueling station design permitting. Frequency and probability data, on the other hand, has focused on leakage failures estimated from generic industrial data and the limited hydrogen-specific data. Yet, little attention has been brought to the occurrence of releases from non-leak failure mechanisms [93]. To properly address the new LH_2-related scenarios, additional studies and data collection methods should refer to:

a) Monitoring the effects of pressure and temperature cycling in liquid hydrogen storage tanks and related piping on failure probabilities. This is also a fundamental aspect to characterize the frequency of failures leading to hydrogen leaks in the system [7].

b) The likelihood and direct consequences of cryogenic liquid hydrogen releases. Depending on the location of the leak and operational conditions present during the release, this may result in hydrogen accumulation, evaporation, and the development of risk scenarios associated with gaseous hydrogen ignition.

c) The indirect consequence of cryogenic liquid hydrogen releases on infrastructure and instrumentation reliability. Low temperature of the leaked fuel can lead to damage and malfunctioning of different components, affecting the frequency of failures. Particularly, this is relevant for adjacent valves, pressure relief devices or other components which are not strictly rated for cryogenic temperatures [94].

Based on the data considerations presented above, several opportunities to expand data collection activities in hydrogen fueling stations are available for future consideration. It should be noted that these aspects can also be addressed through other types of frameworks. This discussion leads into the following Chapter 5.

Chapter 5. Conceptual Development of PHM Framework for LH_2 Storage Systems

The design and implementation of data-driven PHM frameworks in engineering systems require systematic collection and robust processing of data. This chapter presents key aspects concerning condition-monitoring data collection and an overview of selected applications in complex engineering systems to establish common procedures and implementation requirements. This, with the purpose of extending their use to hydrogen systems. This is followed by the conceptual development of a data-driven PHM framework for the studied LH_2 storage system. The selection of monitoring variables is based on the results from Section 3.3.1 as well as from related applications of components similar to those found in this system. This chapter discusses possible condition-monitoring data sources and their application for early fault detection, which can be the first PHM-related task enabled by the current knowledge of the system's operation.

5.1. Methodology

This section refers to the methodology followed to develop an early concept of a PHM framework for a LH_2 storage system. First, as mentioned in Section 2.4, the first stage of a PHM framework is dedicated to data acquisition. For this purpose, key aspects regarding data collection for PHM frameworks are presented.

Second, selected examples of PHM applications in complex engineering systems are used as a means to discuss the diverse set of tools available to use condition-monitoring data for LH_2 systems. The presented case studies include systems whose operation is inherently linked to variable operational conditions and for which no comprehensive

physics-based models exist to characterize either their performance or degradation processes.

Third, based on the relevant aspects identified through the review of data collection procedures and application in engineering systems, the basic foundations of a PHM framework designed for a LH_2 storage system are described. This step is divided into the identification of the potential condition-monitoring sources in the LH_2 system and the definition of the PHM framework design steps.

Finally, the last section of this chapter is dedicated to the discussion regarding the potential integration of PHM and QRA frameworks for risk and reliability analysis of complex systems.

5.2. Data Collection in PHM Applications

In this section, key aspects of condition-monitoring data collection are discussed. This includes a brief review of industrial PHM standards and of commonly used benchmark datasets that have supported the recent surge of data-driven PHM applications in published literature.

5.2.1. Data Types for Diagnostics and Prognostics

The acquisition of both sensor and event data is an initial and one of the most essential steps of PHM frameworks [63]. Sensor data from condition-monitoring systems are the most common source of raw data used in PHM. Measurements collected via a variety of installed sensors whose performance is linked to the overall's system health state are referred to as condition-monitoring data. Collected data types can vary depending on the desired PHM task. Frequently, however, it is the availability of data that limits the

possible applications to any system. Most complex systems have integrated sensors for control and maintenance purposes; it is possible that valuable information can be extracted from currently operating systems.

Sensor data types can be summarized by three categories: value, waveform, and multidimensional [95]. Value data generally refers to measurement time-series. Examples of value data are temperature, pressure, and humidity. It should be noted that ambient conditions may also affect the system's behavior (e.g., ambient temperature, humidity) in unforeseen ways. Waveform data include acoustic emission, vibration, and electrical signals (e.g., current, voltage). Waveform data are particularly popular as they are complemented with a vast knowledge of signal processing techniques. These measurements are also highly linked to CBM, especially for damage and anomaly detection. Finally, multidimensional data mainly refers to images, including those obtained through various data processing methods. A vital component of this sensor data is the corresponding timestamp. Ideal sampling frequency (i.e., the time period between measurement timestamps) depends on the failure mechanisms and the temporal response these produce on the monitored data. Collecting data during operation can allow the characterization of 'normal' and 'anomalous' behavior in the system. This is the basis for health-state diagnostics, which requires system-specific knowledge, e.g., system layout, sensor types, and nominal sensor values. An example is presented in Figure 5-1 [24].

Event data include information from maintenance actions taken in response to adverse events (e.g., failure, breakdown, installation, etc.) which occur in the system. Ideal maintenance records should indicate timestamps of the detected failure and what components were involved. Designing an adequate maintenance record facilitates the use

of other contextual data for diagnostics tasks, such as the specific failure mode experienced by the system. This can include interruptions to normal system operation due to internal or external reasons. Combining this event data with the operational conditions and anomalous behavior recorded by sensors prior to a failure can enable health-state prognostics and estimation of the system's RUL. An example is presented in Figure 5-2 [96].

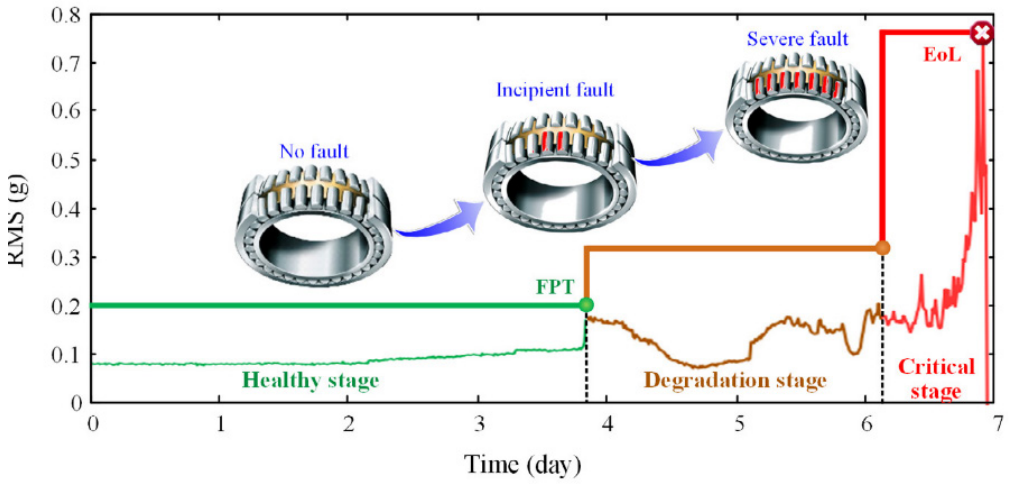

Figure 5-1: Examples of PHM applications: Health-state diagnosis in bearings. Lei et al. (2018).

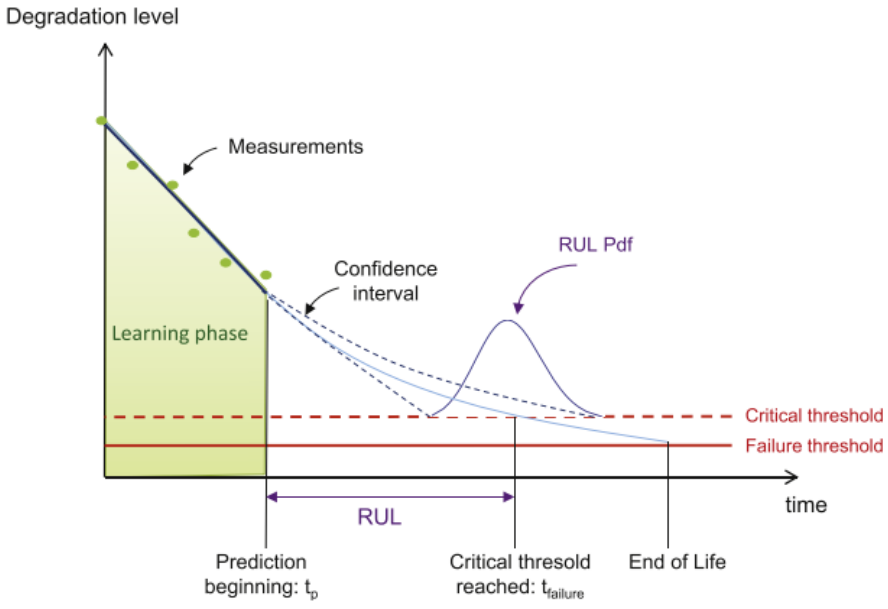

Figure 5-2: Examples of PHM applications: Health-state prognosis. Jouin et al. (2016).

Data collection campaigns for condition-monitoring data require adequate planning and design prior to their implementation. Multi-source monitoring systems yield large amounts of different types of data, increasing the difficulty of effectively analyzing and utilizing this information [97]. For this reason, system-specific analyses of the relative importance of each component and failure mode should be employed to identify and select the most relevant condition-monitoring variables in the system.

5.2.2. PHM-Related Standards

In 2014, the National Institute of Standards and Technology (NIST) published a survey of existing PHM-related standards, with the purpose of guiding the expansion of their application to manufacturing systems [98]. Their work addressed the extent, similarities, and potential gaps of standards present in other industries related to PHM system development. This work summarizes several formal definitions and procedures required to plan, design, and implement PHM within real industrial multi-component systems. These approaches present a stark difference to most recent academic publications, that generally only address component-level aspects of PHM systems.

In this report, PHM-based assessment of failure or degradation is defined as a process requiring performance metrics appropriate to the specific challenge addressed. A distinction should be made between performance metrics developed for detection tasks (to determine the system's health state) and isolation (to identify a root cause for the fault or failure mode) to prognostics tasks (to determine the RUL). A guidance for measurement techniques and diagnostic models is presented in *ISO 17359:2011* and *ISO 13379-1:2012*, respectively. Understanding the relationships between failure mode and measurable symptoms is fundamental for planning and designing PHM frameworks. The

aforementioned standards refer to the incorporation of failure logic analysis such as FMEA and FTA to identify ideal sensor locations for condition-monitoring data collection efficiency. Table 5-1 [98] presents some measurement and diagnostic techniques along with their state of development at the time of the study (2012). The techniques mentioned are categorized as either knowledge-based and data-driven methods and do not explicitly address physics-based methods. Of these, rule-based and statistical methods are the diagnostic models with a higher degree of development, while faults identified through process parameters and the system's performance are more widespread applications.

Table 5-1: Measurement techniques for various diagnostics models. NIST (2014).

Diagnostic model/ monitoring technique	Knowledge-based			Data-driven						
Example of faults	Rule-based	Causal fault	First principle	Statistical methods	Case-based reasoning	Neural Network	Classification trees	Random forest	Logistic regression	Support vector machines
Vibration	M	D	P	M	D	D		D		
Thermography	M			M		D		P		
Oil analysis	M	P		M	D	D		D	D	D
Process parameters	M		D	M	M	M	M	M	M	M
Performance	M		D	M	M	M	M	M	M	M
Acoustic emission	M			M		D	P	D		
Acoustic monitoring	M			M		D		D		
Electrical monitoring	M			M		D				

M: Mature and commonly applied in industrial applications.
D: Under development and some initial applications.
P: Promising and potential

This NIST report concludes that the standards referring to diagnostics and prognostics tools are limited; however, the existing standards are still valuable for industry [98]. The specific contents of the standards are subject to continuous review processes, yet the structure these standards provide for PHM system implementation are valuable guidelines for exploring applications in other areas. The existence of these standards may also provide security to stakeholders to whom these methods are presented as alternatives for CBM and are unsure or unaware of related academic research. It should be noted that this survey does not cover the state-of-the-art developments of the past six years, which has diversified both techniques and applications of PHM, particularly on the development of DL frameworks.

5.2.3. Benchmark Datasets

Applications of PHM and CBM frameworks have addressed a wide variety of engineering problems in electrical and mechanical systems. The state of the art of these applications differ and depend mainly on the available data for technical and engineering reasons. For instance, many electrical systems are equipped with 'virtual sensors' which provide easy and non-intrusive access to condition-monitoring data (e.g., voltage, current, etc.) without requiring the installation of additional sensors. In contrast, applications seeking to monitor crack growth need to rely on indirect measurements (e.g.: vibrations signals and acoustic emissions) as the damage cannot be accessed during the system's operation (i.e., crack growth can be measured through intrusive techniques during inspection or maintenance activities). Machinery prognostics research flourished thanks to the availability of benchmark datasets originating from either simulations or simplified test-rigs to test data-driven architecture performance [24]. Some of these are:

- C-MAPSS turbofan dataset [99]. This dataset was originally released as the data challenge in the IEEE PHM 2008 conference [100] and is composed of multiple run-to-failure data of turbofan engines. The effects of faults and degradations in major rotating components of turbofan engines are simulated using a thermo-dynamical simulation model. A total of twenty-seven outputs (including temperature, pressure, speed, bleed) are utilized to measure the system response and RUL under up to six different operational conditions and two failure modes represented in four sub-datasets.
- FEMTO bearing degradation dataset. This RUL dataset was employed for the prognostic challenge of IEEE PHM conference in 2012 [101], [102]. The data is composed of seventeen run-to-failure data of rolling element bearings acquired from a PRONOSTIA platform. Accelerometers and thermocouples were used to monitor the bearings, but its low sampling frequency (10 Hz) does not allow in-depth analysis.
- Center for Intelligent Maintenance Systems (IMS), University of Cincinnati bearing degradation dataset [103], [104]. It is composed of accelerometer readings at a sampling frequency (1Hz) which does allow the extraction of frequency-domain features to monitor the degradation processes of specific components.
- Milling machine degradation. This dataset includes run-to-failure data acquired from tool wear experiments of a milling machine [105], [106]. Acoustic emission, vibration and current sensors recorded tool wear processes under different realistic industrial operational conditions.

To date, several other datasets have been published including tool wear, gearbox and lithium-ion battery degradation [68]. However, available data does not represent realistic situations in industry, where run-to-failure data is expensive and usually expressed through long-term degradation processes [24]. As mentioned in Chapter 2, this is expected to improve given the future widespread integration of IoT and Industry 4.0.

5.3. PHM Applications in Engineering Systems

As stated in [107], the main challenge in data-driven degradation analysis is to extract useful representative features from raw collected data. Analysis of rotating machinery data has been one of the focus of PHM applications in engineering systems. Given the availability of benchmark datasets and the relative simplicity of experimental setups, bearing failures have been intensively researched. Vibrations, acoustic signals, and temperature monitoring are frequently employed to determine the health state of these components and obtain an accurate prediction of the RUL based on current operational conditions [59].

In the following sections, brief examples of system-specific data processing and common procedures for energy-related systems are discussed. Aspects of the data-driven techniques described below present relevant insight to the design requirements of health-monitoring applications in hydrogen systems.

5.3.1. Variable Renewable Energy Systems

The use of PHM under dynamic operational conditions is a constant challenge to the completeness of the data-driven model's training stage. Such is the case of wind or solar energy systems, where data-driven health-state assessments must incorporate an understanding of external processes, such as the availability of solar and wind energy

sources, to correctly identify failures in the system. Given the limited availability of physics-based degradation models, data-driven tools play an important role in aiding the safer deployment of these technologies. Applications of PHM frameworks in renewable energy systems face unique challenges, particularly in cases in which the systems function under varying operational conditions.

For instance, Stetco et al. [69] present an in-depth analysis of previously published works in which ML methods were applied for PHM frameworks to wind turbine systems. These frameworks have been proposed by several authors as alternatives to reducing maintenance costs, particularly in offshore installations. This meta-analysis classifies the models by data sources, feature selection and extraction, model selection, validation, and decision-making stage development. In this industry, these data-driven applications are mostly focused on fault diagnosis via classification approaches and typically employ techniques such as NN, SVM and Decision Trees (DT). Data-driven approaches are of interest to wind turbine industry per the successful studies in fault detection for rotary machinery data analysis. This industry also benefits from the availability of SCADA systems to collect data, which deliver time-series signals in regular intervals during operation. Frequently, these monitoring systems cover a variety of variables, such as bearing vibration and temperature, phase currents, and wind speed to assess the turbine's operational state. The use of time-frequency processing techniques for signal analysis is common, but implementation is complicated by dynamic operational conditions.

One example of a data-driven application in wind turbines operations is the use of regression models for anomaly or fault detection. Here, data collected under normal operational conditions is used for 'healthy state' modeling. Specific variables, such as

power generation, are replicated based on healthy sensor data and then compared with the observed outputs to identify anomalous behavior. This can be complemented with parametric models, such as power curves, to establish engineering-based criteria to detect anomalous behavior rather than relying only on statistical thresholds. For classification models, failure data is important to enable diagnostic capabilities. This underscores the importance of condition-monitoring applications from an engineering perspective: frequently failing components and their corresponding failure modes must be identified before designing the data collection process. In this context, ML and DL techniques have been introduced to analyze, replicate, and diagnose the health at both the component and system level. A variety of diagnostic and prognostic tasks for wind turbines have been addressed, including blade fault detection, generator brush failure prediction, transmission system fault diagnosis, and lubricant pressure monitoring.

Similar PHM frameworks have been proposed and implemented for fault detection and diagnosis of solar photovoltaic array (PVA) systems [108]. In their review, Mellit et al. summarize the growing number of data-driven applications for fault detection, localization, and diagnosis in PVA systems. Of these, fault localization is the most challenging, as it strongly depends on the monitoring system design. This aspect is of fundamental importance in these systems, in which electrical and thermal faults can be developed over a wide range of spatial and temporal dimensions. For instance, visual and thermal methods are frequently employed to diagnose module-level faults, while electrical methods also allow fault detection at system level. The work developed in this industry has led to the creation of specific guidelines and standards for data-driven fault detection and diagnostic frameworks. Examples are the *Standard IEC 61724: Photovoltaic system*

performance monitoring – Guidelines for measurement, data exchange and analysis, which details the required accuracies and validation procedures for data quality [109].

Applications reviewed in [108] include SVM, k-NN and NN employed to classify known operational conditions and faults or identify anomalous behavior. As with the process described for wind turbines, regression-based fault detection methodologies consist of using parametric or empirical techniques to compare observed states with estimated data. One common approach in PVA systems relies on the prediction of generated power estimated from measured solar irradiance, module temperature, and historic energy generation at the array level. From a monitoring system design perspective, the sampling frequency of the measuring system significantly influences which failures are detected in PVAs. While a lot of research has focused on short-term forecasting and fault detection, current efforts are directed at extending these frameworks for longer-term degradation behavior analysis.

5.3.2. Lithium-ion Batteries and Fuel Cells

At the component level, beyond bearing analysis, considerable research has been focused on the application of data-driven PHM techniques to lithium-ion batteries and fuel cells. Both of these components' performance is affected by the conditions under which they operate (e.g., environment, loads, etc.), which increases the challenges to execute precise prognostic tasks. Case studies differ significantly between these areas, given the complexity of the observed degradation process within these components and the effect over the system's performance.

Research related to the health monitoring of lithium-ion batteries has seen a surge in recent years, encouraged by the widespread demand of this technology as energy carriers

in the electronics, energy, and transport sectors [23]. The main challenge of modeling the performance of these systems is due to the complex electrochemical reactions that occur during operation, especially during transient operation. However, an advantage of PHM applications in battery systems is the prevalent availability of using non-invasive measurements to characterize their performance through variables such as voltage, current, capacity, inner resistance, and working temperatures. These measurements have traditionally been employed to assess the electronic system's performance during normal operation and degraded conditions through various physics-based models [110]. Further, by implementing data-driven approaches, the modeling of the battery's operation can be complemented with methods aimed at estimating two HI critical to the assessment of the RUL: State of Health (SOH) and State of Charge (SOC) [23].

Recently, research has focused on the development of data-driven and hybrid applications, including PF, NN, SVR and GPR. One example characterizing battery faults under real operational conditions through voltage measurements during a yearlong operation of a taxi EV was developed in [111]. These systems operate under an intense regime of varying operational conditions that can lead to the accelerated development of abnormal voltage faults. After a correlation analysis of available measurements, four variables are selected to predict future voltage values through a LSTM model: historical cell and battery pack voltage, the SOC, vehicle speed and a brake pedal stroke measurement. Model-based alarm and warning thresholds were introduced depending on the severity of possible consequences caused by voltage abnormality. Some of the important aspects discussed in this work are: the relevance of including different operational conditions and how selecting adequate prediction horizons has a direct impact

of the usefulness of the framework. In this case, the study considered environmental aspects which vary throughout the year, such as ambient temperature, a variable known to affect battery operation, as shown in Figure 5-3 [111].

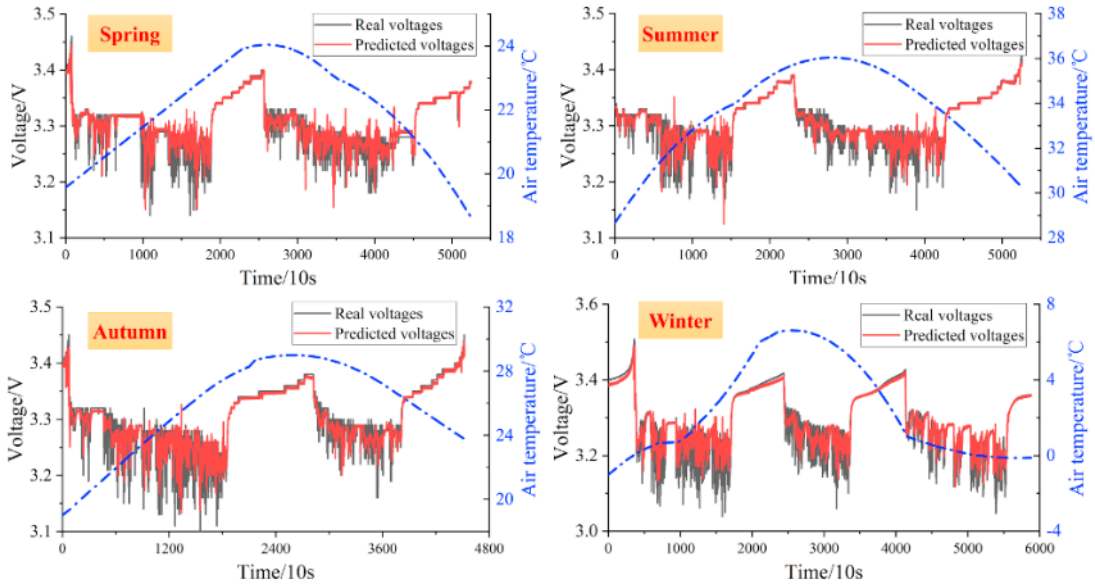

Figure 5-3: The predicted and observed voltage curves in four seasons. Hong, Z. Wang, and Y. Yao (2019).

Authors argue that practical aspects of data collection need to be considered when discussing the selected prediction horizons (i.e., how far in the future the predicted value is expected). In the case of battery systems, collecting data for very short-term predictions (e.g., 1-minute in the future) is impractical in terms of the amount of storage required to analyze extended periods of time. However, these short-term predictions are also fundamental to diagnose rapidly developing high-severity thermal failures (such as thermal runaway) and take the corresponding safety measures in time to avoid high-consequence accidents.

Another example is the study of prognostics in Proton Exchange Membrane Fuel Cells (PEMFC), a relatively new technology with promising applications but which suffers

from reduced lifespans and long-term underperformance [25]. While physics-based models have used voltage, temperature, impedance, and pressure-drop measurements for short-term HIs, model-based long-term failure prognostics is limited by current knowledge of degradation and failure mechanisms [112]. Hence, several works have sought to characterize PEMFC operation through data-driven applications with the purpose of providing useful information about observed long-term degradation processes, aiding both operation and maintenance decisions to extend their useful life.

Diagnostic approaches for fault detection and isolation, as well as RUL estimation in PEMFC have been addressed through model-based, data-driven, and hybrid approaches. In these complex systems, specific events (such as transients) relevant to the performance and corresponding lifespan are difficult to sample under real operation. Under limited available data, SVM and BNs have demonstrated better performance than more complex DL methods [113]. For example, the study presented in [25] proposes a hybrid prognostic method for PEMFC combining a SVM variant (least square support vector machine, LSSVM) and a PF variant method (regularized particle filter, RPF). Using voltage drop as an indicator of the PEMFC's health, the SVM model was trained to replicate the PEMFC's voltage until surpassing a known degradation threshold. Further, based on the predicted voltage values, the RPF provides a RUL probability distribution as a measure of uncertainty, as shown in Figure 5-4 [25].

This combined framework presents higher performance than regular PF and RPF, given that these relied on physics-based voltage models. Although this work only addresses the framework's performance under steady state operational conditions, it is relevant to introduce different achievable results from hybrid data-driven prognostic applications.

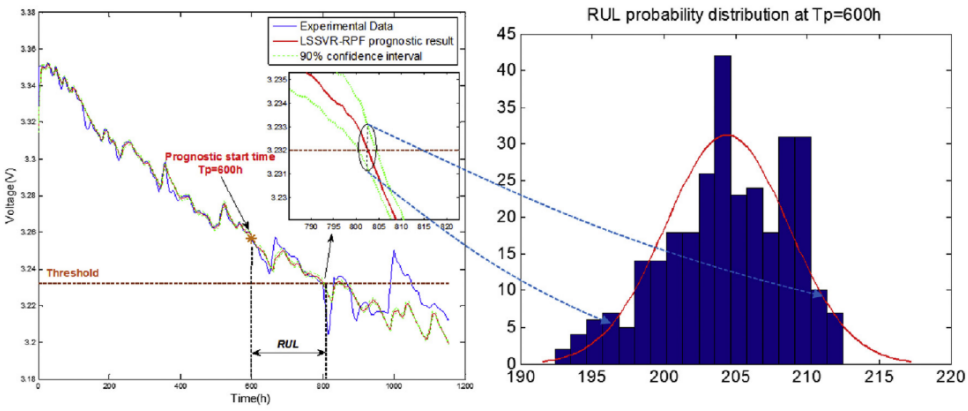

Figure 5-4: Estimated RUL probability distribution. Cheng, Zerhouni, and Lu (2018).

These examples of PHM applications in complex engineering systems for both diagnostic and prognostics tasks illustrate the wide range of opportunities for hydrogen systems to incorporate into maintenance-scheduling and risk assessment activities. In the next section, potential data sources are discussed in the context of LH_2 storage system applications.

5.4. Potential Condition-Monitoring Data Sources in LH_2 Storage Systems

Guidelines for design, maintenance, and installation procedures of hydrogen infrastructure are presented in the CGA documents discussed in Section 2.1.1.2. These guides include descriptions of sensors and testing based on temperature fluctuations, pressure measurements, vibrations, pump electric motor operation, multiphase flow identification, and acoustic signals. Additionally, insights from these codes, design and test procedures refer to normal operation thresholds aiding anomaly detection and diagnosis tasks. This implies that condition-monitoring data can be collected from hydrogen systems to explore the feasibility of applying data-driven models for the system's health

management. In this section, relevant sensor measurements and their possible use for early fault detection in the main components in the system are discussed.

5.4.1. LH_2 Storage Tank and Pipelines

Storage tanks and pipelines are the main components of concern in the studied LH_2 system. Vacuum conditions between double-walled components are monitored for operational safety reasons. The same monitoring could enable detection of thermal insulation loss or leakage from the inner tank [29]. Similarly, failure criteria for composite tanks have been developed through physics models and simulations based on variables such as burst pressure and estimated fatigue lifetimes [114]. For instance, the effects on permeation rates in vehicle fuel high-pressure containers under pneumatic cycling was previously addressed in [94]. Thus, temperature and pressure anomalous variations could be employed as indicators for fault detection in these LH_2 storage system components. Alternatively, identifying precursor operational or ambient conditions leading to leakages can enable prognostic capabilities. Relevant information could include fueling history and ambient temperature fluctuations and other variables related to seasonal effects. This can prove to have a greater effect when applied to elements present in the dispensing systems (hose, connections, etc.), which represent the majority of unscheduled maintenance events in hydrogen fueling stations [115].

Although storage tanks consist of no moving parts, vibration analysis is one viable method for leakage detection. Previously, online monitoring systems have been implemented for damage detection and localization in hydrogen vessels [116] through piezoelectric (PZT) sensor array and vibrations analysis. Yang et al. [116] presents a method for fully automatic detection and localization of defects in hydrogen storage vessels

based on an online monitoring system. This work utilizes guided wave-based techniques that have been successfully employed for localization and detection of micro-crack defects in different structures [117], [118]. Experiments were conducted on a cylindrical hydrogen storage vessel where an array of eighteen surface-mounted PZT transducers were used to identify faults. Induced faults were identified through ellipse localization algorithms based on guided wave paths generated and received by pairs of PZTs at different exciting frequencies and wave velocities. Fault localization was characterized in the vertical (mm) and the azimuth (rad) direction. The minimum combined fault detection errors reach 2.65%. An example of the effect of excited frequencies is shown in Figure 5-5, where the PZT are shown as bright green points and the real damage location is circled in black.

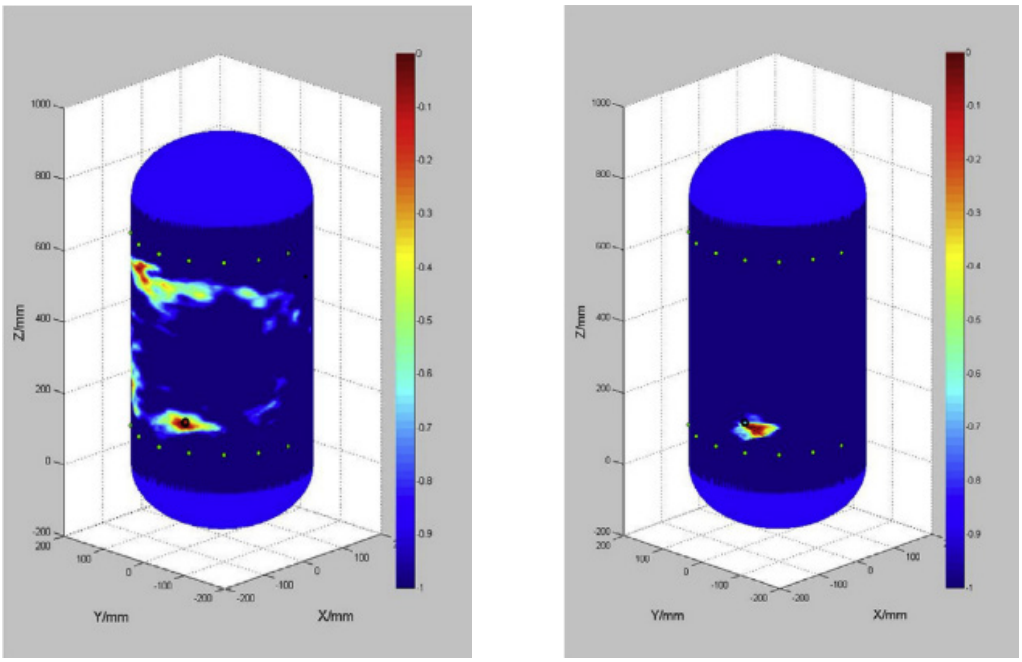

(a) 120 kHz *(b) 250 kHz*

Figure 5-5: Defect localization on the cylinder: effect of excited frequencies. Yang et al. (2019).

Similarly, acoustic wave analysis has been implemented for leak detection in gas pipelines and valves. In [119], a data-driven pipeline fault detection method was developed

based on acoustic signals and the use of specific signal analysis for feature extraction. These are then integrated into SVM models to classify the severity of the leak. As pressurized gas escapes at high velocity through a leak site in a pipeline, the pressure difference between the outside medium and the gas induces vibrations that travel through the pipeline's walls. From an experimental pipeline setup with induced leak sites, specialized wavelet transform procedures are employed to de-noise the received acoustic signals and extract time-frequency features for analysis. An SVM was implemented for a multiclass classification problem consisting of four severity classes: normal (no leak), small leak, middle leak, and large leak; based on the ratio between the leak size and cross-section of the pipeline.

In a similar work [120], a valve leakage detection framework was developed based on acoustic emission signal analysis, Principle Component Analysis (PCA) for model-free feature extraction, and a multiclass SVM model for leakage severity classification. Leaked flowrates and corresponding acoustic responses were measured from an experimental setup and divided into eight severity classes. Following time-frequency feature extraction, PCA was used for dimensionality reduction which were then used as input for the classification model. Different techniques were used, including DT, NN, k-NN and SVM, the latter obtaining over 95% detection and classification accuracy. The applications described in the pressurized vessels and piping sections have achieved high accuracy in experimental setups. However, detailed analysis on sensor location is needed to implement in a real, operational system.

5.4.2. Centrifugal Pump for LH_2 Cryogenic Applications

Another component of interest in the studied LH_2 system is the cryogenic pump. The operation of centrifugal pumps has known 'nominal' operational conditions and so the dynamic behavior of its monitored variables can be used to detect anomalies. Complex components such as cryogenic pumps may require the monitoring of several variables, depending on the specific failure mode to be detected, including differential pressure, flow rate, electric current, electric voltage, vibration, and acoustic emission monitoring. In this case, data-driven models are more convenient than physics-based ones due to the high number of components and their varying operational conditions. For instance, centrifugal pump degradation based on vibration measurements has been used to detect flow blockages and predict impending cavitation [121]. Vibration signatures are extracted using two tri-axial accelerometers, one installed on the pump housing and the other on the bearing housing, at five stages of manual flow blockage and at the start of bubble formation preceding cavitation. In this work, SVM classification models are used to classify these operational conditions based on statistical features extracted from the time-domain vibration signals. Binary ("healthy" vs "blocked") and multiclass (depending on the blockage stage) classifications are compared at different operating speeds of the centrifugal pump. The results show that the classification accuracy for both binary and multiclass experiments increase with the blockage level and pump speed, implying that this procedure is useful for progressive degradation monitoring.

Vibration signals and acoustic emissions have also been preprocessed as images to take advantage of powerful image-processing techniques. In [122], the analysis is focused on detecting normal operation from incipient and developed cavitation regimes through vibration analysis. Following the time-domain analysis of the recorded vibration signals,

several statistical and CNN-based image feature extraction procedures are compared for different multiclass classification models to diagnose the pump's operational state in terms of accuracy and implementation time. Considering the multiple combinations of processing and classification models presented in this paper, it is determined that k-NN, RF and SVM classification models obtain accuracies over 96%. Similarly, [123] analyzed bearing and impeller defects detected with acoustic emission data processed as 2D gray-scale acoustic images.

5.4.3. Proposed Condition-Monitoring Data Sources in LH_2 Storage System

As discussed in the previous sections, there are many fundamentally important variables for PHM applications in LH_2 storage systems. For classification tasks, measurements such as vibrations and acoustic signals suggest promising results for damage detection and localization. While for prognosis, possible use of sensor variables such as temperature and pressure fluctuations could have potential to be employed for prognosis tasks. A list of potential measurements and data sources for LH_2 storage systems are presented in Table 5-2, and a visual representation of the proposed monitoring system layout overlaid with the studied LH_2 storage unit is presented in Figure 5-6.

Table 5-2: Opportunities for PHM applications in LH_2 Storage Systems.

Component	Possible measurements	Possible Outputs
Cryogenic pump & electric motor	• Discharge temperatures & flow rates • Current consumption • Vibrations & acoustic emissions	• Pump & motor degradation • Leak detection
Storage tank & Pressure relief valve	• Pressure in inner vessel/vacuum • Temperature vacuum/outer jacket • Relative humidity in vent stacks	• Leak detection • Thermal insulation degradation
General	• Maintenance logs • Sensor placement & system layout	• Component failure rates • Health-State Prognosis

A significant effort must be applied to develop data collection campaigns to explore data-driven reliability-focused applications in LH_2 systems. The overview of data types presented above was developed by reviewing current PHM research related to other systems. Yet, similarly to the limitations of available traditional reliability data regarding hydrogen systems, data collection should be conducted specifically for liquid systems. Previous work related to anomaly and fault detection techniques suggest that reliability in some components, such as the storage tank, piping, and cryogenic pump, could be complemented with these techniques. While anomaly and fault detection are useful capabilities, prognostics applications and pragmatic considerations (e.g., reducing required safety distances) require characterizing the system-specific degradation processes.

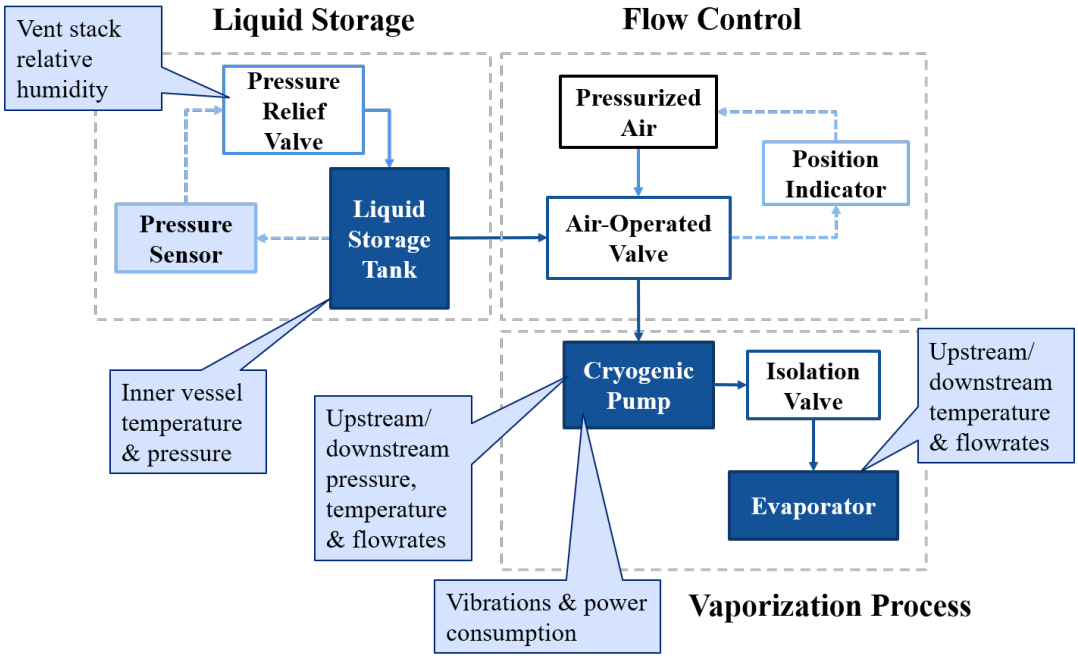

Figure 5-6: Monitoring System Layout for LH_2 Storage Systems.

5.5. PHM Framework Design Stages for LH_2 Storage System

Several works have reviewed the design methodologies behind the implementation of PHM frameworks, including project management aspects, selection of failure modes, and corresponding diagnostic and prognostic tools [124], [125]. For instance, a comprehensive review and a high-level, systematic methodology for PHM architecture design oriented to aircraft maintenance applications was recently presented in [61].

Currently, the *NFPA 2* code establishes minimum requirements of periodic maintenance in hydrogen systems given the manufacturer's recommendation and the necessary corrective action [4]. Given the analysis of the reliability data collected from surveys discussed in Section 4.2.1, small, low-consequence leaks have the greatest effect on the availability of hydrogen stations. Hence, the inclusion of proactive maintenance policies based on PHM frameworks for early failure and leak detection could help to significantly reduce the number of unscheduled maintenance hours, while also providing a means to study long-term component degradation behavior.

Future implementation of data-driven techniques for PHM in LH_2 systems should consist of the phases described in the following subsections. These phases were developed considering the methodological and conceptual aspects of design and the review of applications presented previously.

5.5.1. System Failure Characterization

A component-level breakdown of the studied system is needed to identify relevant components, failure modes and failure detection methods. This can be developed through the analysis of failure and maintenance records, and/or results obtained from FMEA or HAZOP tools for risk screening. ESDs and FTAs can be developed to study specific

failures in the system to aid in the process of selecting important condition-monitoring variables and other HI for the system. Further, this step can be used to design the monitoring and data acquisition system. It must be noted that constructing comprehensive maintenance records can potentially enable the use of traditional probabilistic-based reliability analysis.

5.5.2. System Behavior Characterization

Given a set of measurements related to the operation of the mentioned components, a first phase should be dedicated to analyzing the temporal behavior of these measurements and calculating their statistical parameters. Useful information related to nominal operational values can be retrieved from manufacturer specifications and coupled to historical measurements to determine statistical thresholds of normal operational conditions. Time-series visualization is an important tool to determine the necessary data processing steps by identifying trends or whether there are significant outliers within the data. Representation under different conditions (such as ambient temperature, fueling demand) is important to understand seasonal and periodic fluctuations. For example, Figure 5-7 depicts two applications in which the system's state of health is graphically represented in two or three dimensions [119], [120].

The state of health, known beforehand, is color-coded in these figures, showing 'regions' of operation which can later be used for diagnosis of the system. If the state of health is unknown, other methods can be used to identify possible different regions of operations, such as clustering though k-NN. Figure 5-7a presents an example of dimensionality reduction, where multi-sensor condition-monitoring data has been reduced to an abstract representation through PCA. Meanwhile Figure 5-7b presents an abstract

representation based on identifying the most statistically significance features related to the monitored variable, in this case, vibrations for leak damage detection.

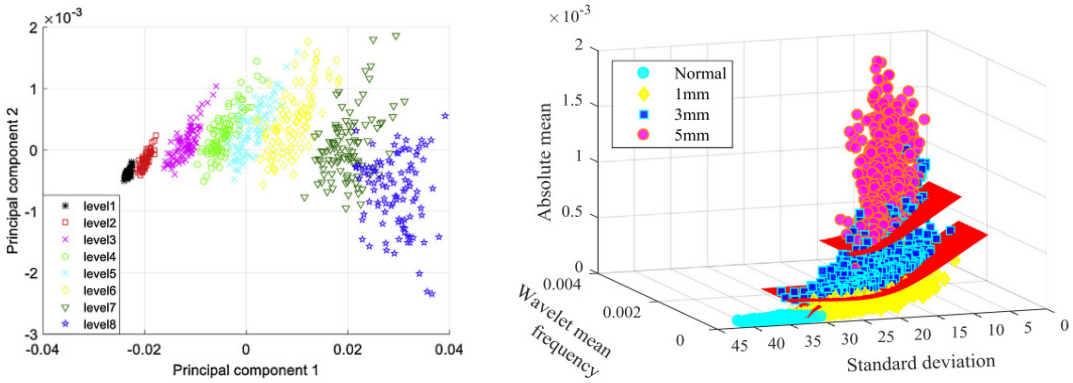

(a) Feature dimension reduction using RBF kernel PCA for eight levels of leak damage in a gas pipeline. Li et. al (2017).

(b) Scatter plot of three most discriminative features for four levels of leak damage in a pipeline. Xiao, Hu, and Li (2019).

Figure 5-7: Examples of dimensionality reduction for system diagnosis.

5.5.3. Anomaly Detection

Although an important element needed to enable maintenance scheduling is the use of failure records, these might not be as informative as required to label the monitored data correctly between 'healthy', 'degraded' and 'faulty' states. For this reason, the known behavior of the system should be replicated through a selected representative variable, e.g., the pump's power consumption time-series, and then compare it with either known or data-extracted performance thresholds. Achieving this can enable simple anomaly detection methods through the comparison between observed and estimated measurements. Here, the use of ML and DL tools have been successfully applied to identify potential differences between operational conditions, either in binary anomaly or fault detection tools, or in multiclass classification tools for damage detection, localization, and diagnosis. While the

first can be explored as an unsupervised task, the latter requires knowledge on the system's failure states. An example of these are methods based on signal reconstruction and subsequent health-state classification through methods such as AE and SVR [126]. Figure 5-8a presents an example of an anomaly detection application for aircraft through acceleration signal reconstruction and threshold infringement [66].

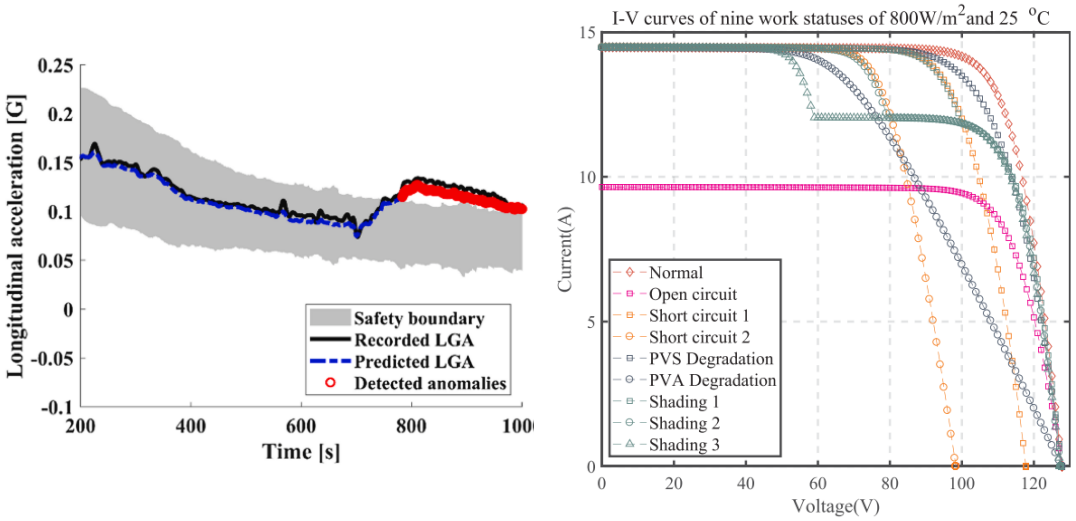

(a) Example of anomaly detection in aircraft through SVR. Lee et al. (2020).

(b) Characterization of I-V curves of PVA simulated under different faults. Chen et al. (2019)

Figure 5-8: Examples of anomaly and fault characterization for diagnosis.

5.5.4. Diagnosis of Faulty Behavior

To employ data-driven methods such as the ones described in Sections 5.3 and 5.4, labeled datasets need to be constructed from the acquired sensor data. The steps needed to acquire representative sensor measurements and process the data vary with each application and are still a topic of discussion in current literature [60], [68]. As a starting point, as mentioned in the previous step, system-specific knowledge can enable binary classification tasks for anomaly or fault detection. Further, as shown with the cited works regarding flow blockage detection in centrifugal pumps, these can be extended to

multiclass classification tasks for various failure modes. Another example of this is shown in Figure 5-8b [127], where different failure modes in a PVA system are characterized through the I-V curve, a frequently-used HI in these systems. When analyzing a multi-component system, a first approach may include identifying the monitored data's behavior during failures in specific components as separate failure modes. Complexity can be increased by comprehensively breaking down component failure modes and specific failure detection methods, enabling more complex tasks such as damage localization and quantification. The main advantage data-driven models possess over traditional, statistical, or rule-based alarm thresholds is that these methods have the flexibility to identify and classify the system's behavior without explicitly relying on system knowledge. While a detailed record of system performance and failures enhances this stage, simplified knowledge of what is considered 'healthy' and 'failure' states is sufficient. However, as mentioned in Section 2.4.3, this can also lead to unexplainable models and are significantly limited by the data quality, particularly in industry settings where noisy and heterogenous data is more likely to be found than in experimental setups.

5.5.5. Prognosis of Future Health States

The prognosis of future health states of a system and the development of tools which correctly predict the RUL at component and system level has captured the attention of recent PHM-related research [24], [128]–[130]. The development of this stage depends on various aspects discussed for the previously described tasks. Methodologically, a difference must be drawn between the 'real' time-to-failure of a component, which might be dynamic based on the operational condition, and the RUL generated labels from recorded failures. An example of RUL prediction for a milling tool in a CNC machine is

presented in Figure 5-9 [128]. Here, the 'Ground truth RUL' labels are constructed as a linear function from the point at which the component failed and up to 4500 seconds prior to this moment.

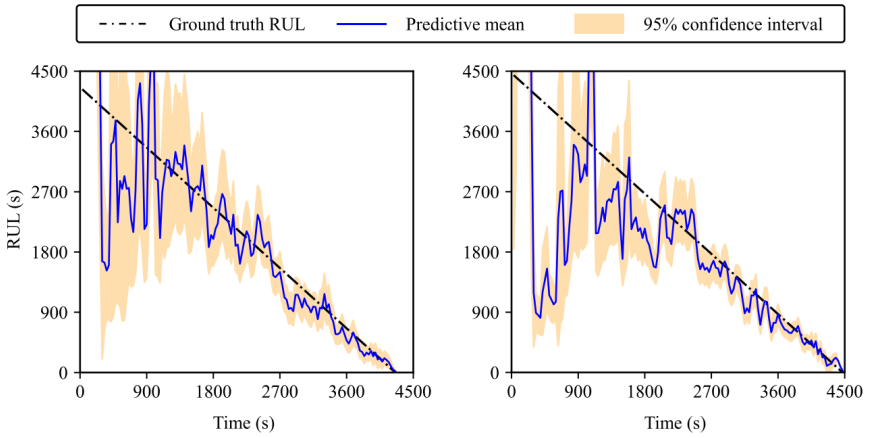

Figure 5-9: Examples of RUL prognosis in a CNC milling machine. Wang et al. (2020).

The implementation of a prognostic tool requires that the collected condition-monitoring data provide evidence of degradation or abnormal behavior prior to or during a previously defined failed state. Hence, the predicted RUL based on this data does not necessarily accurately follow the linear labels until the point at which a clear degradation trend has been identified [128]. Considering this, RUL prediction depends on the system's operation nature (periodical, continuous, on-demand, etc.), failure mode and degradation mechanisms, and ultimately the quality of the data processing and of the sensor data itself. The complexity of these issues and the need to introduce active uncertainty estimation and management techniques for RUL prediction are discussed in detail in [60].

5.5.6. Framework Integration to System Operation

The final objective of integrating a PHM framework into any system's operation may vary between applications and current state of knowledge of its operating and failure

logic. Maintenance scheduling has been one of the most frequent implementations cited in the literature, either through early fault detection or actual calculation of the RUL of a component or system. A summary of tools available, expected outputs and levels of implementations can be found in Table 5-3.

Table 5-3: Design of implementation stages for PHM frameworks.

Design Stage	Tools Available	Expected Outputs	Implementation
System failure characterization	Maintenance records/FMEA/HAZOP for risk screening; ESD/ETA/FTA for failure modeling.	Identification of most relevant components and failure modes to overall system failure.	Offline
System behavior characterization	Time-series analysis of monitored system variables, nominal operational thresholds, dimensionality reduction (PCA); clustering methods (k-NN).	Identification of system's nominal operation through statistical parameters and time series visualization.	Offline
Anomaly detection	Comparison of monitored data with statistical or rule-based thresholds; NN models (AE).	Health indicators based on system operation.	Offline or online
Diagnosis	Various model, physics, and statistical-based methods. Includes ML (SVM, RF, etc.) and DL (NN, CNN, etc.) methods.	Health-state or specific failure type identification, localization, and quantification	Offline or online
Prognosis	Physics-based models when available, data-driven model depending on data quality (SVR, NN, RNN, etc.), hybrid models (PF).	Health-state evolution, RUL	Offline or online

While the first design stages described in this section require offline development, several works have aimed to construct online fault detection, diagnostic, and prognostic tools, i.e., methods which can determine the state of health of a system during operation. However, it should be noted that online applications depend on a series of factors, including data acquisition frequency, system inertia, and degradation behavior. As discussed in the case of solar PVAs (Section 5.3.1), failures in these systems may cover a wide spectrum

of temporal and spatial scales. While detecting thermal or electrical anomalies might be possible within minutes, the detection and diagnosis of long-term degradation effects require other criteria. In contrast, offline applications can be opportunely scheduled during inspection tasks [61].

Given the current knowledge of the LH_2 storage system failures, significant effort is required to implement future data-driven PHM applications. Figure 5-10 presents the sequential data requirements for the construction of a general data-driven framework, where the early-stage research opportunities are highlighted in the dashed box. The implementation of diagnostic and prognostic tools is presently limited under the current state of knowledge of LH_2 system failure behavior and the uncertainty regarding the quality of the deployed data collection abilities of hydrogen stations. However, as mentioned in Section 5.4, studies aimed at fault detection in storage tanks, piping sections and centrifugal pumps serve to illustrate the short-term potential capabilities these tools could present for hydrogen systems.

In both Chapter 3 and Chapter 4, the discussion centered on defining methods and data requirements to improve the state of system knowledge and failure characterization. A crucial aspect to enable any kind of prognostic tool, either data-driven or based on probability theory, is the inclusion of maintenance records in the analysis. These records facilitate reliable estimates of reliability metrics like time-to-failure or filling-cycles-to-failure. Early implementations of this can be seen in Figure 4-6, in which the system-level failure rate of a hydrogen fueling station is estimated based on historic data. Ideally, failure and maintenance records should reflect a comprehensive equipment, component, and failure mode breakdown. The most important components contributing to overall system

failure need to be identified in terms of the risk they represent, considering both the frequency of failure and possible consequences. An analysis of maintenance records will indicate whether it is more valuable to monitor, for example, valve operation than a storage tank, as discussed in Section 4.2.1.

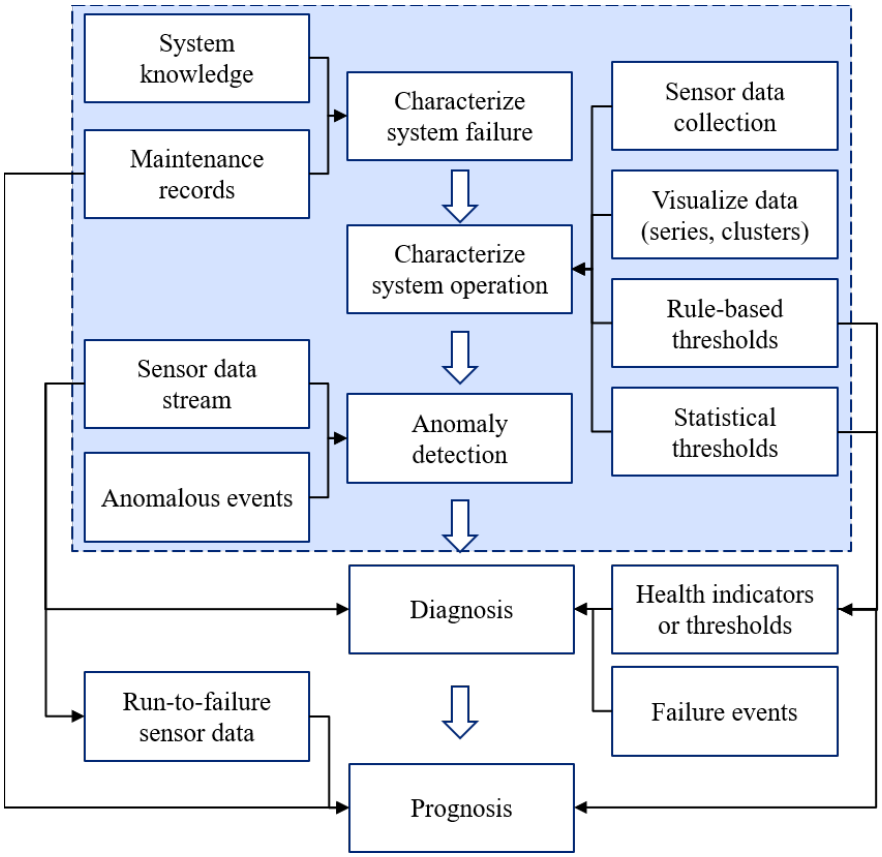

Figure 5-10: Gradual Implementation of PHM Framework based on Available Data.

Additional contextual information, beyond the time-to-failures extracted from maintenance records, periodic inspection and accelerated testing may be collected for use in probabilistic reliability theory. Accordingly, sensor data must be actively collected during operation for the implementation of both condition-based and prognostic tools for proactive maintenance scheduling. In this regard, the quality data acquisition, analysis, and preprocessing stages depicted in Figure 2-10 are arguably the foundation of PHM

frameworks [131]. Several tools have been discussed as candidates to analyze sensor data retrieved from possible sources detailed in Section 5.4. Of these alternative sources for condition-monitoring data, given the relatively easier access to simultaneous monitoring points in different sections of a LH_2 storage system, temperature and pressure fluctuation emerge as promising candidates for as anomaly and fault detection alarms. The implementation of these anomaly detectors could also be used to diagnose loss of insulation and leakage events throughout the piping network system. By monitoring strategic points as depicted in Figure 5-6, such as immediately upstream and downstream of the centrifugal pump, the evaporator, or any major valve, leakage failures in connecting elements could be detected through comparison to either nominal or statistically-defined fluctuation thresholds. The occurrence and recording of anomalous or faulty system states is fundamental to comprehensively implement these detectors while reducing the risk of false alarms. Alternatively, if maintenance records warrant particular attention to certain components, dedicated monitoring could prove to be a useful approach to limit the number of unscheduled maintenance events in these systems. One application of dedicated component monitoring could be fault diagnosis on centrifugal pumps through vibration analysis.

5.6. Proposed PHM and QRA Integration Framework

The previous sections summarized various PHM frameworks, reviewed selected case studies in complex engineering systems, and conceptually formulated possible applications in LH_2 storage systems. A visual representation of the information flow in a PHM framework to support preventive maintenance decision-making is presented in Figure 5-11. The implementation of data-driven models for anomaly detection, fault

diagnosis, and fault prognosis faces several challenges, particularly regarding data quantity and quality.

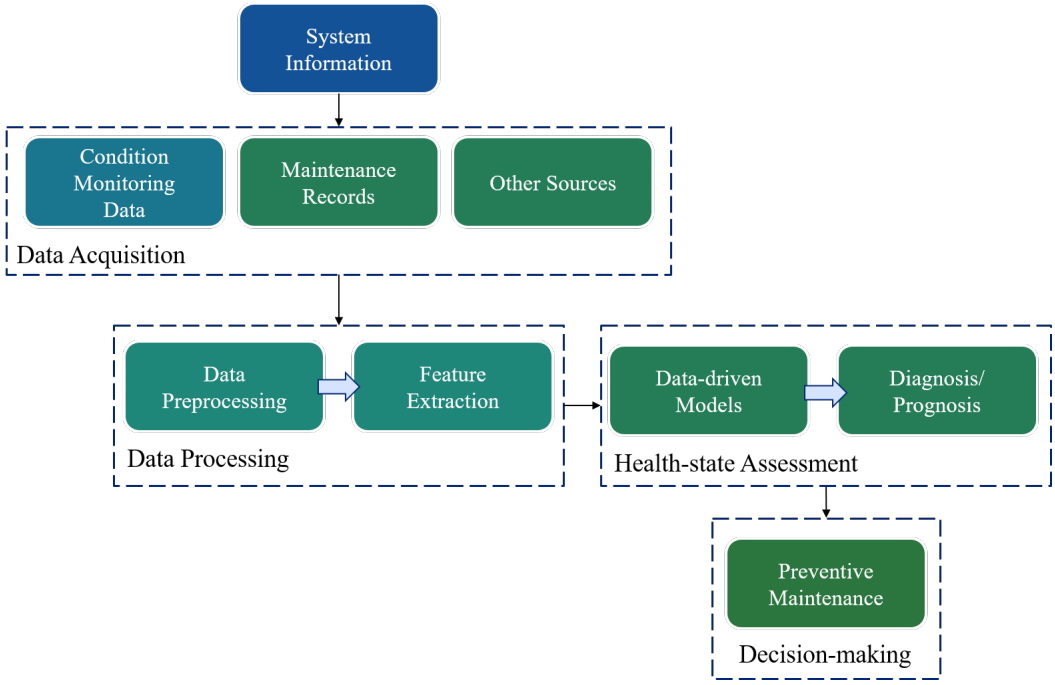

Figure 5-11: Information Flow in PHM Framework for maintenance decisions.

To balance the conversation, it is important to highlight the following positive aspects of data-driven models:

- Data-driven PHM models are based on data collected during the system's normal operation through non-invasive condition-monitoring sensors.
- Several PHM standards have been developed to guide design and implementation in various engineering systems and are intended to close the gap between industrial system management and academic research.
- PHM frameworks consist of several different approaches. This progressively enables tasks depending on the quality and quantity of the data collected, from anomaly detection to fault diagnosis and failure prognosis.

- There is a growing history of successful applications in various engineering problems in electrical and mechanical systems. Although most research focuses on synthetic data or collected under experimental tests, these are promising results paving the road in the Industry 4.0 era.

Previous chapters also discussed the use of QRA in the context of developing risk-informed SCS for hydrogen systems. Selected results from published literature were discussed, highlighting their role in technology deployment. Important steps of this framework related to frequency analysis have been addressed for the generic LH_2 storage system, including FMEA, ESD, and FTA development. In Figure 5-12, the information flow of a QRA process aimed towards standard and code improvement is depicted.

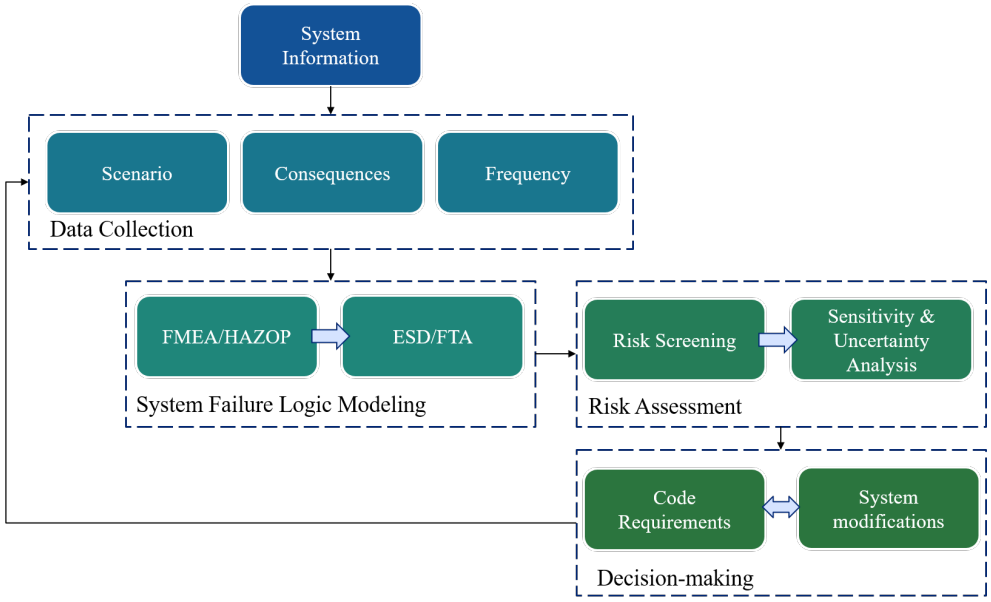

Figure 5-12: Information Flow in QRA for risk-informed code development.

As discussed in previous chapters, data limitations significantly impair the adequate characterization of risk and may lead to unrepresentative requirements in SCS, either by under- or overestimating risk. However, the strengths of QRA lie in:

- The flexibility to merge a variety of data sources to adequately represent contextual information particular to the studied system.
- The existence of well-documented technical standards to develop QRAs and a history of research related to hydrogen risk assessments to build from.
- The flexibility to continuously address and manage risk in a system throughout various stages of technology development, deployment, operations, maintenance, and retirement.

QRA and PHM frameworks currently operate at different temporal and spatial scales. QRA methodology is designed for system-level analysis, including contextual information. As QRAs must consider worst-case scenarios possible when developing and ranking risk scenarios, this has reduced the importance of how these faults are developed in the system and the precision on event frequency. While reliability data is being collected and can finally lead to probabilistic models of station availability, it is also possible to adapt this framework to assess risk in a dynamic way through the inclusion of online data-driven applications. Alternatively, by incorporating QRA aspects to PHM frameworks, a risk perspective could be incorporated into the design and decision-making stage, as portrayed in Figure 5-13.

This concept has already been indirectly addressed through the design of CBM and PHM frameworks based on the study of failure modes, incorporating tools such as FMEA and FTA to guide the design of the sensor monitoring system. For instance, feature extraction and selection processes can be designed from an engineering point of view, i.e., considering the impact and development of specific failure modes and mechanisms in the

system. On the other hand, HIs extracted from analyzing the health state of a system based on sensor monitoring data could be included in a risk-screening process, allowing the development of dynamic risk assessment frameworks.

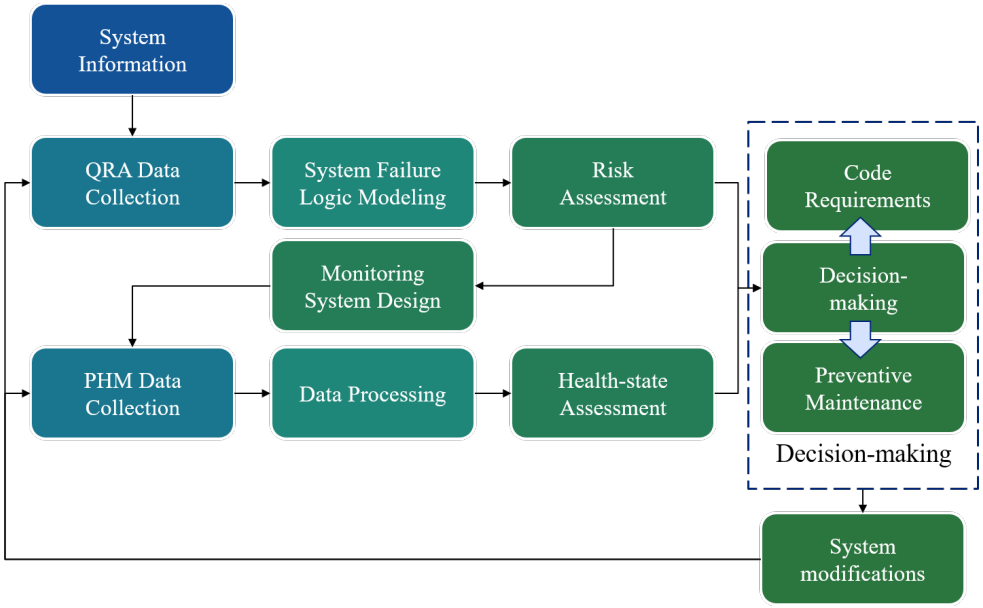

Figure 5-13: Combined QRA-PHM Framework.

Additionally, there are design and operation requirements that contribute to the station's safety which must also be considered when quantifying the risk inherent to a station. Some key design features which are currently specified in hydrogen SCS are interlocked leak detection and isolation capability, emergency manual shut-off switches, process monitoring and safety interlocks, and fail-safe design requirements [6]. On the other hand, operational requirements can include safety procedures for normal operation, monitoring, maintenance, and emergencies in case of major accidents. Quantifying the effects and comparing the costs and benefits of safety measures are complex tasks for SCS. In the context of safety measures, condition-monitoring techniques can be a valuable tool for assessing the current and future health state of a system. Critical aspects of framework

design and integration, such as costs associated with adequate sensor network design, data acquisition, analysis, and storage must be addressed in a system-specific way to avoid overshadowing apparent benefits if these are not planned correctly.

The development of tools based on sensor monitoring data represents an opportunity for hydrogen fueling station stakeholders to take credit for the inclusion of risk-informed barriers and mitigation measures for SCS compliance. Incorporating real-time information collected from hydrogen systems can potentially deliver better estimates of the existing risks in the station and improve passive security measures. Strengthening these passive measures under the established risk acceptance criteria may also lead to the reduction or modification of other SCS requirements in the future.

Chapter 6. Discussion and Conclusions

This thesis analyzed a generic LH_2 storage system in a hydrogen fueling station from a risk assessment perspective with the purpose of identifying data collection priorities to enable future QRA and PHM framework approaches. The main products of this thesis are the identification of data collection opportunities to fill the current gaps of QRAs in LH_2 systems and to explore PHM applications for main components in the system, such as early failure detection. These aspects are summarized in the following section, including technical contributions and limitations, as well as recommendations for future work.

A long-term goal of introducing PHM frameworks to hydrogen systems is to develop end-to-end risk assessment tools which use online monitoring components to enable condition-based decision-making. Ongoing challenges for hydrogen fueling stations include the use of risk-informed SCS to design and permit the operation of these systems. Quantifying the risks associated with LH_2 systems is of critical importance to address safety questions, further enabling the development of standards such as *NFPA 2* and *ISO 19880-1*, and ultimately the widespread deployment of hydrogen infrastructure. Further, the use of data-driven reliability tools such as early failure detection and prediction may enable dynamic maintenance scheduling and increase the reliability and availability of hydrogen stations which currently suffer from frequent low-consequence leakage events and downtime. Station downtime is an increasingly significant barrier to deployment of hydrogen vehicles. Increasing the station reliability is fundamental requirement to enable FCEV deployment and thus plays a critical role in enabling the decarbonization of the transportation sector.

The framework described in Chapter 5 creates possible opportunities to incorporate dynamic risk assessment into the operational phases of a system, rather than solely during the project's design or implementation stages. This work constitutes an initial step in exploring towards these long-term goals, focusing on identifying LH_2 release scenarios and system failure modes, identifying reliability data requirements which support the improvement of PHM and QRA frameworks, and providing a pathway for using PHM to improve system reliability and safety.

6.1. Summary and Technical Contributions

This thesis has been divided into three interrelated tasks addressing: a) the quantitative risk assessment of a bulk LH_2 storage system consisting of FMEA, ESD and FTA to identify, develop and quantify high-risk scenarios and LH_2 release events in the system; b) an analysis of currently available hydrogen-related QRA and reliability data including leak frequencies, accident scenario databases, safety reports from currently operating facilities, and generic industrial failure data from reputable sources used in risk and reliability assessments; and c) a review of data-driven PHM techniques and applications to identify main elements, condition-monitoring data sources and possible outcomes of PHM framework that can be applied to LH_2 storage systems. The main contributions and insights are summarized as follows:

1. A hydrogen fueling station design with a bulk LH_2 storage system corresponding to the expected future state of the industry was characterized and analyzed through an FMEA process. A survey of hydrogen reliability data was conducted for this analysis, based on published literature and available public databases available. Several works refer to generic databases, citing expert knowledge or experimental

results to incorporate site-specific data. Consequence analysis is addressed qualitatively for the purpose of this work. This led to the identification of high-risk failure modes related to the release of LH_2. The three most critical failure scenarios are: leakage events caused by the malfunction of the pressure relief valve system due to cryogenic temperatures, operation failure (fail closed) at prescribed time of the air-operated valve, and hydrogen release caused by a rupture of the evaporator due to either a collision or an external accident.

2. ESD were developed to model the LH_2 hazard scenarios. The proposed ESD updates a general ESD that was included in the HyRAM architecture, but which only included GH_2 releases. The newly developed ESD incorporates liquid and gaseous leakage, dispersion, and ignition events. However, insufficient information on LH_2 release and consequence behavior limits the quantification of these ESDs. To estimate the initiating event related to LH_2 releases in the storage system, a fault tree was developed based on an analysis of generic component failure data and LOC event frequencies using data from OREDA and *The Purple Book*.

3. Based on the previous FMEA, ESD, and FTA results, it was determined that the application of QRA methods for LH_2 systems is limited by poor quality, unrepresentative hydrogen component reliability data and leak frequencies. Proposed data collection strategies should focus on a) monitoring the effects of pressure and temperature cycling on the failure frequencies of the main components to enable PHM, b) estimating LH_2 leak frequencies of specific components of these systems, as recorded frequency data for GH_2 infrastructure cannot be assumed to

be representative, and c) characterizing the indirect effect of cryogenic LH_2 releases on infrastructure and instrumentation reliability.

4. The core elements of a PHM framework for LH_2 storage system were identified. From previous literature, several condition-monitoring variables were proposed to be used as HIs in the storage tank, piping, and centrifugal pump, including temperature, pressure, vibrations, and acoustic emissions. The design and implementation stages of PHM applications were discussed in terms of required data types, available tools, expected outputs and possible integration methods.

6.2. Discussion and Limitations

The work presented in this thesis addresses critical technical gaps and contributes to advancing the state-of-the-art risk assessments currently applied to LH_2 systems. Systems can be engineered for safety and reliability purposes. To achieve the overreaching goals of risk reduction, as well as increased reliability and safety, engineers need insight into how to prevent, mitigate, and recover from system failures and accidents. Additionally, reliability-related research and implementation can reduce costs by proactively mitigating risk throughout the lifecycle, optimizing maintenance costs, preventing major accidents and bad public relations. Risk consists of three concepts: existence of scenarios leading to hazard exposure, frequency of occurrence, and the magnitude of the resulting consequences. A good characterization of risk facilitates the design of prevention and mitigation barriers to maintain tolerable exposure frequency, regulated by technical and societal risk acceptance criteria. While the results summarized in the previous section represent a step forward to better characterize the data requirements to strengthen QRAs

and enable future data-driven PHM applications in hydrogen systems, the following aspects should be noted.

The work is based on a high-level design of a hydrogen station layout which includes liquid and gas storage systems. Modern hydrogen systems are relatively new, and the application of risk assessment techniques for this domain are also new. Few public details are available regarding specific designs and components, particularly regarding valves, connecting elements, instrumentation, and emergency system operation. Hence, the design used in this study allowed the interpretation of the system's failures logic but does not allow for specific failure mode identification for an as-built system. The failure rate data extracted from the OREDA and *The Purple Book* databases have a limited representativeness of the system, in particular because hydrogen is not among the hazardous materials contained in those data sources, nor are fueling stations included in either data source. As discussed in Chapter 2, few published works have addressed the leakage event frequency in LH_2 storage systems, or even the failure modes of unique hydrogen components. Most existing works that do address hydrogen fueling stations are focused on GH_2 systems, which have gradually constructed databases of leak frequencies originating from other industries and updated through Bayesian procedures from a small number of experiments and recorded accidents for over a decade.

As a result, the FMEA developed considers only the list of components extracted from the generic layout and failure modes have been inspired in the limited accident databases and from *The Purple Book*. It should be noted that this analysis has focused exclusively on risks related to LH_2 and have not introduced or presented a comprehensive analysis of GH_2 risks in this station design. Risks referring to GH_2 systems have been

evaluated previously during the development of the HyRAM software and are not re-evaluated in this work. However, some are included to understand the process required to analyze LH_2 risks. Ideally, FMEA procedures are developed in a diverse group of experts over a lengthy process with continuous feedback loops. However, this has not been the case for this work and thus the completeness of the risk-screening process cannot be guaranteed. The high risks identified in the system might have also been overestimated in terms of frequency and consequences, yet this process serves as a comparison point to then define locations of interest in the system. The ESDs developed are inspired in the HyRAM software, but currently HyRAM lacks sufficient data to populate the newly added events in these diagrams. Moreover, the limited experience with liquid systems is a particularly important challenge for developing pooling and cryogenic plume scenarios, as it is unclear what operational conditions lead to these events instead of immediate evaporation from the leak site, which has been the usual assumption employed in these analyses.

The unreliability of the LH_2 storage system was estimated based on the fault tree design, which also serves as a representative initiating event of the developed ESDs. This FTA considers three different classes of failure mechanisms: first, external accidents leading to storage component ruptures; secondly, random leaks which have gone undetected by the emergency systems; and thirdly, failures caused by a combination of events and interactions between the components. To quantify these events, failure rate data representing random events was used, although the structure of the fault tree implies a dependency between these events (as opposed to completely random events). The biggest limitation of this is even though the OREDA database has been thoroughly analyzed by component types and failure modes, many assumptions have been made to correctly match

the failure modes on the components described in the book with the ones identified in the station through the FMEA. The FTA delivers an estimated unreliability of 0.1042 in a year which appears to be a conservative estimate compared those implied by the available maintenance and accident records. However, this only refers to the liquid storage system and does not include the dispensing units, which represent the majority of the unavailability events in these stations.

Finally, the development of the PHM framework is set in the context of exploring new risk assessment applications in hydrogen systems. This, with the purpose of aiding the hydrogen community in incorporating these methodologies for future QRA and system safety applications. The main results of this analysis are a description of what a data-driven PHM framework should look like in a hydrogen system, including the stages needed to define and implement them. The main focus is on the data requirements but in this case, the analysis is conceptually constructed based on other published literature where PHM frameworks have been successfully implemented in other systems, including variable renewable energy systems, lithium-ion batteries, and fuel cells. From the previous experience of PHM applications in complex engineering systems, a list of possible measurements in different components of the LH_2 storage system was developed, as well as the planification of what kind of outcome could be obtained from implementing these data-driven models. As mentioned, this design is on a conceptual level as there is currently no publicly available data that could be used to validate this framework.

6.3. Recommendations and Future Work

In this section, the identified possible actions, and recommendations for the future development of this work are discussed. Regarding the current state of hydrogen system

QRAs, it is important to adequately design new incident report databases and data collection methods for operation, maintenance, and failure of hydrogen systems. It is critical to design these databases in such a way that proves useful for QRA to improve the risk assessments of hydrogen systems and support the development of risk-informed codes and standards.

This leads to another aspect of data challenges, which is the lack of data characterizing operational conditions in hydrogen stations leading towards the leak event. To date, the research in hydrogen safety assessments has focused more heavily on consequences than on frequency analysis, aiming to reduce the risk entirely through consequence reduction. An unintended effect of this has led to unsystematic reliability data collection, analysis, and integration to QRAs. While accident reports have been used to develop credible risk scenarios and consequence models, attention should also be brought towards proactively reducing incidents through predictive maintenance strategies. This is highly relevant to hydrogen fueling stations, as the most reported events causing station unavailability are frequent, low-consequence leaks.

A logical step towards this includes exploring, and if necessary, updating the leak frequency probability distributions and transition event probabilities collected in the HyRAM software in the context of LH_2 infrastructure. On the one hand, this action consists of introducing new components into HyRAM (e.g., pumps, evaporators), as the design of these LH_2 stations is different than those of which the historic gas data has been based on. On the other hand, LH_2 release conditions need to be verified through experimental setups and further quantified to be incorporated in the HyRAM ESD models. Detection, ignition, and dispersion behavior probabilities may need to be updated based on the initiating

conditions of a LH_2 leak, including new scenarios such as pooling or cryogenic plume. **For these reasons, the primary focus of the next stages of developed QRA research must focus on the scenario developments and *system failure data aspects essential in a complete risk assessment.***

As mentioned in Section 2.1.1.1, physics-based models for simulating the behavior of multiphase hydrogen flow within pipelines and liquid release behavior are currently being researched. Further steps may consider monitoring the effects of pressure and temperature cycling in LH_2 components' failure probabilities as mentioned in Section 3.4.3.

Experimental research should also shift towards the study of the physics of failure in hydrogen components, incorporating phenomena such as hydrogen embrittlement and fatigue models to risk assessment procedures from a reliability perspective. It should be noted that physics of failure research would be particularly beneficial for components with limited lifespans, such as seals, hoses, and other connecting elements which are key drivers of safety, despite the fact that much of physics-based safety research in hydrogen has extensively focused on storage tank design (for both LH_2 and GH_2). Counterintuitively, this may result in significant improvement to the hydrogen fueling station reliability by reducing more frequent, lower-consequence leaks in connecting elements rather than less frequent, but high-consequence scenarios in the storage tanks.

While ongoing research is being developed for physics-based models for LH_2 releases, recent advances in CBM and PHM in other engineering systems have yielded promising results which merit further exploration. Risk assessment could benefit from the integration of PHM metrics and techniques along with uncertainty and sensitivity analysis

of diagnosis and prognosis tasks. For instance, monitoring and predicting temperature changes and pressure cycling within storage vessels can allow individual risk estimations associated with hydrogen releases and subsequent combustion-related hazards. For this, it is critical to obtain access to a hydrogen station's system information and, if available, monitored data. It is important to analyze site-specific information, such as fueling history and maintenance records, to tailor the design of a data-driven PHM framework. If monitoring data is not available, a risk-screening process and analysis of reliability data can help identify points of interest in the system for designing future applications.

Relevant applications have been described in terms of the cryogenic pump, storage tanks, and piping health diagnosis applications in the previous chapter. However, it is probable that anomaly and fault detection applications could have a greater impact in improving the reliability and availability dispensing system, as this concentrates the majority of unscheduled maintenance events. **Short-term goals for the implementation of data-driven PHM frameworks in hydrogen systems should explore the connection between PHM frameworks, reliability, and safety.** Including the use of a grid-like temperature and pressure sensors in various locations, e.g., upstream and downstream measurement points surrounding main valves and both the cryogenic pump and the evaporator in the case of LH_2 storage systems provides opportunities to use this data for additional purposes. As implied by the *NFPA 2* and CGA codes as well as the available P&ID, these sensors are likely already be installed in critical points of the system. These could be employed for the monitoring of abnormal conditions or for leakage detection along the piping and connecting elements, thus enhancing system safety. More complex monitoring system interventions include the installation of accelerometers either critical

piping sections such as joints and in the vicinity of main valves, as well as in the centrifugal pump shaft and corresponding bearing housing to study and detect pump degradation.

As highlighted through many applications in other complex engineering systems, data-driven PHM frameworks for fault detection, diagnosis, and prognosis are important tools for modernizing the traditional approach to maintenance policies. While there are many examples of applications in the data-driven reliability area, further work is required to determine how PHM frameworks should be integrated to modern risk assessment strategies. Alternatively, the worth of including risk-screening techniques in the design of a monitoring system for health management in complex systems appears to be in line with the PHM standards developed for industry. Incorporating real-time information from a hydrogen system's operation can potentially improve hazard management and reduce some of the barriers these technologies face.

Appendices

Appendix A. Hydrogen Fuel Properties

Until 2016, renewable energy production accounted for 14% of the global energy mix, where electricity-based technologies have led the transition to cleaner and more sustainable alternatives [132]. Hydrogen has historically been considered as a valuable commodity gas and chemical feedstock, however, in recent years, it has also become a valuable alternative for decarbonizing both heating and transport sector, in particular for light and heavy-duty vehicle fuel purposes [133]. This is particularly important for sustainable development goals, as also is the maturity of the technology for producing *green* hydrogen through renewable energy sources and electrolysis processes as reported in 2018 by the International Renewable Energy Agency (IRENA) [134].

Gaseous hydrogen is non-toxic, environmentally safe, and by having a low radiation level, it also presents a reduced risk of secondary fires [1]. Hydrogen is usually safer than other fuels in the event of leaks [75]. Yet, specific regulations and standards for storage and usage must be implemented, along with detection systems to avoid any accident or components failure due to hydrogen attack or hydrogen embrittlement [75], [135]. The Compressed Gas Association (CGA) H-5 Standard for Bulk Hydrogen Supply Systems [31] describes the main safety hazards to consider when handling and storing hydrogen:

- Hydrogen gas is odorless, asphyxiant gas which can displace oxygen. However, it is lighter than air and can accumulate in high spots. Detonations in open areas are highly unlikely due to its high volatility and release speed (20 m/s) [136].
- Hydrogen gas has a wide flammability range (4%-75% in air), and low ignition level (0.02 mJ), so it is comparatively easier to ignite than other liquids and gases, for instance, than gasoline (0.24 mJ) or methane (0.29 mJ). It also possesses a high laminar burning velocity (2.37 m/s). On the other hand, self-ignition temperature of hydrogen (585 °C) is significantly higher than for gasoline (228–501 °C) and natural gas (540 °C) [135].
- Hydrogen gas burns with almost invisible flame in daylight. It has a wide detonation range (18.3%-59% in air), yet these limits are higher than those for gasoline (1.1–3.3%) and natural gas (5.7–14%).

Currently, compressed GH_2 at ambient temperature and high pressures is the most common and mature technology adopted in various hydrogen systems [137]. On the other hand, liquid storage presents the advantage of having a higher density reaching up to 0.07 kg/L compared to 0.03 kg/L achieved by compressed GH_2 [138]. However, the liquefaction process consumes approximately 40% of its energy content while compressing hydrogen gas has lower losses estimated at 10% [7]. Additionally, liquid storage requires temperatures to be below the hydrogen boiling point of -253°C at atmospheric pressure. The use of liquid hydrogen must also consider all of the mentioned safety aspects, as well as those related exclusively to unsafe releases of cryogenic liquid hydrogen: frostbite, cryogenic burns, hypothermia, ice formation on vents and valves, air condensation, and

oxygen enrichment, moisture within storage due to inadequate purging, damage to boil-off and release valves [40]. Liquid hydrogen will vaporize when allowed in contact warm surfaces and although vaporized hydrogen is lighter than air and will disperse rapidly, containment increases hazard because it slows down the rate of vaporization.

To maintain cryogenic and pressure conditions, double-walled storage tanks are required, consisting of an inner pressure vessel and an external protective jacket. The inner tank is frequently constructed from cold-stretched stainless steel and can be both thermally isolated and maintained in vacuum conditions [77]. Generic design methods are described in the ISO 21009-1:2008 *Cryogenic vessels — Static vacuum-insulated vessels — Part 1: Design, fabrication, inspection and tests* and ISO 21009-2:2015 *Cryogenic vessels — Static vacuum insulated vessels — Part 2: Operational requirements* standards [139], [140]. Certain materials are susceptible to hydrogen embrittlement, particularly high-strength steels, and carbon steel at low temperatures. Hydrogen embrittlement is usually observed at ambient temperatures and its effects below -150°C can be neglected in unstable austenitic stainless steels often used for cryogenic vessels. At low temperatures, although it is a non-corrosive liquid, other effects damaging to material integrity must be considered. For instance, changes in mechanical characteristics, expansion, and contractions phenomena, as well as increased brittleness addressed with proper thermal insulation [78]. Additional to the embrittlement of sealing materials, due to the low temperatures, material selection must also account for ductile to brittle transition temperature (DBTT), plastic deformation at low temperatures, and thermal and pressure cycling.

In hydrogen fueling stations, GH_2 is dispensed into vehicles at 35 MPa or 70 MPa and the most frequently-used storage system is compressed hydrogen gas storage. However, GH_2's low density, in terms of volume use and energy capacity, implies additional safety challenges for bulk storage and transportation. Alternative physical and chemical methods exist for hydrogen storage, such as liquefaction and the use of hydrides as described in [7]. Liquid hydrogen storage design, material selection, and cost are directly related to the effect of cryogenic temperatures over the storage system's different components. At the present, even if LH_2 storage systems are more energetically efficient, challenges remain regarding the energy cost in the hydrogen liquefaction process, the high material costs, evaporation losses, and security [141]. Currently, ongoing research is focused on the nature of liquid hydrogen and whether unsafe releases can lead to risks such as ignition, explosions, and cryogenic-temperature related damage.

Renewable on-site hydrogen production in zero-emission stations accounted for 13% of them, mostly found in the USA and Europe. In 2015 the costs of producing hydrogen varied from \$1.8 to 2.9/H_2 kg for Coal gasification, 2.3–5.8/H_2 kg for steam methane reforming (SMR), \$6–7.4/H_2 kg for wind power, and \$6.3–25.4/H_2 kg for solar photovoltaic (PV) systems, with the lowest cost nearing competitiveness with petroleum fuels [1].

Appendix B. Additional Risk Scenarios and Mitigations in HAZOP study

A-Table 1: P-28 HAZOP Consequences in other system nodes.

#	Deviation	Caused by	Consequences
1.1	High pressure	Operator error – trapped liquid by improper valve sequencing	Hose or line rupture resulting in hydrogen release with possible fire/explosion, equipment damage, and personal injury.
1.6	High flow	Line rupture, valve, or component failure	Hydrogen release with possible fire/explosion, equipment damage, and personal injury.
1.16	Loss of containment	External impacts	Hydrogen release, and possible fire/explosion, equipment damage, and personal injury.
		Natural disasters	
		External fire	PRD functions. Hydrogen release, and possible fire/explosion, equipment damage, and personal injury
		Material defects including gasket/packing leaks	Hydrogen release, and possible fire/explosion, equipment damage, and personal injury.
		Hose rupture or bayonet seal failure	
		Trailer rollaway	
3.4	High temperature	External fire	Demand on thermal relief system with hydrogen release, possible fire/explosion, equipment damage, and personal injury.
3.14	Loss of containment	External impacts	Hydrogen release, and possible fire/explosion, equipment damage, and personal injury.
		Natural disasters	
		External fire	Thermal relief functions. Hydrogen release, and possible fire/explosion, equipment damage, and personal injury.
4.6	High flow	Line rupture	Hydrogen release, possible fire/explosion, equipment damage, and personal injury.
		Customer demand exceeds design rate	Overdraw the system with cold gas or liquid to carbon steel piping with possible line failure, hydrogen release, possible fire/explosion, equipment damage, and personal injury.
4.12	Change of state (vapor to liquid)	Overdraw the vaporizer	Cold gas or liquid to carbon steel piping with possible line failure, hydrogen release, possible fire/explosion, equipment damage, and personal injury.
4.15	Loss of containment	External impacts	Hydrogen release, and possible fire/explosion, equipment damage, and personal injury.
		Natural disasters	
		External fire	PRD functions. Hydrogen release, and possible fire/explosion, equipment damage, and personal injury.
7.2	Material incompatibility	Improper design specification	Component failures, reactions, corrosion, cryogenic brittle fractures with hydrogen release, and possible fire/explosion, equipment damage, and personal injury
		Operator error-inadequate maintenance	

A-Table 2: P-28 Other safeguards for large range consequence scenarios.

#	Deviation	Safeguards
1.1	High pressure	Trailer relief valve. Operating procedures. Trailer's bursting disks. Vent system. Trailer's emergency shutdown. Properly labeled lines and valves.
1.6	High flow	Pneumatic trailer air switch. Operator training. Mechanical integrity program.
1.16	Loss of containment	Proper tank sitting in accordance with NFPA 55. Proper foundation. Properly designed PRD vent system. Mechanical integrity program. Proper material selection (material compatibility). Anti-towaway system (vehicle brake interlock). Wheel chocks.
3.4	High temperature	Proper tank sitting in accordance with NFPA 55. Fire-rated isolation valves. Mechanical integrity program.
3.14	Loss of containment	Proper tank sitting in accordance with NFPA 55. Foundation design.
4.6	High flow	Adequate vaporizer and system design for maximum use demand Low temperature protection system. Mechanical integrity program.
4.12	Change of state (vapor to liquid)	Adequate vaporizer and system design for maximum use demand. Low temperature protection system.
4.15	Loss of containment	Proper tank sitting in accordance with NFPA 55. Area fenced-in location. Remotely operable emergency shutoff valve.
7.2	Material incompatibility	Mechanical integrity program System design- austenitic stainless steel or aluminum Operating procedures and training

Appendix C. Hydrogen Fueling Station P&IDs

The documents presented in this Appendix section correspond to those presented by the Hydrogen Fueling Infrastructure Research and Station Technology (H2FIRST) project initiated by the DOE in 2015 and executed by Sandia National Laboratories and the National Renewable Energy Laboratory (NREL) [70].

C.1. Liquid Storage Subsystem

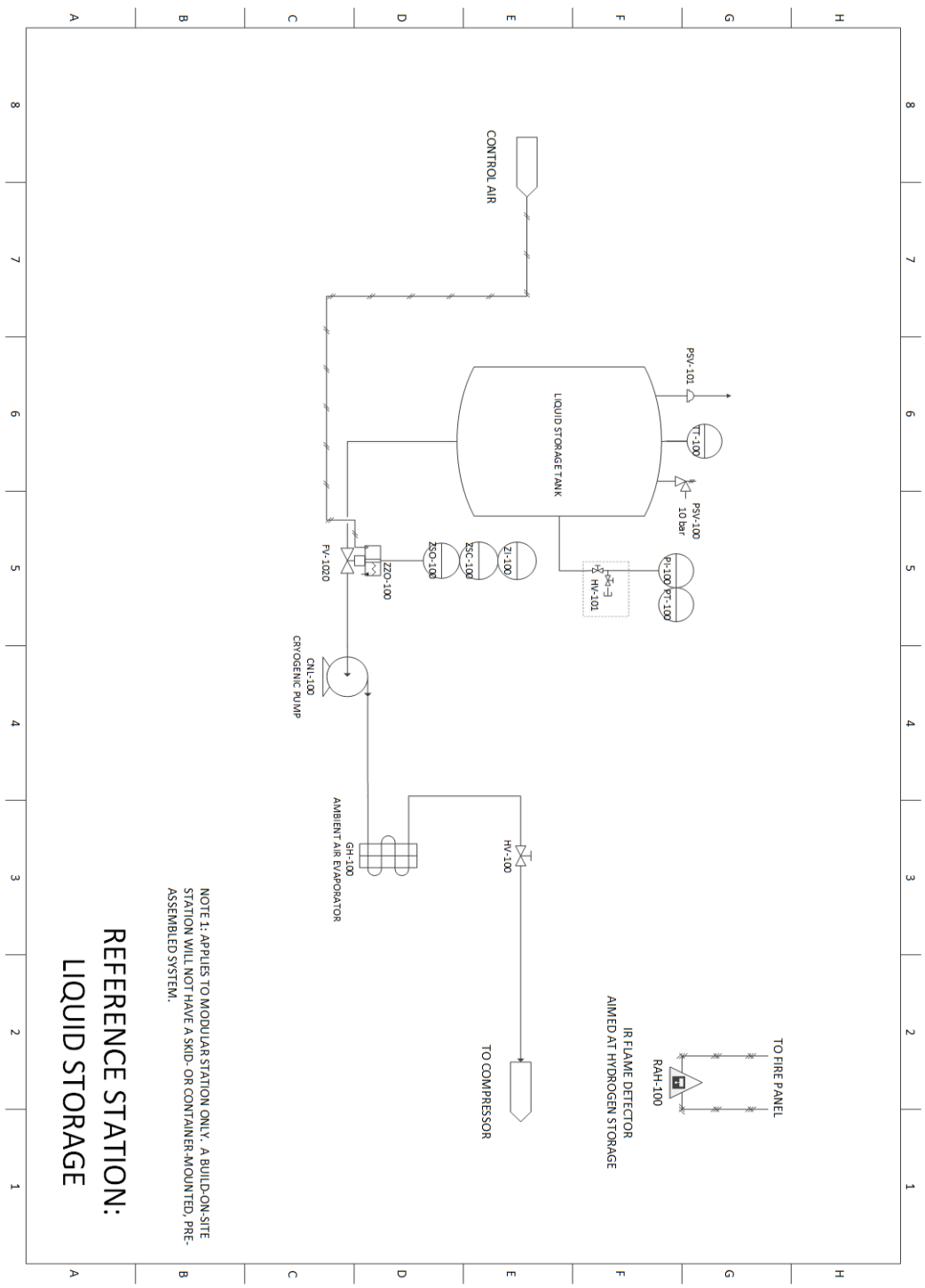

A-Figure 1: Reference Station P&ID - Liquid Storage.

C.2. Compression and Cooling Subsystem

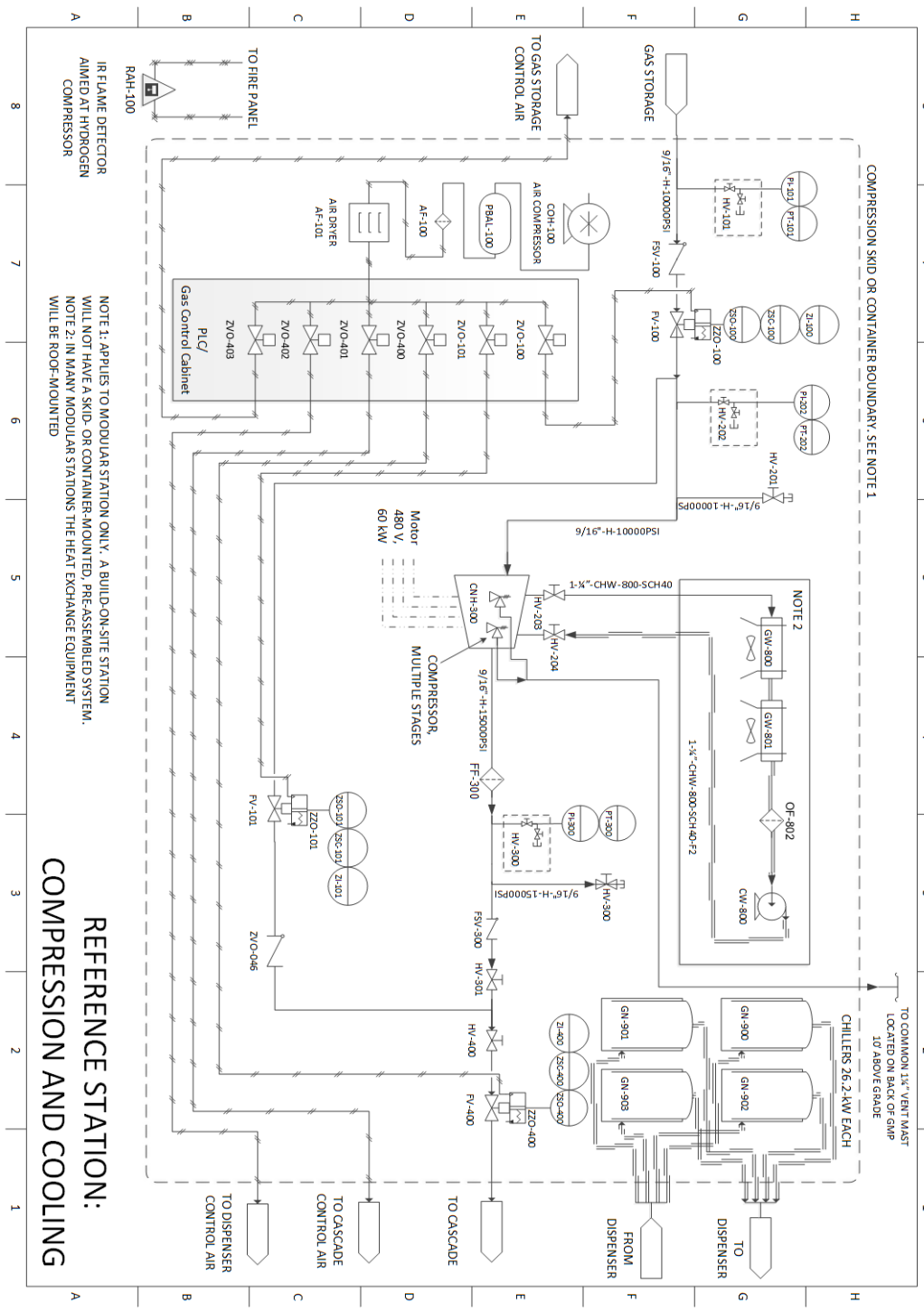

A-Figure 2: Reference Station P&ID - Compression and Cooling.

C.3. Cascade Storage Unit

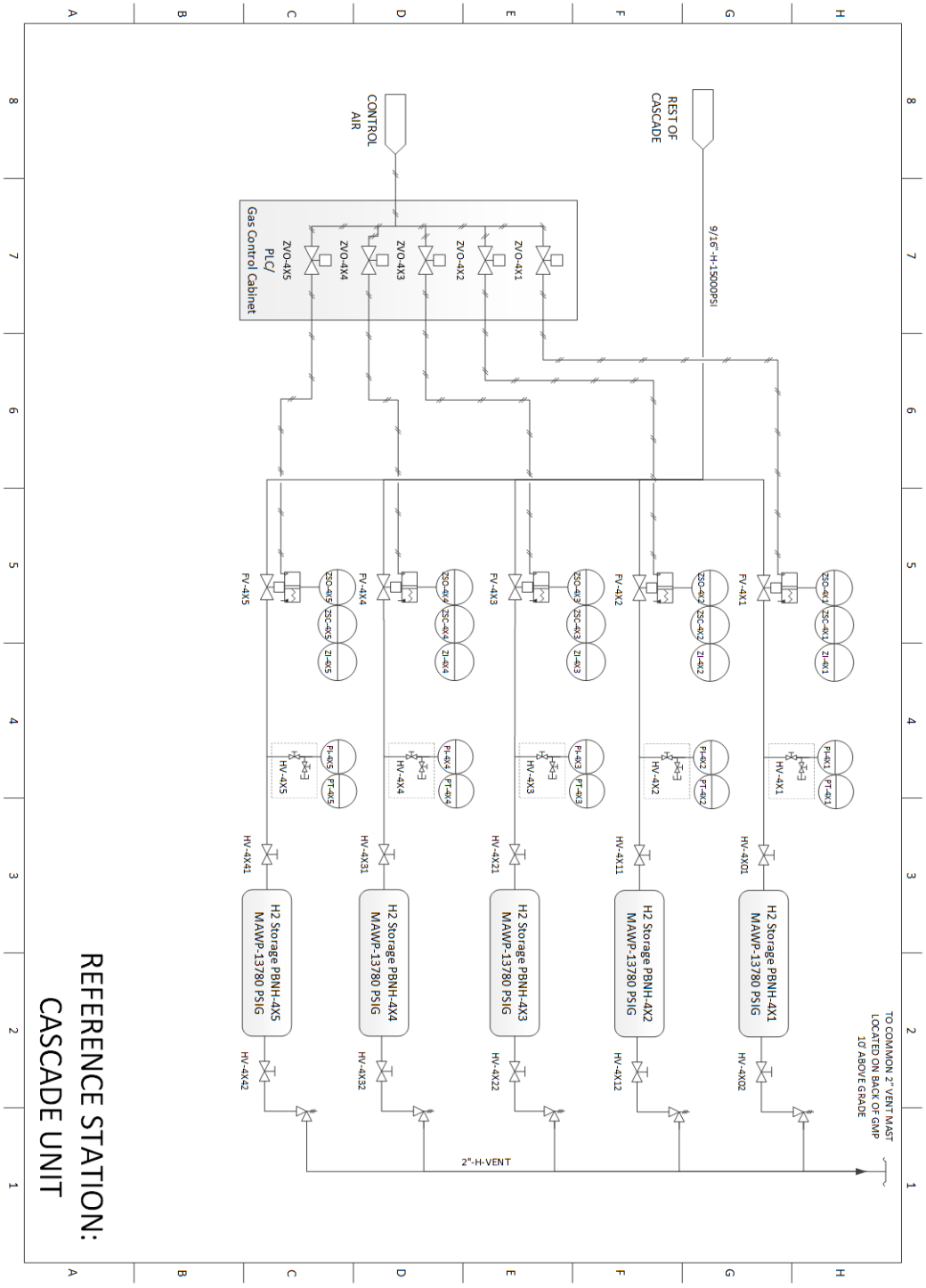

A-Figure 3: Reference Station P&ID – Cascade Gas Storage Unit.

C.4. Cascade Storage System

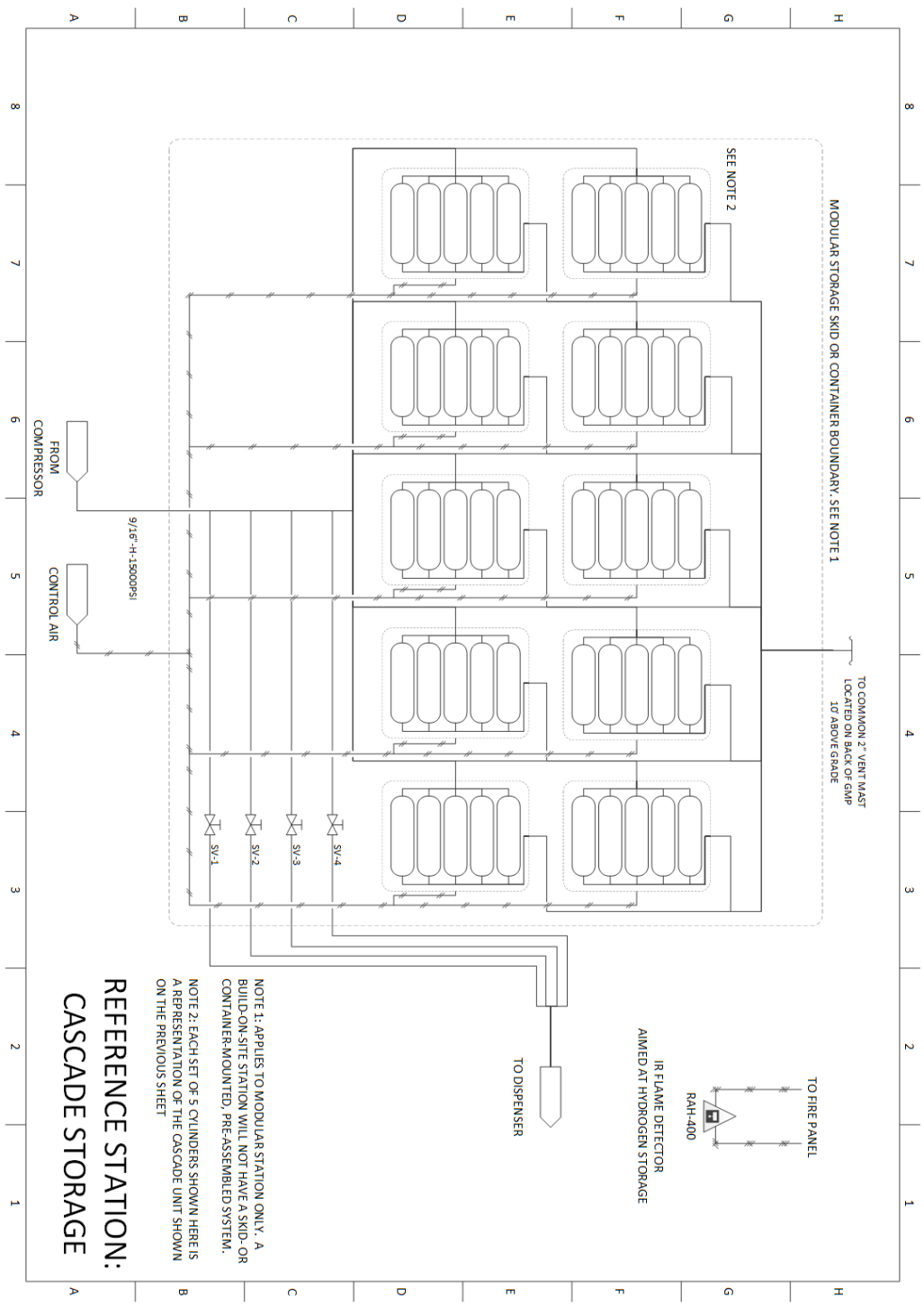

A-Figure 4: Reference Station P&ID - Cascade Storage System.

C.5. Fuel Dispenser Subsystem

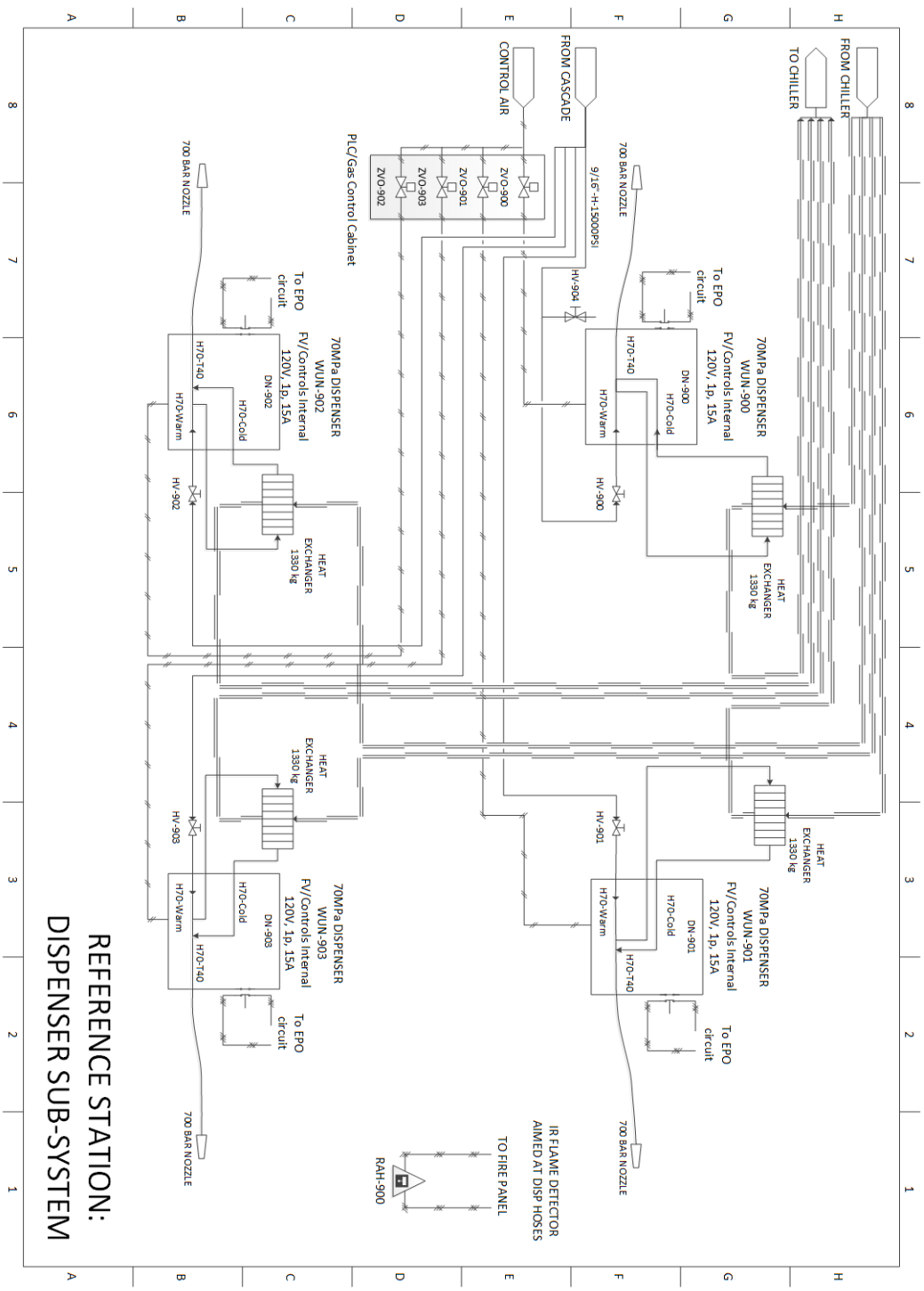

A-Figure 5: Reference Station P&ID – Dispenser.

C.6. Subsystem components by P&ID Nomenclature

A list of the components within each subsystem presented in the previous sections are shown below.

C.6.1. Liquid Storage Subsystem

Using the nomenclature of A-Figure 1 the storage subsystem components are listed as follows:

- Liquid Storage Tank; 800 kg capacity, double wall.
  - Two-way pressure relief valve (PSV-100); pressure switch valve (PSV-101).
  - Temperature transmitter (TT-100).
  - Pressure indicator (PI-100); pressure transmitter (PT-100).
  - Hand valve (HV-101).
- Air-actuated valve, spring return closed; flow valve (FV-1020).
  - Position indicator (ZI-100).
  - Position switch; open (ZSO-100).
  - Position switch; closed (ZSC-100).
  - Position actuator air (ZZO-100).
- Cryogenic Pump (CNL-100).
- Ambient air evaporator (GH-100).
- Hand valve (HV-100).
- IR flame detector aimed at hydrogen storage; radiation alarm high (RAH-100).

C.6.2. Compression and Cooling Subsystem

Using the nomenclature of A-Figure 2, the compression and cooling subsystem components are listed as follows:

- Pressure indicator (PI-101, PI-202, PI-300); pressure transmitter (PT-101, PT-202, PT-300).
  - Ball valve; hand valve (HV-101, HV-202, HV-300).
- Check valve; flow stich valve (FSV-100, FSV-300).
- Air-actuated valve, spring return closed; flow valve (FV-100, FV-101, FV-400).
  - Position indicator (ZI-100, ZI-101, ZI-400).
  - Position switch; open (ZSO-100, ZSO-101, ZSO-400).
  - Position switch; closed (ZSC-100, ZSC-101, ZSC-400).
  - Position actuator air (ZZO-100, ZZO-101, ZZO-400).
- Ball valve; hand valve (HV-201, HV-301. HV-400).
- Multiple Stage Compressor (CNH-300).
  - Ball valve; hand valve (HV-203, HV-204).
  - Air blown cooler (GW-800, GW-801).
  - Water filter (OF-802).
  - Centrifugal water pump (CW-800).
- Flow filter (FF-300).
- Check valve; position valve open (ZVO-046).
- PLC/Gas control cabinet.

    - Position valve open (ZVO-100, ZVO-101, ZVO-400, ZVO-401, ZVO-402, ZVO-403).
- Air compressor COH-100
    - Air dyer; air filter (AF-100, AF-101).
    - PBAL-100.
- IR flame detector aimed at hydrogen compressor; radiation alarm high (RAH-100).
- Chillers (GN-900, GN-901, GN-902, GN-903).

C.6.3. Gas Cascade Storage Subsystem

Using the nomenclature of A-Figure 3 and A-Figure 4, the components of the gas cascade storage are listed as follows:

- Ball valve; switch valve (SV-1, SV-2, SV-3, SV-4).
- Cascade Unit, H_2 storage Unit MAWP-13780 PSIG.
    - Air-actuated valve, spring return closed; flow valve (FV-4X1, FV-4X2, FV-4X3, FV-4X4, FV-4X5).
        - Position indicator (ZI-4X1, ZI-4X2, ZI-4X3, ZI-4X4, ZI-4X5).
        - Position switch; open (ZSO-4X1, ZSO-4X2, ZSO-4X3, ZSO-4X4, ZSO-4X5).
        - Position switch; closed (ZSC-4X1, ZSC-4X2, ZSC-4X3, ZSC-4X4, ZSC-4X5).
        - Position actuator air (ZZO-4X1, ZZO-4X2, ZZO-4X3, ZZO-4X4, ZZO-4X5).
    - PBNH-4X1, PBNH-4X2, PBNH-4X3, PBNH-4X4.
- Pressure indicator (PI-4X1, PI-4X2, PI-4X3, PI-4X4, PI-4X5); pressure transmitter (PT-4X1, PT-4X2, PT-4X3, PT-4X4, PT-4X5).
- Ball valve; hand valve (HV-4X01, HV-4X02, HV-4X11, HV-4X12, HV-4X21, HV-4X22, HV-4X31, HV-4X32, HV-4X41, HV-4X42).
- PLC/Gas control cabinet.
    - Position valve open (ZVO-4X1, ZVO-4X2, ZVO-4X3, ZVO-4X4, ZVO-4X5).
- Unnamed two-way pressure relief valves, five units.

C.6.4. Fuel Dispenser Subsystem

Using the nomenclature of A-Figure 5, the components of the dispenser subsystem are listed as follows:

- Heat exchanger, four unnamed units.
- Dispensers (DN-900, DN-901, DN-902, DN-903).
    - 700 bar nozzles.
    - Hand valve (HV-900, HV-901, HV-902, HV-903).
    - EPO circuit.

Appendix D. Frequency Data Sources

D.1. HyRAM Frequency Data

The event sequence diagram presented in Figure 2-4 refers to the possible scenarios caused by a hydrogen release from a component in a hydrogen fueling station [45]. The frequencies of occurrence for each of these events are:

$$f_{Isolated} = f_{H2\ Release} \times P(Isolated) \quad (3)$$

$$f_{Unignited} = f_{H2\ Release} \times P(\overline{Isolated}) \times (1 - P(Immed.Ignite) - P(Delayed\ Ignite)) \quad (4)$$

$$f_{Jet\ fire} = f_{H2\ Release} \times P(\overline{Isolated}) \times P(Immed.Ignite) \quad (5)$$

$$f_{Explosion} = f_{H2\ Release} \times P(\overline{Isolated}) \times P(Delayed\ Ignite) \quad (6)$$

Here, $f_{H2\ Release}$ is the annual frequency of a hydrogen releases per component, $P(Isolated)$ is the probability of release (leak) detection and isolation before ignition, $P(Immed.Ignite)$ is the probability of immediate ignition, and $P(Delayed\ Ignite)$ is the probability of delayed ignition. These default probability values are:

1. Release Detection and Isolation Probability

The default value for successful detection and isolation of a release is: $P(Isolate) = 0.9$. This value incorporates many considerations on how likely the hydrogen is to detect, including ventilation, sensor placement, leak location, and the ability of the sensor and isolation valve to operate successfully on-demand.

2. Ignition Probabilities

The default hydrogen ignition probabilities are a function of the hydrogen release rate and are obtained from [142] as seen in A-Table 3. It should be noted that both the immediate and delayed ignition probabilities are independent and both relative to a hydrogen release; the delayed ignition probability is not conditional upon the immediate ignition having not occurred. The total probability of ignition of hydrogen is the immediate and delayed ignition probabilities added together.

A-Table 3: HyRAM Probability Data.

Hydrogen release rate (kg/s)	P (Immediate Ignition)	P (Delayed Ignition)
<0.125	0.008	0.004
0.125-6.25	0.053	0.027
>6.25	0.230	0.120

3. Component Leak Frequencies

HyRAM calculates the annual frequency of a hydrogen release for release sizes of 0.01%, 0.1%, 1%, 10%, or 100% with respect to the component pipelines. This annual frequency of random leaks is assumed to be distributed as a lognormal distribution (μ, σ). Given its characteristics, the median value is used in the release calculations. The default

values are generic hydrogen-system annual leak frequencies are found in A-Table 4 and A-Table 5. A particular FTA model has been developed for dispenser releases.

The median of the leak rate $f(t)$ are found as:

$$M[f(t)] = e^{\mu} \quad (7)$$

To incorporate the leakage frequencies into the calculation of the release frequencies, HyRAM uses the following equation, for which an example for 0.01% leaks is showed in A-Figure 6:

$$f_{Random\ Releases,size\ k} = \sum_{i=1} N_{Component_i} \times f_{Leak_{i,k}} \quad (8)$$

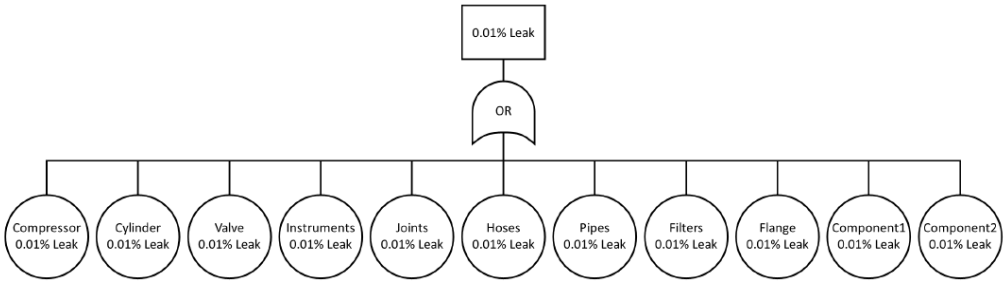

A-Figure 6: Example of HyRAM Fault Tree for Random Leaks.

A-Table 4: Random leak frequency parameters per components. To be continued.

Component	Release size %	μ	σ	*Mean*	5^{th}	*Median*	95^{th}
Compressors	0.01	-1.73	0.22	1.8E-01	1.2E-01	1.8E-01	2.6E-01
	0.1	-3.95	0.50	2.2E-02	8.5E-03	1.9E-02	4.4E-02
	1	-5.16	0.80	7.9E-03	1.5E-03	5.8E-03	2.2E-02
	10	-8.84	0.84	2.1E-04	3.6E-05	1.4E-04	5.7E-04
	100	-11.34	1.37	3.0E-05	1.3E-06	1.2E-05	1.1E-04
Cylinders	0.01	-13.92	0.67	1.1E-06	3.0E-07	9.0E-07	2.7E-06
	0.1	-14.06	0.65	9.6E-07	2.7E-07	7.8E-07	2.3E-06
	1	-14.44	0.65	6.6E-07	1.8E-07	5.4E-07	1.6E-06
	10	-14.99	0.65	3.8E-07	1.1E-07	3.1E-07	9.0E-07
	100	-15.62	0.68	2.1E-07	5.3E-08	1.6E-07	5.0E-07
Filters	0.01	-5.25	1.99	3.8E-02	2.0E-03	5.3E-03	1.4E-01
	0.1	-5.29	1.52	1.6E-02	4.2E-04	5.0E-03	6.1E-02
	1	-5.34	1.48	1.4E-02	4.2E-04	4.8E-03	5.5E-02
	10	-5.38	0.89	6.9E-03	1.1E-03	4.6E-03	2.0E-02
	100	-5.43	0.95	6.9E-03	9.1E-04	4.4E-03	2.1E-02

A-Table 5: Random leak frequency parameters per components. Continued.

Component	Release size %	μ	σ	Mean	5^{th}	$Median$	95^{th}
Flanges	0.01	-3.92	1.66	7.9E-02	1.3E-03	2.0E-02	3.0E-01
	0.1	-6.12	1.25	4.8E-03	2.8E-04	2.2E-03	1.7E-02
	1	-8.33	2.20	2.7E-03	6.4E-06	2.4E-04	9.0E-03
	10	-10.54	0.83	3.7E-05	6.7E-06	2.6E-05	1.0E-04
	100	-12.75	1.83	1.5E-05	1.4E-07	2.9E-06	4.9E-05
Hoses	0.01	-6.83	0.28	1.1E-03	6.8E-04	1.1E-03	1.7E-03
	0.1	-8.73	0.61	1.9E-04	5.9E-05	1.6E-04	4.4E-04
	1	-8.85	0.59	1.7E-04	5.4E-05	1.4E-04	3.8E-04
	10	-8.96	0.59	1.5E-04	4.9E-05	1.3E-04	3.4E-04
	100	-9.91	0.88	7.3E-05	1.2E-05	5.0E-05	2.1E-04
Joints	0.01	-9.58	0.17	7.0E-05	5.2E-05	6.9E-05	9.1E-05
	0.1	-12.92	0.81	3.4E-06	6.4E-07	2.4E-06	9.3E-06
	1	-11.93	0.51	7.5E-06	2.8E-06	6.6E-06	1.5E-05
	10	-12.09	0.58	6.7E-06	2.2E-06	5.6E-06	1.5E-05
	100	-12.22	0.61	6.0E-06	1.8E-06	4.9E-06	1.3E-05
Pipes	0.01	-11.91	0.69	8.5E-06	2.1E-06	6.7E-06	2.1E-05
	0.1	-12.57	0.71	4.5E-06	1.1E-06	3.5E-06	1.1E-05
	1	-13.88	1.14	1.8E-06	1.4E-07	9.3E-07	6.1E-06
	10	-14.59	1.16	9.1E-07	6.8E-08	4.6E-07	3.1E-06
	100	-15.73	1.72	6.4E-07	8.8E-09	1.5E-07	2.5E-06
Valves	0.01	-5.19	0.18	5.7E-03	4.2E-03	5.6E-03	7.5E-03
	0.1	-7.31	0.42	7.3E-04	3.4E-04	6.7E-04	1.3E-03
	1	-9.71	0.98	9.8E-05	1.2E-05	6.0E-05	3.0E-04
	10	-10.34	0.69	4.1E-05	1.0E-05	3.2E-05	1.0E-04
	100	-12.00	1.33	1.5E-05	6.9E-07	6.1E-06	5.5E-05
Instruments	0.01	-7.38	0.71	8.0E-04	1/9E-04	6.2E-04	2.0E-03
	0.1	-8.54	0.82	2.7E-04	5.1E-05	2.0E-04	7.5E-04
	1	-9.10	0.92	1.7E-04	2.4E-05	1.1E-04	5.1E-04
	10	-9.21	1.09	1.8E-04	1.7E-05	1.0E-04	6.0E-04
	100	-10.21	1.49	1.1E-04	3.2E-06	3.7E-05	4.3E-04

D.2. OREDA

OREDA holds a collection of failure data, failure modes and mechanisms recorded for specific components in engineering systems. Given the wide variety of industrial components and failure rates described, this is considered one of the most important

industrial reliability data sources available. To analyze this database, the following definitions needs to be considered [87]:

1. Failure is defined as the termination of the ability of an item to perform its required functions. This can also refer to the degradation of said function below acceptable limits. A failure event can include:
   - A partial or complete breakdown of the item which causes unavailability and requires corrective maintenance action.
   - Damage or degradation discovered during periodical inspection, testing, or preventive maintenance that requires repair.
   - Failure on safety devices or control/monitoring devices that necessitates shutdown, or reduction of the item's capability below specified limits.
2. A failure mechanism is defined as the apparent, immediate cause of the failure and is related to the lowest level in the system's hierarchy where it can be identified.
3. A failure mode is defined as the effect by which a failure is observed on the failed unit, related to the equipment unit level. The failure mode is a description of the various abnormal states/conditions of an equipment unit. Failure modes can be grouped into three main categories (ISO 14224):
   - The desired function is not obtained.
   - Specified function lost or outside accepted operational limits.
   - A failure indication is observed, but there is no immediate and critical impact on the equipment unit function. These are typical non-critical failures related to some degradation or incipient failure condition.
4. Severity classes in the context of failures are used to describe the effect on operational status and the severity of loss of output from the unit.
   - Critical failure: a failure that causes an immediate and complete loss of an equipment unit's capability of providing its output.
   - Degraded failure: a failure which is not critical, but it prevents and equipment unit from providing its output within specifications. Such a failure would usually be gradual or partial and may develop into a critical failure in time.
   - Incipient failure: a failure that does not immediately cause loss of a unit's capability of providing its output, but which, if not attended to, could result in a critical or degraded failure.
   - Unknown: failure severity was not recorded or could not be deduced.

The OREDA database is divided into topside and subsea equipment; the first will be the focus of this analysis. This includes data regarding pumps, electric motor, valves, instrumentation input devices, heat exchangers, process vessels, among others. Equipment types are further subdivided into particular applications, e.g.: pumps include centrifugal pumps for cooling applications. Each equipment type is described as a function of their subcomponents and corresponding *maintainable items*. Each failure mode is associated to the most probable combination of a maintainable item and failure mechanism. A-Table 6 summarized the failure modes identified to be relevant in the analysis of the LH_2 storage system. A list of relative contributions of each maintainable item and failure mechanisms to the total failure rate is presented decomposed for each failure mode. Both these inputs are valuable for FMEA and FTA analysis, primarily, as a method to prioritize failure modes

to monitor in the system. presents the failure modes selected as relevant for the analysis of the LH_2 storage system.

Failure rates $\hat{\lambda}$ are estimated from number of multiple failures of a single component or single failures from multiple components, as shown in Equation (9). A 90% confidence interval is given for every estimated failure rate through a χ^2 distribution. The failure data is formatted as shown in A-Table 7, under two aggregated time assumptions: calendar time and operational time. Calendar time is given with a higher certainty than operational time; however operational time-based failure rates are of importance to stand-by units and on/off components.

A-Table 6: Relevant Failure Modes from OREDA database.

FM	Description	FM	Description
AIR	Abnormal instrument reading	NOI	Noise
AOL	Abnormal output - low	NOO	No output
ELP	External leakage - process medium	OHE	Overheating
ELU	External leakage - utility medium	OTH	Other
ERO	Erratic output	PDE	Parameter deviation
FTF	Fail to function on demand	SER	Minor in-service problems
FTS	Fail to start on demand	SPO	Spurious operation
HIO	High output	STD	Structural deficiency
INL	Internal leakage	UNK	Unknown
LCP	Valve leakage in closed position	VIB	Vibration

$$\hat{\lambda} = \frac{Number\ of\ failures}{Aggregated\ time\ in\ service} = \frac{n}{\tau} \tag{9}$$

A general failure rate is given for each component and is also presented for each failure mode, when available. Further, these are also categorized into severity classes: critical, degraded, incipient and unknown. Additionally, maintenance data is also reported based on the number of demands or cycles of the total population. Active repair times and calendar manhours are reported for the corresponding maintenance action for each failure mode and severity class. However, in several cases these numbers only estimated and heavily depend on the facilities' maintenance procedures and capacity.

The scope of the OREDA handbook covers the following items for the topside equipment:

- A drawing illustrating the boundary of the equipment unit and specification of subunits and maintainable items that are part of the various subunits.
- A listing of all failure modes, classified as *critical, degraded, incipient* or *unknown*.
- The aggregated observed time in service for the equipment unit, classified as *calendar time*, *operational time*, and *number of demands*.
- The observed number of failures for each failure mode.
- An estimate of the constant failure rate for each failure mode with associated uncertainty intervals.

- Mean and maximum values of the *active* repair time, i.e., the elapsed time in hours to repair the failure and restore the function time (time when actual repair work was being done).
- Mean and maximum values of the *manhours* repair time, i.e., the number of manhours requires to repair the failure and restore the function.
- Supportive information, e.g., equipment population and number of installations.
- A cross-tabulation of:
  a) Maintainable item vs Failure mode
  b) Failure mechanism vs Failure mode

In the following sections, failure data related to the components in the LH_2 storage system are discussed.

A-Table 7: OREDA Topside Data Table Format.

Taxonomy no.: 1.3.1.3	**Item - Machinery – Pumps - Centrifugal - Cooling Systems**								
Population: 15 Installations: 1	Aggregated time in service (10e6 hours)					No of demands			
	Calendar time * 0.7033			Operational time † 0.6507					
Failure mode	No of failures	Failure rate (per 10e6 hours)					Active rep. hrs.		Manhours	
		Lower	Mean	Upper	SD	n/t	Mean	Max	Mean	Max
Critical										
VIB										
Degraded										
ELP										
Incipient										
AIR										
Unknown										
ELU										
All modes										
Comments										

D.2.1. Pumps

This equipment type is divided into five subdivisions: power transmission, pump unit, control and monitoring, lubrication system and miscellaneous elements. By analyzing the most frequent maintainable items as shown in A-Figure 7, it can be identified that there is a significant number of failures with no attributable subcomponent (i.e., *unknown* subcomponents), only surpassed by seals. Additionally, external leakage either of process (ELP) or utility (ELU) medium are the most common failure modes related to these maintainable items, as well as abnormal instrument readings (AIR). A-Table 8 lists the failure modes and mechanisms with higher relative contributions to the total failure rate,

while A-Figure 8 presents the relationship between these. Both are consistent identifying that leakage and abnormal instrumentation behavior have a considerable effect on the pump's failures.

Failure rates are available for these main failure modes for centrifugal pumps used in cooling systems, which is the taxonomic classification most similar to the cryogenic pump installed in the LH_2 system (1.3.1.3). As the cryogenic pump operates under demand, the failure rates estimated in *operational time* presented in A-Table 9 are considered more representative values.

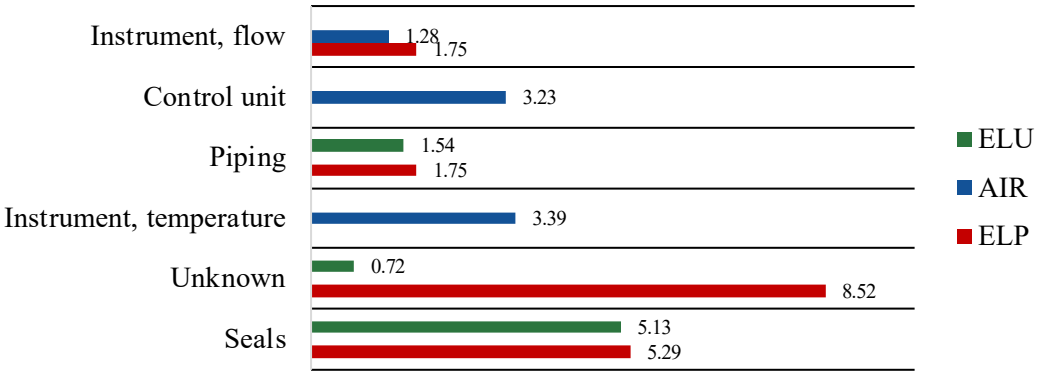

A-Figure 7: Maintainable items relative contribution to the total failure rate, %.

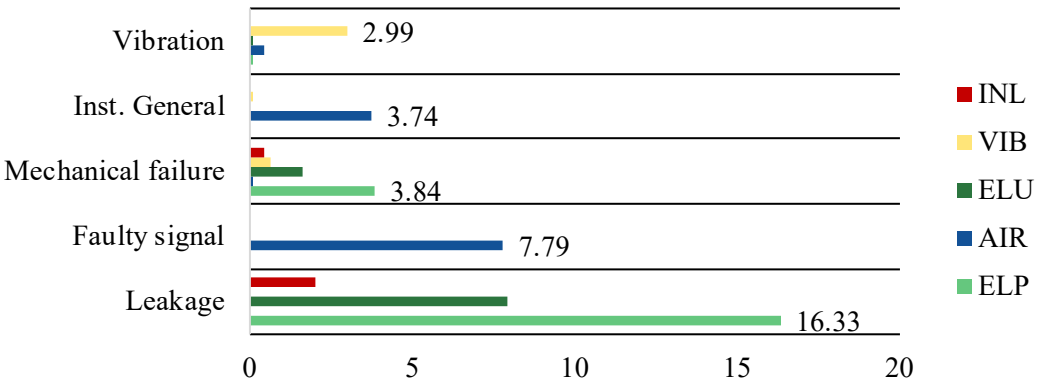

A-Figure 8: Top failure modes and mechanisms in centrifugal pumps, %.

A-Table 8: Top failure mode and mechanisms - Centrifugal pumps.

Failure Modes	Contribution, %	Failure Mechanisms	Contribution, %
INL	4.06	Vibration	4.72
VIB	5.02	Blockage/plugged	5.36
OTH	5.25	Inst. General	5.46
ELU	12.81	Faulty signal	9.07
AIR	19.44	Mechanical failure	10.89
ELP	23.82	Leakage	27.12
Total	70.40	Total	62.62

A-Table 9: Failure rates for Centrifugal Pump in Cooling Systems.

Severity Class	Failure Mode	Mean	SD	n/t	Time
Critical	All	5.69	2.84	5.69	*
		6.15	3.07	6.15	†
	VIB	2.84	2.01	2.84	*
		3.07	2.17	3.07	†
Degraded	All	12.8	4.27	12.8	*
		13.8	4.61	13.8	†
	AIR	1.42	1.42	1.42	*
		1.54	1.54	1.54	†
	ELP	7.11	3.18	7.11	*
		7.68	3.44	7.68	†
	ELU	1.42	1.42	1.42	*
		1.54	1.54	1.54	†
Incipient	All	22.8	5.69	22.8	*
		24.6	6.15	24.6	†
	AIR	7.11	3.18	7.11	*
		7.68	3.44	7.68	†
	ELU	1.42	1.42	1.42	*
		1.54	1.54	1.54	†
	INL	2.84	2.01	2.84	*
		3.07	2.17	3.07	†
	OTH	2.84	2.01	2.84	*
		3.07	2.17	3.07	†
Unknown	All	1.42	1.42	1.42	*
		1.54	1.54	1.54	†
	ELU	1.42	1.42	1.42	*
		1.54	1.54	1.54	†
All modes	All	42.7	7.79	42.7	*
		46.1	8.42	46.1	†

Note: All failure rates are given in (10^{-6}hrs.)

D.2.2. Electric Motor for Centrifugal Pump

This equipment type is divided into five subdivisions: motor, control and monitoring, lubrication system, cooling system, and miscellaneous elements. Failure to start (FTS), vibrations (VIB) and structural deficiencies (STD) are the most common failure modes. A-Table 10 lists the failure modes and mechanisms with higher relative contributions to the total failure rate, while A-Figure 9 presents the relationship between these. Both are consistent identifying that electrical failures and abnormal vibrations have a considerable effect on the motor's failures.

Failure rates are available for these main failure modes for electric motors powering centrifugal pumps used in cooling systems, which is the taxonomic classification most similar to the cryogenic pump installed in the LH_2 system (2.2.2.4). Other failure modes identified as relevant in general applications of electric motors in centrifugal pumps (2.2.2) are also presented. As the cryogenic pump operates under demand, the failure rates estimated in *operational time* presented in A-Table 11 are considered more representative values.

A-Table 10: Top failure mode and mechanisms - Electric motors.

Failure Modes	Contribution, %	Failure Mechanisms	Contribution, %
BRD	6.37	Faulty power	4.55
OHE	6.37	Breakage	4.55
UST	6.37	Inst. General	6.37
ELU	7.27	Control failure	6.37
PDE	7.27	Leakage	7.27
STD	10.01	Vibration	10.00
VIB	10.91	Mechanical failure	14.55
FTS	20.01	Electrical failure	23.64
Total	74.58	Total	77.30

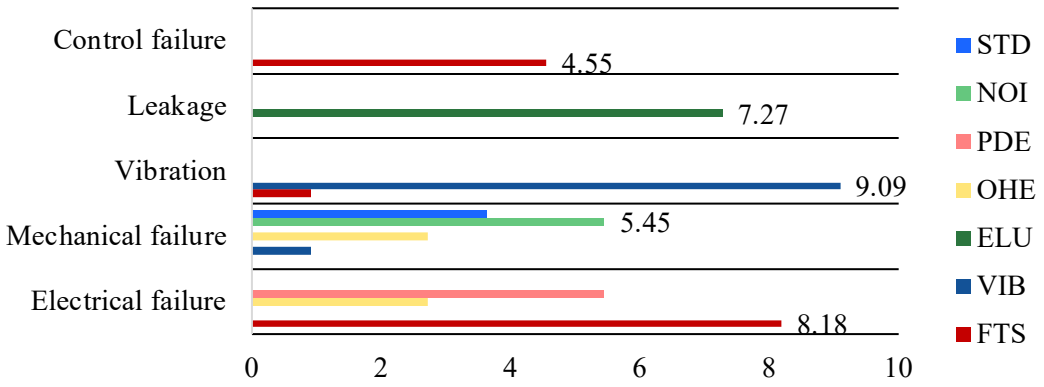

A-Figure 9: Top failure modes and mechanisms in electric motors, %.

A-Table 11: Failure rates for Electric Motors in Centrifugal Pump-Cooling Systems.

Type	Severity Class	Failure Mode	Mean	SD	n/t	Time
Electric Motor, Centrifugal Pump, Cooling Systems	Critical	All	17.44	8.72	17.44	*
			17.44	8.72	17.44	†
		FTS	17.44	8.72	17.44	*
			17.44	8.72	17.44	†
	Degraded	All	8.72	6.17	8.72	*
			8.72	6.17	8.72	†
		PDE	4.36	4.36	4.36	*
			4.36	4.36	4.36	†
		STD	4.36	4.36	4.36	*
			4.36	4.36	4.36	†
	All modes	All	26.16	10.68	26.16	*
			26.16	10.68	26.16	†
Electric Motor, Centrifugal Pump	Critical	ELU	3.47	7.91	1.52	*
			3.68	9.01	1.74	†
		NOI	0.69	0.51	0.87	*
			0.83	0.51	0.99	†
		OHE	0.95	0.77	1.3	*
			1.16	0.77	1.49	†
		VIB	0.48	0.88	0.22	*
			0.55	0.95	0.25	†
	Degraded	ELU	1.00	1.79	0.22	*
			1.13	2.02	0.25	†
		NOI	0.72	1.09	0.65	*
			1.25	2.27	0.74	†

Note: All failure rates are given in (10^{-6} hrs.)

D.2.3. Valves

This equipment type is divided into four subdivisions: valves, actuator, control and monitoring, and miscellaneous elements. Prevalent failure modes differ between different types of valves. Relief and shut-off valves are of interest for this analysis.

(1) Relief Valves

In the case of relief valves, most common failures have undetermined causes, followed by leakage (ELP) and delays in operation (DOP). A-Table 12 lists the failure modes and mechanisms with higher relative contributions to the total failure rate, while A-Figure 10 presents the relationship between these.

Failure rates are available for the listed failure modes for conventional pressure relief valves (PSV), which is the taxonomic classification most similar the PSV present in the LH_2 storage tank in the system (4.4.12.3). As the PSV operates under demand, the failure rates estimated in operational time presented in A-Table 13 are considered more representative values.

A-Table 12: Top failure mode and mechanisms - Relief valves.

Failure Modes	Contribution, %	Failure Mechanisms	Contribution, %
FTO	7.40	Wear	7.410
STD	7.40	Corrosion	11.10
DOP	14.81	Leakage	14.81
ELP	14.81	Other	18.52
OTH	33.33	Unknown	29.61
Total	77.75	Total	81.45

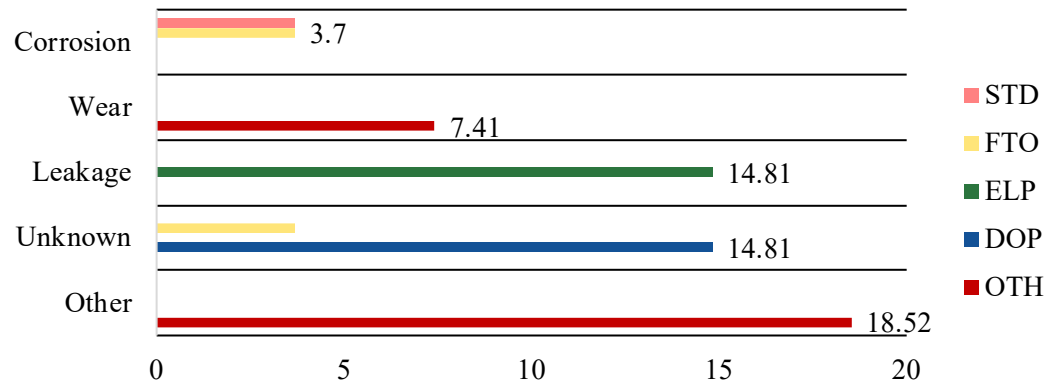

A-Figure 10: Top failure modes and mechanisms in relief valves, %.

A-Table 13: Failure rates for Conventional PSV Relief Valves.

Severity Class	Failure Mode	Mean	SD	n/t	Time
Critical	All	1.02	1.15	1.15	*
		1.03	1.17	1.17	†
	FTO	1.02	1.15	1.15	*
		1.03	1.17	1.17	†
Incipient	All	5.11	4.29	5.75	*
		5.17	4.29	5.83	†
	STD	1.50	1.83	1.15	*
		1.51	1.81	1.17	†
	OTH	4.07	2.3	4.6	*
		4.12	2.33	4.67	†
All modes	All	5.93	5.08	6.9	*
		6	5.08	7	†

Note: All failure rates are given in (10^{-6} hrs.)

(2) Shut-off Valves

In the case of shut-off valves, failure modes have not been described in detail. Most common failures are related to service issues (SER) and leakage when closed (LCP), both related to materials and mechanical failures. A-Table 14 lists the failure modes and mechanisms with higher relative contributions to the total failure rate, while A-Figure 11 presents the relationship between these.

Failure rates are available for the listed failure modes for ball and gate shut-off valves, both taxonomic classifications most similar to the ones present in the system (4.4.13.1 and 4.4.13.3, respectively). As these valves operate under demand, the failure rates estimated in operational time presented in A-Table 15 and A-Table 16 are considered more representative values.

A-Table 14: Top failure mode and mechanisms - Shut-off valves.

Failure Modes	**Contribution, %**	**Failure Mechanisms**	**Contribution, %**
INL	11.11	Leakage	22.22
ELU	22.22	Mechanical failure	22.22
LCP	33.33	Corrosion	22.22
SER	33.33	Material failure	33.33
Total	100.00	Total	100.00

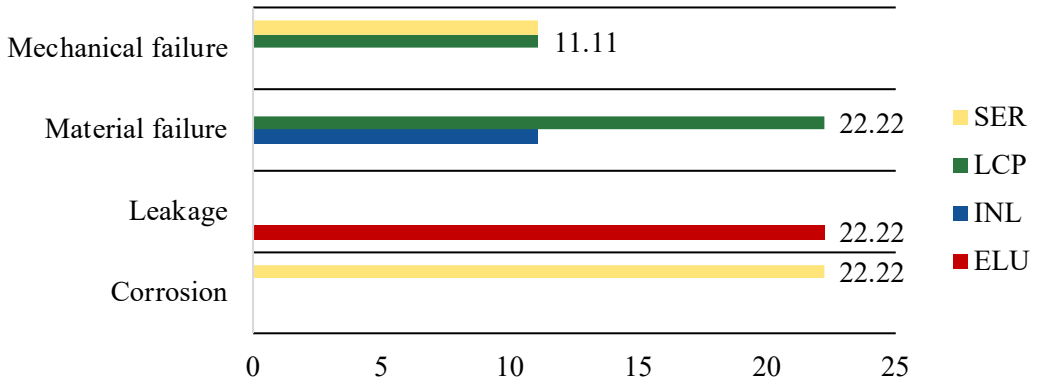

A-Figure 11: Top failure modes and mechanisms in shut-off valves, %.

A-Table 15: Failure rates for Shut-off valves. To be continued.

Type	**Severity Class**	**Failure Mode**	**Mean**	**SD**	**n/t**	**Time**
Shut-off, Ball	Critical	All	24.74	24.74	24.74	*
			24.76	24.76	24.76	†
		ELU	24.74	24.74	24.74	*
			24.76	24.76	24.76	†

Note: All failure rates are given in (10^{-6} hrs.)

A-Table 16: Failure rates for Shut-off valves. Continued

Type	Severity Class	Failure Mode	Mean	SD	n/t	Time
Shut-off, Ball	Degraded	All	24.74	24.74	24.74	*
			24.76	24.76	24.76	†
		ELU	24.74	24.74	24.74	*
			24.76	24.76	24.76	†
	All modes	All	5.93	5.08	6.9	*
			6	5.08	7	†
Shut-off, Gate	All modes	All	4.03	5.7	-	*
			4.03	5.7	-	†

Note: All failure rates are given in (10^{-6} hrs.)

D.2.4. Input Devices

This equipment refers to transmitters, transducers, and switch-type components. As this covers a wide range of different devices, this category is divided into two general subdivisions: control and monitoring and miscellaneous elements. Most common failures are related to service issues (SER) and failure to function on-demand (FTF), mostly related to leakage failures. A-Table 17 lists the failure modes and mechanisms with higher relative contributions to the total failure rate, while A-Figure 12 presents the relationship between these. This data mostly implies that instrumentation is damaged through leakage events and other undetermined reasons.

A-Table 17: Top failure mode and mechanisms - Input devices.

Failure Modes	Contribution, %	Failure Mechanisms	Contribution, %
UNK	4.55	Faulty signal	9.09
AOL	13.64	Mechanical Failure	9.10
FTF	18.19	Unknown	13.64
OTH	22.74	Inst. General	18.20
SER	40.92	Leakage	40.91
Total	100.00	Total	90.94

(3) Pressure Sensors

Pressure sensor devices mostly present the same failure modes and mechanisms as general input devices. These differ in the relative contribution of service issues (SER) and failure to function on-demand (FTF) to the overall failure rate, as shown in A-Table 18. A-Figure 13 presents the relationship between the failure modes and mechanisms. Similarly, this data implies that instrumentation is damaged through leakage events and other undetermined reasons.

Failure rates are available for these general failure modes for various input devices. Failure data referring to temperature (4.2.4) and pressure sensors (4.2.3) are shown in A-Table 19. The latter is discussed more in depth in the following section. In this case, *calendar time* should represent more accurately the monitoring process of the system.

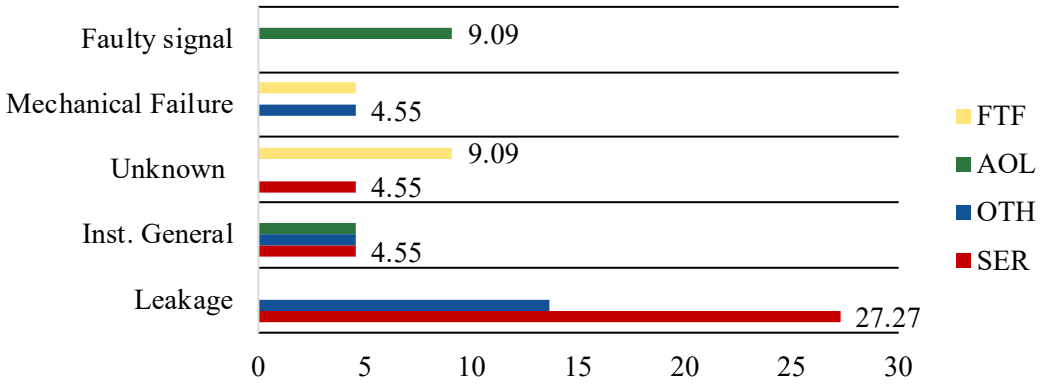

A-Figure 12: Top failure modes and mechanisms in input devices, %.

A-Table 18: Top failure mode and mechanisms - Pressure input devices.

Failure Modes	**Contribution, %**	**Failure Mechanisms**	**Contribution, %**
FTF	14.28	Inst. General	7.14
OTH	35.71	Contamination	7.14
SER	50.00	Earth/isolation fault	7.14
		Mechanical Failure	14.28
		Leakage	64.29
Total	100.00	Total	100.00

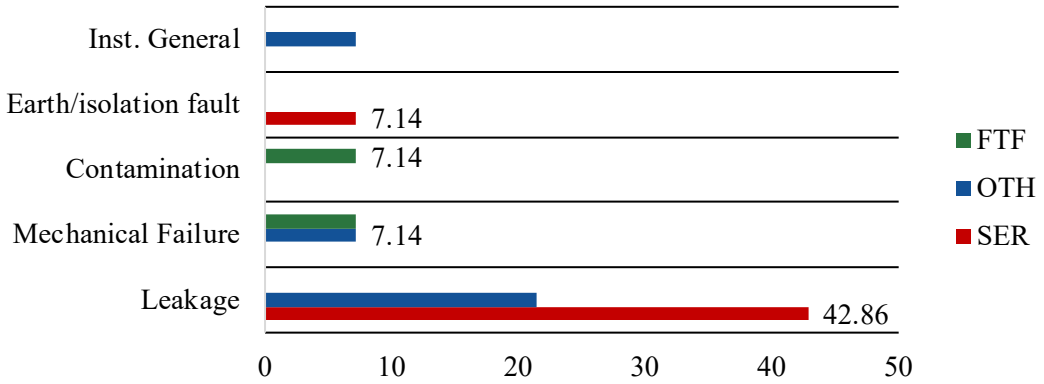

A-Figure 13: Top failure modes and mechanisms in pressure input devices, %.

A-Table 19: Failure rates for various input devices.

Type	Severity Class	Failure Mode	Mean	SD	n/t	Time
Input devices, general	Critical	All	2.15	2.32	0.52	*
			2.16	2.23	0.65	†
		FTF	1.73	2.11	0.29	*
			1.72	2.08	0.37	†
	Degraded	All	3.66	5.04	0.59	*
			3.66	5.02	0.74	†
		AOL	0.65	1.02	0.07	*
			0.65	1.01	0.09	†
	All modes	All	9.98	11.95	1.62	*
			10.00	11.88	2.04	†
Temperature, general	All modes	All	3.63	5.13	-	*
			3.63	5.14	-	†
Temperature, resistance	All modes	All	2.22	3.14	-	*
			2.22	3.14	-	†
Pressure, general	Critical	All	1.05	1.48	1.05	*
			1.09	1.37	1.09	†
		SER	0.51	1.90	0.51	*
			0.51	1.71	0.51	†
		OTH	0.51	1.54	0.51	*
			0.45	1.15	0.45	†
	Degraded	All	2.45	5.42	0.45	*
			2.48	5.41	0.58	†
		SER	1.67	3.59	0.30	*
			1.70	3.57	0.38	†
		OTH	0.88	1.76	0.15	*
			0.90	1.74	0.19	†
	Incipient	All	2.08	2.35	0.23	*
			2.09	2.32	0.29	†
		SER	2.08	2.35	0.23	*
			2.09	2.32	0.29	†
	All modes	All	5.93	5.08	6.90	*
			6.00	5.08	7.00	†

Note: All failure rates are given in (10^{-6} hrs.)

D.2.5. Fire & Gas Detectors

This equipment refers to fire and gas detectors. As this covers a wide range of different devices, this category is divided into three general subdivisions: sensors, interface unit and miscellaneous elements. Most common failures are related to anomalous high and erratic outputs (HIO, ERO), as well as failure to function on-demand (FTF). A-Table 20 lists the failure modes and mechanisms with higher relative contributions to the total failure

rate, while A-Figure 14 presents the relationship between these. This data mostly implies that instrumentation is damaged through contamination events and calibration issues.

Failure rates are available for general failure modes for various detectors devices. Failure data referring generic fire and gas detectors (4.1) are shown in A-Table 21 and A-Table 22. In this case, *calendar time* should represent more accurately the monitoring process of the system.

A-Table 20: Top failure mode and mechanisms - Fire & gas detectors.

Failure Modes	Contribution, %	Failure Mechanisms	Contribution, %
UNK	8.75	Faulty signal	10.00
NOO	10.00	Inst. General	11.25
FTF	17.50	Unknown	17.50
ERO	20.00	Out of adjustment	20.00
HIO	23.75	Contamination	27.50
Total	80.00	Total	86.25

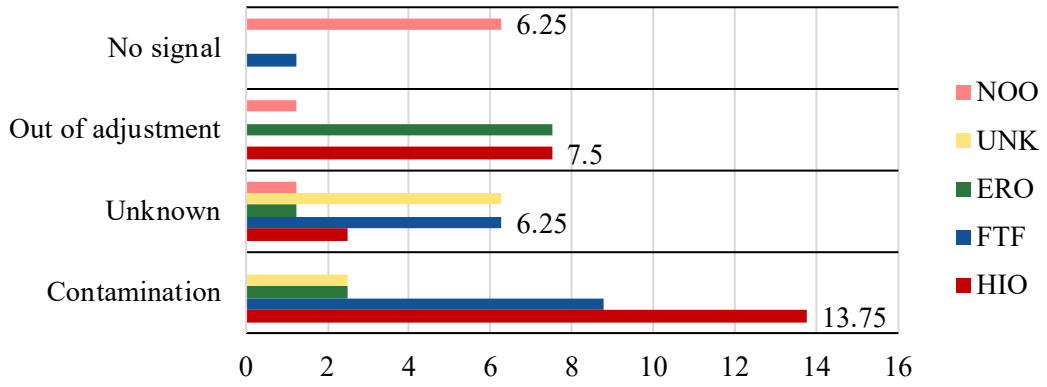

A-Figure 14: Top failure modes and mechanisms in fire & gas detectors, %.

A-Table 21: Failure rates for Fire & gas detectors. To be continued.

Severity Class	Failure Mode	Mean	SD	n/t	Time
Critical	All	2.30	1.61	2.52	*
		2.31	1.64	2.53	†
	FTF	1.02	1.83	1.22	*
		1.04	1.86	1.22	†
	HIO	0.08	0.15	0.09	*
		0.08	0.15	0.09	†
	NOO	0.63	1.11	0.69	*
		0.63	1.12	0.70	†

Note: All failure rates are given in (10^{-6} hrs.)

A-Table 22: Failure rates for Fire & gas detectors. Continued

Severity Class	Failure Mode	Mean	SD	n/t	Time
Degraded	All	3.25	4.67	3.91	*
		3.27	4.73	3.92	†
	ERO	1.33	2.25	1.30	*
		1.34	2.25	1.31	†
	HIO	0.91	3.24	1.56	*
		0.92	3.29	1.57	†
	UNK	0.26	0.53	0.35	*
		0.26	0.54	0.35	†
Incipient	All	0.42	0.19	0.43	*
		0.43	0.19	0.44	†
	ERO	0.08	0.15	0.09	*
		0.08	0.15	0.09	†
	UNK	0.14	0.29	0.17	*
		0.14	0.30	0.17	†
Unknown	All	0.09	0.10	0.09	*
		0.09	0.09	0.09	†
All modes	All	5.96	6.74	6.95	*
		6.00	6.83	6.97	†

Note: All failure rates are given in (10^{-6} hrs.)

D.2.6. Control Logic Devices

Failure data on control logic devices (CLU) is not described in depth in OREDA. A-Table 23 lists the identified failure modes and mechanisms relevant to general CLU components. The data implies that failures refer to unstable functionality, such as spurious operation (SPO), failure to function on-demand (FTF) and erratic output (ERO). As A-Figure 15 indicates, the failure modes are directly related to specific failure mechanisms, i.e., electrical and software failures.

Failure rates are available for the generic failure modes for CLU components (4.3) in A-Table 24. In this case, *calendar time* should represent more accurately the participation of the CLU in the control and monitoring processes of the system.

A-Table 23: Top failure mode and mechanisms – CLUs.

Failure Modes	Contribution, %	Failure Mechanisms	Contribution, %
ERO	25.00	Electrical failure	25.00
FTF	25.00	Software failure	25.00
SPO	50.00	Earth/isolation fault	50.00
Total	100.00	Total	100.00

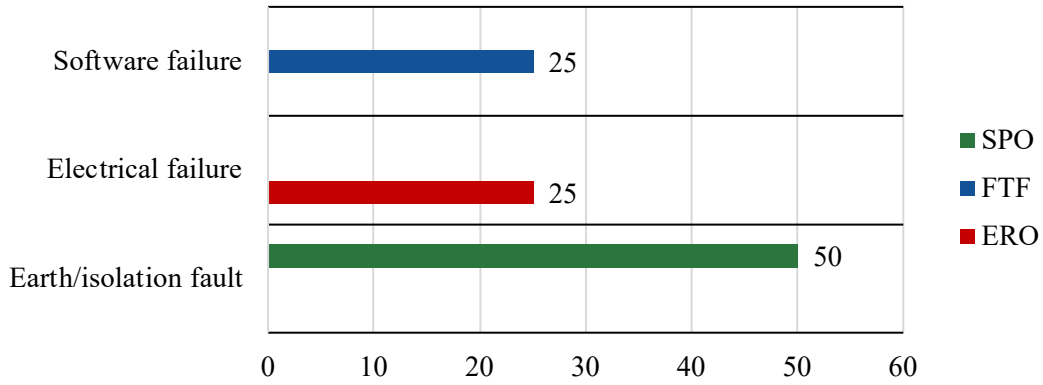

A-Figure 15: Top failure modes and mechanisms in CLU, %.

A-Table 24: Failure rates for CLUs.

Severity Class	Failure Mode	Mean	SD	n/t	Time
Degraded	All	17.37	23.82	11.40	*
		17.40	64.69	11.42	†
	SPO	17.37	23.82	11.40	*
		17.40	23.85	11.42	†
Incipient	All	9.90	11.52	11.40	*
		9.91	11.53	11.42	†
	ERO	5.22	5.77	5.71	*
		5.21	5.76	5.70	†
	FTF	5.21	5.76	5.70	*
		5.22	5.77	5.71	†
All modes	All	24.68	15.35	22.80	*
		24.71	15.38	22.83	†

Note: All failure rates are given in (10^{-6} hrs.)

D.2.7. Heat Exchangers

This equipment type refers to several different designs of heat exchangers. In general, this equipment is divided into four subdivisions: external unit, internal unit, control and monitoring, and miscellaneous elements. Abnormal instrument readings (AIR) and leakage (ELP, ELU) are the most common failure modes. More detail es necessary on the evaporator's characteristics to select relevant failure modes for analysis. A-Table 25 lists the general failure modes and mechanisms with higher relative contributions to the total failure rate, while A-Figure 16 presents the relationship between these. Both are consistent identifying that leakage and abnormal instrumentation readings have a considerable effect on the components' failures.

Failure rates are available for general failure modes for heat exchangers (3.1). Other failure modes are described for various types of heat exchangers and could be more appropriate. However, as e means of simplifying the data collected, A-Table 26 and A-

Table 27 present this generic failure data for heat exchangers. As this component operates under demand, the failure rates estimated in *operational time* are considered more representative values.

A-Table 25: Top failure mode and mechanisms - Heat exchangers.

Failure Modes	Contribution, %	Failure Mechanisms	Contribution, %
STD	11.84	Mechanical failure	7.89
OTH	11.85	Corrosion	7.90
ELP	14.48	Control failure	10.53
ELU	14.48	Unknown	14.48
AIR	23.70	Leakage	19.74
Total	96.10	Total	73.70

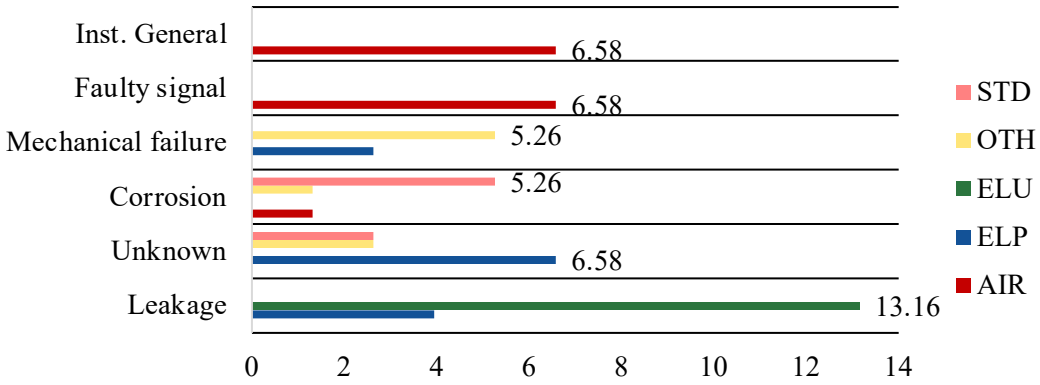

A-Figure 16: Top failure modes and mechanisms in heat exchangers, %.

A-Table 26: Failure rates for Heat Exchangers. To be continued.

Severity Class	Failure Mode	Mean	SD	n/t	Time
Critical	All	16.36	17.43	25.99	*
		17.31	19.49	28.15	†
	AIR	6.64	4.87	8.00	*
		7.11	5.34	8.66	†
	ELP	1.30	0.94	1.33	*
		1.41	1.02	1.44	†
	ELU	3.53	1.95	4.00	*
		3.74	2.31	4.33	†
	STD	2.20	2.15	2.67	*
		2.36	2.36	289.00	†
	OTH	2.46	1.62	2.67	*
		2.65	1.78	2.89	†

Note: All failure rates are given in (10^{-6} hrs.)

A-Table 27: Failure rates for Heat Exchangers. Continued.

Severity Class	Failure Mode	Mean	SD	n/t	Time
Degraded	All	27.51	24.42	18.66	*
		28.27	24.92	20.21	†
	AIR	3.21	4.55	3.33	*
		3.42	4.88	3.61	†
	ELP	2.10	5.88	2.00	*
		2.25	2.05	2.17	†
	ELU	3.03	1.49	3.33	*
		3.28	1.61	3.61	†
	STD	3.66	3.34	2.67	*
		3.81	3.39	2.89	†
	OTH	3.19	2.51	3.33	*
		3.42	2.72	3.61	†
Incipient	All	5.31	7.27	6.00	*
		5.65	7.80	6.50	†
	AIR	0.61	0.67	0.67	*
		0.66	0.72	0.72	†
	ELP	3.70	5.79	4.00	*
		3.93	6.21	4.33	†
	STD	0.70	0.85	0.67	*
		0.75	0.92	0.72	†
All modes	All	50.25	12.22	50.66	*
		53.89	12.14	54.86	†

Note: All failure rates are given in (10^{-6} hrs.)

D.2.8. Vessels

The data presented in the OREDA databases under the taxonomy of 'vessels' is not directly applicable to the storage vessels present in the LH2 storage system. However, they do allow the quantification of the reliability of the system in an initial estimation process. As seen in A-Table 28, most common issues are related to instrumentation (AIR) and leakage (ELP), which can be extended to storage vessels. Failure mechanisms, as shown in A-Figure 17 however, are mostly focused on process control, which does not apply to the studied system.

Failure rates are available for the general failure modes in vessels (3.2). Other sources for relevant failure modes could be required for an appropriate quantification of the reliability of the system. Currently, the failure data presented in A-Table 29 and A-Table 30 for *calendar time*-based failure estimations are considered for the analysis.

A-Table 28: Top failure mode and mechanisms – Vessels.

Failure Modes	Contribution, %	Failure Mechanisms	Contribution, %
STD	9.53	No signal	7.05
OTH	9.92	Out of adjustment	7.88
PDE	12.44	Control failure	14.51
ELP	16.58	Unknown	14.52
AIR	41.05	Faulty signal	17.43
Total	89.52	Total	61.39

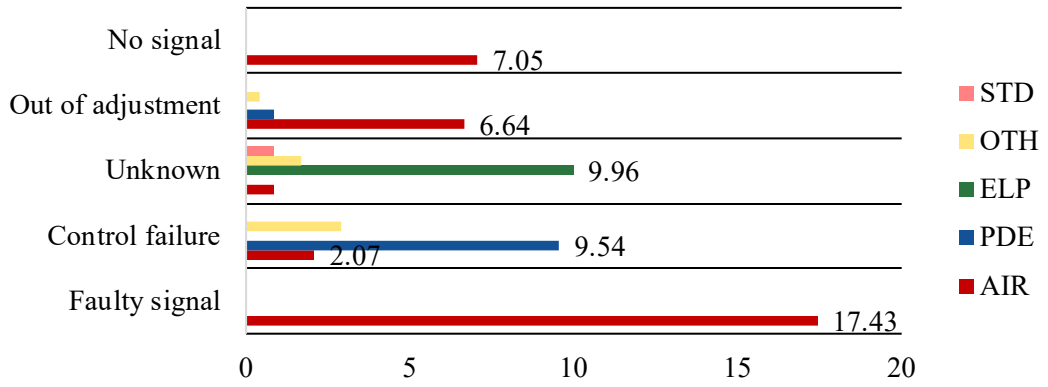

A-Figure 17: Top failure modes and mechanisms in vessels, %.

A-Table 29: Failure rates for Vessels. To be continued.

Severity Class	Failure Mode	Mean	SD	n/t	Time
Critical	All	27.02	48.00	38.78	*
		30.13	53.95	43.78	†
	AIR	13.32	21.20	19.60	*
		14.97	23.80	22.13	†
	ELP	2.86	3.73	2.98	*
		3.19	3.74	3.37	†
	PDE	7.84	19.88	10.23	*
		8.80	22.40	11.55	†
	OTH	1.90	2.00	2.13	*
		2.15	2.24	2.41	†

Note: All failure rates are given in (10^{-6} hrs.)

A-Table 30: Failure rates for Vessels. Continued.

Severity Class	Failure Mode	Mean	SD	n/t	Time
Degraded	All	39.89	27.75	41.33	*
		43.43	28.53	46.66	†
	AIR	13.95	15.67	18.32	*
		15.29	17.13	20.68	†
	ELP	2.59	3.91	4.26	*
		2.93	4.36	4.81	†
	PDE	9.47	11.76	2.56	*
		10.03	12.52	2.89	†
	STD	5.96	2.07	6.39	*
		6.81	2.16	7.22	†
	OTH	4.98	9.66	6.39	*
		5.60	10.87	7.22	†
Incipient	All	14.97	11.97	20.88	*
		17.00	13.15	23.57	†
	AIR	2.73	2.30	3.41	*
		3.09	2.57	3.85	†
	ELP	5.46	9.15	9.37	*
		6.35	10.31	10.58	†
	STD	3.88	4.36	3.41	*
		4.23	4.54	3.85	†
Unknown	All	1.28	1.48	1.70	*
		1.45	1.66	1.92	†
	AIR	0.71	0.74	0.85	*
		0.81	0.83	0.96	†
	ELP	0.37	0.43	0.43	*
		0.42	0.48	0.48	†
All modes	All	82.73	51.08	102.70	*
		91.58	54.72	115.93	†

Note: All failure rates are given in (10^{-6} hrs.)

D.3. Purple Book Loss of Containment Frequency Data

The Purple Book collects a variety of LOC frequency data relevant to the construction of ETAs and FTAs in the context of QRAs. Although this information refers to generic industry data, detailed breakdowns for some components by application and type allow a better characterization than using other databases. LOC data refer the occurrence of random events, estimated through observed failed and operational components in industrial settings. In this document, individual and societal risk are defined as:

a) Individual Risk: Frequency of an individual dying due to LOCs. The individual is assumed to be unprotected and to be present during the total exposure time.

b) Societal Risk: Frequency of having an accident with N ore more people being killed simultaneously. The people involved are assumed to have some means of protection.

As per instructed in *The Purple Book* guideline for constructing relevant QRAs, only LOC that contribute to individual or societal risk should be included under two conditions:

1) The frequency of occurrence is equal to or greater than 10^{-8} per year.
2) Lethal damage (1% probability) occurs outside the establishment's boundary or the transport route.

It is stated that criterion (1) corresponds with present-day practice. A threshold of 10^{-8} per year for including LOCs is considered reasonable since generic LOCs leading to the release of the complete inventory have failure frequencies in the range 10^{-5} to 10^{-7} per year. In the following sections, relevant LOCs for the analysis of the LH_2 storage system are documented [33]. These primarily refer to the LH_2 storage tank. LOC data is also reported for pipelines, pumps, heat exchangers and pressure relief devices. Further, specific indications are suggested to consider the consequences of the reported releases, as shown in A-Table 31.

A-Table 31: Consequence modeling for storage and piping LOC events.

LOC	Installation	To model as:
Instantaneous	Tanks and vessels	Totally ruptured vessel. Gas: no air entrainment during expansion. Liquid: spreading pool
Continuous release	Tanks and vessels	Hole in vessel wall (sharp orifice)
Full bore rupture	Process pipes	Full bore ruptured pipeline
Leak	Process pipes	Outflow through small leak (sharp orifice)
Pressure relief valve	All	Hole in vessel wall (rounded orifice)
Pool evaporation	Tanks and vessels	Pool evaporation
Process scenarios	Tanks and vessels	Specific models

D.3.1. Pressure and Atmospheric Tanks

The LOC frequency data collected for pressurized and atmospheric tanks or vessels cover failures directly related to the structural integrity of the vessel wall and the welded stumps, mounting plates these and of the associated instrumentation pipework. Additionally, the failure frequencies recorded are *default* failure frequencies excluding effects such as corrosion, fatigue due to vibrations, operating errors, and external impacts. Several types of pressurized stationary tanks as well as pressure, process and reactor vessels can be distinguished. These are defined as:

- Pressure vessel: A pressure vessel is a storage vessel in which the pressure is (substantially) more than 1 bar absolute.
- Process vessel: In a process vessel a change in the physical properties of the substance occurs, e.g., temperature or phase. Examples of process vessels are

distillation columns, condensers, and filters. Vessels where only the level of liquid changes can be considered as pressure vessels.

Depending on the application, some storage tanks may have been pressurized to just above 1 bar (abs.). In this case, these can be considered as atmospheric tanks for LOC purposes. This applies, for instance, to cryogenic tanks and atmospheric storage tanks with nitrogen blanketing.

Based on the previous definitions, data for two types of releases are available:

a) Directly to the atmosphere. This refers to single-walled storage tanks.
b) From primary container to unimpaired secondary container or outer shell. This refers to double-walled storage tanks, such as the ones used to store liquid hydrogen.

Data for three distinct failure modes are presented:

1. G_1: Instantaneous release of complete inventory.
2. G_2: Continuous release of the complete inventory in 10 min at a constant rate of release.
3. G_3: Continuous release from a hole with an effective diameter of 10 mm.

Further differentiation is needed between the particular configurations of these tanks resulting in different release scenarios. These types are defined as:

- Single-containment atmospheric tank: Consists of a primary container for the liquid. An outer shell is either present, or not, but when present, primarily intended for the retention and protection of insulation. It is not designed to contain liquid in the event of the primary container's failure.
- Atmospheric tank with a protective outer shell: Consists of a primary container for the liquid and a protective outer shell. The outer shell is designed to contain the liquid in the event of failure of the primary container but is not designed to contain any vapor. The outer shell is not designed to withstand all possible loads, e.g., explosion (static pressure load of 0.3 bar during 300 ms), penetrating fragments and cold (thermal) load.
- Double-containment atmospheric tank: Consists of a primary container for the liquid and a secondary container. The secondary container is designed to contain the liquid in the event of failure of the primary container and to withstand all possible loads, like explosion (static pressure load of 0.3 bar during 300 ms), penetrating fragments and cold (thermal) load. The secondary container is not designed to hold any kind of vapor.
- Full-containment atmospheric tank: Consists of a primary container for the liquid and a secondary container. The secondary container is designed to contain both the liquid and vapor in the event of failure of the primary container, and to withstand all possible loads, like explosion (static pressure load of 0.3 bar during 300 ms), penetrating fragments and cold. The outer roof is supported by the secondary containment and designed to withstand loads e.g., explosion.

Hence, the relevant LOC are extracted from the atmospheric tank section, shown in A-Table 32. It must be noted that failure frequencies for atmospheric vessels are considered to be higher than for pressurized tanks by a factor of 10, to include potential hazardous exposure of the stored substance. Further, for specific failure scenarios, in which

external impact or operating errors cannot be excluded, the given values for LOC G1 and G2 should consider adding 5×10^{-6} per year.

A-Table 32: LOC data for pressure and atmospheric tanks.

Installation/ Release type	**LOC (y^{-1})**					
	G1		G2		G3	
	a	b	a	b	a	b
Pressure vessel	5×10^{-7}		5×10^{-7}		1×10^{-5}	
Process vessel	5×10^{-6}		5×10^{-6}		1×10^{-4}	
Single-contained Atmospheric tank	5×10^{-6}		5×10^{-6}		1×10^{-4}	
Atmospheric tank with protective outer shell	5×10^{-7}	5×10^{-7}	5×10^{-7}	5×10^{-7}		1×10^{-4}
Double-containment atmospheric tank	1.25×10^{-8}	5×10^{-8}	1.25×10^{-8}	5×10^{-8}		1×10^{-4}
Full-containment atmospheric tank	1×10^{-8}					

D.3.2. Pipelines

LOC data for pipelines cover all types of process pipes and inter-unit pipelines above ground of the studied system and are summarized in A-Table 33 based on their nominal diameters. This considers that the pipeline is operating in an environment with no excessive vibration, corrosion, erosion, or thermal cycling stresses. The minimum length of a pipeline is 10 m to included flange failures in the estimations.

Data for two distinct failure modes are presented:

1. G_1: Full-bore rupture. outflow is from both sides of the full-bore rupture.
2. G_2: Leak. outflow is from a leak with effective diameter of 10% of the nominal diameter, with a maximum of 50 mm.

A-Table 33: LOC data for pipelines.

Installation/Release type	**LOC ($m^{-1}y^{-1}$)**	
	G1	G2
Nominal diameter < 75 mm	1×10^{-6}	5×10^{-6}
Nominal diameter (75>, <150) mm	3×10^{-7}	5×10^{-6}
Nominal diameter > 150 mm	1×10^{-6}	5×10^{-6}

D.3.3. Pumps

LOC data for pumps are summarized here based on structural characteristics of the installation, such as the casing, as a release mitigation measure. The failure frequencies presented in A-Table 34 are averages encompassing pump, drive and sealing type as well as rpm speed, among others.

Data for two distinct failure modes are presented:

1. G_1: Catastrophic failure. full-bore rupture of the largest connecting pipeline.
2. G_2: Leak. outflow is from a leak with effective diameter of 10% of the nominal diameter of largest connecting pipeline, with a maximum of 50 mm.

A-Table 34: LOC data for centrifugal pumps.

Installation/ Release type	**LOC (y^{-1})**	
	G1	G2
Pumps without additional provisions	1×10^{-4}	5×10^{-4}
Pumps with a wrought steel containment	5×10^{-5}	2.5×10^{-4}
Canned pumps	1×10^{-5}	5×10^{-5}

D.3.4. Heat Exchangers

LOC data for heat exchangers are summarized in A-Table 35 based on the inner or outer fluid properties, pressure, and structural characteristics of the installation. These consider tube and pipe heat exchanger designs. These estimations are based on expert judgment.

Data for three types of designs are available:

a) Dangerous substance outside pipes.
b) Dangerous substance inside pipes. The design pressure of the outer shell is less than the pressure of dangerous substance.
c) Dangerous substance inside pipes. The design pressure of the outer shell is equal or higher than the pressure of dangerous substance.

Data for six distinct failure modes are presented:

1. G_1: Instantaneous release of complete inventory.
2. G_2: Continuous release of the complete inventory in 10 min at a constant rate of release.
3. G_3: Continuous release from a hole with an effective diameter of 10 mm.
4. G_4: Full-bore rupture of ten pipes simultaneously. outflow from both sides of the full-bore rupture
5. G_5: Full-bore rupture of one of the pipes. outflow from both sides of the full-bore rupture

6. G_6: Leak. outflow from a leak with effective diameter of 10% of the nominal diameter, with a maximum of 50 mm.

For heat exchangers with the dangerous substance inside the pipes, a rupture of ten pipes is assumed to always go simultaneously with failure of the outer shell, resulting in a direct release to the environment.

A-Table 35: LOC data for heat exchangers.

Installation/	**LOC (y^{-1})**					
Release type	G1	G2	G3	G4	G5	G6
Dangerous substance outside pipes.	5×10^{-5}	5×10^{-5}	1×10^{-3}			
Dangerous substance inside pipes. Outer pressure is lower.				1×10^{-5}	1×10^{-3}	1×10^{-2}
Dangerous substance inside pipes. Outer pressure is higher.				1×10^{-6}		

D.3.5. Pressure Relief Devices

LOC data for pressure relief devices (PRD) are summarized in A-Table 36. It must be noted that the opening of a pressure relief valve results in an emission only if the device is in direct contact with the substance and discharges directly to the atmosphere. These estimations are based on expert judgment.

Data for one distinct failure modes are presented:

1. G_1: Discharge of a pressure relief device with maximum discharge rate.

A-Table 36: LOC data for PRDs.

Installation/	**LOC ($m^{-1}y^{-1}$)**
Release type	G1
PRD	2×10^{-5}

Appendix E. Extended QRA Results

E.1. FMEA Full Results

A-Table 37: FMEA Results for System 1.1 Storage Tank. To be continued.

No.	Failure Modes and Causes	Failure Mode Model	Local Effects	Next Higher Level	End Effects	Severity	Probability	Risk Matrix Level	Notes
1.1.1	Leak of hydrogen into vacuum between walls.	Failure to meet functional specifications	Loss of insulative capability	Hydrogen evaporation within outer tank	Overpressure of outer tank causing tank rupture	Critical	Medium	H	Loss of insulation would cause evaporation before effective leakage; hence risk is related to GH2
1.1.2					Embrittlement of outer tank by hydrogen causing leakage	Moderate	Medium	M	
1.1.3	Puncture of outer tank due to debris or collision	Failure conditions caused by the operational environment			Overpressure of inner tank causing tank rupture	Critical	Low	M	
1.1.4					Leakage of gaseous hydrogen (embrittlement of inner tank)	Minor	Low	L	
1.1.5	Failure of outer tank wall due to external fire				Overpressure of inner tank causing tank rupture	Critical	Low	M	
1.1.6	Tank rupture due to accident or collision		Tank Rupture	Release of high quantity of liquid hydrogen	Cryogenic risks	Critical	Low	M	Evaporation rate is required to assess liquid/gaseous release scenario
1.1.7	Fittings fail due to manufacturing defect or installation error	Failure to meet functional specifications	Leakage	Release of minor quantity of liquid hydrogen	Evaporation of released hydrogen	Minor	Medium	L	

A-Table 38: FMEA Results for System 1.1 Storage Tank. Continued.

No.	Failure Modes and Causes	Failure Mode Model	Local Effects	Next Higher Level	End Effects	Severity	Probability	Risk Matrix Level	Notes
1.1.8	Overpressure from failed PSV operation	Failure to operate at prescribed time	Leakage	Release of minor quantity of liquid hydrogen	Evaporation of released hydrogen	Moderate	Medium	M	Small leakage allows evaporation before liquid accumulation; hence risk is related to GH2
1.1.9			Tank Rupture	Release of high quantity of liquid hydrogen	Cryogenic/Evaporation risks	Critical	Medium	H	Evaporation rate is required to assess liquid/gaseous release scenario
1.1.10	Mechanical failure due to pressure cycling fatigue	Failure to meet functional specifications	Loss of insulation vacuum through cracking at piping penetrations	Hydrogen evaporation within outer tank	Embrittlement by hydrogen causing leakage	Moderate	Medium	M	Loss of insulation would cause evaporation before effective leakage; hence risk is related to GH2
1.1.11					Overpressure of inner tank causing tank rupture	Critical	Medium	H	
1.1.12			Leakage by cracking at piping penetrations	Release of minor quantity of liquid hydrogen	Evaporation of released hydrogen	Moderate	Medium	M	Small leakage allows evaporation before liquid accumulation; hence risk is related to GH2

A-Table 39: FMEA Results for System 1.2-1.4 PSV. To be Continued.

No.	Failure Modes and Causes	Failure Mode Model	Local Effects	Next Higher Level	End Effects	Severity	Probability	Risk Matrix Level	Notes
1.2.1-1.3.1	Circuit failure due to external accident	Failure conditions caused by the operational environment	No pressure control	-	Unable to control tank overpressure	Moderate	Low	L	Early detection of malfunction should reduce potential risk.
1.2.2-1.3.2	Circuit malfunction due to cryogenic temperatures					Moderate	Low	L	
1.2.3-1.3.3	Circuit malfunction	Failure to meet functional specifications				Moderate	Low	L	
1.4.1	Controller failure to stop hydrogen release	Failure to cease operation at prescribed time	Additional release of GH2		Release of excess GH2	Moderate	Low	L	Not a risk if hydrogen is not continuously evaporating and creating overpressure
1.4.2	Controller malfunction, operation when not needed	Premature operation				Minor	Low	L	

A-Table 40: FMEA Results for System 1.2-1.4 PSV. Continued.

No.	Failure Modes and Causes	Failure Mode Model	Local Effects	Next Higher Level	End Effects	Severity	Probability	Risk Matrix Level	Notes
1.4.3	Controller failure to commence operation	Failure to operate at prescribed time	Inner tank damage	Hydrogen evaporation within outer tank	Overpressure of outer tank causing tank rupture	Critical	Low	M	Loss of insulation would cause evaporation before effective leakage; hence risk is related to GH2
1.4.4					Embrittlement of outer tank by hydrogen causing leakage	Moderate	Low	L	
1.4.5	Malfunction due to cryogenic temperatures	Failure conditions caused by the operational environment	Inner tank damage		Overpressure of outer tank causing tank rupture	Critical	High	H	
1.4.6					Embrittlement of outer tank by hydrogen causing leakage	Moderate	High	H	

A-Table 41: FMEA Results for System 1.5 Block-and-bleed valve.

No.	Failure Modes and Causes	Failure Mode Model	Local Effects	Next Higher Level	End Effects	Severity Class	Probability Class	Risk Matrix Level	Notes
1.5.1	Controller failure to stop hydrogen release (bleed)	Failure to cease operation at prescribed time	Additional release of GH2	-	Release of excess GH2	Moderate	High	H	Small release of GH2-related risk
1.5.2	Controller failure to commence operation (bleed)	Premature operation				Minor	Low	L	
1.5.3	Leakage	Failure to meet functional specifications	Leakage of LH2 (small)	LH2 Evaporation	GH2 release (small)	Minor	High	M	Small leakage allows evaporation before liquid accumulation; hence risk is related to GH2
1.5.4	Controller failure to commence operation (bleed)	Failure to operate at prescribed time	Inner tank damage	Hydrogen evaporation within outer tank	Embrittlement of outer tank by hydrogen causing leakage	Moderate	High	H	Loss of insulation would cause evaporation before effective leakage; hence risk is related to GH2

A-Table 42: FMEA Results for System 2.1 Air-operated valve (FV).

No.	Failure Modes and Causes	Failure Mode Model	Local Effects	Next Higher Level	End Effects	Severity Class	Probability Class	Risk Matrix Level	Notes
2.1.1	Mechanical failure, unable to close	Failure to meet functional specifications	Lack of appropriate flow of cryogenic pump	Cavitation of cryogenic pump	Potential explosion and release of LH2	Minor	Medium	L	Evaporation rate is required to assess liquid/gaseous release scenario
2.1.2	Operation failure	Premature operation				Critical	Low	M	
2.1.3		Failure to operate at prescribed time				Critical	High	H	
2.1.4			Potential overpressure in piping and tank upstream	-	Potential release of LH2	Moderate	High	H	
2.1.5	Leakage	Failure to meet functional specifications	Leakage of LH2 (small)	LH2 Evaporation	GH2 release (small)	Minor	Medium	L	Small leakage allows evaporation before liquid accumulation; hence risk is related to GH2

A-Table 43: FMEA Results for System 2.2-2.6 FV Control System.

No.	Item	Failure Modes and Causes	Failure Mode Model	Local Effects	Next Higher Level	End Effects	Severity Class	Probability Class	Risk Matrix Level	Notes
2.2.1	Position Actuator	Controller malfunction	Premature operation	No pressure control	-	Unable to control tank overpressure	Moderate	Low	L	Very detailed. Condense to 'Air-actuated valve control system'
2.2.2		Operation failure	Failure to meet functional specifications				Moderate	Medium	M	
2.3.1	Position Indicator						Moderate	Low	L	
2.4.1	Position switch Open						Moderate	Low	L	
2.5.1	Position switch Closed						Moderate	Low	L	
2.6.1	Process air	Supplies ZZO for FV operation	Air supply malfunction	Failure to operate at prescribed time	No pressure control	Unable to control tank overpressure	Critical	Low	M	External component availability

A-Table 44: FMEA Results for System 3.1 Cryogenic Pump.

No.	Failure Modes and Causes	Failure Mode Model	Local Effects	Next Higher Level	End Effects	Severity Class	Probability Class	Risk Matrix Level	Notes
3.1.1	Leakage from pump due to seal failure or installation error	Failure to meet functional specifications	Leakage of LH2 (small)	LH2 Evaporation	GH2 release (small)	Minor	Medium	L	Small leakage allows evaporation before liquid accumulation; hence risk is related to GH2
3.1.2			Leakage of LH2 (large)	-	Cryogenic LH2 release	Moderate	Medium	M	Evaporation rate is required to assess liquid/gaseous release scenario
3.1.3	Pump fails to deliver LH2	Failure to operate at prescribed time	No flow of LH2 to Evaporator	Increased pressure upstream	Increased leakage of valves	Minor	High	M	Small leakage allows evaporation before liquid accumulation; hence risk is related to GH2
3.1.4	Pump operates prematurely due to controller failure	Premature operation	Unwanted flow of LH2 to Evaporator	Overpressure of piping towards Evaporator	Potential rupture of piping and release of LH2	Critical	Low	M	Evaporation rate is required to assess liquid/gaseous release scenario
3.1.5	Pump fails to perform adequately	Failure to meet functional specifications	Lack of appropriate LH2 flow	Increased pressure upstream	Increased leakage of valves	Minor	Medium	L	Small leakage allows evaporation before liquid accumulation; hence risk is related to GH2

A-Table 45: FMEA Results for System 3.2 Isolation Hand Valve.

No.	Failure Modes and Causes	Failure Mode Model	Local Effects	Next Higher Level	End Effects	Severity Class	Probability Class	Risk Matrix Level	Notes
3.2.1	Controller failure to commence operation	Failure to operate at prescribed time	Potential overpressure in piping/pump upstream	-	Leakage failure in piping/pump	Moderate	Low	L	Evaporation rate is required to assess liquid/gaseous release scenario
3.2.2	Controller failure to stop operation		Potential overpressure in piping/evaporator downstream	-	Leakage failure in piping/evaporator	Moderate	Low	L	
3.2.3	Leakage	Failure to meet functional specifications	Leakage of LH2 (small)	LH2 Evaporation	GH2 release (small)	Minor	High	M	Small leakage allows evaporation before liquid accumulation; hence risk is related to GH2

A-Table 46: FMEA Results for System 3.3 Ambient air Evaporator.

No.	Failure Modes and Causes	Failure Mode Model	Local Effects	Next Higher Level	End Effects	Severity Class	Probability Class	Risk Matrix Level	Notes
3.3.1	Rupture due to collision or accident	Failure conditions caused by the operational environment	Release of mixture of liquid/gaseous hydrogen	-	Release of mixture of liquid/gaseous hydrogen	Critical	Medium	H	Evaporation rate is required to assess liquid/gaseous release scenario
3.3.2	Leakage from fittings and connecting piping	Failure to meet functional specifications				Moderate	Medium	M	
3.3.3	Leakage to/from internal piping	Failure to meet functional specifications	Mixture of ambient air and LH2/GH2 within evaporator		Leakage by embrittlement	Minor	Medium	L	Small leakage allows evaporation before liquid accumulation; hence risk is related to GH2

A-Table 47: FMEA Results for System 4.1 Piping Lines.

No.	Failure Modes and Causes	Failure Mode Model	Local Effects	Next Higher Level	End Effects	Severity Class	Probability Class	Risk Matrix Level	Notes
4.1.1	Leakage due to mechanical failure or installation error	Failure conditions caused by the operational environment	Leakage of LH2 (small)	LH2 Evaporation	GH2 release (small)	Minor	Medium	L	Small leakage allows evaporation before liquid accumulation; hence risk is related to GH2
4.1.2			Leakage of LH2 (large)	LH2 release	Cryogenic risks	Moderate	Medium	M	Evaporation rate is required to assess liquid/gaseous release scenario
4.1.3	Leakage due to material failure (fatigue)	Failure to meet functional specs	Leakage of LH2 (small)	LH2 Evaporation	GH2 release (small)	Minor	Medium	L	Small leakage allows evaporation before liquid accumulation; hence risk is related to GH2
4.1.4			Leakage of LH2 (large)	LH2 release	Cryogenic risks	Moderate	Medium	M	Evaporation rate is required to assess liquid/gaseous release scenario

E.2. Full Fault Tree

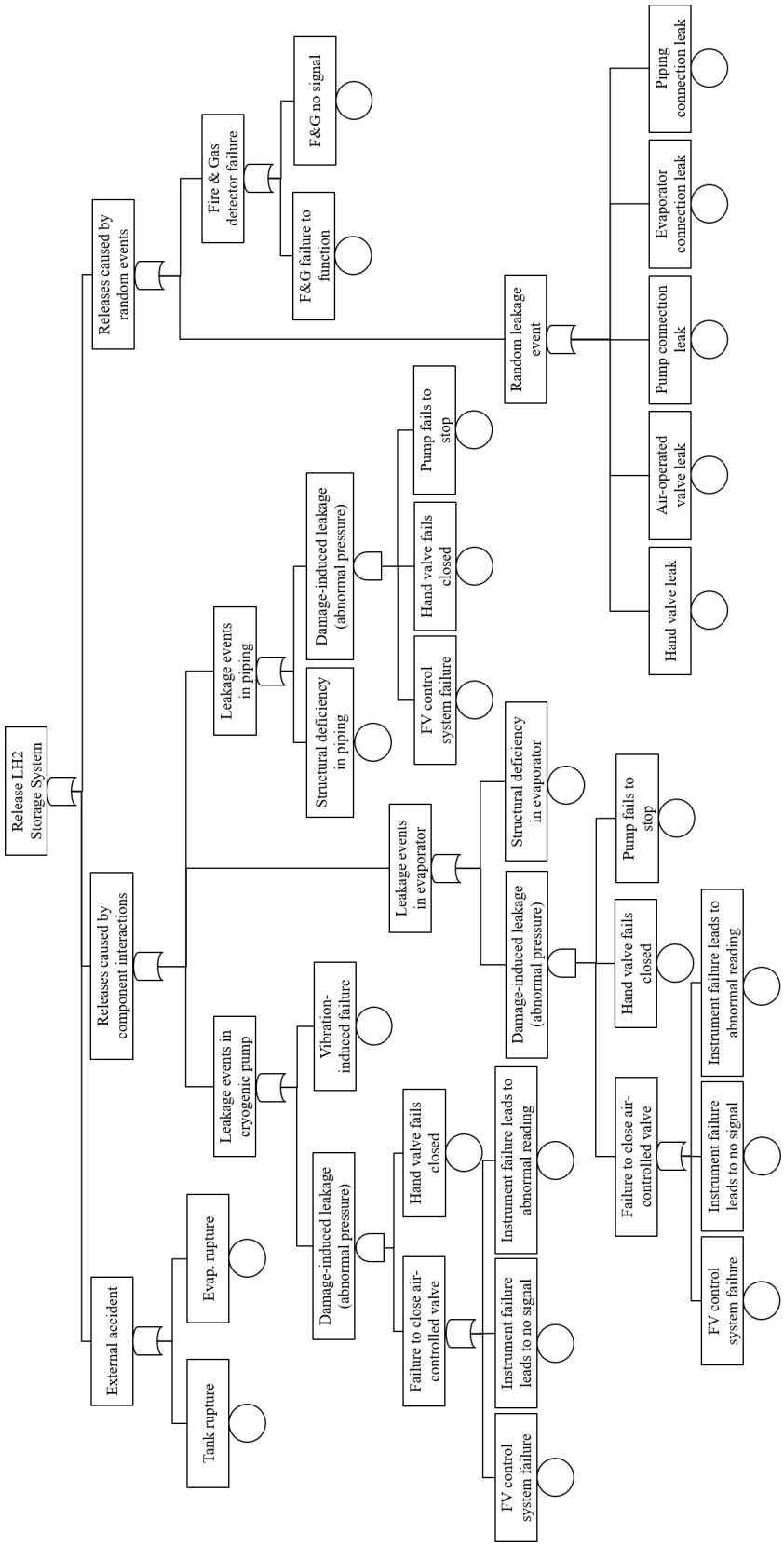

A-Figure 18: Complete Fault Tree for LH2 Release Top Event.

References

[1] J. Alazemi and J. Andrews, "Automotive hydrogen fuelling stations: An international review," *Renew. Sustain. Energy Rev.*, vol. 48, pp. 483–499, Aug. 2015.

[2] Hydrogen and Fuel Cell Technologies Office (HFTO), "Hydrogen and Fuel Cell Technologies Office Multi-Year Research, Development, and Demonstration Plan," 2015. [Online]. Available: https://www.energy.gov/eere/fuelcells/downloads/hydrogen-and-fuel-cell-technologies-office-multi-year-research-development.

[3] S. Satyapal, "U.S. Department of Energy Hydrogen and Fuel Cells Program: 2019 Annual Merit Review and Peer Evaluation Report; April 29 - May 1, 2019, Arlington, Virginia," 2020.

[4] National Fire Protection Association, "NFPA 2 Hydrogen Technologies Code." 2020.

[5] J. M. Schneider, G. Dang-Nhu, and N. Hart, "ISO 19880-1, Hydrogen Fueling Station and Vehicle Interface Technical Specification," *ECS Trans.*, vol. 71, no. 1, pp. 155–172, Feb. 2016.

[6] J. LaChance, A. Tchouvelev, and J. Ohi, "Risk-informed process and tools for permitting hydrogen fueling stations," *Int. J. Hydrogen Energy*, vol. 34, no. 14, pp. 5855–5861, Jul. 2009.

[7] R. Moradi and K. M. Groth, "Hydrogen storage and delivery: Review of the state of the art technologies and risk and reliability analysis," *Int. J. Hydrogen Energy*, vol. 44, no. 23, pp. 12254–12269, May 2019.

[8] R. M. Souza, E. G. S. Nascimento, U. A. Miranda, W. J. D. Silva, and H. A. Lepikson, "Deep learning for diagnosis and classification of faults in industrial rotating machinery," *Comput. Ind. Eng.*, vol. 153, p. 107060, Mar. 2021.

[9] N. Li, N. Gebraeel, Y. Lei, X. Fang, X. Cai, and T. Yan, "Remaining useful life prediction based on a multi-sensor data fusion model," *Reliab. Eng. Syst. Saf.*, vol. 208, p. 107249, Apr. 2021.

[10] IEA, "The Future of Hydrogen for G20," *Int. Energy Agency*, no. June, 2019.

[11] "National Fire Protection Association (NFPA)," 2020. [Online]. Available: https://www.nfpa.org/. [Accessed: 08-Jun-2020].

[12] J. L. LaChance, B. Middleton, and K. M. Groth, "Comparison of NFPA and ISO approaches for evaluating separation distances," *Int. J. Hydrogen Energy*, vol. 37, no. 22, pp. 17488–17496, Nov. 2012.

[13] K. M. Groth, J. L. LaChance, and A. P. Harris, "Design-stage QRA for indoor vehicular hydrogen fueling systems," *Safety, Reliab. Risk Anal. Beyond Horiz. - Proc. Eur. Saf. Reliab. Conf. ESREL 2013*, pp. 2247–2255, 2014.

[14] A. C. LaFleur, A. B. Muna, and K. M. Groth, "Application of quantitative risk assessment for performance-based permitting of hydrogen fueling stations," *Int. J. Hydrogen Energy*, vol. 42, no. 11, pp. 7529–7535, Mar. 2017.

[15] J. M. Schneider, G. Dang-Nhu, and N. Hart, "ISO 19880-1, Hydrogen Fueling Station and Vehicle Interface Technical Specification," *Int. Conf. Hydrog. Saf.*, vol. 71, no. 1, pp. 155–172, Feb. 2015.

[16] K. M. Groth and E. S. Hecht, "HyRAM: A methodology and toolkit for quantitative

risk assessment of hydrogen systems," *Int. J. Hydrogen Energy*, vol. 42, no. 11, pp. 7485–7493, Mar. 2017.
[17] K. M. Groth, E. Hecht, J. T. Reynolds, M. L. Blaylock, I. W. Ekoto, and G. W. Walkup, "HyRAM (Hydrogen Risk Assessment Models), Version 1.0." Sandia National Laboratories, 2016, software available at http://hyram.sandia.gov.
[18] K. M. Groth, E. Hecht, J. T. Reynolds, M. L. Blaylock, and E. Carrier, "HyRAM (Hydrogen Risk Assessment Models), Version 1.1." Sandia National Laboratories, (2/28/2017), software available at http://hyram.sandia.gov.
[19] B. D. Ehrhart *et al.*, "HyRAM (Hydrogen Risk Assessment Models), Version 2.0." Sandia National Laboratories (4/29/2019); software available at http://hyram.sandia.gov, 2019.
[20] B. D. Ehrhart *et al.*, "HyRAM (Hydrogen Risk Assessment Models), Version 3.0." Sandia National Laboratories (9/30/2020), software available at http://hyram.sandia.gov, 2020.
[21] N.-H. Kim, D. An, and J.-H. Choi, *Prognostics and Health Management of Engineering Systems*. Cham: Springer International Publishing, 2017.
[22] S. Khan and T. Yairi, "A review on the application of deep learning in system health management," *Mech. Syst. Signal Process.*, vol. 107, pp. 241–265, 2018.
[23] H. Meng and Y. F. Li, "A review on prognostics and health management (PHM) methods of lithium-ion batteries," *Renewable and Sustainable Energy Reviews*, vol. 116. Pergamon, p. 109405, 01-Dec-2019.
[24] Y. Lei, N. N. Li, L. Guo, N. N. Li, T. Yan, and J. Lin, "Machinery health prognostics: A systematic review from data acquisition to RUL prediction," *Mech. Syst. Signal Process.*, vol. 104, pp. 799–834, May 2018.
[25] Y. Cheng, N. Zerhouni, and C. Lu, "A hybrid remaining useful life prognostic method for proton exchange membrane fuel cell," *Int. J. Hydrogen Energy*, vol. 43, no. 27, pp. 12314–12327, Jul. 2018.
[26] D. Apostolou and G. Xydis, "A literature review on hydrogen refuelling stations and infrastructure. Current status and future prospects," *Renew. Sustain. Energy Rev.*, vol. 113, p. 109292, Oct. 2019.
[27] U.S. Department of Energy's Office of Energy Efficiency & Renewable Energy's Vehicle Technologies Office, "Alternative Fueling Station Locator," *Alternative Fuels Data Center*..
[28] J. LaChance, "Risk-informed separation distances for hydrogen refueling stations," *Int. J. Hydrogen Energy*, vol. 34, no. 14, pp. 5838–5845, Jul. 2009.
[29] Compressed Gas Association, "CGA P-28--2014 OSHA Process Safety Management and EPA Risk Management Plan Guidance Document for Bulk liquid Hydrogen Supply Systems - Fourth Edition," 2014.
[30] "Compressed Gas Association (CGA)," 2021. [Online]. Available: https://www.cganet.com/.
[31] Compressed Gas Association, "CGA H-5-2014 Standard For Bulk Hydrogen Supply Systems - Second Edition," 2014.
[32] Compressed Gas Association, "CGA H-3-2013 Cryogenic Hydrogen Storage - Second Edition," 2014.
[33] P. A. M. Uijt de Haag, B. J. M. Ale, and J. G. Post, "The 'Purple Book,'" in *Loss Prevention and Safety Promotion in the Process Industries*, Elsevier, 2001, pp.

1429–1438.
[34] K. Groth, E. Hecht, J. T. Reynolds, M. L. Blaylock, and E. E. Carrier, "Methodology for assessing the safety of Hydrogen Systems: HyRAM 1.1 technical reference manual," Albuquerque, NM, and Livermore, CA (United States), Mar. 2017.
[35] J. C. H. Schüller, J. L. Brinkman, P. J. Van Gestel, and R. W. Van Otterloo, *Methods for determining and processing probabilities: Red Book*. Committee for the Prevention of Disasters, 1997.
[36] I. W. Ekoto *et al.*, "Liquid Hydrogen Release and Behavior Modeling: State-of-the-Art Knowledge Gaps and Research Needs for Refueling Infrastructure Safety," Albuquerque, NM, 2014.
[37] J. LaChance, A. Tchouvelev, and A. Engebo, "Development of uniform harm criteria for use in quantitative risk analysis of the hydrogen infrastructure," *Int. J. Hydrogen Energy*, vol. 36, no. 3, pp. 2381–2388, Feb. 2011.
[38] G. Saur, S. Sprik, J. Kurtz, S. Oronato, S. Gilleon, and E. Winkler, "Hydrogen Station Data Collection and Analysis," in *DOE Hydrogen and Fuel Cells Program 2019 Annual Merit Review and Peer Evaluation Meeting*, 2019, pp. 53–57.
[39] M. Peters, N. Menon, M. Ruple, J. Martin, and E. Winkler, "H2First: Dispenser Reliability," in *2019 DOE Annual Merit Review*, 2019, vol. 1, pp. 1–29.
[40] A. M. Abdalla, S. Hossain, O. B. Nisfindy, A. T. Azad, M. Dawood, and A. K. Azad, "Hydrogen production, storage, transportation and key challenges with applications: A review," *Energy Convers. Manag.*, vol. 165, no. January, pp. 602–627, Jun. 2018.
[41] S. Kikukawa, H. Mitsuhashi, and A. Miyake, "Risk assessment for liquid hydrogen fueling stations," *Int. J. Hydrogen Energy*, vol. 34, no. 2, pp. 1135–1141, Jan. 2009.
[42] H.-R. R. Gye, S.-K. K. Seo, Q.-V. V. Bach, D. Ha, and C.-J. J. Lee, "Quantitative risk assessment of an urban hydrogen refueling station," *Int. J. Hydrogen Energy*, vol. 44, no. 2, pp. 1288–1298, Jan. 2019.
[43] K. Tsunemi, T. Kihara, E. Kato, A. Kawamoto, and T. Saburi, "Quantitative risk assessment of the interior of a hydrogen refueling station considering safety barrier systems," *Int. J. Hydrogen Energy*, vol. 44, no. 41, pp. 23522–23531, Aug. 2019.
[44] P. Russo, A. De Marco, M. Mazzaro, and L. Capobianco, "Quantitative risk assessment on a hydrogen refuelling station," *Chem. Eng. Trans.*, vol. 67, 2018.
[45] B. Ehrhart and E. Hecht, "Hydrogen Risk Assessment Models (HyRAM) Version 3.0 Technical Reference Manual.," SAND2020-10600. September 2020., Albuquerque, NM, and Livermore, CA (United States), Sep. 2020.
[46] M. Casamirra, F. Castiglia, M. Giardina, and C. Lombardo, "Safety studies of a hydrogen refuelling station: Determination of the occurrence frequency of the accidental scenarios," *Int. J. Hydrogen Energy*, vol. 34, no. 14, pp. 5846–5854, Jul. 2009.
[47] S. Kikukawa, F. Yamaga, and H. Mitsuhashi, "Risk assessment of Hydrogen fueling stations for 70 MPa FCVs," *Int. J. Hydrogen Energy*, vol. 33, no. 23, pp. 7129–7136, Dec. 2008.
[48] T. Suzuki *et al.*, "Quantitative risk assessment using a Japanese hydrogen refueling station model," *Int. J. Hydrogen Energy*, Dec. 2020.
[49] K. Tsunemi, K. Yoshida, T. Kihara, T. Saburi, and K. Ono, "Screening-Level Risk Assessment of a Hydrogen Refueling Station that Uses Organic Hydride," *Sustainability*, vol. 10, no. 12, p. 4477, Nov. 2018.

[50] M. Kodoth *et al.*, "Leak frequency analysis for hydrogen-based technology using bayesian and frequentist methods," *Process Saf. Environ. Prot.*, vol. 136, pp. 148–156, Apr. 2020.
[51] Y. Huang and G. Ma, "A grid-based risk screening method for fire and explosion events of hydrogen refuelling stations," *Int. J. Hydrogen Energy*, vol. 43, no. 1, pp. 442–454, Jan. 2018.
[52] A. Al-Shanini, A. Ahmad, and F. Khan, "Accident modelling and safety measure design of a hydrogen station," in *International Journal of Hydrogen Energy*, 2014, vol. 39, no. 35, pp. 20362–20370.
[53] H. J. Pasman and W. J. Rogers, "Risk assessment by means of Bayesian networks: A comparative study of compressed and liquefied H 2 transportation and tank station risks," *Int. J. Hydrogen Energy*, vol. 37, no. 22, pp. 17415–17425, Nov. 2012.
[54] B. J. Lowesmith, G. Hankinson, and S. Chynoweth, "Safety issues of the liquefaction, storage and transportation of liquid hydrogen: An analysis of incidents and HAZIDS," in *International Journal of Hydrogen Energy*, 2014, vol. 39, no. 35, pp. 20516–20521.
[55] S. Pique, B. Weinberger, V. De-Dianous, and B. Debray, "Comparative study of regulations, codes and standards and practices on hydrogen fuelling stations," *Int. J. Hydrogen Energy*, vol. 42, no. 11, pp. 7429–7439, Mar. 2017.
[56] R. Zhao, R. Yan, Z. Chen, K. Mao, P. Wang, and R. X. Gao, "Deep learning and its applications to machine health monitoring," *Mech. Syst. Signal Process.*, vol. 115, pp. 213–237, Jan. 2019.
[57] M. L. Hoffmann Souza, C. A. da Costa, G. de Oliveira Ramos, and R. da Rosa Righi, "A survey on decision-making based on system reliability in the context of Industry 4.0," *Journal of Manufacturing Systems*, vol. 56. Elsevier B.V., pp. 133–156, 01-Jul-2020.
[58] ISO 13381-1:2015, "Condition monitoring and diagnostics of machines — Prognostics — Part 1: General guidelines.".
[59] X. Li, W. Zhang, and Q. Ding, "Deep learning-based remaining useful life estimation of bearings using multi-scale feature extraction," *Reliab. Eng. Syst. Saf.*, vol. 182, pp. 208–218, Feb. 2019.
[60] O. Fink, Q. Wang, M. Svensén, P. Dersin, W.-J. Lee, and M. Ducoffe, "Potential, challenges and future directions for deep learning in prognostics and health management applications," *Eng. Appl. Artif. Intell.*, vol. 92, p. 103678, Jun. 2020.
[61] R. Li, W. J. C. Verhagen, and R. Curran, "A systematic methodology for Prognostic and Health Management system architecture definition," *Reliab. Eng. Syst. Saf.*, vol. 193, p. 106598, Jan. 2020.
[62] R. Moradi and K. M. Groth, "Modernizing risk assessment: A systematic integration of PRA and PHM techniques," *Reliab. Eng. Syst. Saf.*, vol. 204, p. 107194, Dec. 2020.
[63] V. Atamuradov, K. Medjaher, P. Dersin, B. Lamoureux, and N. Zerhouni, "Prognostics and health management for maintenance practitioners - review, implementation and tools evaluation," *Int. J. Progn. Heal. Manag.*, vol. 8, no. Special Issue 7, pp. 1–31, 2017.
[64] P. Marti-Puig, A. Blanco-M, J. J. Cárdenas, J. Cusidó, and J. Solé-Casals, "Effects of the pre-processing algorithms in fault diagnosis of wind turbines," *Environ.*

Model. Softw., vol. 110, pp. 119–128, Dec. 2018.
[65] K. T. P. Nguyen and K. Medjaher, "A new dynamic predictive maintenance framework using deep learning for failure prognostics," *Reliab. Eng. Syst. Saf.*, vol. 188, pp. 251–262, Aug. 2019.
[66] H. Lee, G. Li, A. Rai, and A. Chattopadhyay, "Real-time anomaly detection framework using a support vector regression for the safety monitoring of commercial aircraft," *Adv. Eng. Informatics*, vol. 44, p. 101071, Apr. 2020.
[67] G. Niu, *Data-driven technology for engineering systems health management: Design approach, feature construction, fault diagnosis, prognosis, fusion and decision*. 2016.
[68] B. Rezaeianjouybari and Y. Shang, "Deep learning for prognostics and health management: State of the art, challenges, and opportunities," *Meas. J. Int. Meas. Confed.*, vol. 163, p. 107929, Oct. 2020.
[69] A. Stetco *et al.*, "Machine learning methods for wind turbine condition monitoring: A review," *Renew. Energy*, vol. 133, pp. 620–635, Apr. 2019.
[70] B. D. Ehrhart *et al.*, "Hydrogen Refueling Reference Station Lot Size Analysis for Urban Sites.," Albuquerque, NM, and Livermore, CA (United States), Mar. 2020.
[71] M. Modarres, M. P. Kaminskiy, and V. Krivtsov, *Reliability Engineering and Risk Analysis*. Third edition. | Boca Raton: Taylor & Francis, a CRC title,: CRC Press, 2016.
[72] M. Cristina Galassi *et al.*, "HIAD - Hydrogen incident and accident database," *Int. J. Hydrogen Energy*, vol. 37, no. 22, pp. 17351–17357, Nov. 2012.
[73] Online Data & Information Network (ODIN), "HIAD 2.0: Hydrogen Incidents and Accidents Database," *European Comission Joint Research Center (JRC)*, 2020. [Online]. Available: https://odin.jrc.ec.europa.eu/giada/.
[74] Pacific Northwest National Laboratory, "Lessons Learned | Hydrogen Tools," *DOE Office of Energy Efficiency and Renewable Energy's Fuel Cell Technologies Office*, 2020. [Online]. Available: https://h2tools.org/lessons.
[75] CEC, "Failure modes and effects analysis for hydrogen fueling options. CEC-600-2005-0012004," California Energy Commission: California.
[76] O. R. Hansen, "Liquid hydrogen releases show dense gas behavior," *Int. J. Hydrogen Energy*, vol. 45, no. 2, pp. 1343–1358, Jan. 2020.
[77] G. Petitpas and S. M. Aceves, "Modeling of sudden hydrogen expansion from cryogenic pressure vessel failure," *Int. J. Hydrogen Energy*, vol. 38, no. 19, pp. 8190–8198, Jun. 2013.
[78] H. Barthelemy, M. Weber, and F. Barbier, "Hydrogen storage: Recent improvements and industrial perspectives," *Int. J. Hydrogen Energy*, vol. 42, no. 11, pp. 7254–7262, Mar. 2017.
[79] K. Groth, C. Wang, and A. Mosleh, "Hybrid causal methodology and software platform for probabilistic risk assessment and safety monitoring of socio-technical systems," *Reliab. Eng. Syst. Saf.*, vol. 95, no. 12, pp. 1276–1285, Dec. 2010.
[80] G. Saur, S. Gilleon, and S. Sprik, "Fueling Station Component Validation," in *H2@Scale Working Group*, 2020.
[81] NREL National Fuel Cell Technology Evaluation Center, "Hydrogen System Component Validation," *DOE Annual Merit Review Meeting (June 2017)*, 2017. [Online]. Available: https://www.nrel.gov/hydrogen/hydrogen-component-

validation.html.
[82] NREL National Fuel Cell Technology Evaluation Center, "Hydrogen Fueling Infrastructure Analysis," *NREL Composite Data Products (April 2020)*, 2020. [Online]. Available: https://www.nrel.gov/hydrogen/hydrogen-infrastructure-analysis.html.
[83] NREL, "Hydrogen Compressor Reliability Investigation and Improvement - Cooperative Research and Development Final Report," no. March, 2016.
[84] L-B-Systemtechnik GmbH, "Handbook for Approval of Hydrogen Refuelling Stations," *European Comission CORDIS EU Research Results*, 2007. [Online]. Available: https://cordis.europa.eu/project/id/19813/reporting/fr.
[85] R. Wurster *et al.*, "Hyapproval: Final handbook for approval of hydrogen refuelling stations," in *16th World Hydrogen Energy Conference 2006, WHEC 2006, 13-16 June 2006, Lyon, France*, 2006.
[86] E. Funnemark, J. E. Eldor, and G. P. Haugom, "HyApproval: Identification and review of databases for reliability data," Tech. Rep. Deliverable 4.4, WP4 HyApproval-Handbook for Approval of Hydrogen Refuelling Stations, 2006.
[87] SINTEF Technology and Society, Norges teknisk-naturvitenskapelige Universitet, and DNV GL, *OREDA: Offshore and Onshore Reliability Data Handbook.*, 6th ed., no. v. 1. OREDA Participants, 2015.
[88] P. D. S. D. Handbook, "Reliability data for safety instrumented systems," *PDS Data Handbook, SINTEF*, 2010.
[89] D. Mahar, W. Fields, and J. Reade, "Nonelectronic Parts Reliability Data (NPRD-2016)," *Quanterion Solut. Inc.*, 2015.
[90] Swedpower AB, *T-book. Reliability data of components in Nordic nuclear power plants.*, 6th Editio. Stockholm, Sweden: TUD Office, 2005.
[91] D. Lyons, *Western European cross-country oil pipelines 30-year performance statistics*, vol. 17, no. 2. Brussels: CONCAWE, 2002.
[92] M. Kodoth, S. Aoyama, J. Sakamoto, N. Kasai, T. Shibutani, and A. Miyake, "Evaluating uncertainty in accident rate estimation at hydrogen refueling station using time correlation model," *Int. J. Hydrogen Energy*, vol. 43, no. 52, pp. 23409–23417, Dec. 2018.
[93] C. San Marchi *et al.*, "Overview of the DOE hydrogen safety, codes and standards program, part 3: Advances in research and development to enhance the scientific basis for hydrogen regulations, codes and standards," *Int. J. Hydrogen Energy*, vol. 42, no. 11, pp. 7263–7274, Mar. 2017.
[94] M. McDougall and D. Stephens, "Cumulative Fuel System Life Cycle and Durability Testing of Hydrogen Containers (Report No. DOT HS 811 832)," Washington, DC, 2013.
[95] K. L. Tsui, N. Chen, Q. Zhou, Y. Hai, and W. Wang, "Prognostics and Health Management: A Review on Data Driven Approaches," *Math. Probl. Eng.*, vol. 2015, pp. 1–17, 2015.
[96] M. Jouin, R. Gouriveau, D. Hissel, M. C. Péra, and N. Zerhouni, "Degradations analysis and aging modeling for health assessment and prognostics of PEMFC," *Reliab. Eng. Syst. Saf.*, vol. 148, pp. 78–95, 2016.
[97] M. Huang, Z. Liu, and Y. Tao, "Mechanical fault diagnosis and prediction in IoT based on multi-source sensing data fusion," *Simul. Model. Pract. Theory*, vol. 102,

p. 101981, Jul. 2020.
[98] G. W. Vogl, B. A. Weiss, and M. A. Donmez, "Standards Related to Prognostics and Health Management (PHM) for Manufacturing," Gaithersburg, MD, Jun. 2014.
[99] A. Saxena and K. Goebel, "Turbofan Engine Degradation Simulation Data Set, NASA Ames Prognostics Data Repository," NASA Ames Research Center, Moffett Field, CA, 2008.
[100] A. Saxena and K. Goebel, "PHM08 Challenge Data Set, NASA Ames Prognostics Data Repository," NASA Ames Research Center, Moffett Field, CA, 2008.
[101] IEEE, "PHM 2012 Prognostic Challenge. Outline, Experiments, Scoring of results, Winners.," 2012. [Online]. Available: http://www.femto-st.fr/f/d/IEEEPHM2012-Challenge-Details.pdf.
[102] P. Nectoux *et al.*, "PRONOSTIA: An experimental platform for bearings accelerated degradation tests.," 2012.
[103] H. Qiu, J. Lee, J. Lin, and G. Yu, "Wavelet filter-based weak signature detection method and its application on rolling element bearing prognostics," *J. Sound Vib.*, vol. 289, no. 4–5, pp. 1066–1090, Feb. 2006.
[104] J. Lee, H. Qiu, G. Yu, J. Lin, and Rexnord Technical Services., "'Bearing Data Set", NASA Ames Prognostics Data Repository," NASA Ames Research Center, Moffett Field, CA, 2007.
[105] A. Agogino, K. Goebel, BEST lab, and UC Berkeley, "'Milling Data Set", NASA Ames Prognostics Data Repository," NASA Ames Research Center, Moffett Field, CA, 2007.
[106] K. Goebel, "Management of Uncertainty for Sensor Validation, Sensor Fusion, and Diagnosis Using Soft Computing Techniques." Ph. D. Thesis, University of California at Berkeley, Berkeley. Addison …, 1996.
[107] W. Ahmad, S. A. Khan, M. M. M. Islam, and J. M. Kim, "A reliable technique for remaining useful life estimation of rolling element bearings using dynamic regression models," *Reliab. Eng. Syst. Saf.*, vol. 184, pp. 67–76, Apr. 2019.
[108] A. Mellit, G. M. Tina, and S. A. Kalogirou, "Fault detection and diagnosis methods for photovoltaic systems: A review," *Renew. Sustain. Energy Rev.*, vol. 91, no. March, pp. 1–17, 2018.
[109] International Electrotechnical Commission (IEC), "Standard IEC 61724: Photovoltaic system performance monitoring – Guidelines for measurement, data exchange and analysis," *IEC 61724-1:2017*, 2017. [Online]. Available: https://webstore.iec.ch/publication/33622.
[110] Institute of Electrical and Electronics Engineers (IEEE), "IEEE Standard Framework for Prognostics and Health Management of Electronic Systems," *IEEE Standard 1856-2017*, 2017. [Online]. Available: https://ieeexplore.ieee.org/document/8227036. [Accessed: 04-Feb-2021].
[111] J. Hong, Z. Wang, and Y. Yao, "Fault prognosis of battery system based on accurate voltage abnormity prognosis using long short-term memory neural networks," *Appl. Energy*, vol. 251, p. 113381, Oct. 2019.
[112] H. Liu, J. Chen, M. Hou, Z. Shao, and H. Su, "Data-based short-term prognostics for proton exchange membrane fuel cells," *Int. J. Hydrogen Energy*, vol. 42, no. 32, pp. 20791–20808, Aug. 2017.
[113] R. H. Lin, X. N. Xi, P. N. Wang, B. D. Wu, and S. M. Tian, "Review on hydrogen

fuel cell condition monitoring and prediction methods," *Int. J. Hydrogen Energy*, vol. 44, no. 11, pp. 5488–5498, Feb. 2019.
[114] M. Zhang, H. Lv, H. Kang, W. Zhou, and C. Zhang, "A literature review of failure prediction and analysis methods for composite high-pressure hydrogen storage tanks," *Int. J. Hydrogen Energy*, vol. 44, no. 47, pp. 25777–25799, Oct. 2019.
[115] G. Saur, S. Gilleon, and S. Sprik, "Fueling Station Component Validation," in *H2@Scale Working Group*, 2020.
[116] B. Yang *et al.*, "Damage localization in hydrogen storage vessel by guided waves based on a real-time monitoring system," *Int. J. Hydrogen Energy*, vol. 44, no. 40, pp. 22740–22751, Aug. 2019.
[117] Y. Ren, L. Qiu, S. Yuan, and Z. Su, "A diagnostic imaging approach for online characterization of multi-impact in aircraft composite structures based on a scanning spatial-wavenumber filter of guided wave," *Mech. Syst. Signal Process.*, vol. 90, pp. 44–63, Jun. 2017.
[118] A. De Fenza, A. Sorrentino, and P. Vitiello, "Application of Artificial Neural Networks and Probability Ellipse methods for damage detection using Lamb waves," *Compos. Struct.*, vol. 133, pp. 390–403, Dec. 2015.
[119] R. Xiao, Q. Hu, and J. Li, "Leak detection of gas pipelines using acoustic signals based on wavelet transform and Support Vector Machine," *Measurement*, vol. 146, pp. 479–489, Nov. 2019.
[120] Z. Li, H. Zhang, D. Tan, X. Chen, and H. Lei, "A novel acoustic emission detection module for leakage recognition in a gas pipeline valve," *Process Saf. Environ. Prot.*, vol. 105, pp. 32–40, Jan. 2017.
[121] A. K. Panda, J. S. Rapur, and R. Tiwari, "Prediction of flow blockages and impending cavitation in centrifugal pumps using Support Vector Machine (SVM) algorithms based on vibration measurements," *Measurement*, vol. 130, pp. 44–56, Dec. 2018.
[122] Q. Hu, E. F. Ohata, F. H. S. Silva, G. L. B. Ramalho, T. Han, and P. P. Rebouças Filho, "A new online approach for classification of pumps vibration patterns based on intelligent IoT system," *Meas. J. Int. Meas. Confed.*, vol. 151, p. 107138, Feb. 2020.
[123] A. Kumar, C. P. P. Gandhi, Y. Zhou, R. Kumar, and J. Xiang, "Improved deep convolution neural network (CNN) for the identification of defects in the centrifugal pump using acoustic images," *Appl. Acoust.*, vol. 167, p. 107399, Oct. 2020.
[124] H. M. Elattar, H. K. Elminir, and A. M. Riad, "Prognostics: a literature review," *Complex Intell. Syst.*, vol. 2, no. 2, pp. 125–154, Jun. 2016.
[125] G. W. Vogl, B. A. Weiss, and M. Helu, "A review of diagnostic and prognostic capabilities and best practices for manufacturing," *J. Intell. Manuf.*, vol. 30, no. 1, pp. 79–95, Jan. 2019.
[126] Y. Wang, H. Yang, X. Yuan, Y. Schardt, C. Yang, and W. Gui, "Deep learning for fault-relevant feature extraction and fault classification with stacked supervised auto-encoder," *J. Process Control*, vol. 92, pp. 79–89, Aug. 2020.
[127] Z. Chen, Y. Chen, L. Wu, S. Cheng, and P. Lin, "Deep residual network based fault detection and diagnosis of photovoltaic arrays using current-voltage curves and ambient conditions," *Energy Convers. Manag.*, vol. 198, p. 111793, Oct. 2019.
[128] B. Wang, Y. Lei, T. Yan, N. Li, and L. Guo, "Recurrent convolutional neural

network: A new framework for remaining useful life prediction of machinery," *Neurocomputing*, vol. 379, pp. 117–129, Feb. 2020.
[129] C. Che, H. Wang, Q. Fu, and X. Ni, "Combining multiple deep learning algorithms for prognostic and health management of aircraft," *Aerospace Science and Technology*, vol. 94. Elsevier Masson, p. 105423, 01-Nov-2019.
[130] Y. Chen, G. Peng, Z. Zhu, and S. Li, "A novel deep learning method based on attention mechanism for bearing remaining useful life prediction," *Appl. Soft Comput. J.*, vol. 86, p. 105919, Jan. 2020.
[131] N. Omri, Z. Al Masry, N. Mairot, S. Giampiccolo, and N. Zerhouni, "Industrial data management strategy towards an SME-oriented PHM," *J. Manuf. Syst.*, vol. 56, pp. 23–36, Jul. 2020.
[132] IEA, "Statistics - Key Renewables Trends (Renewables Information, 2016 edition)," 2016.
[133] D. Parra, L. Valverde, F. J. Pino, and M. K. Patel, "A review on the role, cost and value of hydrogen energy systems for deep decarbonisation," *Renewable and Sustainable Energy Reviews*, vol. 101. Pergamon, pp. 279–294, 01-Mar-2019.
[134] IRENA, *Hydrogen From Renewable Power: Technology outlook for the energy transition*, no. September. 2018.
[135] G. Zini and P. Tartarini, *Solar Hydrogen Energy Systems*. Milano: Springer Milan, 2012.
[136] G. Cipriani *et al.*, "Perspective on hydrogen energy carrier and its automotive applications," *International Journal of Hydrogen Energy*, vol. 39, no. 16. Pergamon, pp. 8482–8494, 27-May-2014.
[137] Z. Yanxing, G. Maoqiong, Z. Yuan, D. Xueqiang, and S. Jun, "Thermodynamics analysis of hydrogen storage based on compressed gaseous hydrogen, liquid hydrogen and cryo-compressed hydrogen," *Int. J. Hydrogen Energy*, vol. 44, no. 31, pp. 16833–16840, Jun. 2019.
[138] S. Niaz, T. Manzoor, and A. H. Pandith, "Hydrogen storage: Materials, methods and perspectives," *Renewable and Sustainable Energy Reviews*, vol. 50. Pergamon, pp. 457–469, 01-Oct-2015.
[139] International Organization for Standardization (ISO), "Cryogenic vessels — Static vacuum-insulated vessels — Part 1: Design, fabrication, inspection and tests (ISO 21009-1:2008)." International Organization for Standardization (ISO).
[140] International Organization for Standardization (ISO), "Cryogenic vessels — Static vacuum insulated vessels — Part 2: Operational requirements (ISO 21009-2:2015)." International Organization for Standardization (ISO), 2015.
[141] T. Sinigaglia, F. Lewiski, M. E. Santos Martins, and J. C. Mairesse Siluk, "Production, storage, fuel stations of hydrogen and its utilization in automotive applications-a review," *Int. J. Hydrogen Energy*, vol. 42, no. 39, pp. 24597–24611, Sep. 2017.
[142] A. V Tchouvelev, "Risk Assessment Studies of Hydrogen and Hydrocarbon Fuels," vol. 2, no. 416, pp. 1–86, 2008.